MICROARRAY AND GENOME-WIDE SEQUENCING APPROACHES TO CHARACTERIZING DNA BINDING MOLECULES

Thesis by

James William Puckett

In Partial Fulfillment of the Requirements

for the Degree of

Doctor of Philosophy

California Institute of Technology

Pasadena, California

2009

(Defended May 12, 2009)

Acknowledgements

I would like to thank my graduate research advisor, Professor Peter Dervan, for providing laboratory space, research funding, and helpful advice when asked. Thank you for providing me with a wonderful environment in which to learn as a researcher. I would like to thank the members of my thesis committee, Professor Robert Grubbs, Professor Stephen Mayo, and Professor Linda Hsieh-Wilson for their support.

I have had the opportunity to meet and work alongside many wonderful people during my tenure in the Dervan laboratories. I would like to acknowledge my collaborators in lab: Katy Muzikar, Carey Hsu, Nicholas Nickols, and Fei Yang, whose strong work ethics, scientific insight, and perseverance have made much of this work possible. Working in Church 316 has afforded the opportunity to interact daily with Carey Hsu, Sherry Tsai, Fei Yang, and Dan Gubler, all wonderful coworkers. I would like to thank all of the members of the Dervan lab for their friendship, especially my classmates Carey Hsu and Justin Cohen, and a more senior student, Nicholas Nickols, with whom the graduate student journey has been a true pleasure. I would like to thank John Phillips for carpooling with me from West Los Angeles to Pasadena during my final year of graduate study.

I would like to acknowledge the graduate students of the Dervan group during my tenure: Timothy Best, Michael Brochu, David Chenoweth, Raymond Doss, Benjamin Edelson, Michelle Farkas, Eric Fechter, Claire Jacobs, Benjamin Li, David Montgomery, Katy Muzikar, Julie Poposki, Adam Poulin-Kerstien, and Jim Sanchez; and postdoctoral scholars Hans-Dieter Arndt, Christian Dose, Mareike Goeritz, Bogdan Olenyuk, and Anne Viger.

Much of the research performed was in collaboration with the Gottesfeld Laboratory at the Scripps Research Institute in La Jolla, California (TSRI), the Ansari Laboratory at the University of Wisconsin, Madison, the Wells Laboratory at Texas A&M University, and the Pandolfo Laboratory at Université Libre de Bruxelles—Hôpital Erasme. From these laboratories I would like to thank the principal investigators as well as Ryan Burnett

(TSRI), Myriam Raï (Brussels), Leslie Son (Texas), Josh Tietjen (Wisconsin), and Christopher Warren (Wisconsin). Their collaborative efforts have greatly expanded the scope of research that could be studied with polyamides.

I would like to thank members of the Wold laboratory at Caltech for helpful discussions on ChIP-Seq studies: Ali Mortazavi, Anthony Kirilusha, Ken McCue, Brian Williams, and Diane Trout. Dr. Ryan Baugh and Oren Schaedel of the Sternberg lab were kind to show me how to use their fluorometer and allow me use of it. Thanks to Lorian Schaefer of the Millard and Muriel Jacobs Genetics and Genomics Laboratory for processing the ChIP-Seq experiments.

I would like to thank the Caltech staff, especially Professor Dervan's administrative assistant, Ms. Lynne Martinez. Steve Gould and Lillian Kremar have ensured prompt placement of orders. Thanks to Joe Drew and Ron Koen for their prompt delivery of received shipments.

for Joanne and my parents

Abstract

Hairpin and linear beta-alanine linked pyrrole-imidazole (Py-Im) polyamides are programmable oligomers that bind the DNA minor groove sequence-specifically with affinities comparable to those of DNA-binding proteins found in nature. These small molecules have been observed to localize within the nucleus of living cells and modulate endogenous gene expression. Herein, we demonstrate the utility of a linear beta-alanine linked pyrrole-imidazole polyamide to upregulate *frataxin* mRNA and protein expression in a cell line derived from a Friedreich's Ataxia patient. We examine the binding affinities and specificities of additional linear beta-alanine linked polyamides. We examine binding specificities of a Cy3-fluorescently labeled version of the *frataxin* expression modulating-polyamide and a Cy3-labeled polyamide known to downregulate expression of the Vascular Endothelial Growth Factor using DNA microarrays composed of hairpins harboring all 524,800 unique 10 bp DNA sequences. We experimentally verify the correlation of Cy3 fluorescence intensity with quantitative DNase I footprint derived binding affinities. We find that Cy3 dye placement on the polyamide tail versus labeling of an internal pyrrole does not significantly alter DNA specificity. Finally, we examine the genome-wide binding preferences of Androgen Receptor (AR) in LNCaP cells using ChIP-Seq (chromatin immunoprecipitation followed by high-throughput DNA sequencing). We observe the canonical ARE motif to be present in a majority of the immunoprecipitated binding regions. We observe a secondary sequence motif that may be the dimerization of AR with a forkhead protein, an interaction known in the literature but without a defined sequence motif. We also define AR occupancy with respect to location in and about known genes. We correlate gene expression profiles from mRNA microarray data with the ChIP-Seq data.

Table of Contents

List of Figures and Tables

Page

Chapter 1

Chapter 2A

Chapter 2B

Chapter 3

Chapter 4

Appendix A

Appendix B

Appendix C

Appendix D

Chapter 1

Introduction

Deoxyribonucleic Acid (DNA)

Deoxyribunocleic acid is the double-stranded, double-helical biopolymer that encodes all heritable information necessary to maintain life and the complex networks of gene expression and protein expression that ultimately result from its sequence. All combinations of DNA sequence polymers can be made from four monomers called nucleotides: deoxyadenosine (A), deoxycytidine (C), deoxyguanosine (G), and deoxythymidine (T), each connected to one another on a phosphodiester-linked deoxyribose sugar backbone. For each double-stranded duplex, there are rules that govern pairing of each of the four nucleotides: A pairs with T, and T with A; C pairs with G, and G with C. Several sequence and context dependent forms of DNA exist, such as A-form, B-form, and Z-form.[1,2] Of these, I will focus the discussion on B-form DNA as it will be most relevant to this thesis.

An X-ray crystal structure of B-form DNA is shown in Figure 1.1.[1] The three-dimensional structure of the clefts within DNA can be subdivided into a "major" groove and a "minor" groove. The phosphodiester-linked deoxyribose sugar backbone of DNA is highlighted in blue, and the individual bases are shown in a silver color. Each base pair is oriented perpinduclarly to the helical axis of DNA. Ten base pairs of DNA represent a full turn of the DNA helix. Space-filling representations of A·T and G·C base pairs are shown in Figure 1.1. Two hydrogen bonds form between A·T base pairs and three between G·C base pairs. Beneath each base pair is shown the minor groove hydrogen bonding pattern.

Protein-DNA Recognition

The three billion base pairs of DNA within a human cell nucleus contains the information which encodes 20,000 to 25,000 protein-coding genes.[3] DNA is transcribed into mRNA, which forms the template for the synthesis of proteins, a process called translation. Some of the proteins produced function as transcription factors which regulate the expression of genes at the DNA→mRNA level. These proteins recognize and bind specific sequences of DNA. An example of five such proteins is denoted in Figure 1.2.

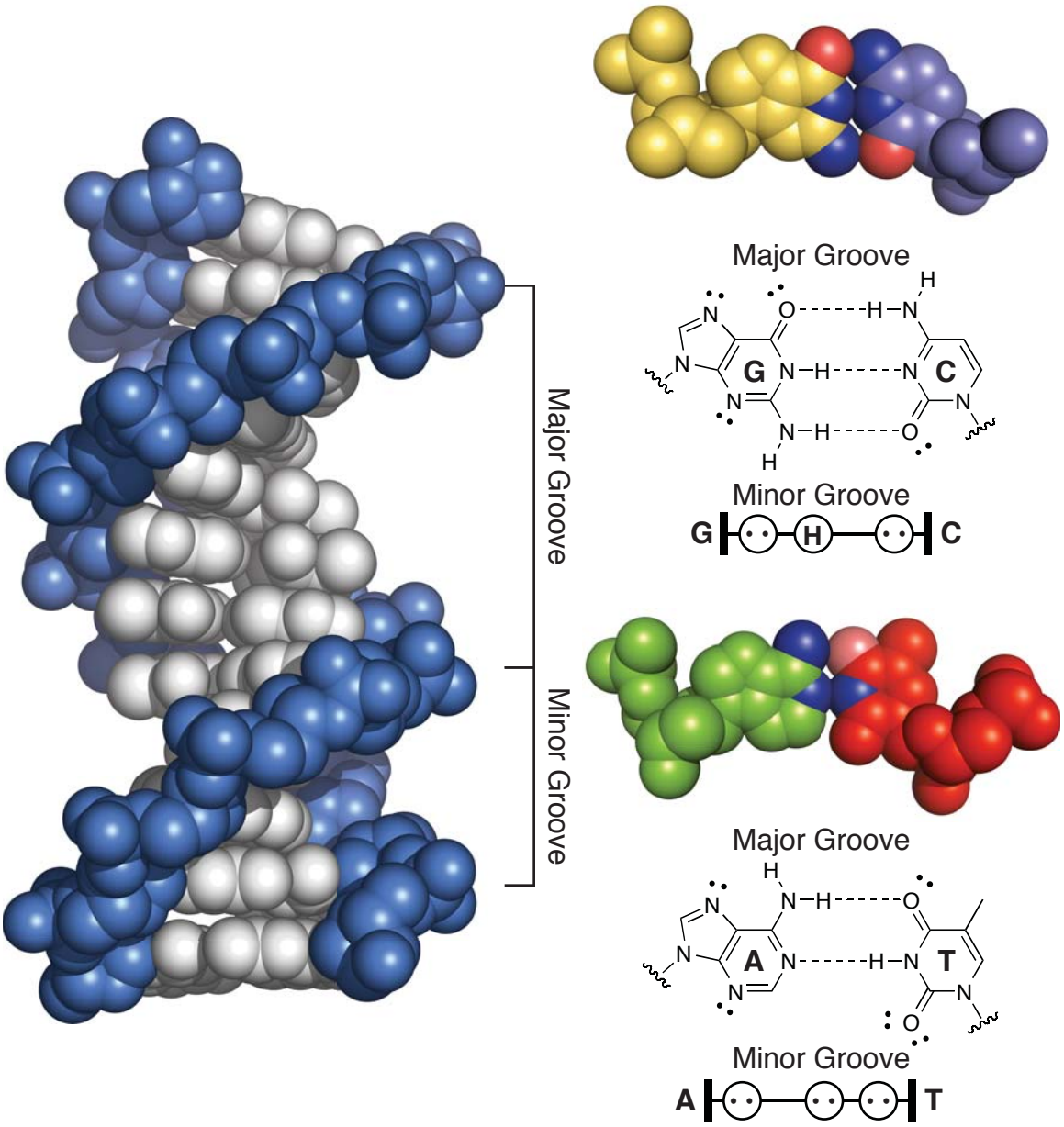

Figure 1.1. X-ray crystal structure (PDB 1BNA) of double-stranded DNA and examination of individual DNA base pairs

Transcription factors can be segmented into three recognition groups: a group that targets the minor groove of DNA, a group that binds the major groove, and a group that binds a hybrid of the two grooves. Of the proteins shown in Figure 1.2, NF-κB (p50/p65 heterodimer), Zif268, and Ets-1 recognize the major groove of DNA.[4–6] TATA-Binding Protein (TBP) and LEF-1 each recognize the minor groove of DNA.[7,8] Of these proteins, zinc finger proteins (such as Zif268) have been evolved to target new sequences of 9–18 base pairs.[9]

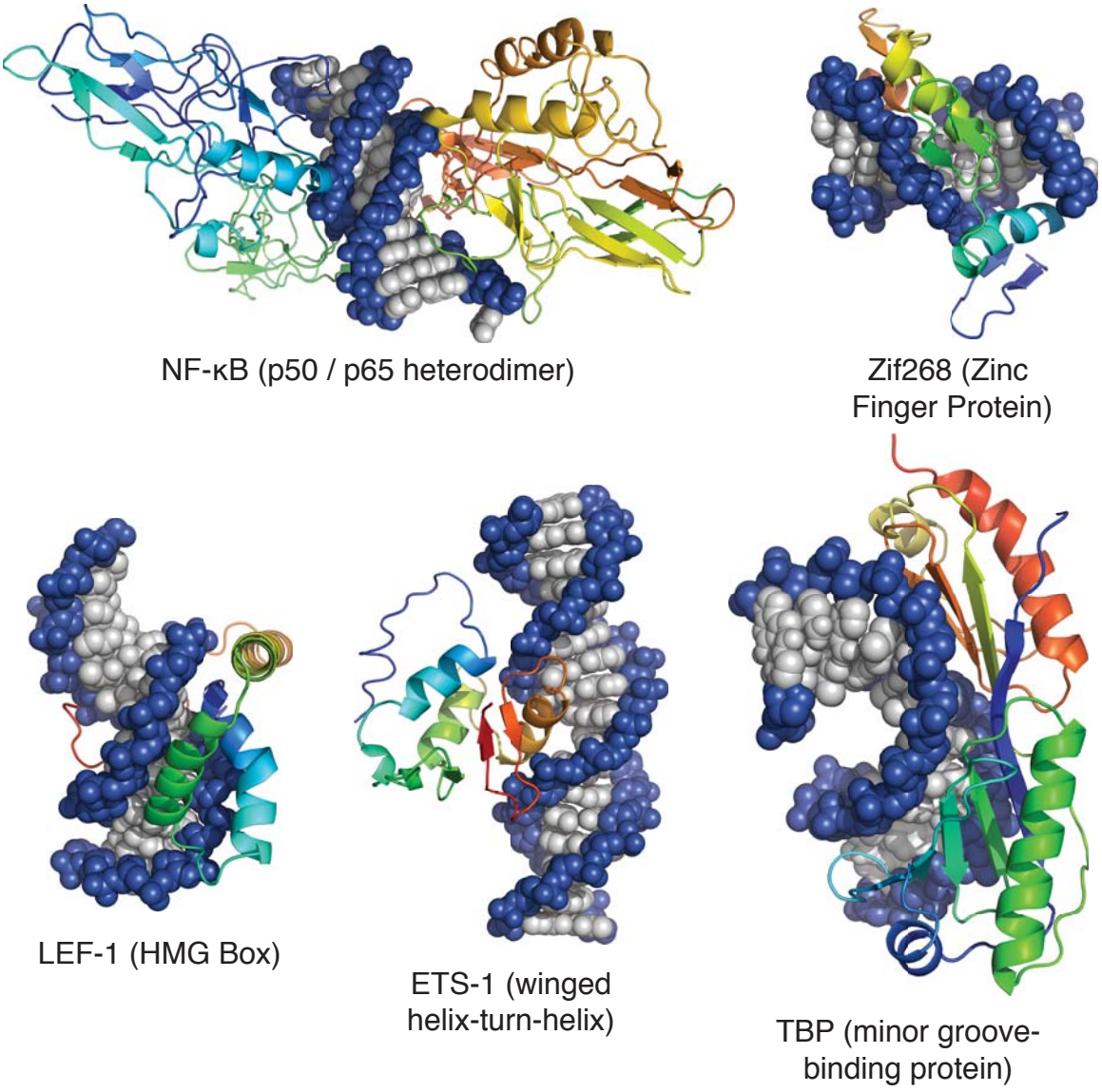

Figure 1.2. X-ray crystal and NMR structures of five protein–DNA complexes: NF-κB–DNA (PDB 1VKX), Zif268–DNA (PDB 1ZAA), LEF-1–DNA (PDB 2LEF), ETS-1–DNA (PDB 2STW), and TBP–DNA (PDB 1TGH)

Specificities of *in vitro* binding preferences for transcription factors have been studied by selective mutation studies to known binding sites and by SELEX (Systematic Evolution of Ligands by Exponential Enrichment), which gives rise to a preferred match site for the protein.[10–13] These *in vitro* binding data have been cataloged in both the TRANSFAC database and the JASPAR database.[14,15] More recent work has examined protein-DNA specificity by using fluorophore-labeled (using both covalent and non-covalent labeling schemes) proteins in conjunction with custom DNA microarrays to rank-order sequence preferences and extract sequence motifs.[16–19]

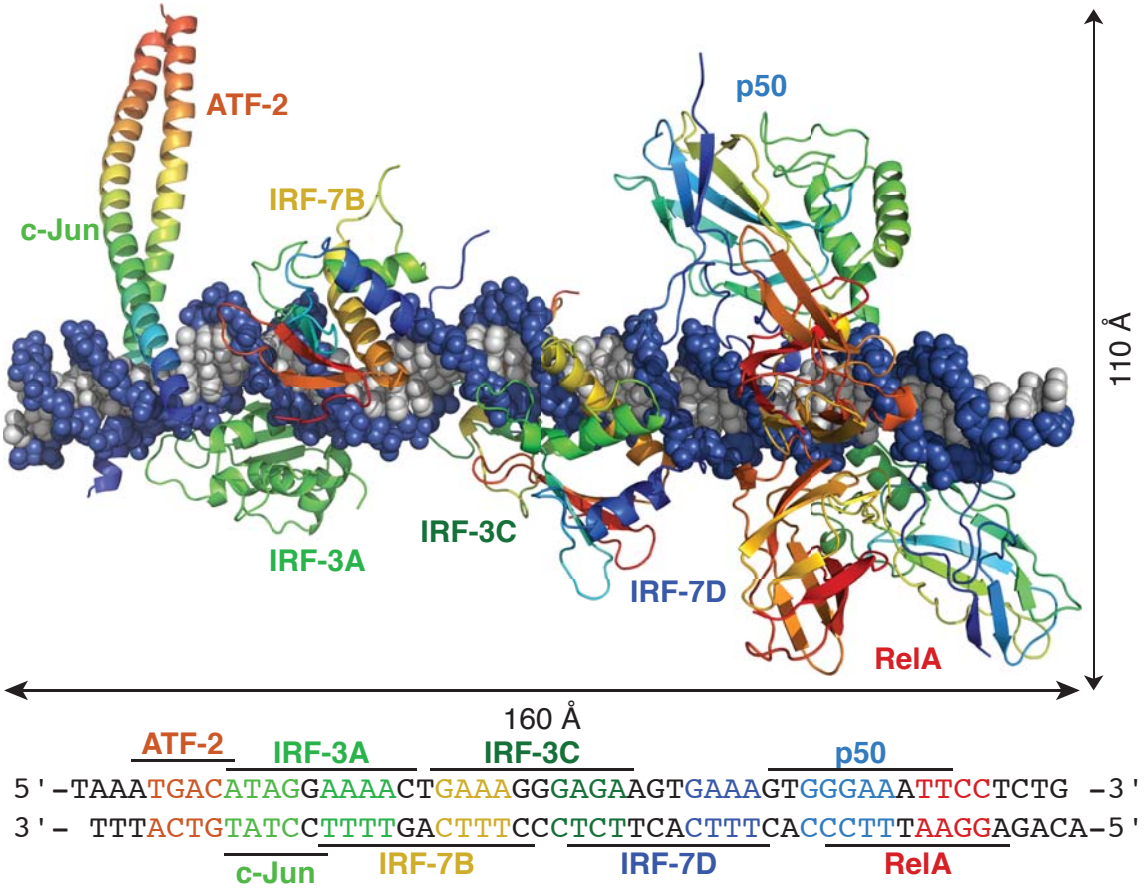

Figure 1.3. The interferon beta enhanceosome: a composite model of allosterically-driven protein–DNA recognition created from overlayed X-ray crystal structures (PDB 2O6G, 2O61)

Allosteric Recognition of DNA

The first example of allosterically modulated protein-DNA specificity on an enhancer was recently observed by Harrison, Maniatis, and co-workers, who used two crystal structures of proteins complexed with DNA (ATF-2/c-Jun, IRF-3A, IRF-7B, IRF-3C, IRF-7D, p50, and RelA) to create a model structure of the interferon-beta enhanceosome (Figure 1.3).[20] There are no protein-protein contacts between any of the proteins on this DNA sequence. Thus, it has been proposed that structural alterations to the DNA, such as widening or narrowing of the major or minor groove by individual protein-DNA interactions creates optimum binding shape and structure for other proteins, in a cooperative interaction.[20]

Higher Order DNA Structures

While discussion of DNA to this point has examined its structure in the absence and presence of proteins, the structure found inside cellular environments is far more complex. To demonstrate the layers of folding that occur as DNA is compacted inside of a cell nucleus, Figure 1.4 shows the progression from naked DNA (Figure 1.4A)[1] to the nucleosome (Figure 1.4B)[21] to the tetranucleosome (Figure 1.4C).[22] These are the known high-resolution structures. Packing continues to chromatin fibre, which has been modeled,[22] and with more structural proteins, eventually to a single chromosome. The transition of DNA to the nucleosome is facilitated by an histone octamer, consisting of two copies each of histones H2A, H2B, H3, and H4. Duplex DNA wraps twice about the histone octamer, forming a 146–147 bp nucleosome.[21] Until recently, this was the only high-resolution structural data known about the repeating unit in chromatin packing. An X-ray crystal structure of a tetranucleosome solved at 9 Å resolution answered the long-standing question of how four nucleosomes would pack together.[22]

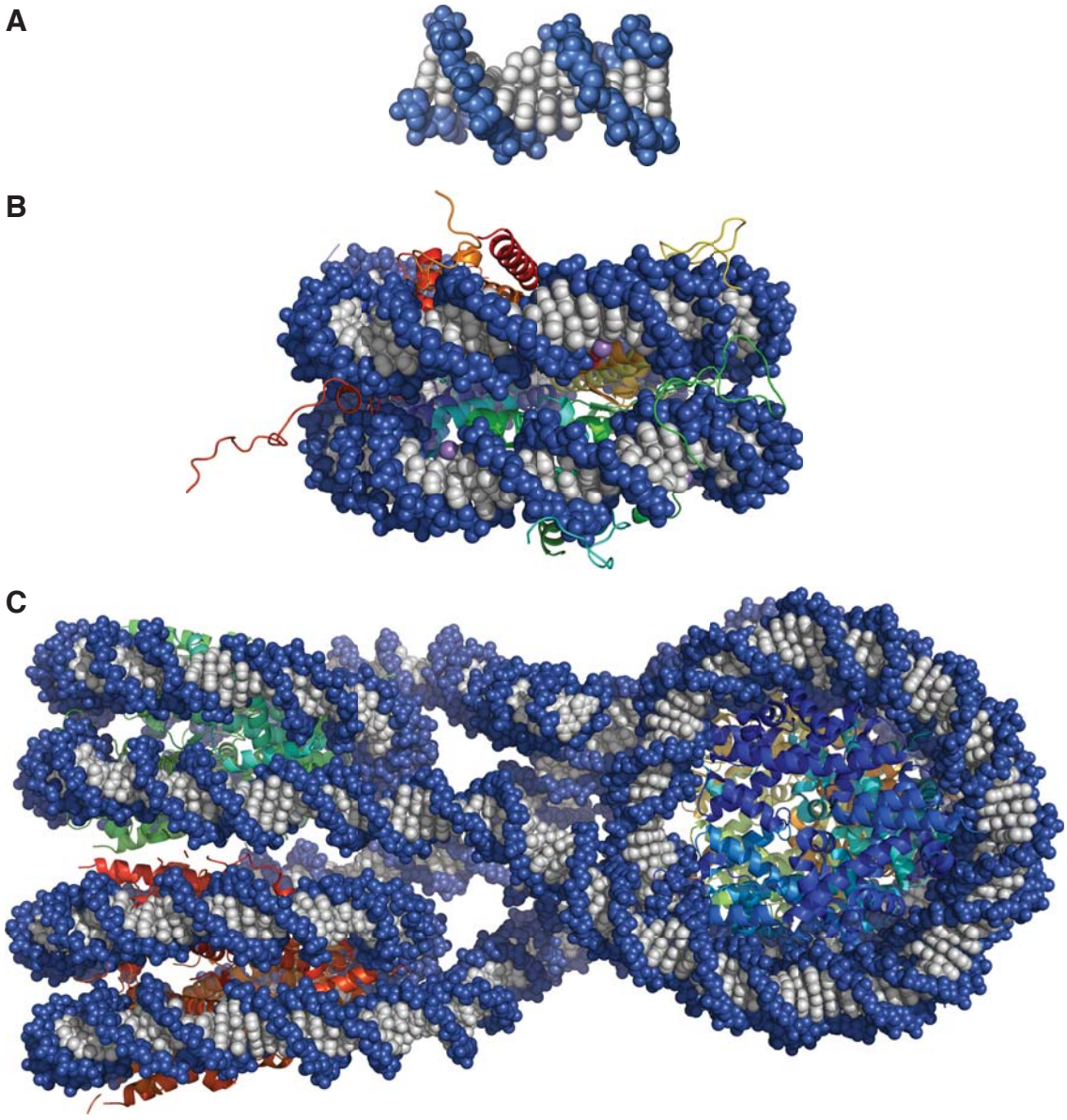

Figure 1.4. Known X-ray Crystal Structures Demonstrating Higher-order DNA Packing. a) X-ray crystal structure of double-stranded DNA (PDB 1BNA). b) X-ray crystal structure of 147 bp nucleosome core particle (PDB 1KX5). c) X-ray crystal structure of tetranucleosome, showing how nucleosomes pack (PDB 1ZBB)

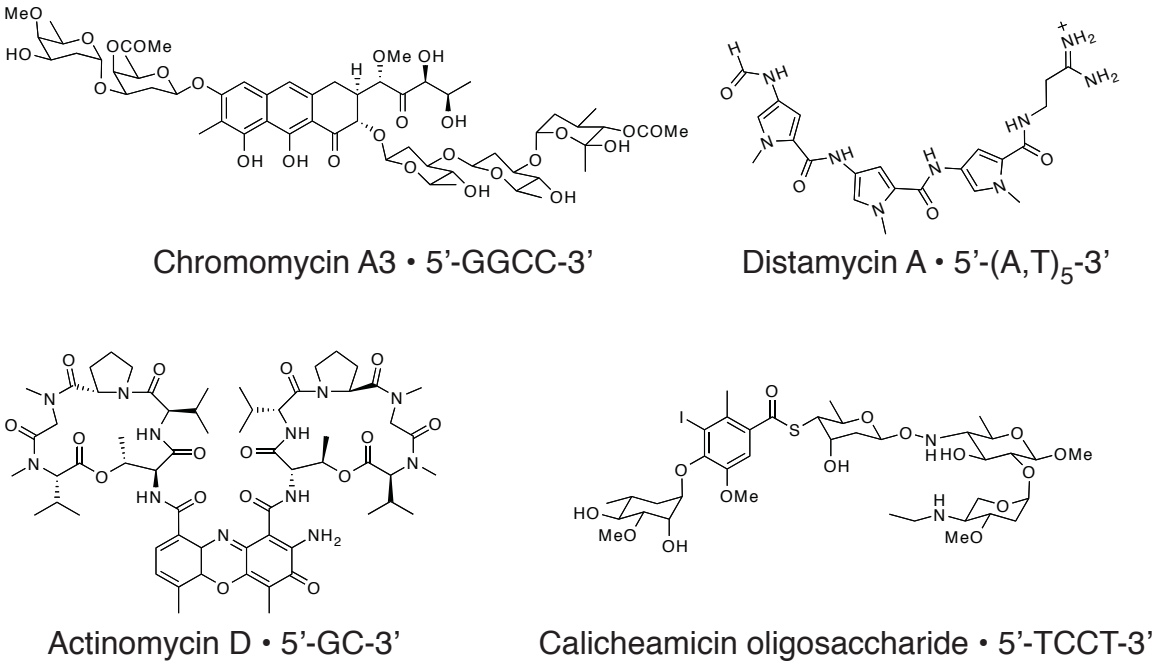

Figure 1.5. Natural products that recognize DNA: chromomycin, distamycin, actinomycin D, and calicheamicin oligosaccharide

Natural Products that Recognize DNA

In addition to the nuclear proteins that recognize and bind DNA, there are numerous natural products that bind DNA in a sequence-specific fashion. Four are shown in Figure 1.5: chromomycin, distamycin, actinomycin D, and calicheamicin oligosaccharide. Chromomycin recognizes the minor groove of DNA, targets the sequence 5'-GGCC-3,' and binds in a 2:1 ligand:DNA stoichiometry. Chromomycin is believed to be biologically active by interfering with replication and transcription.[23] Actinomycin D intercalates DNA preferentially at 5'-GC-3' sequences in a 1:1 ligand:DNA stoichiometry. It has been used as a chemotherapeutic and is known to inhibit transcription and potentially DNA replication as well.[24,25] Calicheamicin oligosaccharide binds the DNA minor groove as a monomer and recognizes 5'-TCCT-3.'[26]

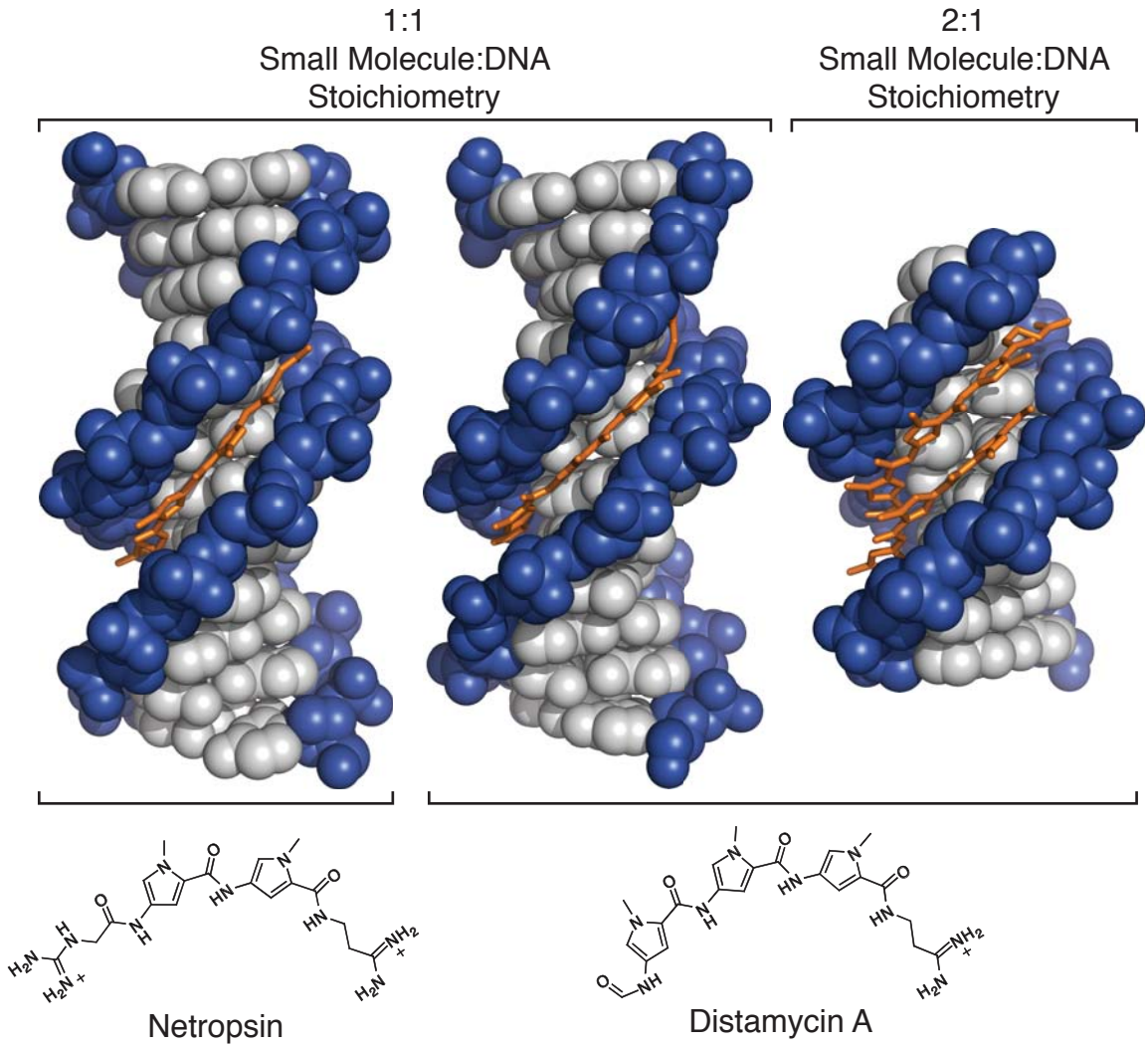

Figure 1.6. X-ray crystal structures showing the molecular recognition of DNA by netropsin (PDB 6BNA) and distamycin (PDB 2DND in a 1:1 complex with DNA and PDB 378D in a 2:1 complex with DNA), both oligopyrrole natural products

Molecular Recognition of DNA by Distamycin and Netropsin

Distamycin and netropsin are both low molecular weight oligomers of *N*-methylpyrrole carboxamides, with distamycin containing three monomer units and netropsin containing two.[27,28] X-ray crystal structures of netropsin and distamycin are shown in Figure 1.6.[27,29–31] Netropsin and distamycin each recognize A,T tracts of DNA. Netropsin is known to bind in a 1:1 ligand:DNA complex,[29] whereas distamycin can bind both in a 1:1 and 2:1 ligand:DNA stoichiometry.[30,31] The positively charged tails at the N- and C- termini of netropsin likely prevent 2:1 binding stoichiometry.

Binding in 1:1 and 2:1 ligand:DNA stoichiometries alters the width and depth of the minor groove of DNA. In the 1:1 ligand:DNA binding cases, the minor groove of DNA narrows and deepens upon ligand binding.[27,29,30] In the 2:1 ligand:DNA binding case, distamycin binds as an antiparallel dimer and widens the minor groove. The hydrogen bonding patterns present in the minor groove are presented more closely to the distamycin, making a shallower groove.[31] Through the X-ray crystal structures of these ligands, it was originally suggested that the minor groove-protruding exocyclic amine of guanine in G·C base pairs may be accommodated by utilizing *N*-methylimidazole in place of *N*-methylpyrrole.[27,29] This substitution[32–34] lead to the beginnings of a pairing code for binding of synthetically modified distamycin-like molecules, which have been called polyamides.[35,36]

Polyamide Recognition of the DNA Minor Groove

The incorporation of *N*-methylimidazole (Im) into a distamycin-like polymer: Im-Py-Py-Dp yielded not a 5'-SWW-3' (S = G,C; W = A,T) recognition sequence but rather 5'-WGWCW-3,' from which it was proposed that a 2:1 ligand:DNA binding stoichiometry could account for the observation.[32,33,35] These side-by-side minor groove ring pairings would form the basis for recognition of all four DNA base pairs. G·C, C·G, and A·T/T·A could be targeted using *N*-methylimidazole (Im) and *N*-methylpyrrole ligands (Py) bound side-by-side. When Im was adjacent to Py (Im / Py), G·C was read. Py / Im reads C·G, and Py / Py reads A·T or T·A. The specificity problem between A·T and T·A minor groove recognition was soon resolved with the introduction of the *N*-methyl-3-hydroxypyrrole monomer (Hp). In this case, Hp / Py reads T·A, while Py / Hp reads A·T.[37] When lengthening oligomers to read more base pairs, it was hypothesized that the polyamides were overcurved relative to the minor groove of DNA. Beta-alanine (β) was introduced as a substitute for Py that enables the curvature of the polyamide to be reset to better align with longer sequences of DNA, while maintaining the same recognition properties as

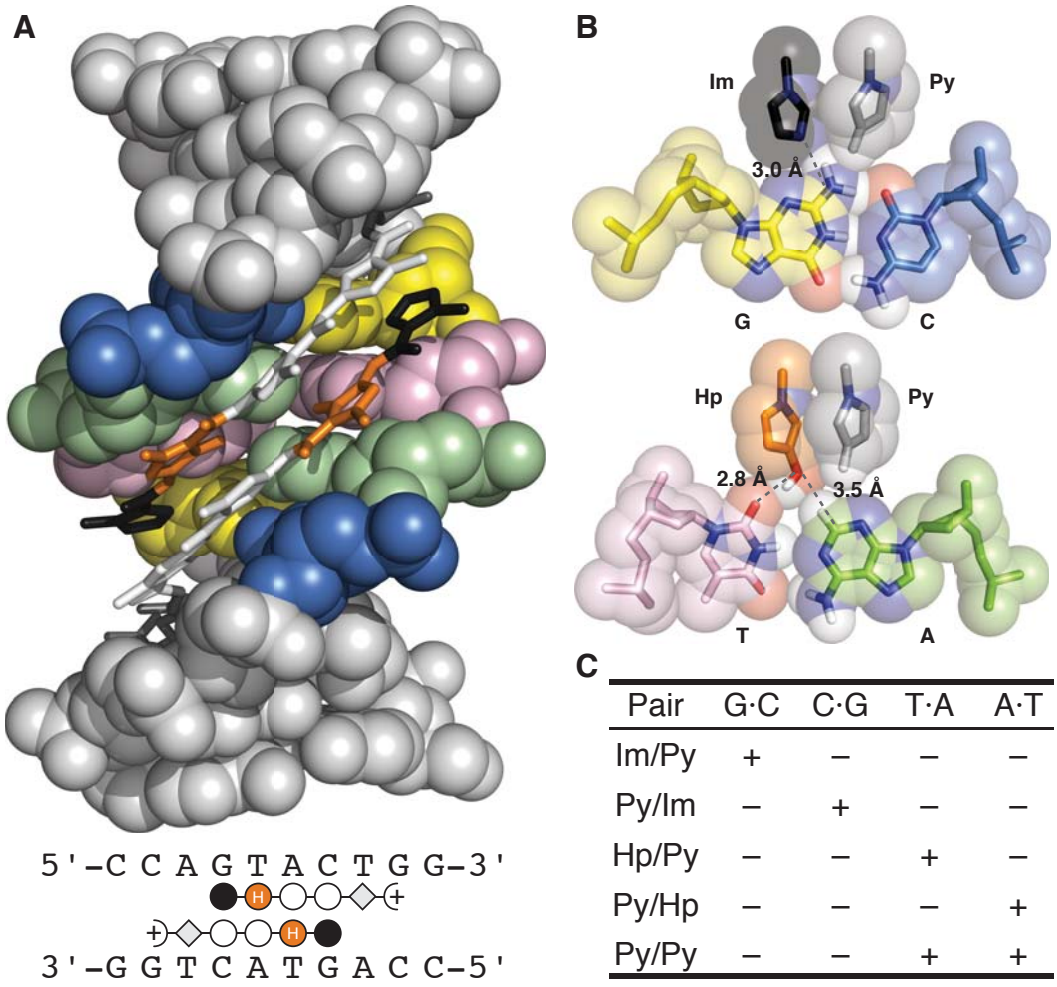

C

Pair	G·C	C·G	T·A	A·T
Im/Py	+	–	–	–
Py/Im	–	+	–	–
Hp/Py	–	–	+	–
Py/Hp	–	–	–	+
Py/Py	–	–	+	+

Figure 1.7. Recognition of all four base pairs of DNA by designed ligands based on the natural product distamycin. a) X-ray crystal structure of a 2:1 ligand:DNA decamer complex bound by the polyamide ligand Im-Hp-Py-Py-*β*-Dp (PDB 407D). Filled circles represent Im; orange circles with white H, Hp; hollow circles, Py; greyed diamonds, *β*; and half-circle with plus sign, Dp. b) Putative hydrogen-bond contacts made between polyamide monomers and individual base pairs. c) Polyamide pairing code for minor groove recognition of duplex DNA. A "+" denotes a favored interaction, and a "–" denotes a disfavored interaction.

Py.[38,39] Each of these monomers is shown in Figure 1.9B.

X-ray crystallography enabled the full structural understanding of DNA minor-groove recognition by polyamides, first for the basis for the G·C specific recognition[40] and then for A·T specific recognition (Figure 1.7).[41] The 2:1 binding polyamides generally orient themselves from N-terminus to C-terminus relative to DNA read 5' to 3.'[42]

While the 2:1 binding stoichiometry enabled all four base pairs to be read, linear beta-

A

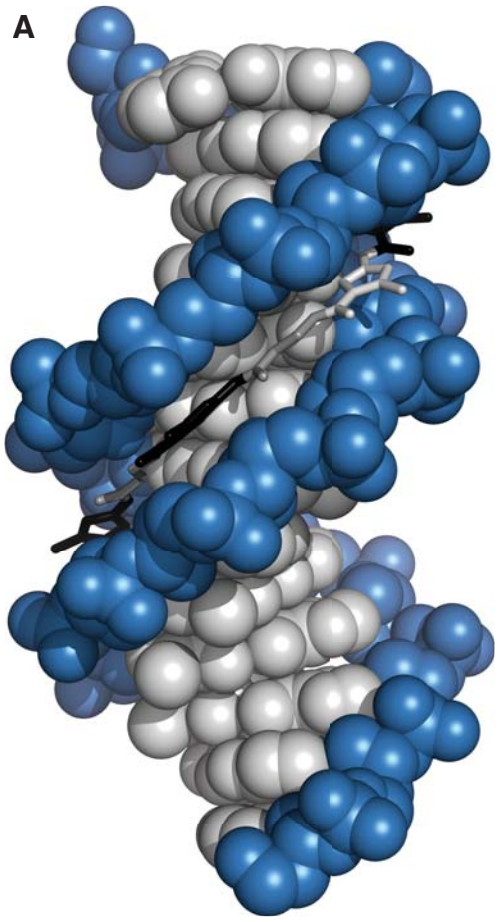

B

Ring	G·C	C·G	T·A	A·T
Im	+	+	+	+
Py	–	–	+	+
β	–	–	+	+
Hp	–	–	–	+

Figure 1.8. Molecular recognition of narrow, minor groove DNA tracts by linear beta-alanine linked polyamides. a) Average NMR structure of Im-Py-*β*-Im-*β*-Im-Py-*β*-Dp (PDB 1LEJ). In the ball-and-stick polyamide structure, filled circles represent Im, hollow circles Py, greyed diamonds β, and half-circle with a plus sign, Dp. b) Observed specificity of polyamide monomers in a 1:1 polyamide:DNA complex. A "+" indicates a favored interaction, and a "–" indicates a disfavored interaction.

alanine linked (*β*-linked) polyamides enable the targeting of narrow minor groove tracts, typically purine-rich strands of DNA, such as 5'-AAAGAGAAG-3' in a 1:1 ligand:DNA stoichiometry (Figure 1.8).[43–45] Im, Py, *β*, and Hp have been studied in the linear *β*-linked

Figure 1.9. DNA minor groove hydrogen bond recognition elements. a) Minor groove hydrogen bond donors and acceptors for all four base pairs. b) Monomers found in polyamides. The ball-and-stick symbols as well as abbreviations are listed below the chemical structures. c) Potential hydrogen bonds formed between 5'-WTACGW-3' and a hairpin polyamide, Ct-Py-Py-Im-(*R*)^{H2N}γ-Py-Im-Py-Py-*β*-Dp. d) Potential hydrogen bonds formed between 5'-AAGAAGAAG-3' and a linear *β*-linked polyamide, Im-Py-*β*-Im-Py-*β*-Im-*β*-Dp

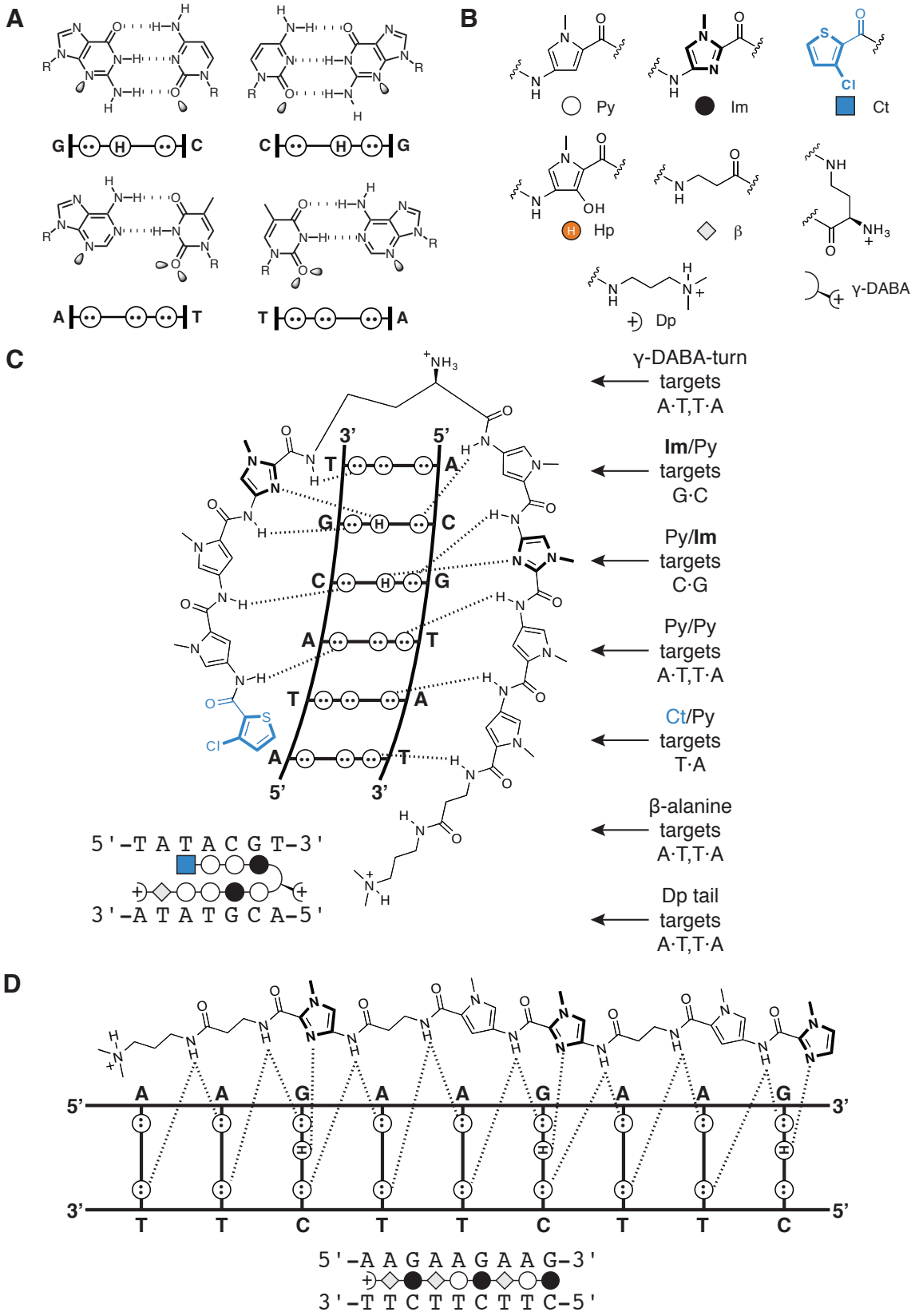
A
B
Py
Im
Ct
Hp
β
γ-DABA
Dp
C
γ-DABA-turn
targets
A·T,T·A
Im/Py
targets
G·C
Py/Im
targets
C·G
Py/Py
targets
A·T,T·A
Ct/Py
targets
T·A
β-alanine
targets
A·T,T·A
Dp tail
targets
A·T,T·A
5'-T A T A C G T-3'
3'-A T A T G C A-5'
D
5'-A A G A A G A A G-3'
3'-T T C T T C T T C-5'

polyamide class—Im is degenerate for all four base pairs, Py and *β* prefer W (A,T) over S (G,C), and Hp prefers A·T in the homo-purine strand, although at lower binding affinity.[44] The linear *β*-linked polyamides orient themselves from N-terminus to C-terminus relative to DNA read from 3' to 5' on the purine-rich strand of DNA.[43–45] The NMR structure of a linear *β*-linked polyamide in complex with DNA has been solved.[45] Figure 1.9D shows an example of the hydrogen bond recognition between a polypurine tract of DNA and a linear *β*-linked polyamide that targets 5'-AAGAAGAAG-3.'

Polyamides that are currently used are generally derived from 2:1 binding class and less frequently from the 1:1 binding class. To prepay the entropic costs of polyamide dimerization, a hairpin "turn-unit," γ-aminobutyric acid, was used to covalently attach the two polyamide oligomers in an antiparallel fashion (Figure 1.9C).[46] This covalent modification allowed subnanomolar concentrations of ligands to target 5'-WGTACW-3.'[47] Other covalent linkages have been utilized: the H-pin polyamide motif,[48] the U-pin polyamide motif,[49] and the cyclic polyamide motif,[50] although the hairpin motif has been most widely studied. Because hairpin polyamides occasionally align N-terminus to C-terminus against DNA read 3' to 5,' the γ-aminobutyric acid linker was modified to an (*R*)-2,4-diaminobutyric acid, which increased binding affinity and enforced an N to C terminus alignment with DNA read 5' to 3.'[42,51] Hairpin polyamides typically are constructed from eight aromatic heterocycles, or "rings," and target six base pairs.

Recent work has completed a library of all possible eight-ring hairpin polyamides that have an N-terminal *N*-methylimidazole monomer.[52] Much of the scope of known sequences that hairpin polyamides can target is shown in Table 1.1.[52]

Table 1.1. Imidazole-capped eight-ring polyamides recognize a diverse library of DNA sequences

General (5'→3')	Polyamide	K_a (M^{-1})	Sequence context
1 WW**G**WWWW		3×10^{9}	5'-TA**G**TATT-3'
2 WW**GG**WWW		5×10^{8}	5'-CT**GG**TTA-3'
3 WW**G**W**G**WW		4×10^{9}	5'-TA**G**T**G**AA-3'
4 WW**G**WW**G**W		9×10^{9}	5'-TA**G**TA**G**T-3'
5 WW**G**WW**C**W		3×10^{10}	5'-TA**G**TA**C**T-3'
6 WW**G**W**C**WW		2×10^{9}	5'-GA**G**T**C**TA-3'
7 WW**GC**WWW		5×10^{9}	5'-AT**GC**AAA-3'
8 WW**GGG**WW		3×10^{8}	5'-AA**GGG**AA-3'
9 WW**GG**W**G**W		1×10^{10}	5'-TA**GG**T**G**T-3'
10 WW**GG**W**C**W		1×10^{10}	5'-AT**GG**T**C**A-3'
11 WW**GGC**WW		4×10^{8}	5'-AA**GGC**AT-3'
12 WW**G**W**GG**W		4×10^{10}	5'-TA**G**T**GG**T-3'
13 WW**G**W**GC**W		2×10^{9}	5'-AT**GAGC**T-3'
14 WW**GCG**WW		2×10^{9}	5'-AT**GCG**TA-3'
15 WW**GC**W**G**W		2×10^{9}	5'-TA**GCAG**T-3'
16 WW**GC**W**C**W		9×10^{9}	5'-AT**GCTC**A-3'
17 WW**G**W**CG**W		1×10^{10}	5'-AT**GACG**T-3'
18 WW**G**W**CC**W		2×10^{9}	5'-TA**GACC**A-3'
19 WW**GCC**WW		7×10^{8}	5'-AT**GCC**TA-3'
20 WW**GGGG**W		2×10^{8}	5'-GA**GGGG**T-3'
21 WW**GCGG**W		9×10^{8}	5'-AT**GCGG**T-3'
22 WW**GGCG**W		2×10^{8}	5'-CA**GGCG**T-3'
23 WW**GGGC**W		1×10^{8}	5'-CT**GGGC**A-3'
24 WW**GCCG**W		2×10^{9}	5'-AT**GCCG**T-3'
25 WW**GGCC**W		9×10^{9}	5'-AT**GGCC**A-3'
26 WW**GCGC**W		3×10^{9}	5'-AT**GCGC**A-3'
27 WW**GCCC**W		1×10^{9}	5'-AT**GCCC**A-3'

Polyamides for Control of Gene Expression

The selective modulation of gene networks by programmable oligomers that specify short DNA sequences holds promise for new approaches to molecular medicine. The DNA minor groove-binding-polyamides have been utilized in several instances to modulate gene expression in cell culture (Figure 1.10). This ability did not come without three key studies on nuclear localization of polyamides in live cell culture.[53,54] Hypoxia inducible factor 1α (HIF-1α) is a transcription factor that drives the expression of vascular endothelial growth factor (VEGF), a gene responsible for the vascularization of tumors. HIF-1α targets the Hypoxic Response Element (HRE) consensus sequence, 5'-TACGTG-3,' a subset of which is recognized by Ct-Py-Py-Im-(*R*)-^{H2N}γ-Py-Im-Py-Py-Dp-IPA (**1**). HeLa and U251 cells have been dosed with **1** and induced with deferoxamine (DFO). HIF-1α-modulated genes have much lower inductions in the presence of polyamide **1**. In the presence of a polyamide that does not bind the HRE (**2**), a statistically insignificant change in VEGF expression occurs. Microarray experiments have shown that polyamide **1** downregulates a subset of genes upregulated by DFO induction. Furthermore, chromatin immunoprecipitation (ChIP) experiments demonstrated a reduced occupancy of HIF-1α at the VEGF HRE in the presence of polyamide **1**, suggesting that the polyamide acts in a sequence programmed, specific manner.[55–57]

Gene expression regulated by androgen receptor (AR) is critical in the development and progression of prostate cancer. Prostate specific antigen (PSA) is a well-studied marker gene that correlates with the presence of prostate cancer. Androgen receptor binds as a homodimer to the androgen response element (ARE), 5'-GGTACAnnnTGTTCT-3,' a sequence which can readily be targeted by an eight-ring Py/Im hairpin polyamide, Im-Py-Py-Py-(*R*)-^{H2N}γ-Im-Py-Py-Py-Dp-IPA (**3**). In the presence of dihydrotestosterone (DHT) induction, LNCaP cells dosed with polyamide **3** exhibit suppressed PSA induction. A mismatch control polyamide targeting 5'-WGWCGW-3' (Im-Py-Py-Im-(*R*)-^{H2N}γ-Py-Im-Py-Py-Dp-IPA, **4**) has a much smaller effect on mRNA transcript levels of PSA. Microarray

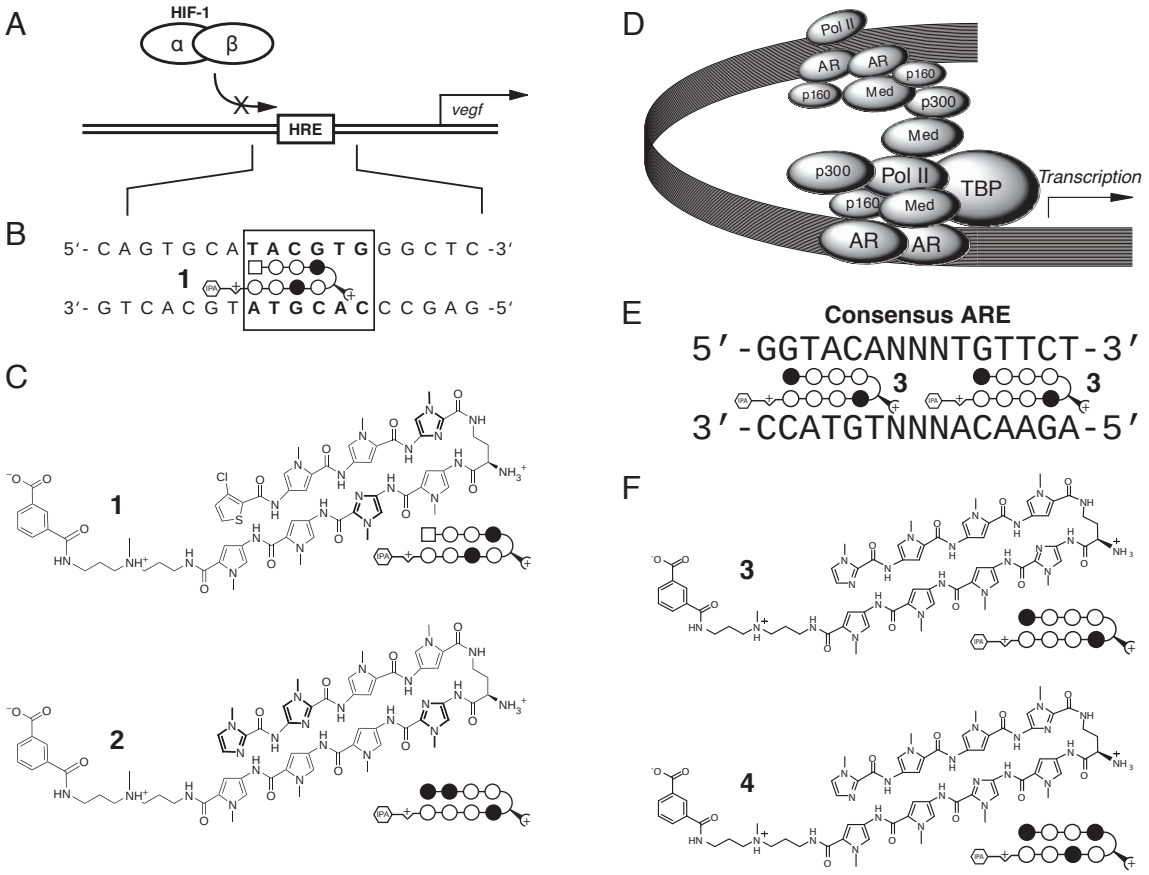

Figure 1.10. Examples of polyamides used for modulation of gene expression in living cell culture. a) Structure of VEGF promoter showing inhibition of HRE binding by the HIF-1α/HIF-1*β* dimer inhibits gene transcription. b) HRE enhancer binding sequence shown with match polyamide **1**. c) Match (**1**) and mismatch (**2**) polyamides utilized to target the HRE. d) Model of the androgen receptor transcription complex. e) Consensus ARE targeted by match polyamide **3**. f) Match (**3**) and mismatch (**4**) polyamides utilized to target the ARE.

experiments on **3** and **4** showed **3** to disrupt induction by DHT for a subset of the DHT-induced genes. ChIP experiments on **3** and **4** again suggest the disruption of a protein-DNA interface as a potential mechanism for polyamide activity.[58]

Scope of this Thesis

In Chapter 2, we explore the use of a linear *β*-linked polyamide for upregulation of frataxin expression in cell culture. We also explore binding properties of other linear *β*-linked polyamides by DNase I footprint titrations (also in Appendix B).[59] In Chapter 3, we utilize DNA microarrays to examine the binding preferences of the linear *β*-linked

polyamide that modulated frataxin expression in Chapter 2. We also examine the binding preferences of the hairpin polyamide utilized to disrupt HIF-1α binding (**1**). Because the microarrays necessitate a fluorophore label, we study the ramifications of different labeling positions, terminal and internal. We find that the polyamide core, and not the label position, drives DNA binding specificity of the polyamide (Appendix C). Finally, in Chapter 4, we move from *in vitro* preferences of synthetic ligands to *in vivo* preferences of protein transcription factors. We study androgen receptor binding preferences in a living cell (LNCaP cells) using ChIP-Seq, chromatin immunoprecipitation followed by high-throughput DNA sequencing. We map the genome-wide binding landscape of androgen receptor. This marks a first step toward creating a negative occupancy map of genomic regions polyamide **3** prevents androgen receptor binding.

References

(1) Drew, H. R.; Wing, R. M.; Takano, T.; Broka, C.; Tanaka, S.; Itakura, K.; Dickerson, R. E. *Proc. Natl. Acad. Sci. U. S. A.* **1981**, *78*, 2179–83.

(2) Dickerson, R. E.; Drew, H. R.; Conner, B. N.; Wing, R. M.; Fratini, A. V.; Kopka, M. L. *Science* **1982**, *216*, 475–85.

(3) Consortium, I. H. G. S. *Nature* **2004**, *431*, 931–45.

(4) Pavletich, N. P.; Pabo, C. O. *Science* **1991**, *252*, 809–17.

(5) Werner, M. H.; Clore, G. M.; Fisher, C. L.; Fisher, R. J.; Trinh, L.; Shiloach, J.; Gronenborn, A. M. *J. Biomol. NMR* **1997**, *10*, 317–28.

(6) Chen, F. E.; Huang, D. B.; Chen, Y. Q.; Ghosh, G. *Nature* **1998**, *391*, 410–3.

(7) Love, J. J.; Li, X.; Case, D. A.; Giese, K.; Grosschedl, R.; Wright, P. E. *Nature* **1995**, *376*, 791–5.

(8) Juo, Z. S.; Chiu, T. K.; Leiberman, P. M.; Baikalov, I.; Berk, A. J.; Dickerson, R. E. *J. Mol. Biol.* **1996**, *261*, 239–54.

(9) Jamieson, A. C.; Miller, J. C.; Pabo, C. O. *Nat. Rev. Drug Discov.* **2003**, *2*, 361–8.

(10) Roulet, E.; Busso, S.; Camargo, A. A.; Simpson, A. J.; Mermod, N.; Bucher, P. *Nat. Biotechnol.* **2002**, *20*, 831–5.

(11) Klug, S. J.; Famulok, M. *Mol. Biol. Rep.* **1994**, *20*, 97–107.

(12) Roulet, E.; Bucher, P.; Schneider, R.; Wingender, E.; Dusserre, Y.; Werner, T.; Mermod, N. *J. Mol. Biol.* **2000**, *297*, 833–48.

(13) Fields, D. S.; He, Y.; Al-Uzri, A. Y.; Stormo, G. D. *J. Mol. Biol.* **1997**, *271*, 178–94.

(14) Wingender, E.; Dietze, P.; Karas, H.; Knuppel, R. *Nucleic Acids Res.* **1996**, *24*, 238–41.

(15) Sandelin, A.; Alkema, W.; Engstrom, P.; Wasserman, W. W.; Lenhard, B. *Nucleic Acids Res.* **2004**, *32*, D91–4.

(16) Berger, M. F.; Philippakis, A. A.; Qureshi, A. M.; He, F. S.; Estep, P. W., 3rd; Bulyk,

M. L. *Nat. Biotechnol.* **2006**, *24*, 1429–35.

(17) Bulyk, M. L.; Gentalen, E.; Lockhart, D. J.; Church, G. M. *Nat. Biotechnol.* **1999**, *17*, 573–7.

(18) Bulyk, M. L.; Huang, X.; Choo, Y.; Church, G. M. *Proc. Natl. Acad. Sci. U. S. A.* **2001**, *98*, 7158–63.

(19) Badis, G.; Chan, E. T.; van Bakel, H.; Pena-Castillo, L.; Tillo, D.; Tsui, K.; Carlson, C. D.; Gossett, A. J.; Hasinoff, M. J.; Warren, C. L.; Gebbia, M.; Talukder, S.; Yang, A.; Mnaimneh, S.; Terterov, D.; Coburn, D.; Li Yeo, A.; Yeo, Z. X.; Clarke, N. D.; Lieb, J. D.; Ansari, A. Z.; Nislow, C.; Hughes, T. R. *Mol. Cell* **2008**, *32*, 878–87.

(20) Panne, D.; Maniatis, T.; Harrison, S. C. *Cell* **2007**, *129*, 1111–23.

(21) Davey, C. A.; Sargent, D. F.; Luger, K.; Maeder, A. W.; Richmond, T. J. *J. Mol. Biol.* **2002**, *319*, 1097–113.

(22) Schalch, T.; Duda, S.; Sargent, D. F.; Richmond, T. J. *Nature* **2005**, *436*, 138–41.

(23) Hou, M. H.; Robinson, H.; Gao, Y. G.; Wang, A. H. *Nucleic Acids Res.* **2004**, *32*, 2214–22.

(24) Kamitori, S.; Takusagawa, F. *J. Am. Chem. Soc.* **1994**, *116*, 4154–4165.

(25) Hou, M. H.; Robinson, H.; Gao, Y. G.; Wang, A. H. *Nucleic Acids Res.* **2002**, *30*, 4910–7.

(26) Bifulco, G.; Galeone, A.; Nicolaou, K. C.; Chazin, W. J.; Gomez-Paloma, L. *J. Am. Chem. Soc.* **1998**, *120*, 7183–7191.

(27) Kopka, M. L.; Yoon, C.; Goodsell, D.; Pjura, P.; Dickerson, R. E. *Proc. Natl. Acad. Sci. U. S. A.* **1985**, *82*, 1376–80.

(28) Arcamone, F.; Penco, S.; Orezzi, P.; Nicolella, V.; Pirelli, A. *Nature* **1964**, *203*, 1064–5.

(29) Kopka, M. L.; Yoon, C.; Goodsell, D.; Pjura, P.; Dickerson, R. E. *J. Mol. Biol.* **1985**, *183*, 553–63.

(30) Coll, M.; Frederick, C. A.; Wang, A. H.; Rich, A. *Proc. Natl. Acad. Sci. U. S. A.*

1987, *84*, 8385–9.

(31) Mitra, S. N.; Wahl, M. C.; Sundaralingam, M. *Acta Crystallogr.* **1999**, *D55*, 602–9.

(32) Mrksich, M.; Wade, W. S.; Dwyer, T. J.; Geierstanger, B. H.; Wemmer, D. E.; Dervan, P. B. *Proc. Natl. Acad. Sci. U. S. A.* **1992**, *89*, 7586–90.

(33) Wade, W. S.; Mrksich, M.; Dervan, P. B. *J. Am. Chem. Soc.* **1992**, *114*, 8783–8794.

(34) Geierstanger, B. H.; Mrksich, M.; Dervan, P. B.; Wemmer, D. E. *Science* **1994**, *266*, 646–50.

(35) Dervan, P. B. *Bioorg. Med. Chem.* **2001**, *9*, 2215–35.

(36) Dervan, P. B.; Edelson, B. S. *Curr. Opin. Struct. Biol.* **2003**, *13*, 284–99.

(37) White, S.; Szewczyk, J. W.; Turner, J. M.; Baird, E. E.; Dervan, P. B. *Nature* **1998**, *391*, 468–71.

(38) Trauger, J. W.; Baird, E. E.; Mrksich, M.; Dervan, P. B. *J. Am. Chem. Soc.* **1996**, *118*, 6160–6166.

(39) Turner, J. M.; Swalley, S. E.; Baird, E. E.; Dervan, P. B. *J. Am. Chem. Soc.* **1998**, *120*, 6219–6226.

(40) Kielkopf, C. L.; Baird, E. E.; Dervan, P. B.; Rees, D. C. *Nat. Struct. Biol.* **1998**, *5*, 104–9.

(41) Kielkopf, C. L.; White, S.; Szewczyk, J. W.; Turner, J. M.; Baird, E. E.; Dervan, P. B.; Rees, D. C. *Science* **1998**, *282*, 111–5.

(42) White, S.; Baird, E. E.; Dervan, P. B. *J. Am. Chem. Soc.* **1997**, *1997*, 8756–8765.

(43) Dervan, P. B.; Urbach, A. R. In *Essays in Contemporary Chemistry*; Quinkert, G., Kisakürek, M. V., Eds.; Verlag Helvetica Chimica Acta: Zurich, 2000, p 327–339.

(44) Urbach, A. R.; Dervan, P. B. *Proc. Natl. Acad. Sci. U. S. A.* **2001**, *98*, 4343–8.

(45) Urbach, A. R.; Love, J. J.; Ross, S. A.; Dervan, P. B. *J. Mol. Biol.* **2002**, *320*, 55–71.

(46) Mrksich, M.; Parks, M. E.; Dervan, P. B. *J. Am. Chem. Soc.* **1994**, *116*, 7983–7988.

(47) Trauger, J. W.; Baird, E. E.; Dervan, P. B. *Nature* **1996**, *382*, 559–61.

(48) Greenberg, W. A.; Baird, E. E.; Dervan, P. B. *Chem.-Eur. J.* **1998**, *4*, 796–805.

(49) Heckel, A.; Dervan, P. B. *Chem.-Eur. J.* **2003**, *9*, 3353–66.

(50) Cho, J.; Parks, M. E.; Dervan, P. B. *Proc. Natl. Acad. Sci. U. S. A.* **1995**, *92*, 10389–92.

(51) Herman, D. M.; Baird, E. E.; Dervan, P. B. *J. Am. Chem. Soc.* **1998**, *120*, 1382–1391.

(52) Hsu, C. F.; Phillips, J. W.; Trauger, J. W.; Farkas, M. E.; Belitsky, J. M.; Heckel, A.; Olenyuk, B. Z.; Puckett, J. W.; Wang, C. C.; Dervan, P. B. *Tetrahedron* **2007**, *63*, 6146–6151.

(53) (a) Belitsky, J. M.; Leslie, S. J.; Arora, P. S.; Beerman, T. A.; Dervan, P. B. *Bioorg. Med. Chem.* **2002**, *10*, 3313–8. (b) Best, T. P.; Edelson, B. S.; Nickols, N. G.; Dervan, P. B. *Proc. Natl. Acad. Sci. U. S. A.* **2003**, *100*, 12063–8.

(54) Edelson, B. S.; Best, T. P.; Olenyuk, B.; Nickols, N. G.; Doss, R. M.; Foister, S.; Heckel, A.; Dervan, P. B. *Nucleic Acids Res.* **2004**, *32*, 2802–18.

(55) Olenyuk, B. Z.; Zhang, G. J.; Klco, J. M.; Nickols, N. G.; Kaelin, W. G., Jr.; Dervan, P. B. *Proc. Natl. Acad. Sci. U. S. A.* **2004**, *101*, 16768–73.

(56) Nickols, N. G.; Jacobs, C. S.; Farkas, M. E.; Dervan, P. B. *ACS Chem. Biol.* **2007**, *2*, 561–71.

(57) Nickols, N. G.; Jacobs, C. S.; Farkas, M. E.; Dervan, P. B. *Nucleic Acids Res.* **2007**, *35*, 363–70.

(58) Nickols, N. G.; Dervan, P. B. *Proc. Natl. Acad. Sci. U. S. A.* **2007**, *104*, 10418–23.

(59) Trauger, J. W.; Dervan, P. B. *Methods Enzymol.* **2001**, *340*, 450–66.

Chapter 2

Linear β-linked Polyamides Target GAA Repeats and Alleviate Transcription Repression in Friedreich's Ataxia Cell Culture

The text of this chapter was taken in part from a manuscript co-authored with Ryan Burnett, Christian Melander, Leslie S. Son, Professor Robert D. Wells (Texas A & M Health Science Center), Professor Joel M. Gottesfeld (The Scripps Research Institute), and Professor Peter B. Dervan (California Institute of Technology).

(Burnett, R.; Melander, C.; Puckett, J. W.; Son, L. S.; Wells, R. D.; Dervan, P. B.; Gottesfeld, J. M. "DNA sequence-specific polyamides alleviate transcription inhibition associated with long GAA·TTC repeats in Friedreich's ataxia." *Proc. Natl. Acad. Sci. U. S. A.* **2006**, *103*, 11497–11502.)

Chapter 2A

DNA sequence-specific polyamides alleviate transcription inhibition associated with long GAA·TTC repeats in Friedreich's Ataxia

Abstract

The DNA abnormality found in 98% of Friedreich's ataxia (FRDA) patients is the unstable hyperexpansion of a GAA·TTC triplet repeat in the first intron of the frataxin gene. Expanded GAA·TTC repeats result in decreased transcription and reduced levels of frataxin protein in affected individuals. *β*-Alanine-linked pyrrole–imidazole polyamides bind GAA·TTC tracts with high affinity and disrupt the intramolecular DNA·DNA-associated region of the sticky-DNA conformation formed by long GAA·TTC repeats. Fluorescent polyamide-BODIPY conjugates localize in the nucleus of a lymphoid cell line derived from a FRDA patient. The synthetic ligands increase transcription of the frataxin gene in cell culture, resulting in increased levels of frataxin protein. DNA microarray analyses indicate that a limited number of genes are significantly affected in FRDA cells. Polyamides may increase transcription by altering the DNA conformation of genes harboring long GAA·TTC repeats or by chromatin opening.

Introduction

The neurodegenerative disease Friedreich's ataxia (FRDA) is caused by hyperexpansion of GAA·TTC repeats in the first intron of a nuclear gene that encodes the essential mitochondrial protein frataxin.[1–4] Normal frataxin alleles have 6–34 repeats, whereas FRDA patient alleles have 66–1,700 repeats. Intronic GAA·TTC repeats interfere with gene transcription.[5–7] Longer repeats cause a more profound frataxin deficiency and are associated with earlier onset and increased severity of the disease.[4] Biochemical studies have documented that expanded GAA·TTC repeats adopt unusual non-B DNA structures, such as triplexes, containing two purine GAA strands along with one pyrimidine TTC strand, flanking a single-stranded pyrimidine region[5,8] as well as intramolecular "sticky" DNA.[6,9–12] Long $(GAA{\cdot}TTC)_n$ repeat sequences form sticky DNA with two separate long $(GAA{\cdot}TTC)_n$ repeating tracts associated within a single closed plasmid DNA. The interaction of the two tracts requires the repeats oriented in the direct repeat orientation, negative supercoiling and the presence of divalent metal ions to stabilize the DNA·DNA-associated region.[8–10] We have demonstrated the capacity of sticky DNA to form both *in vitro*[10,13] and *in vivo*.[11–13] Triplexes and/or sticky DNA block elongation by RNA polymerase II.[5] Another study using artificial transgenes has shown that expanded GAA·TTC repeats induce repressive heterochromatin *in vivo* in a manner reminiscent of position-effect variegation.[14] This effect was augmented by coexpression of heterochromatin protein 1. Here, we address whether minor-groove DNA-binding small molecules can alleviate transcription repression of the frataxin gene.

Molecules that reverse triplex/sticky DNA and/or heterochromatin formation in the frataxin gene may increase successful elongation through expanded GAA·TTC repeats, thereby relieving the deficiency in frataxin mRNA and protein in FRDA cells.[11,14,15] Pyrrole–imidazole polyamides are cell-permeable small molecules that can be programmed to recognize a broad repertoire of DNA sequences.[16] Two classes of polyamides are well established: hairpin polyamides bind mixed-sequence DNA with high affinity and

specificity,[16,17] and linear *β*-alanine-linked polyamides are available for targeting purine tracts of DNA, such as GAGAA·TTCTC repeats.[18,19] *β*-Alanine-linked polyamides have been shown to bind GAGAA repeats in *Drosophila* satellite DNA both *in vitro* and in cytological chromosome spreads.[19] These molecules induce chromatin opening and reverse heterochromatin-mediated position-effect gene silencing when administered to *Drosophila* embryos.[19,20]

Structural studies indicate that *β*-alanine-linked polyamides bind the minor groove of canonical B DNA.[21] Given the high affinity of *β*-alanine-linked polyamides for purine tracts,[18] these molecules might act as a thermodynamic "sink" and lock GAA·TTC repeats into double-stranded B DNA. Such an event would disfavor duplex unpairing, which is necessary for formation of FRDA triplexes and sticky DNA. Although single polyamides bound within coding regions of genes do not appear to block transcription elongation,[22–24] we cannot be certain that multiple polyamides have the potential to relieve transcription repression at expanded GAA·TTC repeats. Alternatively, polyamides may relieve heterochromatin-mediated repression by opening the chromatin domain containing the frataxin gene.[20]

Results and Discussion

Targeting GAA·TTC Repeat DNA with High-Affinity Ligands.

We synthesized two *β*-alanine-linked polyamides of different length, **1** (Im-Py-*β*-Im-Py-*β*-Im-*β*-Dp, where Py is pyrrole, Im is imidazole, *β* is *β*-alanine, and Dp is dimethylaminopropylamine) to target the 9-bp site 5'-AAGAAGAAG-3' and **3** (Im-Py-*β*-Im-Py-*β*-Im-Py-*β*-Im-*β*-Dp) to target the 12-bp site 5'-AAGAAGAAGAAG-3' (Figure 2.1A). Quantitative DNase I footprinting[25] demonstrates that **1** binds to a radiolabeled PCR product containing a $(GAA{\cdot}TTC)_6$ sequence with an apparent dissociation constant (K_d) of 0.1 nM (Figure 2.2A and Table 2.1). Polyamide **3** exhibits a K_d of ≈ 3 pM in footprinting experiments performed at low DNA concentrations (Figure 2.2C, and Table

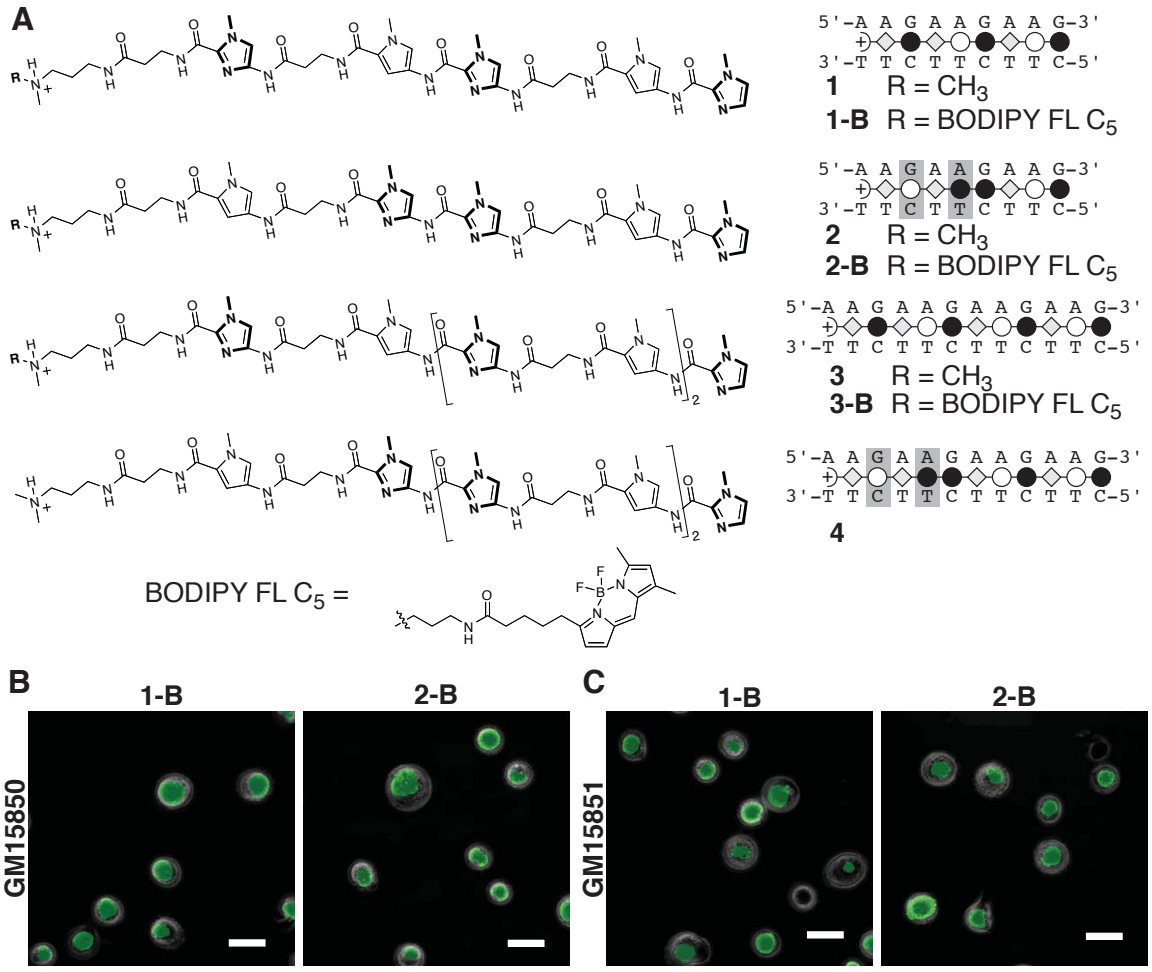

Figure 2.1. Polyamide structures, binding models and nuclear localization in cell culture. a) Structures of polyamides **1**, **2**, **3**, and **4** (R = methyl) and their BODIPY conjugates **1-B**, **2-B**, and **3-B** (R = *N*-propylbutanamide linked BODIPY FL C_5). Polyamide structures are represented schematically as binding models. Filled and open circles are Im and Py rings, respectively; diamonds are *β*-alanine; and, the semicircle with a plus sign is dimethylaminopropylamine. Linear polyamides bind in a carboxyl- to amino-terminal orientation with respect to the 5' to 3' sequence of their DNA target site.[18] Mismatches formed with polyamides **2** and **4** are indicated with shaded boxes. b)-c) Deconvolution microscopy of unfixed lymphoid cells (GM15850, derived from an FRDA patient, shown in b), and GM15851 derived from a healthy sibling, shown in c)), incubated with BODIPY conjugates of each of the indicated polyamides, at 2 μM concentration in cell culture medium for 16 h prior to visualization, as described.[35] The bars represent 10 microns.

2.1); however, this value may be an underestimation of the affinity of this molecule for GAA·TTC repeat DNA, because our K_d measurements are limited by a minimum DNA concentration of ≈2 pM in the binding reaction. Two mismatch controls, **2** (Im-Py-*β*-Im-Im-*β*-Py-*β*-Dp) (Figure 2.1A) and **4** (Im-Py-*β*-Im-Py-*β*-Im-Im-*β*-Py-*β*-Dp), have binding affinities for the $(GAA{\cdot}TTC)_6$ target sequence that are three orders of magnitude lower than those of the match polyamides (Figures 2B and 2D and Table 2.1). Polyamide **1** is

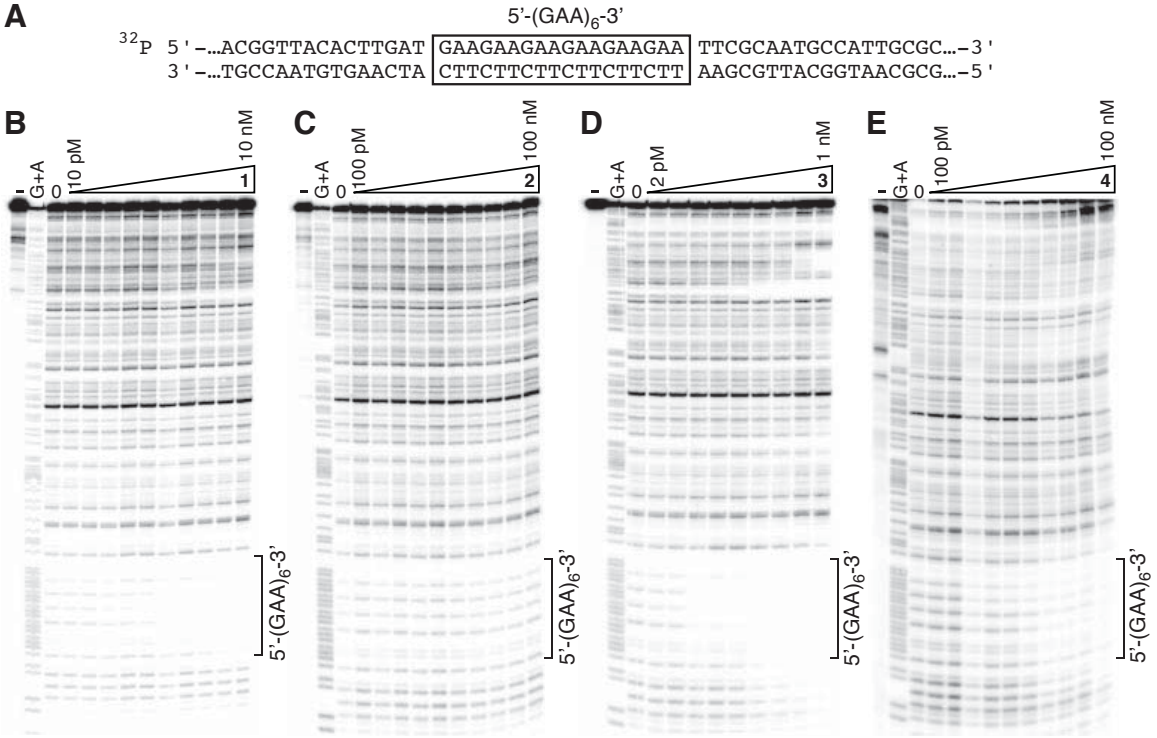

Figure 2.2. DNA binding properties of the polyamides. Quantitative DNase I footprint analysis for polyamide binding to a radiolabeled PCR product containing a $(GAA{\cdot}TTC)_6$ repeat sequence, labeled on the purine strand. DNA (at ≈20 pM for b), c) and e) and ≈2 pM for d)) and polyamide were allowed to equilibrate for 16 h, with the indicated ranges of polyamide concentrations, prior to DNase digestion and gel analysis.[25] The phosphorimage of each gel is shown, with undigested DNA in the lane marked "-"; a G+A sequencing reaction of the same DNA is shown along with DNase-treated DNA in the absence of polyamide (in the lane marked "0"). a) An excerpt of the DNA sequence cloned in pCR2.1 DNA, used to generate the PCR product for footprinting reactions is referenced for b) – e). b) Polyamide **1** targeting 5'-AAGAAGAAG-3'; c) Polyamide **2**, mismatch control for **1**; d) Polyamide **3** targeting 5'-AAGAAGAAGAAG-3'; e) Polyamide **4**, mismatch control for **3**

Table 2.1. Polyamides designed to target GAA·TTC repeats in the frataxin gene

Polyamide sequence	$(GAA{\cdot}TTC)_n$ repeat no. in target site, *n*	Binding affinity (K_d, nM)*
1: Im-Py-*β*-Im-Py-*β*-Im-*β*-Dp	3	0.11 ± 0.02
2: Im-Py-*β*-Im-<u>Im</u>-*β*-<u>Py</u>-*β*-Dp	3	>100
3: Im-Py-*β*-Im-Py-*β*-Im-Py-*β*-Im-*β*-Dp	4	0.003 ± 0.001
4: Im-Py-*β*-Im-Py-*β*-Im-<u>Im</u>-*β*-<u>Py</u>-*β*-Dp	4	2.0 ± 0.4

Mismatch amino acids are underlined. Im, imidazole; Py, pyrrole, *β*, *β*-alanine; Dp, dimethylaminopropylamine

*Binding affinities (mean values of the K_d from a minimum of two determinations, and standard deviations) determined by quantitative DNase I footprinting, as in Figure 2.2

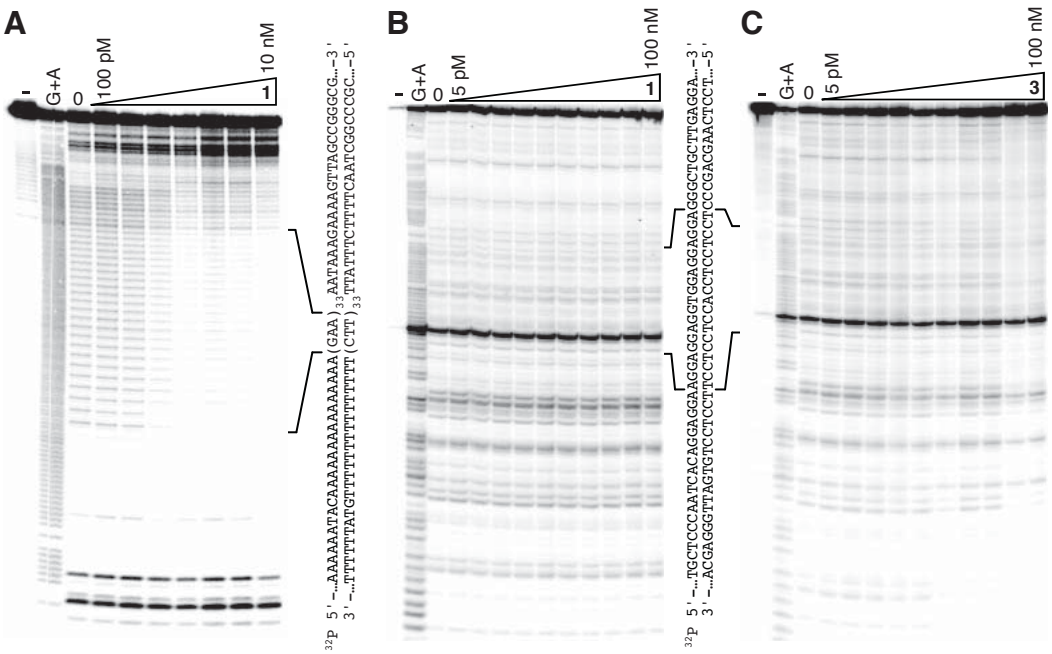

Figure 2.3. DNase I footprint analysis for polyamide **1** binding to a radiolabeled $(GAA{\cdot}TTC)_{33}$ PCR product derived from plasmid pMP142 DNA,[5] labeled on the purine strand; quantitative DNase I footprint analysis for polyamides **1** and **3** binding to a radiolabeled DNA containing a mismatch DNA sequence (5'-AGGAGGAGGTGGAGGAG-GA-3', derived by PCR amplification of the promoter region of the erbB2 gene). DNA (at ≈20 pM concentration) and polyamide were allowed to equilibrate for 16 h, with the indicated range of polyamide concentrations, before DNase digestion and gel analysis. The PhosphorImages are shown, with undigested DNA in the lane marked "–"; a G+A sequencing reaction of the same DNA is shown, along with DNase-treated DNA in the absence of polyamide (in the lane marked "0"). The sequence of the surrounding region is shown adjacent to each gel. a) Polyamide **1** targeting 5'-$(GAA{\cdot}TTC)_{33}$. b) Polyamide **1** targeting 5'-AGGAGGAGG-3'. c) Polyamide **3** targeting 5'-AGGAGGAGGTGG-3'. The sequence of the region surrounding the GGA·TCC repeats is shown between b) and c).

also able to bind extended regions of GAA·TTC repeats $[(GAA{\cdot}TTC)_{33}]$ with no loss in affinity, with several molecules of **1** bound per DNA molecule (Figure 2.3). As another test for sequence specificity, footprinting experiments with **1** and **3** and a radiolabeled DNA fragment containing a mismatch DNA sequence (5'- . . . AGGAGGAGGTGGAGGAGGA . . . -3') were performed. Neither polyamide **1** nor polyamide **3** bound this DNA sequence at polyamide concentrations up to 100 nM (Figure 2.4). Polyamide **1** binds other polypurine DNA tracts with single G-to-A transitions, maintaining similar or slightly reduced binding affinities compared with the 5'-AAGAAGAAG-3' site. A sequence harboring two transitions (A-to-G and G-to-A), giving rise to 5'-AAAAGGAAG-3', increases the K_d of **1** by more than three orders of magnitude. Truncation of **1** to Im-Py-*β*-Im-*β*-Dp increases its

K_d on 5'-AAGAAGAAG-3' by more than four orders of magnitude (see Chapter 2B for data and discussion).

Figure 2.4. Quantitative DNase I footprint analysis for polyamide **1-B**, the BODIPY conjugate of **1**, binding to a radiolabeled $(GAA{\cdot}TTC)_6$ PCR product. Lanes are labeled as per Figures 2.2 and 2.3. Quantitation of this experiment by PhosphorImage analysis reveals a K_d of 1.3 nM. The amplicon sequence is depicted in Figure 2.2A.

Nuclear Localization of Fluorescent Polyamides.

Fluorescent versions of the match polyamides **1** and **3** (**1-B** and **3-B**, respectively) and mismatch polyamide **2** (**2-B**) were synthesized, where the dye BODIPY FL (C5) was attached at the carboxyl terminus of the polyamide (Figure 2.1A). Quantitative DNase I footprinting demonstrated that polyamides **1-** and **3-B** exhibit 13- to 20-fold losses in binding affinity for $(GAA{\cdot}TTC)_6$ DNA, compared with the parent polyamides (for **1-B**, K_d = 1.3 nM) (Figure 2.5; for **3-B**, K_d = 0.04 nM). Epstein–Barr virus-transformed lymphoblast cell lines from an FRDA patient (line GM15850) and from an unaffected sibling (line GM15851) were obtained from the NIGMS Human Genetic Cell Repository (Coriell Institute, Camden, NJ). Both the match **1-B** and mismatch **2-B** conjugates localize in the nucleus of live, unfixed normal and FRDA lymphoid cells after 16 h incubation in culture medium, as determined by deconvolution microscopy (Figure 2.1B). The BODIPY-conjugate of the longer polyamide **3**, **3-B**, also localizes in the nucleus of the FRDA cells.

GAA·TTC-Specific Polyamides Increase Frataxin mRNA and Protein.

To assess whether polyamides alleviate transcription inhibition caused by expanded GAA·TTC repeats in the frataxin gene, we used real-time quantitative qRT-PCR to monitor

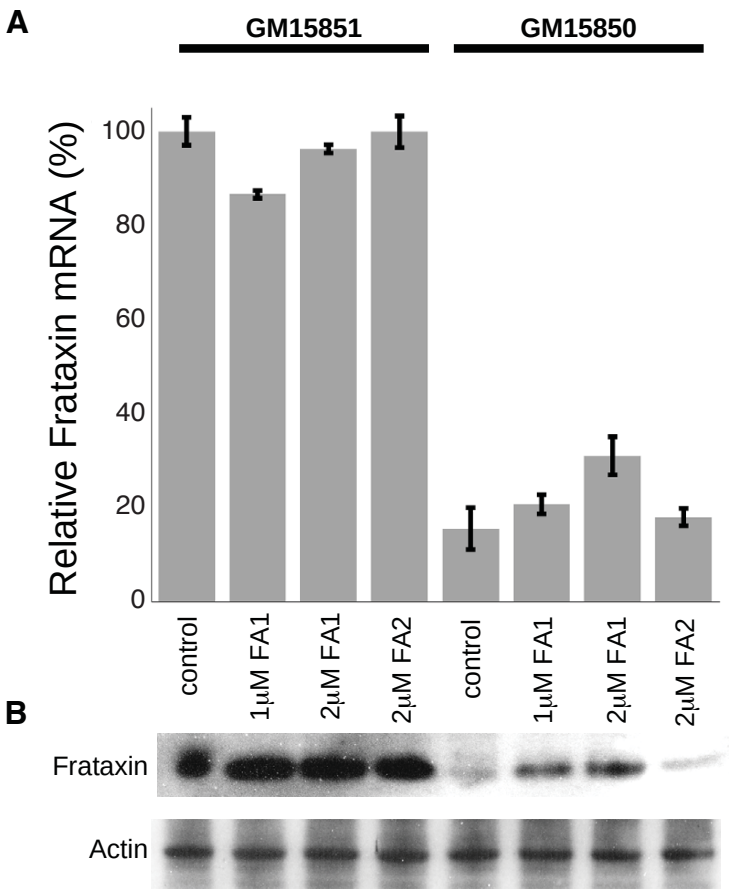

Figure 2.5. Polyamide **1** increases the levels of frataxin mRNA and protein in an FRDA lymphoid cell line. a) Measurement of frataxin mRNA levels, relative to that of GAPDH, in cell lines derived from an unaffected individual (GM15851), and an FRDA patient (GM15850) by qRT-PCR.[35] Polyamides **1** and **2** were included in the cell culture medium at the indicated concentrations, and frataxin and GAPDH mRNA were determined after 7 days, with media and polyamide replenished on days 3 and 5. Error bars are derived from the percent error of the average and standard deviation of the change in cycle threshold between frataxin and GAPDH for triplicate experiments, with triplicate qRT-PCR determinations for each experiment. b) Effects of polyamides on frataxin protein in cultured lymphoid cells. FRDA or control cells were incubated as in panel a) prior to western blot analysis with antibody to human frataxin or actin. Equivalent amounts of total cell extract protein were loaded in each lane.

frataxin mRNA levels in the lymphoid cell lines described above, with the levels of GAPDH mRNA as an internal control for each RNA sample. No differences in GAPDH mRNA levels were found between the two cell lines. As expected, the FRDA cell line had a markedly lower level of frataxin mRNA compared with the cell line from the normal individual (Figure 2.6A; 13 ± 6%, for 20 determinations, Table 2.2). We incubated the FRDA and control cells with various concentrations of each of the polyamides for various lengths of time and found that only polyamide **1** increased frataxin mRNA levels after 7 days incubation in culture medium. No changes in frataxin mRNA levels were observed on shorter incubation times. Over the concentrations of 1–8 μM, we find that polyamides are not cytotoxic to the lymphoid cell lines (as determined by trypan blue exclusion and measurements of ATP levels) and do not affect cell growth rates. Importantly, the level of frataxin mRNA in the FRDA GM15850 cell line was increased

2.5-fold by incubation with polyamide **1** (at 2 μM, Figure 2.6A). The average fold increase observed with 2 μM **1** in the FRDA cell line is 2.2 ± 0.6 (in 20 experiments), resulting in an average of ≈27% of the level of frataxin mRNA found in the normal cell line (Table 2.2). We note that polyamide concentrations greater than the K_d for *in vitro* binding are required for increasing frataxin transcription, presumably because of the large number of potential polyamide-binding sites in the human genome and availability of these sites in the cell nucleus. Despite the fact that **1** binds the 9-bp 5'-AAGAAGAAG-3' repeat with high affinity, the sequence landscape of all possible high-affinity sites for this class of *β*-linked oligomers has not yet been fully characterized.[26] Neither higher concentrations of **1** nor longer incubation times increased frataxin transcription above the levels observed at 2 μM on 7 day incubations. Polyamide **1** did not increase frataxin mRNA levels in the cell line derived from the normal individual. Similar incubations with the mismatch polyamide **2** were without significant effect in either cell line. The levels of GAPDH mRNA were not changed by polyamide treatment in either cell line.

Table 2.2. Collected data showing the average ΔCt for normal cells (GM15851) and FRDA cells (GM15850) before and after treatment with **1** at 2 μM

Exp.	GM15851 Ave ΔCt	GM15850 Ave ΔCt	GM15850+1 Ave ΔCt	Ave ΔΔCt	Rel. exp. 850:851	Rel. exp. 850+1:851	Fold change 850+1:850
1	8.088	11.234	10.628	3.146	11.30	17.19	1.52
2	7.584	11.088	9.923	3.505	8.81	19.76	2.24
3	7.484	10.850	10.057	3.366	9.70	16.81	1.73
4	7.363	11.230	10.785	3.868	6.85	9.33	1.36
5	8.566	10.765	10.083	2.200	21.77	34.94	1.61
6	7.683	10.649	9.206	2.966	12.80	34.80	2.72
7	8.523	12.130	10.748	3.607	8.21	21.39	2.61
8	7.973	11.468	10.959	3.496	8.87	12.62	1.42
9	9.176	12.885	11.241	3.710	7.64	23.89	3.13
10	7.823	11.244	9.837	3.421	9.34	24.75	2.65
11	8.387	11.976	10.607	3.589	8.31	21.46	2.58
12	8.636	11.636	10.551	3.000	12.50	26.52	2.12
13	7.855	11.638	9.812	3.783	7.26	25.74	3.54
14	8.608	12.082	10.804	3.474	9.00	21.82	2.42
15	8.150	10.601	9.653	2.451	18.29	35.29	1.93
16	8.607	11.589	10.402	2.982	12.66	28.83	2.28
17	8.540	11.165	10.316	2.625	16.21	29.19	1.80
18	8.271	9.959	9.425	1.688	31.04	44.93	1.45
19	7.739	10.136	8.515	2.397	18.99	58.43	3.08
20	8.586	10.763	10.024	2.177	22.12	36.92	1.67
Averages	**8.182**	**11.254**	**10.179**	**3.072**	**13.08**	**27.23**	**2.19**
SD (±)	**0.482**	**0.707**	**0.662**	**0.623**	**6.42**	**11.44**	**0.64**

Exp., experiment; Ave, average; Rel. exp., relative expression; 850, GM15850 cell line; 851, GM15851 cell line

We next examined the effect of removal of polyamide **1** from the culture medium on frataxin transcription. After induction of frataxin mRNA synthesis by **1** (7 days at 2 μM), transfer of the cells to fresh medium lacking polyamide caused frataxin mRNA levels to decrease to their original levels after 96 h (data not shown). Thus, polyamides must be continuously present to maintain active transcription of FRDA frataxin alleles. The finding that incubation periods of 7 days or more are necessary to observe increases in frataxin mRNA suggests that multiple rounds of DNA replication are necessary for the compound to alter either the DNA or chromatin structure of expanded frataxin alleles, leading to active transcription, and removal of the polyamide causes the frataxin gene to readopt its inactive DNA or chromatin conformation. To test whether cellular proliferation is required for frataxin gene activation, we serum-starved FRDA and control cells, leading to cell cycle arrest (confirmed by fluorescence activated cell sorting, data not shown), and then incubated the arrested cells with polyamide **1** for 7 days before qRT-PCR analysis. We find no increase in frataxin mRNA with polyamide **1** under these conditions, suggesting that cell division is a requirement for upregulation of transcription by the polyamide.

It was curious that the highest-affinity compound, **3**, did not increase frataxin mRNA levels, because the fluorescent version of this molecule, **3-B**, localized in the nucleus of FRDA lymphoid cells. Previous studies have established that nuclear localization is sensitive to polyamide composition and structure and, especially, the nature of the carboxyl terminus;[27,28] therefore, the nonfluorescent version of **3** may not enter the nucleus. To test this hypothesis, we monitored the levels of frataxin mRNA after incubation with **3-B**, and found an approximately two to threefold increase in relative levels of frataxin mRNA (compared with GAPDH) after 2- to 4-day incubations (data not shown). Thus, polyamide **3** may not have the optimum chemical properties for nuclear localization or DNA binding in the context of cellular chromatin. In contrast, polyamide **1-B** did not increase frataxin mRNA levels in experiments where positive effects were found with polyamide **1**.

Because the primary transcripts from FRDA frataxin genes contain long stretches of

GAA repeat RNA sequence, it is conceivable that this RNA will not be correctly processed into mature frataxin mRNA, and frataxin protein will not be produced. To test whether polyamide **1** leads to increased levels of frataxin protein in treated lymphoid cells, total-cell extracts from polyamide-treated (1–2 μM for 7 days), and untreated GM15851 control and GM15850 FRDA cells were subjected to SDS/PAGE and the corresponding blots probed with anti-frataxin or anti-actin antibodies (Figure 2.6B). An approximately two to threefold increase in frataxin protein is observed with **1** in the FRDA cells, which correlates well with the observed increase in frataxin mRNA (Figure 2.6A).

Effects of Polyamides on Global Gene Expression.

DNA microarray analyses were performed with RNA isolated from GM15850 FRDA and GM15851 normal lymphoid cells that were either untreated or treated with polyamides **1** (at 1 and 2 μM) or **2** (at 2 μM) for 7 days on Affymetrix Human Genome U133 Plus 2.0 GeneChips. Polyamide **1** was found to affect the mRNA levels for a limited number of genes in the FRDA cell line (at $P \leq 0.005$, 51 genes affected by 1 μM **1**, 16 genes affected by 2 μM **1**) and only 2 genes in the normal cell line (Table 2.3). Although more genes were called affected by **1** at 1 μM than at 2 μM, this difference is largely due to genes whose mRNA levels change by $<\approx$ 25% in either direction. At 2 μM **1**, 15 genes were increased in expression by >50%, and 1 gene was decreased by 45%. At 1 μM **1**, only 3 genes had comparable changes in their mRNA levels. For GM15851 cells, 2 genes were up-regulated by **1**, and no genes were down-regulated. For the frataxin gene, untreated GM15850 cells showed 17% of the frataxin mRNA found in untreated GM15851 cells, and incubation with **1** at 2 μM increases frataxin mRNA by 2.5-fold, bringing the frataxin mRNA level in GM15850 cells to 42% of that found in GM15851 cells. These values are comparable with those obtained by qRT-PCR (Figure 2.6A). Transcript levels for frataxin were not changed by **2** in either cell line, and **2** affected only a small number of genes in either cell line (at $P \leq 0.005$, 3 genes affected by 2 μM **2** in GM15850 cells, and 1 gene

Table 2.3. Potential match and degenerate binding sites for polyamide **1** in significant genes listed for class comparisons where $P \leq 0.005$. GeneChip data were normalized using RMAExpress (version 0.4 alpha 7) and analyzed by class comparisons among groups of arrays by BRB ArrayTools. Genes are listed in order from increasing to decreasing expression levels according to each comparison. Genomic sequences were identified by using the Affymetrix probe set target sequence to perform a BLAT search (http://genome.ucsc.edu/). When a representative gene was present, both strands were analyzed to determine the total number of occurrences of each sequence.

Class comparison	Parametric *P* value	Fold change	Probe set ID	Description	Number of times sequence appears on both strands in genomic DNA			
					AAGAAG	AAGAAGA	AAGAAGAA	AAGAAGAAG
GM15851 control vs GM15851 1μM 1								
1	4.65E-03	1.56	219298_at	Enoyl Coenzyme A hydratase domain containing 3	27	9	3	1
GM15851 control vs GM15851 2μM 1								
1	4.83E-03	1.74	1569106_s_at	Hypothetical protein FLJ10707	54	16	7	0
GM15851 control vs GM15851 2μM 2								
1	1.89E-03	1.70	219298_at	Enoyl Coenzyme A hydratase domain containing 3	27	9	3	1
GM15850 control vs GM15850 1μM 1								
1	4.51E-03	2.24	213060_s_at	Chitinase 3-like 2	14	3	1	1
2	3.41E-03	1.66	239862_at	Tumor protein D52	150	43	17	3
3	3.37E-03	1.52	237626_at	RB1-inducible coiled-coil 1	94	49	22	4
4	1.82E-03	1.50	243149_at	Eukaryotic translation initiation factor 4 gamma, 3	281	120	62	19
5	2.64E-03	1.39	239188_at	Chromosome 14 open reading frame 24	29	14	10	1
6	1.97E-03	1.38	227232_at	Enah/Vasp-like	155	55	23	6
7	2.77E-03	1.33	242456_at	MRE11 meiotic recombination 11 homolog A (*S. cerevisiae*)	81	27	11	3
8	3.23E-03	1.32	240174_at	Hypothetical LOC388903	245	93	43	18
9	9.00E-07	1.28	232773_at	Hypothetical protein MGC13057	17	7	3	1
10	3.38E-03	1.20	1564639_at	Hypothetical LOC389908		No representative gene		
11	4.37E-03	1.20	1569714_at	Zinc finger, FYVE domain containing 20	19	9	4	1
12	4.09E-04	1.17	239648_at	Hypothetical protein MGC48972	43	15	4	0
13	1.84E-04	1.12	231958_at	Hypothetical protein BC015088	30	16	8	0
14	2.20E-03	1.11	233681_at	Keratin associated protein 3-3	0	0	0	0
15	3.83E-03	1.10	1562516_at	Hypothetical protein FLJ10300	64	21	12	3
16	4.97E-03	1.09	227532_at	Hypothetical protein MGC14816	31	15	9	0
17	2.67E-03	1.08	1560021_at	Ribosomal protein S20		No representative gene		
18	5.76E-04	1.07	239773_at	Hypothetical protein BC004923	43	18	7	1
19	4.45E-03	1.06	1553618_at	Tripartite motif-containing 43	9	4	1	0
20	1.69E-03	1.04	1563540_at	MRNA; cDNA DKFZp686O0511 (from clone DKFZp686O0511)		No representative gene		
21	4.15E-03	1.04	233616_at	Candidate tumor suppressor protein	318	126	58	22
22	2.51E-03	0.96	213453_x_at	Glyceraldehyde-3-phosphate dehydrogenase	4	1	0	0
23	1.71E-03	0.93	242404_at	Transcribed locus		No representative gene		
24	1.54E-03	0.90	222130_s_at	FtsJ homolog 2 (*E. coli*)	4	3	2	0
25	3.83E-03	0.89	1562524_at			No representative gene		
26	4.76E-03	0.89	1554820_at	Hypothetical protein LOC340351	155	70	24	4
27	2.83E-03	0.87	1559403_at	High mobility group nucleosomal binding domain 3	28	8	1	0
28	6.44E-04	0.87	237619_at	Chromosome 6 open reading frame 146	5	1	0	0
29	2.22E-03	0.87	237124_at	Transcribed locus		No representative gene		
30	3.48E-03	0.87	1553672_at	Enabled homolog (*Drosophila*)	167	64	26	4
31	3.01E-03	0.86	244770_at	Hypothetical gene supported by AK091718		No representative gene		
32	3.15E-03	0.85	228787_s_at	Breast carcinoma amplified sequence 4	41	14	9	2
33	4.43E-03	0.84	218494_s_at	SLC2A4 regulator	1	0	0	0
34	4.13E-03	0.83	1561391_at	Staufen, RNA binding protein, homolog 2 (*Drosophila*)	354	128	56	8
35	3.97E-04	0.83	207253_s_at	Ubinuclein 1	32	15	8	3
36	4.81E-03	0.82	210776_x_at	Transcription factor 3 (E2A immunoglobulin enhancer binding factors E12/E47)	17	4	0	0
37	1.20E-03	0.81	201793_x_at	Chromosome 1 open reading frame 16	94	36	15	5
38	3.23E-03	0.81	222138_s_at	WD repeat domain 13	2	0	0	0
39	4.21E-04	0.80	229269_x_at	Single-stranded DNA-binding protein 4	7	1	0	0
40	4.68E-03	0.80	215176_x_at	HRV Fab 027-VL	479	186	81	18
41	2.31E-03	0.80	223409_at			No representative gene		
42	2.62E-03	0.80	233982_x_at	Dual-specificity phosphatase 24 (putative)		No representative gene		
43	4.91E-04	0.78	201234_at	Integrin-linked kinase	7	3	0	0
44	3.28E-03	0.78	1554907_a_at	Hydrocephalus inducing	242	85	35	5
45	6.76E-04	0.77	205112_at	Phospholipase C, epsilon 1	334	118	44	13
46	4.31E-03	0.75	218954_s_at	BRF2, subunit of RNA polymerase III transcription initiation factor, BRF1-like	3	0	0	0
47	2.48E-03	0.75	202383_at	Smcy homolog, X-linked (mouse)	27	9	1	0
48	4.57E-03	0.75	204908_s_at	B cell CLL/lymphoma 3	4	2	0	0
49	2.27E-03	0.75	1564129_a_at	Quinolinate phosphoribosyltransferase (nicotinate-nucleotide pyrophosphorylase (carboxylating))	7	2	1	0
50	2.36E-03	0.72	220306_at	Family with sequence similarity 46, member C	23	5	2	1
51	2.97E-03	0.63	219348_at	Uncharacterized hematopoietic stem/progenitor cells protein MDS032	3	1	1	0
GM15850 control vs GM15850 2μM 1								
1	3.80E-05	19.61	203290_at	Major histocompatibility complex, class II, DQ alpha 1	4	1	0	0
2	2.15E-05	6.02	213060_s_at	Chitinase 3-like 2	14	3	1	1
3	2.20E-03	3.12	211633_x_at	Immunoglobulin heavy constant gamma 1 (G1m marker)	371	175	56	10
4	4.87E-03	2.95	203324_s_at	Caveolin 2	12	5	1	0
5	3.60E-03	2.75	211634_x_at	Immunoglobulin heavy constant mu	837	378	121	24
6	2.62E-03	2.48	205565_s_at	Frataxin	36	13	10	8
7	1.92E-03	2.32	230735_at	Interferon (alpha, beta and omega) receptor 2	36	13	8	2
8	4.62E-03	2.25	217022_s_at	Immunoglobulin heavy constant alpha 1 /// immunoglobulin heavy constant alpha 2 (A2m marker) /// hypothetical protein MGC27165	320	141	48	10
9	1.52E-03	2.18	208029_s_at	Lysosomal associated protein transmembrane 4 beta	57	15	7	1
10	1.05E-03	2.15	208767_s_at	Lysosomal associated protein transmembrane 4 beta	57	15	7	1
11	4.49E-03	2.02	225133_at	Kruppel-like factor 3 (basic)		No representative gene		
12	3.67E-03	2.00	227198_at	Lymphoid nuclear protein related to AF4		No representative gene		
13	2.33E-03	1.71	242399_at	Hypothetical protein FLJ33708	319	122	52	12
14	2.58E-03	1.65	1558186_s_at	Noncoding transcript (CLLU1 gene), splice variant 3		No representative gene		
15	4.45E-03	1.50	230961_at			No representative gene		
16	3.87E-03	0.55	203892_at	WAP four-disulfide core domain 2	8	3	1	0
GM15850 control vs GM15850 2μM 2								
1	3.78E-03	1.83	1552287_s_at	AFG3 ATPase family gene 3-like 1 (yeast)	8	3	1	0
2	1.50E-03	1.78	228503_at	CDNA: FLJ22648 fis, clone HSI07329		No representative gene		
3	4.43E-03	0.60	201169_s_at	Basic helix-loop-helix domain containing, class B, 2	4	1	0	0

affected in GM15851 cells) (Table 2.3).

To examine the overall changes in gene-expression profiles in treated and untreated populations of FRDA and control cells, we first determined the genes whose expression was called significantly different among all conditions of untreated and treated GM15851 and GM15850 cells. At a *P* value of ≤0.005, this class comparison generated a total of 632 genes. We then generated a correlation graph of the difference in geometric means of intensities for these genes between untreated and treated cells for each experimental condition (Figure 2.7). Neither the match polyamide **1** nor mismatch **2** affected the profile of GM15851 cells (slope of the correlation between conditions = –0.04 to +0.04, Figure 2.7A–D), whereas polyamide **1**-treated GM15850 FRDA cells (at 2 μM) have a gene-expression profile that approaches that of untreated GM15851 cells compared with untreated FRDA cells (Figure 2.7, compare G with E; slope = 0.69 compared with 0.97,

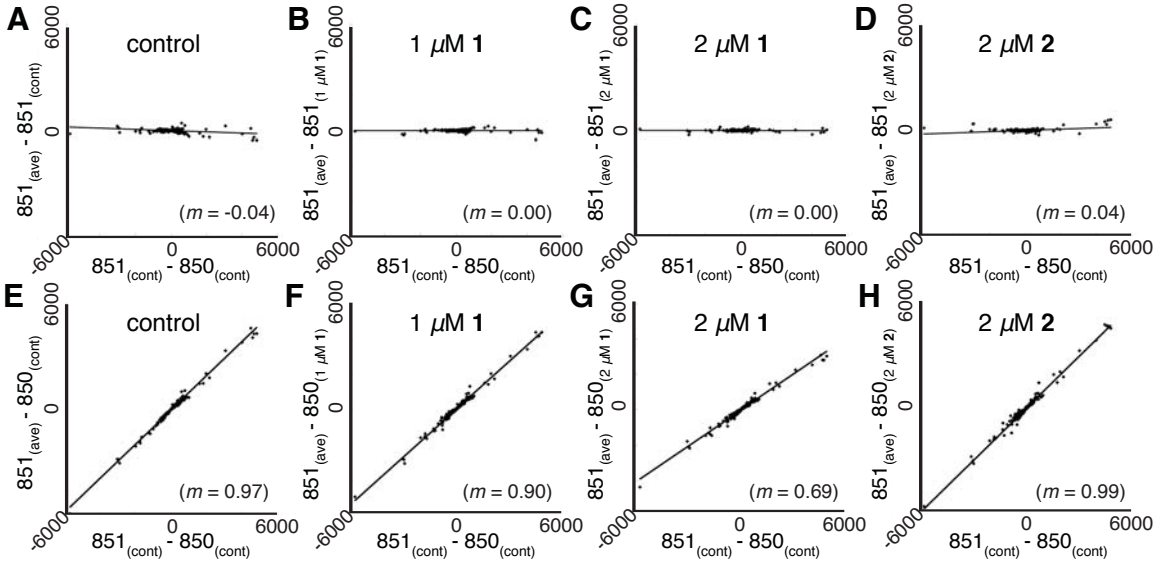

Figure 2.6. Microarray analysis of polyamide effects on global gene expression. Correlation of significant genes called from a class comparison of all arrays (*n* = 632 genes at *P* ≤ 0.005). Cells were cultured with and without the addition of **1** at 1 μM or 2 μM or **2** at 2 μM for 7 days prior to RNA extraction. Each graph represents the difference between the geometric mean of intensities (from an average of the logged RMA data for each condition[38]) of untreated GM15851 cells (denoted 851 in the graphs) and untreated GM15850 cells (denoted 850) plotted versus the difference between the average from all GM15851 geometric means of intensities and each of the individual cell types and conditions. Thus the untreated controls for GM15851 and GM15850 cells should give slopes for the least squares fit line approaching zero and one, respectively. Graphs for normal GM15851 cells are shown for a) the untreated control and b) cells treated with **1** at 1 μM, c) 2 μM, and d) **2** at 2 μM. Graphs for FRDA GM15850 cells are shown for e) the untreated control and f) cells treated with **1** at 1 μM, g) 2 μM, and h) **2** at 2 μM.

respectively). This effect is seen to a lesser degree at 1 μM polyamide **1** (Figure 2.7F), but was not seen with the mismatch polyamide **2** (Figure 2.7H). These changes in gene expression in the affected cell line may be a consequence of changes in frataxin protein levels,[29,30] or some could be direct effects of the polyamide, as suggested by the occurrence of **1** binding sites in up-regulated genes (Table 2.2). Taken together, these data lead us to conclude that polyamide **1** increases frataxin gene expression and, perhaps, downstream targets of frataxin, but this molecule has a limited effect on global gene expression. A search of the GenBank database reveals that most regions of the GAA·TTC DNA sequence [$(GAA{\cdot}TTC)_6$ or longer] are present in nontranscribed repetitive DNA elements (including Alu sequences) in the human genome.[31] Polyamide **1** has no effects on lymphoid cell morphology, metabolism, or growth in culture.

Influence of Polyamides on Sticky-DNA Conformation.

The capacity of sequence-specific polyamides to disrupt the intramolecular sticky-DNA structure formed by GAA·TTC repeat tracts was investigated. Plasmids harboring the sticky-DNA structure are visualized by gel electrophoresis after restriction endonuclease cleavage (Figure 2.7A). Linear DNA is indicative of disruption of the sticky-DNA structure by a polyamide, whereas the cleaved sticky-DNA band that migrates with a much slower mobility reveals no influence of the ligand. Plasmid pRW4886, which contains two tracts of $(GAA{\cdot}TTC)_{176}$ in a direct-repeat orientation,[10] was incubated with each of the polyamides **1**–**4** at concentrations ranging from 0 to 50 μM. The polyamide-bound DNA was then digested with EcoNI and electrophoresed on 1% agarose gels to determine the amount of the EcoNI-cleaved sticky-DNA retarded band present (Figure 2.7B). Incubation of pRW4886 DNA with **3** shifted the equilibrium from a maximum amount of sticky DNA to a complete loss of the EcoNI-cleaved sticky-DNA retarded band at a concentration of 50 nM. Polyamide **4**, which is a mismatch of **3** and has a K_d value ≈1,000 times higher than **3** (Table 2.1), did not affect the stability of sticky DNA in pRW4886 until a concentration

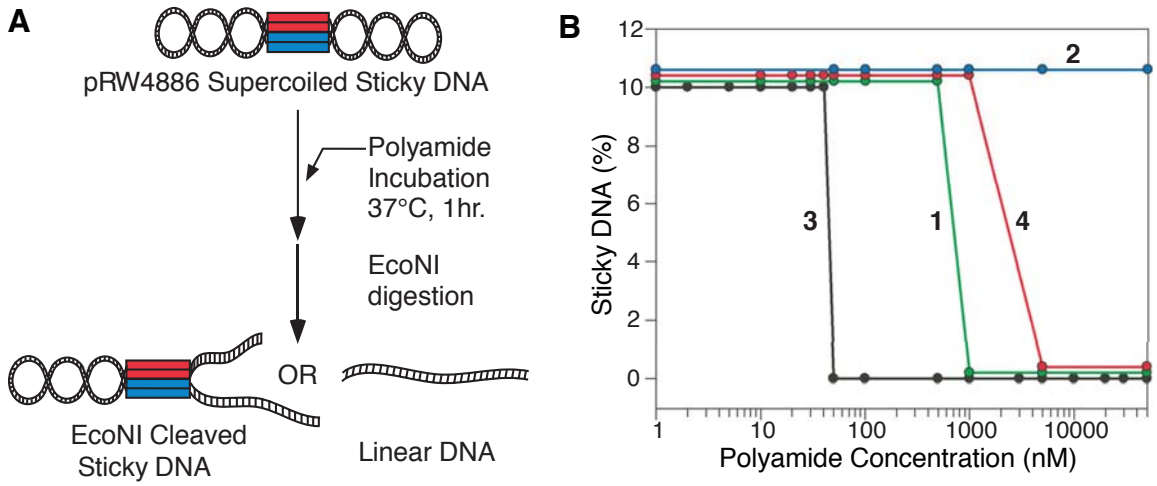

Figure 2.7. Effect of polyamide binding to plasmid DNA on sticky DNA stability. a) Illustration showing the assay for influence of polyamides on sticky DNA conformation. b) The capacity of a polyamide to disrupt the DNA·DNA associated region in the sticky DNA structure was revealed by the formation of linearized pRW4886 rather than the EcoNI cleaved sticky DNA, which showed the absence of a perturbing influence of the ligands. The polyamides that had higher K_d values required higher concentrations to observe the disruption of the DNA·DNA associated region of sticky DNA. The polyamides used were: **1** (green), **2** (blue), **3** (black) and **4** (red).

of 5 μM. For polyamide **1**, a 1 μM concentration was needed to dissociate the DNA·DNA structure-forming region. The mismatched polyamide **2**, having the highest K_d value of all of the polyamides tested, showed no effect on sticky-DNA stability, even at a 100 μM concentration. Thus, the binding affinities of the polyamides for the GAA·TTC sequence had an intimate relationship with the concentration needed to shift the equilibrium from the DNA·DNA-associated structure to the duplex conformation (Figure 2.7B). The absence of the EcoNI-cleaved sticky-DNA-retarded band demonstrated the capacity of the sequence specific polyamide binding to shift the non-B–B-DNA equilibrium toward a conventional DNA duplex conformation in supercoiled plasmids. Because sticky DNA inhibits transcription,[5,32] and because the polyamides destabilize this conformation by shifting the structural equilibrium to duplex B DNA, increases in frataxin mRNA observed with polyamide **1** may be due to this structural transition, although other mechanisms, such as heterochromatin desilencing, must be considered.[19]

Conclusions

Increased frataxin transcription with GAA·TTC-specific polyamides may be due to a change in DNA structure, as suggested by reversal of sticky DNA, which then allows for transcription through expanded GAA·TTC-repeat DNA, or by reversing heterochromatin caused by expanded GAA·TTC repeats.[14] Polyamides designed to target the related sequence GAGAA·TTCTC repeat DNA, which is found in *Drosophila* satellite V, have been shown to alter gene expression in developing embryos by opening the chromatin domains containing these repeated sequences[14,19] and to displace heterochromatin protein 1 (HP1) and the other chromosomal proteins D1 and topoisomerase II.[33] Interestingly, in the transgene study reported by Festenstein and colleagues,[14] HP1 was found to promote gene silencing by expanded GAA·TTC-repeat DNA. Thus, polyamides targeting GAA·TTC-repeat DNA may increase transcription of genes that harbor these sequences by displacement of similar repressor proteins and reversal of inactive heterochromatin to a more active chromatin structure.

Materials and Methods

Polyamide Synthesis and Characterization.

Polyamides were synthesized by solid-phase methods[18,34] and their identity and purity verified by MALDI-TOF MS and analytical HPLC. Fluorescent conjugates were prepared by coupling BODIPY FL C5 (Molecular Probes) to the carboxyl terminus.[27] Binding affinities for match and mismatch sites were determined by quantitative DNase I footprinting. A plasmid harboring six GAA·TTC repeats was constructed by cloning the oligonucleotide 5’-GCCTTACGGTTACACTTGATGAAGAAGAAGAAGAAGA ATTCGCAATGCCATTGCGCTATGA-3’·3’-ACGGAATGCCAATGTGAACTACTT CTTCTTCTTCTTCTTAAGCGTTACGGTAACGCGATAC-5’ in the pCR2.1 TOPO vector (Invitrogen), and 251-bp singly end-labeled PCR product was generated from this plasmid with the following oligonucleotides: 5’-GAAAGACCCGTGTGTAAAGCC-3’

and 5'-CTCGATATCTGCAGAATTGCC-3', where the second oligonucleotide was labeled with γ-[^{32}P]-ATP and polynucleotide kinase, by using standard procedures, to generate a PCR product labeled on the GAA strand. A 204-bp singly end-labeled PCR product was derived from plasmid pMP142 DNA, containing 33 GAA·TTC repeats,[5] with the following oligonucleotides: 5'-GGCCAACATGGTGAAACC-3' and 5'-GTAGCTGGGATTACAGGCGC-3'. The first oligonucleotide shown was radiolabeled as above to generate a PCR product labeled on the GAA strand. A 150-bp PCR product containing a $(GGA{\cdot}TCC)_3$ mismatch sequence was derived from the erbB2 (Her2-neu) promoter in human genomic DNA with the following oligonucleotides: 5'-CTTGTTGGAATGCAGTTGGA-3' and 5'-GGTTTCTCCGGTCCCAAT-3', with the first oligonucleotide radiolabeled.

Cell Culture.

Epstein–Barr virus-transformed lymphoblast cell lines GM15850 from a FRDA patient (alleles with 650 and 1,030 GAA·TTC repeats in the frataxin gene, from the Coriell Cell Repository) and GM15851 from an unaffected sibling (normal range of repeats) were propagated in RPMI medium 1640 with 2 mM L-glutamine and 15% FBS at 37°C in 5% CO_2. Cell growth and morphology were monitored by phase-contrast microscopy and viability by trypan blue exclusion and an ATP assay (ApoSENSOR; BioVision). Polyamides were added directly to the culture medium in PBS, and incubations were for the times indicated in the text and figure legends. Nuclear localization of the polyamides was verified by deconvolution microscopy, as described.[35]

Real-Time qRT-PCR.

Real-time qRT-PCR analysis was performed essentially as described,[36] by using the following primers for the frataxin gene: 5'-CAGAGGAAACGCTGGACTCT-3' and 5'-AGCCAGATTTGCTTGTTTGG-3'. RNA was standardized by quantification

of GAPDH mRNA,[37] and all values are expressed relative to GAPDH. qRT-PCR was performed by using iScript One-Step RT-PCR kit with SYBR green (Bio-Rad). Statistical analysis was performed on three independent qRT-PCR experiments for each RNA sample, and triplicate cell incubations were performed.

Western Blot Analysis.

Total-cell extracts were used for SDS/PAGE and Western blotting with antibodies to human frataxin (Chemicon) or actin (Santa Cruz Biotechnology) as a control for cell number and protein loading. Signals were detected by chemiluminescence after probing the blot with HRP-conjugated secondary antibody (Supersignal West; Pierce). To quantify the relative levels of proteins, autoradiograms (within the linear response range of x-ray film) were converted into digital images and the signals quantified by using Molecular Dynamics ImageQuant software.

DNA Microarrays.

FRDA and control lymphoid cells were incubated with polyamide **1** (at 1 or 2 μM) or **2** (at 2 μM), or in the absence of polyamide, in triplicate for 7 days before RNA purification and microarray analysis at the California Institute of Technology microarray facility. Affymetrix U133A Plus 2.0 GeneChips were hybridized in groups of eight for each of the three replicates. Raw GeneChip data were normalized with RMAExpress,[38] and the normalized data were filtered to remove probe sets called absent on 24 of 24 chips from class comparisons. The Affymetrix probe set-level data were imported to BRB Arraytools (Version 3.3.0 Beta 3a), selecting the U133 chips used in the experiment and leaving all filters off. For class comparisons between groups of arrays, unpaired samples were used, and the random variance model was selected, with the univariate significance threshold set to 0.005. The restrictions for the univariate test were maintained as the default values of 10 for the maximum number of false discovered genes, 0.1 for the maximum proportion

of false discoveries, and a 90% confidence level. Because of poor data correlation in one set of replicates, class comparisons were performed by using all chips for the control group versus two of the three replicates for the treatment group (five groups are the minimum number required for class comparisons). Microarray data (accession no. GSE5040) have been deposited at Gene Expression Omnibus.

Effects of Polyamides on Sticky DNA.

Plasmid pRW4886, which contains two tracts of $(GAA{\cdot}TTC)_{176}$ in a direct repeat orientation[10] and forms sticky DNA,[13] was treated with polyamides at concentrations of 0–50 μM at 37°C for 1 h. Restriction digestion with EcoNI after the polyamide incubation enabled visualization of the presence or absence of an EcoNI-cleaved sticky-DNA band that runs with decreased mobility compared with the linearized plasmid on 1% agarose gels.[13] Quantitation was by densitometric analysis using FluorChem (Version 3.04; Alpha Innotech).

We thank Malcolm Wood for assistance with deconvolution microscopy, Steve Head for statistical analysis of microarray data, and members of the Millard and Muriel Jacobs Genetics and Genomics Laboratory at California Institute of Technology for technical assistance and data analysis. This work was supported by National Institutes of Health Grants NS048989 (to J.M.G.), GM27681 (to P.B.D.), and NS37554 and ES11347 (to R.D.W.); the Friedreich's Ataxia Research Alliance; and the Seek-a-Miracle Foundation (Muscular Dystrophy Association).

References

(1) Campuzano, V.; Montermini, L.; Molto, M. D.; Pianese, L.; Cossee, M.; Cavalcanti, F.; Monros, E.; Rodius, F.; Duclos, F.; Monticelli, A.; Zara, F.; Canizares, J.; Koutnikova, H.; Bidichandani, S. I.; Gellera, C.; Brice, A.; Trouillas, P.; De Michele, G.; Filla, A.; De Frutos, R.; Palau, F.; Patel, P. I.; Di Donato, S.; Mandel, J. L.; Cocozza, S.; Koenig, M.; Pandolfo, M. *Science* **1996**, *271*, 1423–7.

(2) Montermini, L.; Richter, A.; Morgan, K.; Justice, C. M.; Julien, D.; Castellotti, B.; Mercier, J.; Poirier, J.; Capozzoli, F.; Bouchard, J. P.; Lemieux, B.; Mathieu, J.; Vanasse, M.; Seni, M. H.; Graham, G.; Andermann, F.; Andermann, E.; Melancon, S. B.; Keats, B. J.; Di Donato, S.; Pandolfo, M. *Ann. Neurol.* **1997**, *41*, 675–82.

(3) Wells, R. D.; Warren, S. T., eds. *Genetic Instabilities and Hereditary Neurological Diseases*; Academic Press: San Diego, 1998.

(4) Pandolfo, M. *Semin. Pediatr. Neurol.* **2003**, *10*, 163–72.

(5) Ohshima, K.; Montermini, L.; Wells, R. D.; Pandolfo, M. *J. Biol. Chem.* **1998**, *273*, 14588–95.

(6) Bidichandani, S. I.; Ashizawa, T.; Patel, P. I. *Am. J. Hum. Genet.* **1998**, *62*, 111–21.

(7) Grabczyk, E.; Usdin, K. *Nucleic Acids Res.* **2000**, *28*, 2815–22.

(8) Sakamoto, N.; Chastain, P. D.; Parniewski, P.; Ohshima, K.; Pandolfo, M.; Griffith, J. D.; Wells, R. D. *Mol. Cell* **1999**, *3*, 465–75.

(9) Vetcher, A. A.; Napierala, M.; Wells, R. D. *J. Biol. Chem.* **2002**, *277*, 39228–34.

(10) Vetcher, A. A.; Napierala, M.; Iyer, R. R.; Chastain, P. D.; Griffith, J. D.; Wells, R. D. *J. Biol. Chem.* **2002**, *277*, 39217–27.

(11) Napierala, M.; Dere, R.; Vetcher, A.; Wells, R. D. *J. Biol. Chem.* **2004**, *279*, 6444–54.

(12) Vetcher, A. A.; Wells, R. D. *J. Biol. Chem.* **2004**, *279*, 6434–43.

(13) Son, L. S.; Bacolla, A.; Wells, R. D. *J. Mol. Biol.* **2006**, *360*, 267–84.

(14) Saveliev, A.; Everett, C.; Sharpe, T.; Webster, Z.; Festenstein, R. *Nature* **2003**, *422*, 909–13.

(15) Grabczyk, E.; Usdin, K. *Nucleic Acids Res.* **2000**, *28*, 4930–7.

(16) Dervan, P. B.; Edelson, B. S. *Curr. Opin. Struct. Biol.* **2003**, *13*, 284–99.

(17) Trauger, J. W.; Baird, E. E.; Dervan, P. B. *Nature* **1996**, *382*, 559–61.

(18) Urbach, A. R.; Dervan, P. B. *Proc. Natl. Acad. Sci. U. S. A.* **2001**, *98*, 4343–8.

(19) Janssen, S.; Durussel, T.; Laemmli, U. K. *Mol. Cell* **2000**, *6*, 999–1011.

(20) Janssen, S.; Cuvier, O.; Muller, M.; Laemmli, U. K. *Mol. Cell* **2000**, *6*, 1013–24.

(21) Urbach, A. R.; Love, J. J.; Ross, S. A.; Dervan, P. B. *J. Mol. Biol.* **2002**, *320*, 55–71.

(22) Gottesfeld, J. M.; Belitsky, J. M.; Melander, C.; Dervan, P. B.; Luger, K. *J. Mol. Biol.* **2002**, *321*, 249–63.

(23) Shinohara, K.; Narita, A.; Oyoshi, T.; Bando, T.; Teraoka, H.; Sugiyama, H. *J. Am. Chem. Soc.* **2004**, *126*, 5113–8.

(24) Dickinson, L. A.; Burnett, R.; Melander, C.; Edelson, B. S.; Arora, P. S.; Dervan, P. B.; Gottesfeld, J. M. *Chem. Biol.* **2004**, *11*, 1583–94.

(25) Trauger, J. W.; Dervan, P. B. *Methods Enzymol.* **2001**, *340*, 450–66.

(26) Warren, C. L.; Kratochvil, N. C.; Hauschild, K. E.; Foister, S.; Brezinski, M. L.; Dervan, P. B.; Phillips, G. N., Jr.; Ansari, A. Z. *Proc. Natl. Acad. Sci. U. S. A.* **2006**, *103*, 867–72.

(27) Best, T. P.; Edelson, B. S.; Nickols, N. G.; Dervan, P. B. *Proc. Natl. Acad. Sci. U. S. A.* **2003**, *100*, 12063–8.

(28) Edelson, B. S.; Best, T. P.; Olenyuk, B.; Nickols, N. G.; Doss, R. M.; Foister, S.; Heckel, A.; Dervan, P. B. *Nucleic Acids Res.* **2004**, *32*, 2802–18.

(29) Coppola, G.; Choi, S. H.; Santos, M. M.; Miranda, C. J.; Tentler, D.; Wexler, E. M.; Pandolfo, M.; Geschwind, D. H. *Neurobiol. Dis.* **2006**, *22*, 302–11.

(30) Schoenfeld, R. A.; Napoli, E.; Wong, A.; Zhan, S.; Reutenauer, L.; Morin, D.;

Buckpitt, A. R.; Taroni, F.; Lonnerdal, B.; Ristow, M.; Puccio, H.; Cortopassi, G. A. *Hum. Mol. Genet.* **2005**, *14*, 3787–99.

(31) Clark, R. M.; Dalgliesh, G. L.; Endres, D.; Gomez, M.; Taylor, J.; Bidichandani, S. I. *Genomics* **2004**, *83*, 373–83.

(32) Sakamoto, N.; Ohshima, K.; Montermini, L.; Pandolfo, M.; Wells, R. D. *J. Biol. Chem.* **2001**, *276*, 27171–7.

(33) Blattes, R.; Monod, C.; Susbielle, G.; Cuvier, O.; Wu, J. H.; Hsieh, T. S.; Laemmli, U. K.; Kas, E. *EMBO J.* **2006**, *25*, 2397–408.

(34) Baird, E. E.; Dervan, P. B. *J. Am. Chem. Soc.* **1996**, *118*, 6141–6146.

(35) Dudouet, B.; Burnett, R.; Dickinson, L. A.; Wood, M. R.; Melander, C.; Belitsky, J. M.; Edelson, B.; Wurtz, N.; Briehn, C.; Dervan, P. B.; Gottesfeld, J. M. *Chem. Biol.* **2003**, *10*, 859–67.

(36) Chuma, M.; Sakamoto, M.; Yamazaki, K.; Ohta, T.; Ohki, M.; Asaka, M.; Hirohashi, S. *Hepatology* **2003**, *37*, 198–207.

(37) Pattyn, F.; Speleman, F.; De Paepe, A.; Vandesompele, J. *Nucleic Acids Res.* **2003**, *31*, 122–3.

(38) Bolstad, B. M.; Irizarry, R. A.; Astrand, M.; Speed, T. P. *Bioinformatics* **2003**, *19*, 185–93.

Chapter 2B

Footprinting Studies of Polyamides Targeting the [AAG]$_3$ Triplet Repeat and Related Sequences

Abstract

The recent discovery of a linear, beta-alanine linked polyamide that reverses the transcription defect of Friedreich Ataxia (FRDA) has generated the impetus to more fully characterize the binding properties of this polyamide and other related ligands. Polyamides are a class of programmable, sequence-specific minor groove DNA-binding small molecules, derived from the natural product distamycin, that hold promise for sequence-specific transcriptional modulation. The newly discovered ligand belongs to a subset of polyamides that bind narrower tracts of B DNA in a 1:1 ligand:DNA stoichiometry. This class of polyamides has received less attention due to its presumed sequence promiscuity. Interestingly, few genes beyond frataxin were found to be affected by the polyamide in genomic microarray transcript analysis. To more fully understand the binding properties of this and other related linear, beta-linked polyamides, we have synthesized eleven polyamides to study representative effects of polyamide length, polyamide amino acid mismatches, polyamide dye conjugates, and an altered polyamide tail on binding affinity and specificity for polypurine tracts of DNA. Polyamides with fewer than seven monomers appear to be the poorest DNA binders. The other synthesized polyamides maintained binding affinities of at least 10^8 M^{-1}.

Introduction

Friedreich Ataxia (FRDA), a neurodegenerative disorder characterized by the intronic 5'-GAA-3' trinucleotide repeat hyperexpansion (Figure 2.8A) that affects roughly 1 of 30,000 Caucasians,[1] may be caused by an equilibrium shift from B DNA toward a higher-order DNA structure[2–6] or by heterochromatin stabilization[7] that impedes transcription of the frataxin gene.[8–10] A ligand that stabilizes B DNA may shift the equilibrium towards B DNA or may aide heterochromatin opening,[7,11] enabling transcription. Polyamides, minor-groove binding, B DNA stabilizing small molecules, effect increased frataxin transcription in immortalized FRDA cell culture at micromolar concentrations.[12] Traditionally, the polyamide core contains *N*-methylimidazoles (Im), *N*-methylpyrroles (Py), and beta-alanines (β) that specify bases read from minor groove hydrogen bond contacts. A binding code relating polyamide structure to DNA sequence exists for hairpin polyamides and their unlinked and less entropically favored progenitors, the 2:1 binding polyamides.[13–17]

Despite the breadth of data studied for the hairpin and 2:1 binding polyamides, a 1:1 binding linear β-linked polyamide aptly targeted 5'-AAGAAGAAG-3' (Figure 2.8B) and increased frataxin mRNA transcript levels.[12] It is believed that this class of polyamides binds narrower DNA tracts, such as some polypurine sequences. Previous studies on a linear β-linked

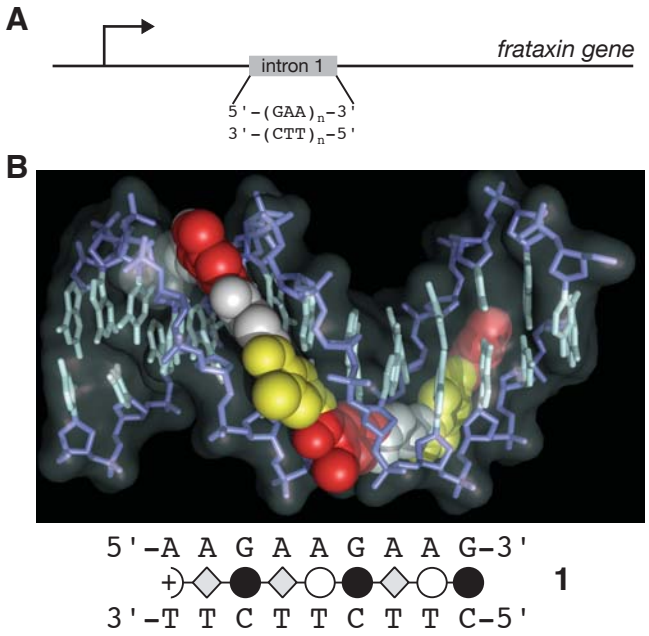

Figure 2.8. Frataxin gene structure and model of polyamide-DNA binding. a) A schematic showing the location of the 5'-GAA-3' repeat expansion in the frataxin gene. For afflicted individuals, $x < n < 1{,}800$. b) A model of polyamide **1** binding its target sequence. Red residues represent imidazoles, yellow residues pyrroles, white residues beta-alanines, and gray, the Dp tail. A ball-and-stick model oriented analogously to the 3D-model is shown below with filled circles representing imidazoles, hollow circles pyrroles, greyed diamonds beta-alanines, and the semi-circle with a plus, the Dp tail.

polyamide known to bind 5'-AAGAG-3' telomeric repeats[11,18] provided the foundations for further examination of binding preferences for this class of polyamides.[19–21] A preliminary binding code derived from quantitative DNase I footprinting and from Fe(II)-EDTA affinity cleavage experiments of the polyamide Im-*β*-Im-Py-*β*-Im-*β*-Im-Py-*β*-Dp (-EDTA) aligns the polyamide from N-terminus to C-terminus with respect to the polypurine DNA strand read from 3' to 5', pairing *N*-methylimidazole (Im) with any base pair and *N*-methylpyrrole (Py) or *β*-alanine (*β*) with A·T or T·A base pairs.[19–21] These rules enabled the design of Im-Py-*β*-Im-Py-*β*-Im-*β*-Dp (Figure 2.9, polyamide **1**), targeting 5'-AAGAAGAAG-3'. A constitutional isomer of **1**, Im-Py-*β*-Im-Im-*β*-Py-*β*-Dp (Figure 2.9, polyamide **2**) fails to bind 5'-AAGAAGAAG-3' and consequently does not increase frataxin transcription.[12] Strikingly, while polyamide **1** may bind any sequence of the composition 5'-WWNWWNWWN-3', only a handful of genes beyond frataxin are modulated in its presence. The binding preferences of polyamides **1** and **2**, have not been elucidated. One goal of this chapter is to establish the preferred binding orientation, to study the preferred binding stoichiometry, and to examine other polypurine tracts polyamide **1** may bind. Likewise, this chapter seeks to establish that polyamide **2** binds DNA.

Because of the biological ramifications of polyamides **1** and **2**, it is necessary to explore other small molecules that may alleviate the transcription defect of the frataxin gene. While polyamide **1** upregulates frataxin expression in Epstein-Barr virus immortalized cell culture samples,[12] a variety of polyamides harboring similar binding affinities and specificities may increase chances of successful frataxin upregulation in an FRDA mouse model.[22] A polyamide consists of aromatic heterocycle and aliphatic amino acid monomers as well as a tail, which is typically 3-(dimethylamino)-1-propylamine (Dp). Polyamide **1** offers two obvious modification points, the truncation of eight monomers to fewer and the alteration of the Dp tail.

While polyamide **2** effected no change in frataxin mRNA transcript levels,[12] this polyamide contains two mutations from polyamide **1**. It is unclear if this double mutation

is necessary to prevent binding to 5'-AAGAAGAAG-3'. Single amino acid mutation polyamides should bind 5'-AAGAAGAAG-3' more poorly than polyamide **1**. Their relative affinity for this site as compared to **2** will be studied.

Polyamide-dye conjugate compounds enable the visualization of polyamide nuclear localization[12,23–25] and may aide the likelihood of nuclear localization and subsequent cellular activity.[25,26] A final consideration studies the energetic penalty of attaching a fluorescent dye to polyamide **1**.

The characterization of this series of ten polyamides by quantitative DNase I footprinting and in one instance methidium-propyl EDTA (MPE) footprinting, and a polyamide-EDTA conjugate by affinity cleavage footprinting marks a first step toward expanding and understanding the known repertoire of 1:1 binding linear *β*-linked polyamides.

Results

Eleven polyamides have been synthesized (Figure 2.9) related to the match polyamide **1** and the mismatch polyamide **2** that were originally used in immortalized cell culture frataxin expression studies.[12] Polyamides were incubated with pJWP2, pJWP5, or pJWP10, as noted, for 14 h prior to DNase I cleavage, methidium propyl EDTA (MPE) digestion, or affinity cleavage. Initial specificity studies of polyamides **1** and **2** are reported. Furthermore, the effects of four variables relating to polyamide **1** or **2** on binding affinity were studied—the length of the DNA binding ligand, the composition of the charged carboxy-terminal tail appended to the polyamide, the mutation of a single amino acid on the ligand, and the presence of the BODIPY FL dye (Figure 2.9).

Plasmid Design

Three plasmids, pJWP2, pJWP5, and pJWP10 were designed to harbor binding sites for polyamides **1**–**8** and polyamides **9**–**10** (Figure 2.10). Plasmid pJWP2 contains

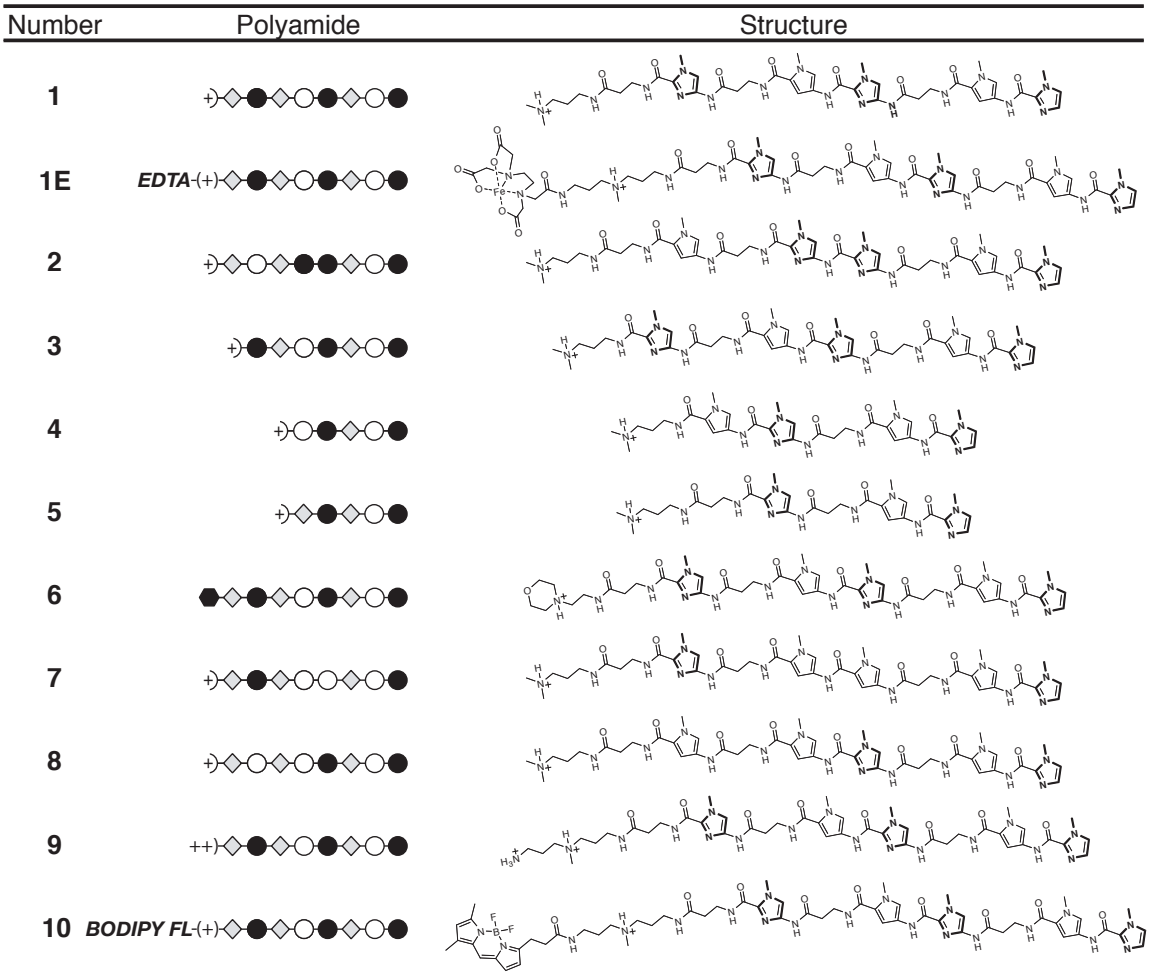

Figure 2.9. A list of polyamide structures utilized in footprinting studies on $[AAG]_3$ repeats. The ball-and-stick structures contain filled circles (*N*-methylimidazoles), empty circles (*N*-methylpyrroles), and greyed diamonds (β-alanines), connected by straight lines (amide bonds). The semi-circle with a plus represents 3-(dimethylamino)-1-propylamine, the filled hexagon represents 4-(2-aminoethyl) morpholine, and the double-plus or a plus in parentheses represents 3,3'-diamino-*N*-methyl-dipropylamine. Dyes and EDTA are represented by their written name appended to the C-terminal tail.

four binding sites – 5'-AAGAAGAAG-3' (Figure 2.10, Site **III**) for polyamide **1**, 5'-AAAAGGAAG-3' (Figure 2.10, Site **IV**) for polyamide **2**, 5'-AAAAAGAAG-3' (Figure 2.10, Site **V**) for polyamide **7**, and 5'-AAGAAAAAG-3' (Figure 2.10, Site **VI**) for polyamide **8**. Binding sites **V** and **VI** contain single mismatch transitions (G to A) relative to binding site **III**; binding site **IV** contains a double mismatch transition (G to A and A to G), enabling specificity of *N*-methylpyrrole and *N*-methylimidazole to be tested for several of the eight monomer polyamides. The spacer sequence between binding sites has been held constant – 5'-CCGGGGCC-3' – analogous to the spacers originally used to

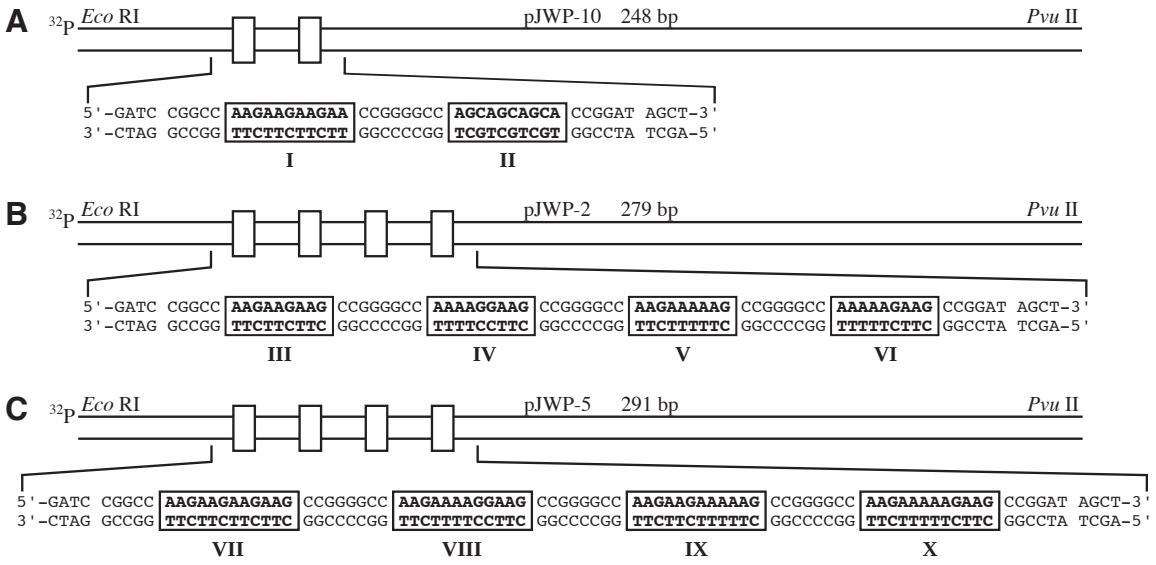

Figure 2.10. Plasmid insert sequences utilized for footprinting $[AAG]_3$-targeting polyamides. a) Schematic showing the sequence of the hybridized insert, 5'-^{32}P label position, and PCR amplicon for pJWP10 plasmid containing the boxed 11-base pair and 10-base pair 1:1 and 2:1 stoichiometry binding sites, **I** and **II**, respectively. b) Schematic showing the sequence of the hybridized insert, 5'-^{32}P label position, and PCR amplicon for pJWP2 plasmid containing the boxed 9-base pair target sites **III**, **IV**, **V**, and **VI**. c) Schematic showing the sequence of the hybridized insert, 5'-^{32}P label position, and PCR amplicon for pJWP5 plasmid containing the boxed 12-base pair target sites **VII**, **VIII**, **IX**, and **X**.

study binding specificity and affinity of 1:1 binding β-linked linear polyamides.[20] Plasmid pJWP5 contains the same sequence composition as pJWP2 but with 5'-AAG-3' appended immediately flanking the 5' portion of each binding site (Figure 2.10)—dye conjugate **10** is substantially longer than polyamide **1**. Plasmid pJWP10 contains binding sites for the 1:1 ligand:DNA stoichiometry, 5'-AAGAAGAAGAA-3' (Figure 2.10, Site **I**) and 2:1 ligand:DNA stoichiometry 5'-AGCAGCAGCA-3' (Figure 2.10, Site **II**). Site **I** enables the elucidation of the binding orientation for polyamide **1** against the polypurine strand of DNA.

Characterization of Polyamide 1 Binding Affinity, Stoichiometry, and Orientation

Polyamide **1** has been footprinted on the amplicon from pJWP10 to examine preference for 1:1 polyamide:DNA binding stoichiometry versus 2:1 polyamide:DNA binding stoichiometry. Figure 2.11A shows the DNase I footprints of polyamide **1** for

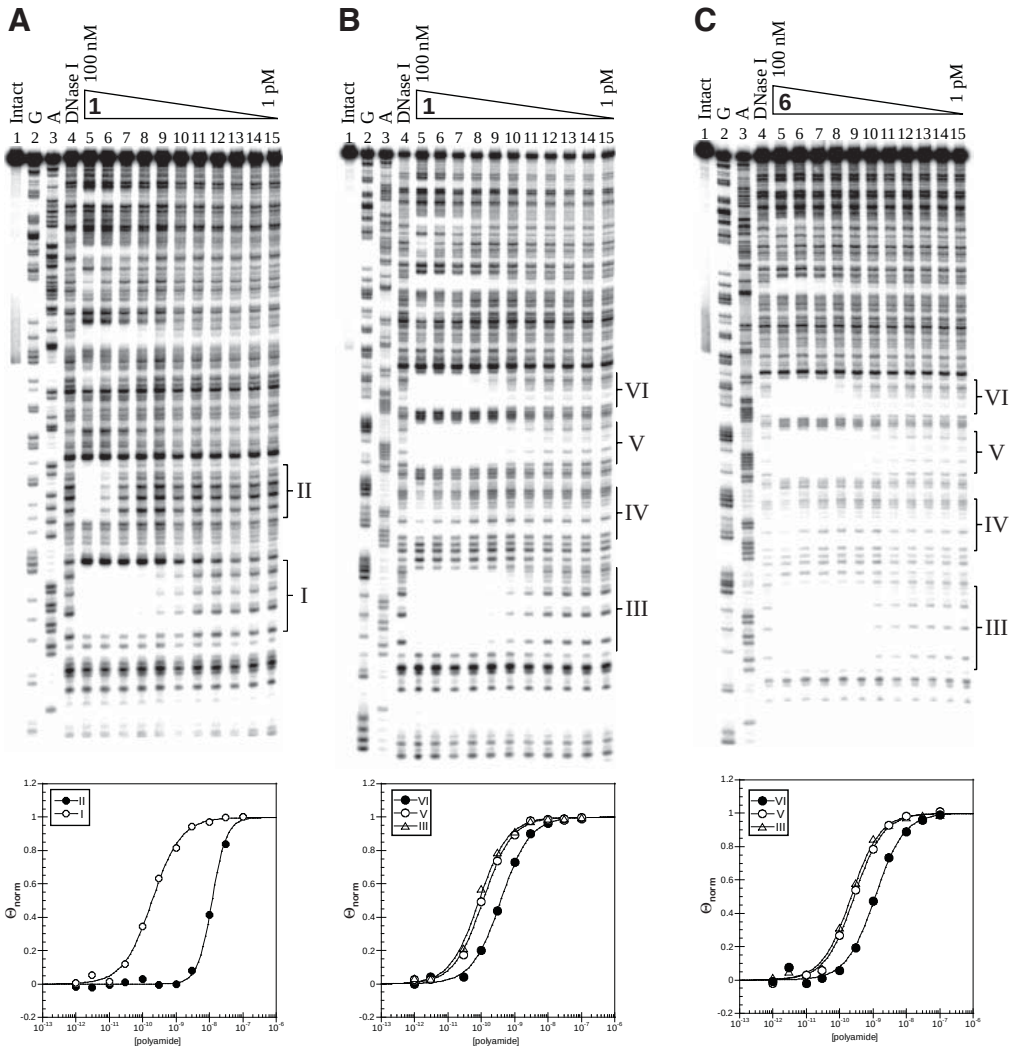

Figure 2.11. Quantitative DNase I footprint titrations for an $[AAG]_3$-targeting polyamide and a 4-(2-aminoethyl) morpholine tail variant. Binding stoichiometry preferences (**A**) and a limited set of binding preferences (**B**) for polyamide **1** and (**C**) for polyamide **2**. Lane 1 contains intact DNA from pJWP10 (**A**) or pJWP2 (**B, C**); lanes 2 and 3 contain G and A chemical sequencing reactions; and lane 4 contains DNase I digested DNA. Lanes 5–15 contain 100 nM, 30 nM, 10 nM, 3 nM, 1 nM, 300 pM, 100 pM, 30 pM, 10 pM, 3 pM, and 1 pM polyamide concentrations, respectively along with DNA from pJWP10 (**A**) or pJWP2 (**B, C**). DNase I digestion of lanes 5–15 proceeds under identical conditions to lane 4. Binding sites from pJWP10 and pJWP2 are identified as roman numerals to the right of each gel. Binding isotherms are shown directly beneath each gel. Hollow circles represent binding site **I** and filled circles binding site **II** for **A**. Hollow triangles represent binding site **III**, hollow circles binding site **V**, and filled circles binding site **VI** for **B**.

these two binding sites and the corresponding binding isotherms derived from these footprints. Table 2.4 shows the corresponding binding affinity data for polyamide **1** on pJWP10. Like the previously reported polyamide, Im-*β*-Im-Py-*β*-Im-*β*-Im-Py-*β*-Dp that targets 5'-AAAGAGAAGAG-3' with 31.5-fold preference over 5'-AGCGCAGCGCT-3',[21]

Table 2.4. Binding affinities (K_a, M^{-1}) of polyamide **1** to sites **I** and **II**. Columns are divided by binding site, with sequences listed 5' to 3' below the binding site number. Values reported are the mean values from at least three DNase I footprinting titration experiments, with the standard deviation given in parentheses. Bracketed numbers below the binding affinities represent the fold decrease in binding affinity relative to the highest affinity site in the row.

Number	Polyamide	I AAGAAGAAGAA	II AGCAGCAGCA
1		**4.6 (± 0.5) × 10^9** **[1]**	8.2 (± 0.3) × 10^7 **[57]**

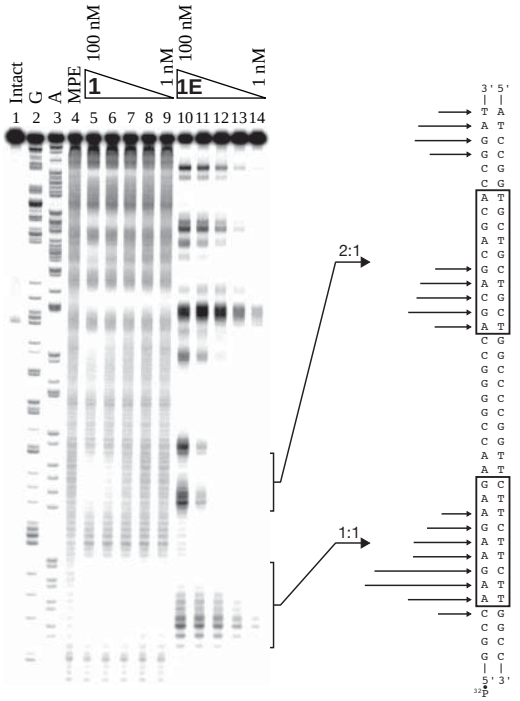

Figure 2.12. Methidium-propyl EDTA (MPE) footprinting of polyamide **1** and affinity cleavage of polyamide **1E** on pJWP10. The affinity cleavage sites for the 1:1 binding stoichiometry site (**I**) and 2:1 binding stoichiometry site (**II**) are shown schematically to the right of the gel. Arrows representing the affinity cleavage sites are drawn proportional to the radiation intensity, as calculated from lane 11. Lane 1 contains intact DNA from pJWP10; lanes 2 and 3 contain G and A chemical sequencing reactions; and lane 4 contains MPE digested DNA. Lanes 5–9 and lanes 10–14 contain 100 nM, 30 nM, 10 nM, 3 nM, and 1 nM polyamide **1** or polyamide **1E** concentrations, respectively as indicated, along with DNA from pJWP10. Lanes 5–9 were treated with MPE in an identical fashion to lane 4.

polyamide **1** prefers to bind DNA in a 1:1 stoichiometry (site **I**, non-cooperative binding isotherms $n = 1$) with 57-fold preference over the 2:1 polyamide:DNA binding mode (site **II**, cooperative binding isotherms $n = 2$). Affinity cleavage experiments of **1E** on pJWP10 (Figure 2.12) present cleavage patterns in concordance with the observed binding modes from the DNase I footprint derived isotherms. Additionally, the cleavage patterns of **1E** at site **I** confirm polyamide orientation of N-terminus to C-terminus read from 3' to 5' against the polypurine strand of DNA. This binding orientation agrees with that previously observed for Im-*β*-Im-Py-*β*-Im-*β*-Im-Py-*β*-Dp.[21]

Intriguingly, polyamide **1** exhibits a 2.4-fold higher affinity to binding site **III** (Figure 2.11B and Table 2.5) than to binding site **I** (Figure 2.11A and Table 2.4) even though the core 5'-AAGAAGAAG-3' sequence remains the same. This disparity in affinity is likely due to unique DNA microstructures resulting from a difference in 3'-flanking sequence between the two binding sites. Site **I** has a 3'-flanking sequence of 5'-AACC-3', whereas

that for site **III** is 5'-CCGG-3'.

Polyamide Length/Affinity Titration

Polyamides **1** and **3**–**5** were synthesized to study the effect of number of monomers per polyamide (length) on binding affinity to 5'-AAGAAGAAG-3' (Figure 2.9). Figures 2.11 and 2.13 show the DNase I footprints of these compounds and the corresponding binding isotherms derived from these footprints. Table 2.5 summarizes the binding affinity data for polyamides **1** and **3**–**5**. Polyamide **1,** composed of 8 monomers, binds site **III** with highest affinity in this series (K_a = 1.1 × 10^{10} M^{-1}). The seven-monomer polyamide **3** removed the C-terminal *β*-alanine, creating a fourfold energetic penalty for binding site **III** (K_a = 2.5 × 10^9 M^{-1}). Further truncation proves to be energetically unfavorable. Two 5-monomer, truncated polyamides were synthesized, polyamides **4** and **5**. Polyamide **4** removes three monomers from the C-terminus of polyamide **1**; polyamide **5** removes three monomers from the N-terminus of polyamide **1** (Figure 2.9). While polyamide **4** harbors a threefold higher binding affinity than polyamide **5** (K_a = 1.8 × 10^6 M^{-1} for **4** versus K_a = 6.3 × 10^5 M^{-1} for **5**), polyamide **4** almost fully coats DNA at 100 mM concentration (Figure 2.13). No signs of coating were observed for polyamide **5**. In comparison to polyamide **1**, polyamides **4** and **5** have 6,100-fold and 17,000-fold lower binding affinities,

Table 2.5. Polyamide length titration series. Polyamide ball-and-stick structures and their corresponding numbers are identified in columns to the left of the reported K_a values (M^{-1}). Values reported are the mean values from at least three DNase I footprinting titration experiments, with the standard deviation given in parentheses. Bracketed values underneath each K_a represent the fold decrease in binding affinity relative to this highest affinity binder for the row. Bracketed values to the right of each K_a represent the fold decrease in binding affinity relative to the highest affinity binder in the column. Assays were performed at 25 ºC.

		III	IV	V	VI
Number	Polyamide	**AAGAAGAAG**	**AAAAGGAAG**	**AAGAAAAAG**	**AAAAAGAAG**
1	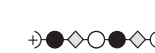	**1.1 (± 0.05) × 10^{10} [1]** **[1]**	≤ 1 × 10^7 **[1]** **[≥1,100]**	9.4 (± 0.5) × 10^9 **[1]** **[1.2]**	2.7 (± 0.3) × 10^9 **[1]** **[4.1]**
3		2.5 (± 0.2) × 10^9 **[4.4]** **[1]**	≤ 1 × 10^7 **[1]** **[≥250]**	2.2 (± 0.2) × 10^9 **[4.3]** **[1.1]**	1.0 (± 0.2) × 10^9 **[2.7]** **[2.5]**
4	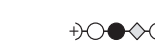	1.8 (± 0.6) × 10^6 **[6,100]** **[1.1]**	≤ 3.3 × 10^5 **[≥6.1]**	1.2 (± 0.3) × 10^6 **[7,800]** **[1.7]**	2.0 (± 0.4) × 10^6 **[1,300]** **[1]**
5		6.3 (± 1.6) × 10^5 **[17,000]** **[1]**	≤ 1 × 10^4 **[≥63]**	2.4 (± 0.6) × 10^5 **[39,000]** **[2.6]**	5.0 (± 0.7) × 10^5 **[5,400]** **[1.3]**
6		3.8 (± 0.7) × 10^9 **[2.9]** **[1]**	≤ 1 × 10^7 **[≥380]**	3.2 (± 0.6) × 10^9 **[2.9]** **[1.2]**	8.0 (± 1.1) × 10^8 **[3.4]** **[4.8]**

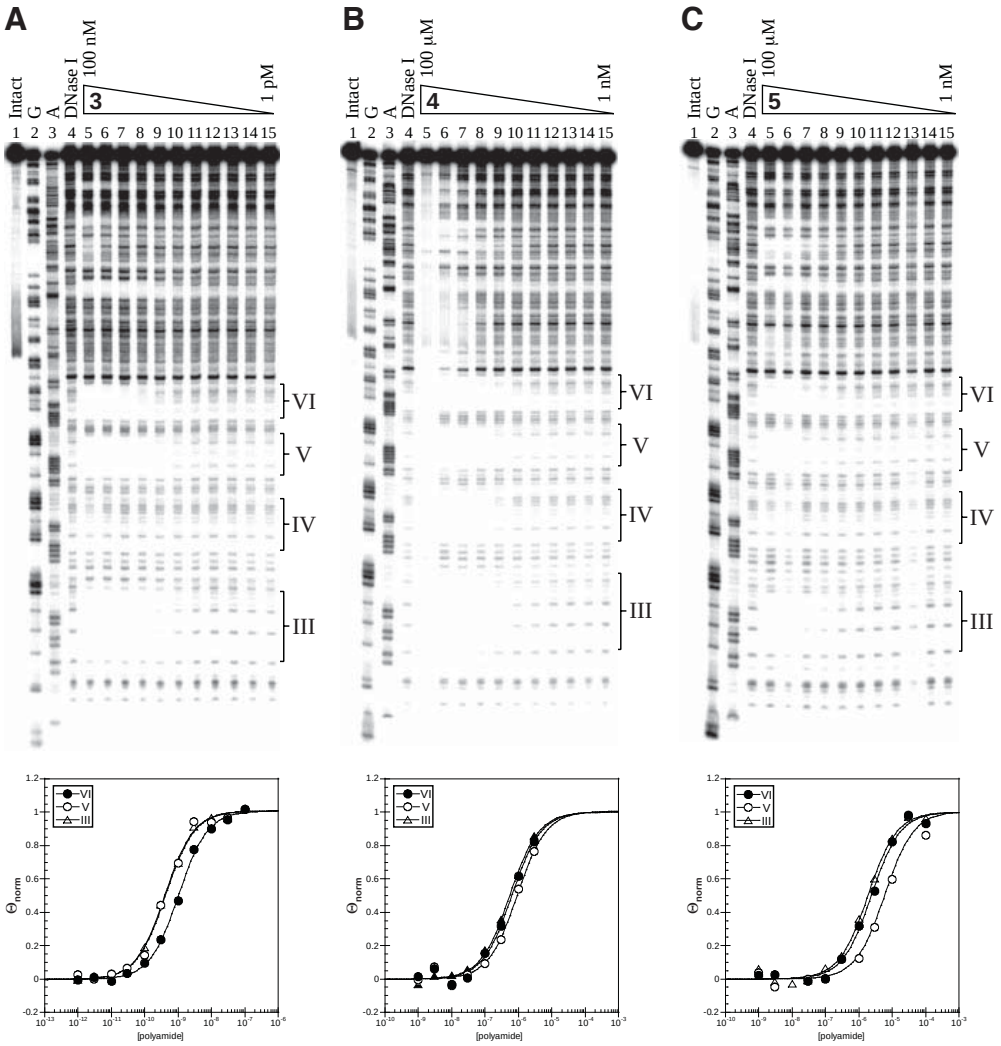

Figure 2.13. Quantitative DNase I footprint titrations showing effects of polyamide length on binding preferences and affinities. Lane 1 contains intact DNA from pJWP2; lanes 2 and 3 contain G and A chemical sequencing reactions; and lane 4 contains DNase I digested DNA. Lanes 5–15 contain 100 nM, 30 nM, 10 nM, 3 nM, 1 nM, 300 pM, 100 pM, 30 pM, 10 pM, 3 pM, and 1 pM of polyamide **3**, respectively for **A**. Lanes 5–15 contain 100 mM, 30 mM, 10 mM, 3 mM, 1 mM, 300 nM, 100 nM, 30 nM, 10 nM, 3 nM, and 1 nM of polyamide **4** or **5**, respectively for **B** and **C**. DNase I digestion of lanes 5–15 proceeds under identical conditions to lane 4. Binding sites from pJWP2 are identified as roman numerals to the right of each gel. Binding isotherms are shown directly beneath each gel. Hollow triangles represent binding site **III**, hollow circles binding site **V**, and filled circles binding site **VI**.

respectively.

Binding Affinity and Specificity of Polyamide 1 and Its Ethyl-Morpholino Derivative

Polyamides **1** and **6** were synthesized to study their relative binding affinities for designed match and mismatch sites. It is believed that the 4-(2-aminoethyl)-morpholine

tail may enhance the *in vitro* and *in vivo* potency of the polyamide bearing the core sequence Im-Py-*β*-Im-Py-*β*-Im-*β*.[27] Figures 2.11 and 2.13 show the DNase I footprints of these compounds and the corresponding binding isotherms derived from these footprints. Table 2.5 summarizes the binding affinity data comparing polyamides **1** and **6**. Polyamide **1** binds site **I** with threefold higher affinity than polyamide **6** ($K_a = 3.8 \times 10^9$ M^{-1}). The preference for site **III** over sites **IV**–**VI** is roughly comparable between polyamides **1** and **6**. Neither compound binds the double transition mismatch site **IV** at 30 nM concentrations. While some binding begins to occur at a concentration of 100 nM, there is an insufficient concentration range to accurately calculate the binding affinity at this site. Both compounds display little preference for the single transition mismatch site **V** over binding site **III**, and each has four or fivefold preference for site **III** over site **VI**, another single transition mismatch site.

Polyamide Single and Double Amino Acid Mutations

Three mismatch polyamides were designed and synthesized that should fail to bind site **III** of pJWP2 (Figure 2.9, polyamides **2**, **7**, and **8**). Figure 2.14 shows the DNase I footprints of these compounds and the corresponding binding isotherms derived from these footprints. Table 2.6 summarizes the binding affinity data comparing polyamides **2**, **7**, and **8**. Here, we report that polyamide **2** binds site **IV** with modest affinity ($K_a = 2.4 \times 10^8$ M^{-1}) and fails to bind sites **III** and **V**. A footprint begins to appear in binding site **VI**, a single G to A transition placed adjacent to an imidazole, although insufficient data precludes the calculation of an affinity for this site.

Polyamide **2** was formed by swapping two residues from polyamide **1**, an Im and a Py, to generate a constitutional isomer of polyamide **1**. Polyamides **7** and **8** represent single amino acid mutations from polyamide **1** (Figure 2.9). Polyamide **7** mutates an internal Im amino acid of polyamide **1** to a Py, forming a compound that should target binding site **V**. Polyamide **8** mutates the C-terminal Im amino acid of polyamide **1** to a Py, forming a

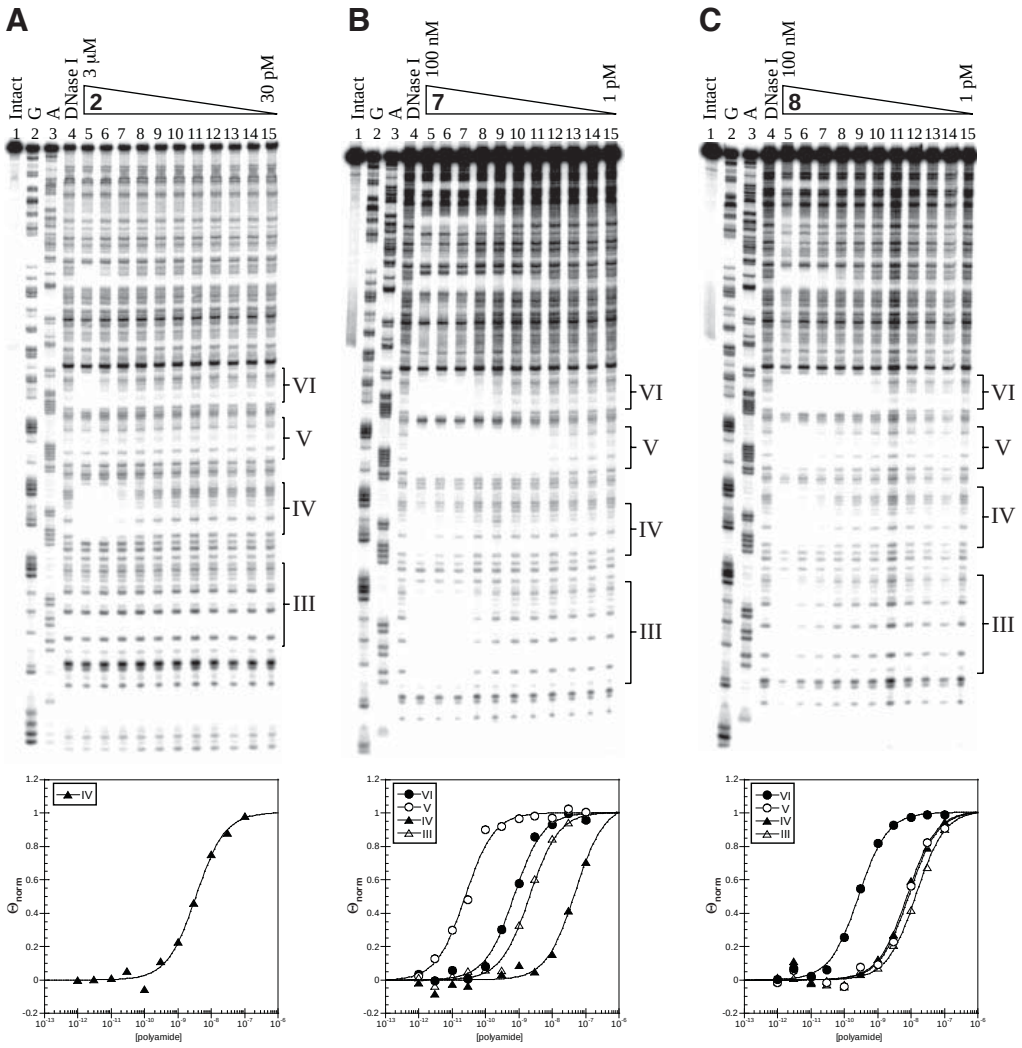

Figure 2.14. Quantitative DNase I footprint titrations examining binding affinities and preferences of double amino acid mismatch versus single amino acid mismatch polyamides on pJWP2. Lane 1 contains intact DNA from pJWP2; lanes 2 and 3 contain G and A chemical sequencing reactions; and lane 4 contains DNase I digested DNA. Lanes 5–15 contain 3 μM, 1 μM, 300 nM, 100 nM, 30 nM, 10 nM, 3 nM, 1 nM, 300 pM, 100 pM, and 30 pM polyamide **2**, respectively for **A**. Lanes 5–15 contain 100 nM, 30 nM, 10 nM, 3 nM, 1 nM, 300 pM, 100 pM, 30 pM, 10 pM, 3 pM, and 1 pM polyamide **7** or polyamide **8**, respectively for **B** and **C**. DNase I digestion of lanes 5–15 proceeds under identical conditions to lane 4. Binding sites from pJWP2 are identified as roman numerals to the right of each gel. Binding isotherms are shown directly beneath each gel. Hollow triangles represent binding site **III**, filled triangles binding site **IV**, hollow circles binding site **V**, and filled circles binding site **VI**.

compound that should target site **VI**. As predicted, polyamide **7** binds site **V** with $K_a = 4.3 \times 10^{10}$ M^{-1}, fourfold more strongly than polyamide **1** binds site **III**; polyamide **8** binds site **VI** with $K_a = 4.2 \times 10^9$ M^{-1}, 2.6-fold more poorly than polyamide **1** binds site **III**. A single

Table 2.6. Polyamide alternative mismatch control series. Polyamide ball-and-stick structures and their corresponding numbers are identified in columns to the left of the reported K_a's (M^{-1}). Values reported are the mean values from at least three DNase I footprinting titration experiments, with the standard deviation given in parentheses. Bracketed values underneath each K_a represent the fold decrease in binding affinity relative to this highest affinity binder for the row. Bracketed values to the right of each K_a represent the fold decrease in binding affinity relative to the highest affinity binder in the column. Assays were performed at 25 ºC.

		III	IV	V	VI
Number	Polyamide	**AAGAAGAAG**	**AAAAGGAAG**	**AAGAAAAAG**	**AAAAAGAAG**
1		**1.1 (± 0.05) × 10^{10} [1]** **[1]**	≤ 1 × 10^{7} **[≥24]** **[≥1,100]**	9.4 (± 0.5) × 10^{9} **[4.6]** **[1.2]**	2.7 (± 0.3) × 10^{9} **[1.6]** **[4.1]**
2		≤ 3.3 × 10^{5} **[≥33,000]** **[≥730]**	**2.4 (± 0.4) × 10^{8} [1]** **[1]**	≤ 3.3 × 10^{5} **[≥130,000]** **[≥730]**	≤ 1 × 10^{6} **[≥4,200]** **[≥240]**
7	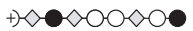	4.9 (± 0.9) × 10^{8} **[22]** **[88]**	2.7 (± 1.5) × 10^{7} **[8.9]** **[1,600]**	**4.3 (± 0.4) × 10^{10} [1]** **[1]**	1.3 (± 0.1) × 10^{9} **[3.2]** **[33]**
8		7.5 (± 0.9) × 10^{7} **[150]** **[56]**	1.3 (± 0.2) × 10^{8} **[1.9]** **[32]**	1.3 (± 0.2) × 10^{8} **[330]** **[32]**	**4.2 (± 0.9) × 10^{9} [1]** **[1]**

transition (A to G, site **III**) reduces binding affinity 88-fold for polyamide **7**, a double transition (site **VI**) only 33-fold, and a triple transition (site **IV**) 1600-fold. Polyamide **8** harbors similar levels of specificity as polyamide **7**. It binds both single and double transition mismatch sites **IV** and **V** 32-fold more poorly than its match site. A second single transition mismatch site (site **III**) lowers the binding affinity 56-fold.

Polyamide Dye Conjugate

Polyamide dye conjugates have functioned to identify the nuclear localization of a polyamide.[23–25] One polyamide-fluorophore conjugate was synthesized (Figure 2.9, compound **10**) to study the energetic penalty resulting from the attachment of a fluorescent BODIPY FL dye as compared to the energetic baseline provided by polyamide **9**. The DNase I footprinting gels and binding isotherms of polyamides **9**–**10** are shown in Figure 2.15. The corresponding binding affinities to sites **VII**–**X** are shown in Table 2.7.

Polyamide **9** binds site **VII** on pJWP5 with $K_a = 1.5 \times 10^{10}$ M^{-1}. It binds degenerately to sites **IX** and **X** with roughly sixty percent the affinity it has to site **VII**. It binds with 63-fold lower affinity to site **VIII**. Attaching BODIPY FL to polyamide **9** yields polyamide **10**, which harbors 21-fold lower affinity to binding site **VII** ($K_a = 7.3 \times 10^{8}$ M^{-1}). The

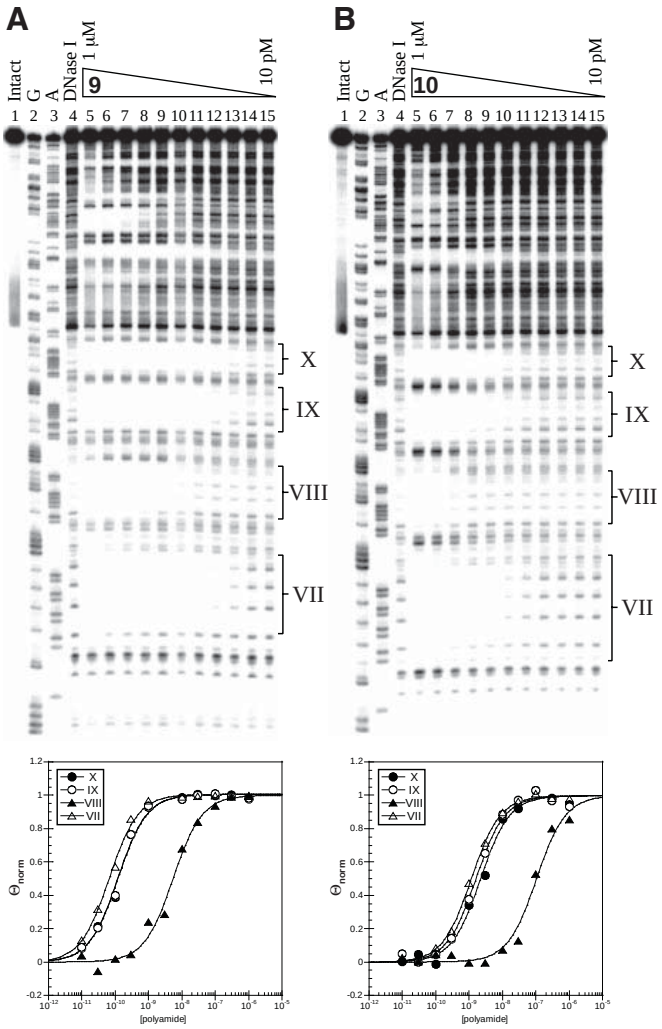

Figure 2.15. Quantitative DNase I footprint titrations showing the effects of BODIPY FL conjugation on binding preferences and affinities. Lane 1 contains intact DNA from pJWP5; lanes 2 and 3 contain G and A chemical sequencing reactions; and lane 4 contains DNase I digested DNA. Lanes 5-15 contain 1 μM, 300 nM, 100 nM, 30 nM, 10 nM, 3 nM, 1 nM, 300 pM, 100 pM, 30 pM, and 10 pM polyamide **9** or **10**, respectively for **A** and **B**. DNase I digestion of lanes 5–15 proceeds under identical conditions to lane 4. Binding sites from pJWP5 are identified as roman numerals to the right of each gel. Binding isotherms are shown directly beneath each gel. Hollow triangles represent binding site **VII**, filled triangles binding site **VIII**, hollow circles binding site **IX**, and filled circles binding site **X**.

Table 2.7. Polyamide dye conjugate series. Polyamide ball-and-stick structures and their corresponding numbers are identified in columns to the left of the reported K_a values (M^{-1}). Values reported are the mean values from at least three DNase I footprinting titration experiments, with the standard deviation given in parentheses. Bracketed values underneath each K_a represent the fold decrease in binding affinity relative to this highest affinity binder for the row. Bracketed values to the right of each K_a represent the fold decrease in binding affinity relative to the highest affinity binder in the column. Assays were performed at 25 ºC.

		VII	VIII	IX	X
Number	Polyamide	**AAGAAGAAGAAG**	**AAGAAAAGGAAG**	**AAGAAGAAAAAG**	**AAGAAAAAGAAG**
9	++)-◇●◇○●◇○●	**1.5 (± 0.1) × 10^{10} [1] [1]**	2.4 (± 0.8) × 10^{8} **[1] [63]**	9.3 (± 0.7) × 10^{9} **[1] [1.6]**	9.6 (± 1.2) × 10^{9} **[1] [1.6]**
10	***BODIPY FL***-(+)-◇●◇○●◇○●	7.3 (± 1.4) × 10^{8} **[21] [1]**	1.3 (± 0.5) × 10^{7} **[19] [56]**	6.1 (± 0.2) × 10^{8} **[15] [1.2]**	4.3 (± 0.5) × 10^{8} **[22] [1.7]**

specificity of binding in polyamide **10** remains roughly comparable to that seen without the dye.

Discussion

From the array of footprinting data, one can observe three trends: a minimum polyamide length required for high binding affinity, an energetic penalty associated with increased molecular weight in polyamide-dye conjugate, and a confirmation of the pairing rules originally established for 1:1 binding *β*-linked linear polyamides, including binding orientation and preferred binding stoichiometry.[20] For the 5'-AAGAAGAAG-3' tract of DNA, a minimum of seven monomers (present as Im, Py, or *β*) facilitates reasonable polyamide binding affinity. The appendage of BODIPY FL for tracking nuclear localization invokes a moderate energetic penalty on the binding affinity with minimal change to binding specificity.

The original sequence specificity studies on linear *β*-linked polyamides observed a tendency for pyrrole to pair adjacent to A·T or T·A base pairs and for imidazole to have no discernible preference for any of the base pairs.[20] While the current reported footprinting studies do not exhaustively place A·T, T·A, C·G, and G·C base pairs over an imidazole, a pyrrole, or a *β*-alanine, they both confirm and relax some of the prior observations. Four core polyamide sequences (containing Im, Py, or *β* monomers) have been studied in this footprinting series—Im-Py-*β*-Im-Py-*β*-Im-*β* (as per polyamides **1**, **6**, and **9**–**10**), Im-Py-*β*-Im-Im-*β*-Py-*β* (as per polyamide **2**), Im-Py-*β*-Py-Py-*β*-Im-*β* (as per polyamide **7**), and Im-Py-*β*-Im-Py-*β*-Py-*β* (as per polyamide **8**)—and enable the further elucidation of pairing rules in polypurine tracts of DNA.

Examining the sequence specificity for pyrrole (polyamides **7** and **8**, binding sites **III**–**VI**), one confirms a general preference for A·T base pairs over G·C. However, there is insufficient data to correlate the location of the pyrrole monomer within the polyamide to the level of sequence specificity observed. Polyamide **7** prefers to place an internal pyrrole monomer adjacent to A·T versus G·C with 88-fold specificity (binding site **V** versus binding

site **III**). Polyamide **8** places a pyrrole closer to the C-terminus adjacent to A·T versus G·C with 56-fold specificity (binding site **VI** versus binding site **III**). Placing an internally located pyrrole of polyamide **8** adjacent to G·C reduces binding affinity 32-fold (binding site **IV** versus binding site **VI**).

For imidazoles, there may be a slight preference for binding G·C base pairs over A·T base pairs in homopurine tracts of DNA. When placing a centrally located imidazole adjacent to an A·T base pair (polyamide **1** adjacent to site **V**), there appears to be no energetic penalty. A fourfold penalty exists when placing a more C-terminal imidazole adjacent to an A·T base pair (polyamide **1** adjacent to site **VI**). Polyamide **6** exhibits at least 240-fold specificity for G·C over A·T adjacent to an internal imidazole (binding site **IV** versus binding site **VI**). Interestingly, placing imidazole adjacent to an A·T base pair either internally (polyamide **8**, binding site **V**) or more C-terminally (polyamide **7**, binding site **VI**) may temper the energetic penalty of placing a pyrrole adjacent to a G·C base pair. It is also possible that this tempering effect results from altered DNA microstructure that better complements the polyamide sequence.

Of important consequence from these experiments is the elucidation of a series of molecules that may harbor biologically significant effects in Friedreich Ataxia cell culture. A threshold has been established for minimum polyamide length to promote reasonable binding affinities. Because of its similar binding properties, a polyamide with an ethyl-morpholino tail may improve the biological efficacy of polyamide **1**. Two new single amino acid mismatch control compounds have been characterized (polyamides **7** and **8**) that harbor high affinities for a polypurine tract of DNA but exhibit high specificity (56-fold to 88-fold) for their match site over a 5'-AAGAAGAAG-3' binding site. These new compounds can begin to answer whether a high binding affinity linear *β*-linked polyamide alone can effect increased frataxin expression.

While polyamide **1** has been observed to bind four other DNA sites beyond 5'-AAGAAGAAG-3', an exhaustive quantitative DNase I footprinting study of 9-base

pair DNA sequences is impractical, necessitating 131,072 unique binding sites. The global sequence preferences of Polyamide **1** will be studied using cognate site identifier (CSI) microarrays.[28]

MATERIALS AND METHODS

Chemicals

Polyamides **1**–**10** were synthesized by solid-phase methods on Boc-*β*-ala-PAM resin (Peptides International, Louisville, KY),[29] on Kaiser oxime resin (Nova Biochem, Laufelfingen, Switzerland),[30] or on Marshall-Liener resin (Nova Biochem, Laufelfingen, Switzerland).[31] Each step of the polyamide synthesis reaction was monitored by analytical HPLC. The polyamide-BODIPY FL conjugate was prepared as previously described.[24] The polyamide-EDTA conjugate (**1E**) was prepared essentially as previously described,[32] although dropwise addition of polyamide **9** in NMP over 1 hour to the vigorously stirred solution of EDTA-dianhydride, Hünig's base, and 1:1 DMSO:NMP was required. The

Table 2.8. MALDI-TOF Mass Spectral Data for Polyamides

Compound	Calc'd $[M+H]^+$	Obsv'd $[M+H]^+$	$\lambda_{max\ (nm)}$	ε ($L \cdot mol^{-1} \cdot cm^{-1}$)
1	914.45	914.55	289	43,125
1E	1231.57	1231.50	289	43,125
2	914.45	914.46	289	43,125
3	843.41	843.37	289	43,125
4	649.33	649.72	285	34,500
5	598.32	598.30	283	25,875
6	942.44	942.54	289	43,125
7	913.45	913.44	289	43,125
8	913.45	913.40	289	43,125
9	957.49	957.50	289	43,125
10	1231.60	1231.52	289	43,125

purity and identification of the final products were verified by analytical HPLC and MALDI-TOF MS. Mass spectral data and UV maxima, along with their estimated extinction coefficients are included for each compound in Table 2.8. *N*-methylpyrrolidinone, di-isopropylethylamine, 3-(Dimethylamino)-1-propylamine, 3,3'-diamino-*N*-methyl-dipropylamine, 4-(2-aminoethyl)morpholine, dimethylformamide, dichloromethane, dimethylsulfoxide, and EDTA-dianhydride were purchased from Sigma-Aldrich. Trifluoroacetic acid was purchased from Halocarbon. Acetic anhydride was from EMD Biosciences and methanol from Fluka. HBTU and Boc-*β*-Ala-OH were purchased from Peptides International. The Boc-*β*-Im-OH dimer was utilized in place of coupling *β*-alanine to *N*-methylimidazole, increasing the polyamide synthesis yield. BODIPY FL succinimidyl ester was purchased from Invitrogen. All commercially available reagents were used as received without additional purification.

Plasmid Preparation

Plasmids were constructed by ligating (Rapid DNA Ligation Kit, Roche) the following hybridized inserts (Integrated DNA Technologies, Coralville, IA) into the *Bam*HI / *Hin*DIII (Roche Biosciences) polycloning site in pUC19 (Sigma):

pJWP2. 5'-GATCCGGCCAAGAAGAAGCCGGGGCCAAAAGGAAGCCGGGGCCAAGAAAAAGCCGGGGCCAAAAAGAAGCCGGAT-3'·5'-AGCTATCCGGCTTCTTTTTGGCCCCGGCTTTTTCTTGGCCCCGGCTTCCTTTTGGCCCCG-GCTTCTTCTTGGCCG-3'.

pJWP5. 5'-GATCCGGCCAAGAAGAAGAAGCCGGGGCCAAGAAAAGGAAGCCGGGGCCAAGAAGAAAAAGCCGGGGCCAAGAAAAAGAAGCCGGAT-3'·5'-AGCTATCCGGCTTCTTTTTCTTGGCCCCGGCTTTTTCTTCTTGGCCCC-GGCTTCCTTTTCTTGGCCCCGGCTTCTTCTTCTTGGCCG-3'.

pJWP10. 5'-GATCCGGCCAAGAAGAAGAACCGGGGCCAGCAGCAGCACCGGAT-3'·5'-AGCTATCCGGTGCTGCTGCTGGCCCCGGTTCTTCTTCTTGGCCG-3'.

The ligated plasmid was then transformed into JM109 subcompetent cells (Promega).

Colonies were selected for a-complementation on 25 mL Luria-Bertani agar plates containing 50 mg/L ampicillin (Sigma), 120 mg/L IPTG (ICN Biomedicals), and 40 mg/L X-gal (Invitrogen) after overnight growth at 37 ºC. Cells were harvested after 16 h growth at 37 ºC in LB medium containing 50 mg/L ampicillin. Plasmid purification was performed using WizardPlus Midi Preps (Promega). The presence of the desired inserts was determined by capillary electrophoresis dideoxy sequencing methods.

Preparation of 5'-End-Labeled Fragments

Two 21 base-pair primer oligonucleotides, 5'-AATTCGAGCTCGGTACCCGGG-3' (forward) and 5'-CTGGCACGACAGGTTTCCCGA-3' (reverse) were constructed for PCR amplification (Integrated DNA Technologies). The forward primer was radiolabeled using [γ-^{32}P]-dATP (MP Biomedicals) and polynucleotide kinase (Roche), followed by purification using ProbeQuant G-50 spin columns (GE Healthcare). The desired DNA segment was amplified as previously described.[33] The labeled fragment was loaded onto a 7% nondenaturing preparatory polyacrylamide gel (5% cross-link), and the desired 279 (pJWP2), 291 (pJWP5), or 248 (pJWP10) base-pair band was visualized by autoradiography and isolated. Chemical sequencing reactions were performed according to published protocols.[33]

Quantitative DNase I Footprint Titrations, Affinity Cleavage, and Methidium Propyl EDTA (MPE) Footprinting Methods

All reactions were carried out in a volume of 400 mL according to published protocols.[33] Quantitation by storage phosphor autoradiography and determination of equilibrium association constants were as previously described.[33]

We thank the Caltech Sequence and Structure Analysis Facility for sequencing the insert regions of the plasmids. Funding was provided by the Friedreich Ataxia Research Alliance and the National Institutes of Health (GM27681).

References

(1) Campuzano, V.; Montermini, L.; Molto, M. D.; Pianese, L.; Cossee, M.; Cavalcanti, F.; Monros, E.; Rodius, F.; Duclos, F.; Monticelli, A.; Zara, F.; Canizares, J.; Koutnikova, H.; Bidichandani, S. I.; Gellera, C.; Brice, A.; Trouillas, P.; DeMichele, G.; Filla, A.; DeFrutos, R.; Palau, F.; Patel, P. I.; DiDonato, S.; Mandel, J. L.; Cocozza, S.; Koenig, M.; Pandolfo, M. *Science* **1996**, *271*, 1423–1427.

(2) Sakamoto, N.; Chastain, P. D.; Parniewski, P.; Ohshima, K.; Pandolfo, M.; Griffith, J. D.; Wells, R. D. *Mol. Cell.* **1999**, *3*, 465–475.

(3) Vetcher, A. A.; Napierala, M.; Iyer, R. R.; Chastain, P. D.; Griffith, J. D.; Wells, R. D. *J. Biol. Chem.* **2002**, *277*, 39217–39227.

(4) Vetcher, A. A.; Napierala, M.; Wells, R. D. *J. Biol. Chem.* **2002**, *277*, 39228–39234.

(5) Vetcher, A. A.; Wells, R. D. *J. Biol. Chem.* **2004**, *279*, 6434–6443.

(6) Napierala, M.; Dere, R.; Vetcher, A.; Wells, R. D. *J. Biol. Chem.* **2004**, *279*, 6444–6454.

(7) Saveliev, A.; Everett, C.; Sharpe, T.; Webster, Z.; Festenstein, R. *Nature* **2003**, *422*, 909–913.

(8) Bidichandani, S. I.; Ashizawa, T.; Patel, P. I. *Am. J. Hum. Genet.* **1998**, *62*, 111–121.

(9) Ohshima, K.; Montermini, L.; Wells, R. D.; Pandolfo, M. *J. Biol. Chem.* **1998**, *273*, 14588–14595.

(10) Grabczyk, E.; Usdin, K. *Nucleic Acids Res.* **2000**, *28*, 2815–2822.

(11) Janssen, S.; Durussel, T.; Laemmli, U. K. *Mol. Cell* **2000**, *6*, 999–1011.

(12) Burnett, R.; Melander, C.; Puckett, J. W.; Son, L. S.; Wells, R. D.; Dervan, P. B.; Gottesfeld, J. M. *Proc. Natl. Acad. Sci. U. S. A.* **2006**, *103*, 11497–11502.

(13) Dervan, P. B.; Edelson, B. S. *Curr. Opin. Struct. Biol.* **2003**, *13*, 284–299.

(14) Foister, S.; Marques, M. A.; Doss, R. M.; Dervan, P. B. *Bioorg. Med. Chem.* **2003**,

11, 4333–4340.

(15) Edayathumangalam, R. S.; Weyermann, P.; Gottesfeld, J. M.; Dervan, P. B.; Luger, K. *Proc. Natl. Acad. Sci. U. S. A.* **2004**, *101*, 6864–6869.

(16) Doss, R. M.; Marques, M. A.; Foister, S.; Dervan, P. B. *Chem. Biodivers.* **2004**, *1*, 886–899.

(17) Marques, M. A.; Doss, R. M.; Foister, S.; Dervan, P. B. *J. Am. Chem. Soc.* **2004**, *126*, 10339–10349.

(18) Janssen, S.; Cuvier, O.; Muller, M.; Laemmli, U. K. *Mol. Cell* **2000**, *6*, 1013–1024.

(19) Urbach, A. R.; Love, J. J.; Ross, S. A.; Dervan, P. B. *J. Mol. Biol.* **2002**, *320*, 55–71.

(20) Urbach, A. R.; Dervan, P. B. *Proc. Natl. Acad. Sci. U. S. A.* **2001**, *98*, 4343–4348.

(21) Dervan, P. B.; Urbach, A. R. In *Essays in Contemporary Chemistry: From Molecular Structure towards Biology*; Quinkert, G., Kisakürek, M. V., Eds.; Verlag Helvetica Chimica Acta: Zürich, 2001, p 327–339.

(22) Miranda, C. J.; Santos, M. M.; Ohshima, K.; Smith, J.; Li, L. T.; Bunting, M.; Cossee, M.; Koenig, M.; Sequeiros, J.; Kaplan, J.; Pandolfo, M. *FEBS Lett.* **2002**, *512*, 291–297.

(23) Belitsky, J. M.; Leslie, S. J.; Arora, P. S.; Beerman, T. A.; Dervan, P. B. *Bioorg. Med. Chem.* **2002**, *10*, 3313–3318.

(24) Best, T. P.; Edelson, B. S.; Nickols, N. G.; Dervan, P. B. *Proc. Natl. Acad. Sci. U. S. A.* **2003**, *100*, 12063–12068.

(25) Edelson, B. S.; Best, T. P.; Olenyuk, B.; Nickols, N. G.; Doss, R. M.; Foister, S.; Heckel, A.; Dervan, P. B. *Nucleic Acids Res.* **2004**, *32*, 2802–2818.

(26) Nickols, N. G.; Jacobs, C. S.; Farkas, M. E.; Dervan, P. B. *Nucleic Acids Res.* **2007**, *35*, 363–370.

(27) Kaizerman, J. A.; Gross, M. L.; Ge, Y. G.; White, S.; Hu, W. H.; Duan, J. X.; Baird,

E. E.; Johnson, K. W.; Tanaka, R. D.; Moser, H. E.; Burli, R. W. *J. Med. Chem.* **2003**, *46*, 3914–3929.

(28) Warren, C. L.; Kratochvil, N. C. S.; Hauschild, K. E.; Foister, S.; Brezinski, M. L.; Dervan, P. B.; Phillips, G. N.; Ansari, A. Z. *Proc. Natl. Acad. Sci. U. S. A.* **2006**, *103*, 867–872.

(29) Baird, E. E.; Dervan, P. B. *J. Am. Chem. Soc.* **1996**, *118*, 6141–6146.

(30) Belitsky, J. M.; Nguyen, D. H.; Wurtz, N. R.; Dervan, P. B. *Bioorg. Med. Chem.* **2002**, *10*, 2767–2774.

(31) Stafford, R. L., Ph. D. Thesis. California Institute of Technology, 2008.

(32) Herman, D. M.; Baird, E. E.; Dervan, P. B. *J. Am. Chem. Soc.* **1998**, *120*, 1382–1391.

(33) Trauger, J. W.; Dervan, P. B. *Methods Enzymol.* **2001**, *340*, 450–466.

Chapter 3

Quantitative Microarray Profiling of DNA Binding Molecules

The text of this chapter was taken in part from a manuscript co-authored with Katy A. Muzikar (California Institute of Technology), Josh Tietjen (University of Wisconsin, Madison), Christopher L. Warren (University of Wisconsin, Madison), Professor Aseem Z. Ansari (University of Wisconsin, Madison), and Professor Peter B. Dervan (California Institute of Technology).

(Puckett, J. W.; Muzikar, K. A.; Tietjen, J.; Warren, C. L.; Ansari, A. Z.; Dervan, P. B. "Quantitative Microarray Profiling of DNA Binding Molecules." *J. Am. Chem. Soc.* **2007**, *129*, 12310–12319.)

Abstract

A high-throughput Cognate Site Identity (CSI) microarray platform interrogating all 524,800 10-base pair variable sites is correlated to quantitative DNase I footprinting data of DNA binding pyrrole-imidazole polyamides. An eight-ring hairpin polyamide programmed to target the 5 bp sequence 5'-TACGT-3' within the hypoxia response element (HRE) yielded a CSI microarray-derived sequence motif of 5'-WWACGT-3' (W = A,T). A linear β-linked polyamide programmed to target a $(GAA)_3$ repeat yielded a CSI microarray-derived sequence motif of 5'-AARAARWWG-3' (R = G,A). Quantitative DNase I footprinting of selected sequences from each microarray experiment enabled quantitative prediction of K_a values across the microarray intensity spectrum.

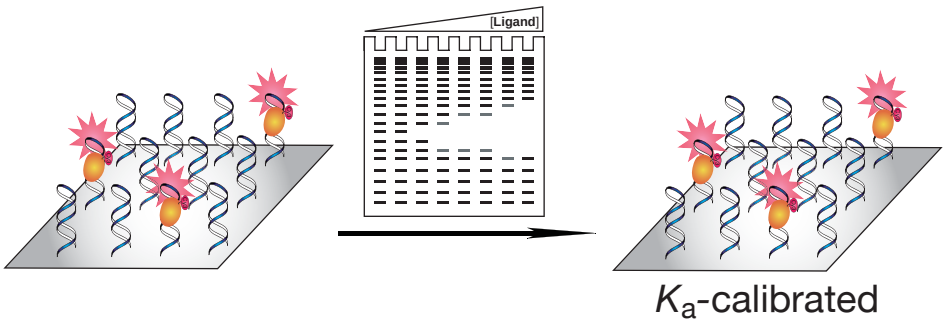

Introduction.

Cell-permeable small molecules which bind specific DNA sequences and are able to interfere with protein-DNA interfaces would be useful in modulating eukaryotic gene expression. For targeting the regulatory elements of eukaryotic genes, knowledge of the preferred binding landscape of the ligand and the energetics of each site would guide gene regulation studies. Pyrrole-imidazole polyamides are a class of cell permeable oligomers which can be programmed, based on simple aromatic amino acid pairing rules, to bind a broad repertoire of DNA sequences.[1] Knowledge of polyamide match sites has allowed us to pursue the characterization of the equilibrium association constants and hence, free energies, of hairpin polyamides for cognate DNA sites by quantitative footprint titration methods. Despite the predictive power of simple pairing rules, the sequence dependent variability of DNA minor groove shape affords significant variability in the range of affinities for match as well as all formal single and double base pair mismatch sites.[1]

Quantitative Footprint Titrations. Characterization of polyamide binding preferences has been studied using quantitative DNase I footprinting titrations, affording binding isotherms that enable rigorous determination of equilibrium association constant, K_a.[2] The resolution of footprinting is conservatively limited to association constants of twofold difference or greater. Polyamide binding preferences have frequently been interrogated using DNA fragments roughly 100 bp in size containing as many as four 6–10 bp binding sites, which are identical with the exception of a single position that iteratively exhibits A·T, T·A, C·G, and G·C base pairs. Each binding site is interspersed with an 8 or more base pair spacer region to prevent interaction between the binding sites.[3] Obtaining high quality data limits a ^{32}P end-labeled DNA fragment to four unique binding sites due to the resolving power of a polyacrylamide gel in a quantitative footprint titration. While DNase I footprinting has enabled the elucidation of a binding code for hairpin polyamides, a relatively limited set of binding sites has been studied. To comprehensively interrogate all four encoded positions of an eight-ring hairpin polyamide, one would need 136 unique

binding sites. In addition, interrogation of the base pairs flanking the polyamide core would necessitate 2,080 (for 6 bp total) or 32,896 (for 8 bp total) binding sites.

CSI Microarray Platform. Several high-throughput platforms have been developed to characterize the binding properties of ligand-DNA interactions.[4] Of these, two have explicitly studied the binding preferences of polyamides. The fluorescence intercalator displacement assay has interrogated polyamide binding to 512 unique 5 bp sequences in a microplate format.[4b] The more recently developed cognate site identifier (CSI) microarray platform presents all 32,896 unique eight-mers (scalable to all unique ten-mers) to fluorescently labeled polyamides, enabling an unbiased interrogation of binding preference.[4c] By coupling DNase I footprinting with the CSI microarray data, the binding affinities (K_a values) of a given DNA-binding molecule (such as a polyamide) for any DNA sequence can be determined (Figure 3.1). To date, CSI microarray intensities of hairpin polyamide-Cy3 conjugates have been linearly correlated to the K_a values of unlabeled polyamides.[4c] We will examine whether this relationship between DNase I footprint

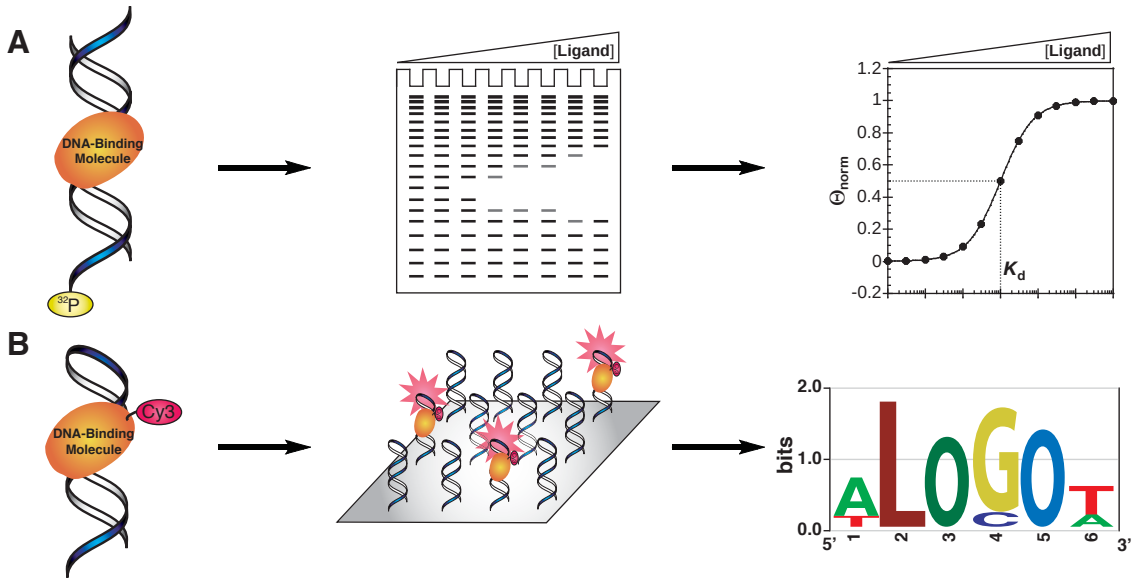

Figure 3.1. Methods for analyzing DNA binding specificity. (a) Quantitative DNase I footprinting gives rise to a defined equilibrium association constant at a specified binding site for a given DNA binding molecule. (b) The CSI microarray platform gives rise to relative binding preferences of an entire sequence space for the same molecule with a sequence logo as a standard summary output.

titration-derived K_a values for Cy3-labeled polyamides and the corresponding microarray data remains true for additional polyamide binding architectures. Because the Cy3-polyamide conjugate may alter sequence specificity when compared with its biologically active counterpart, the sequence specificities of fluorophore-labeled polyamide and the biologically relevant polyamide will also be determined.

A CSI microarray harbors immense sequence specificity data; determining how to best represent this data is critical. The first reported CSI work[4c] represented binding preferences as a sequence logo[5] derived from several motif-finding algorithms[6] that searched the highest *Z*-score bins (the ~300 highest intensities on the array), assigning equal weight to each sequence. It also examined the relative abundance of each sequence motif mutation within its respective *Z*-score bin.[4c] In this paper we observe that K_a-weighting sequence motifs does not alter the sequence logo appreciably. In addition, a comprehensive single base pair mutational analysis is performed, which quantifies the specificities encoded by the polyamide at each position the polyamide interacts with DNA.

Two Cy3-labeled polyamides of biological interest[7] are examined on the CSI microarray that displays all unique 10 base pair sequences. These polyamides include a hairpin structure whose sequence specificities can be predicted from the extensive DNase I footprinting data characterizing other pyrrole-imidazole polyamides[1] and a linear β-linked structure whose sequence specificity is less well understood.[8] In order to correlate the CSI relative affinities (intensities) to absolute affinities (K_a values), DNase I footprinting was performed on a subset of these sequences for both the Cy3-polyamide conjugates and the related, unlabeled polyamides of known biological activity.

Results and Discussion.

Polyamide Design. Two polyamide core sequences have been chosen as representative of both hairpin and linear β-linked polyamide architectures. These core recognition sequences exhibit biologically significant roles, modulating transcription in

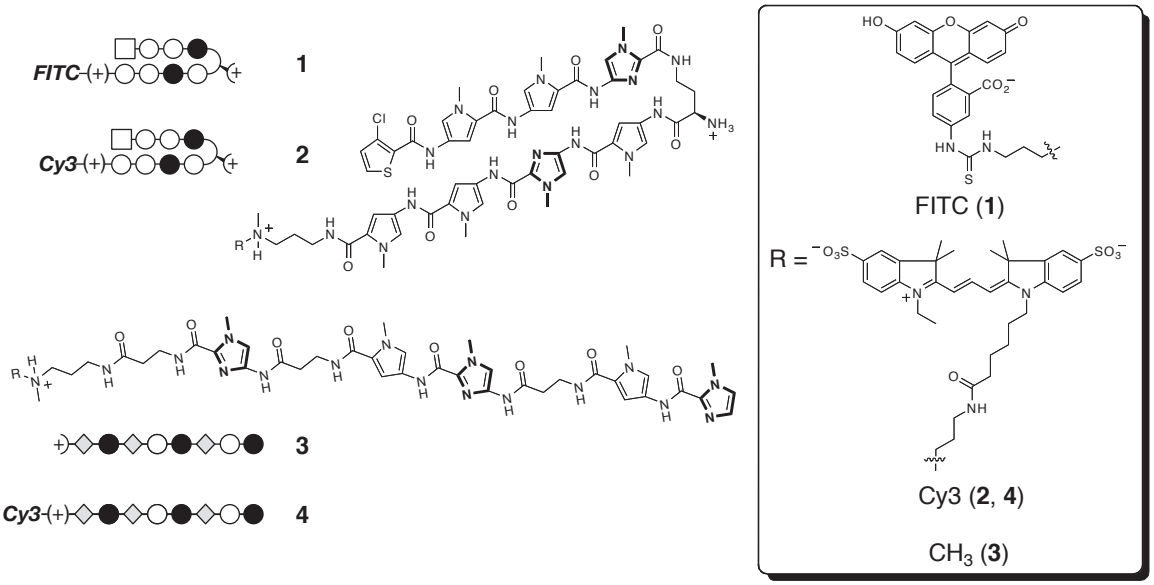

Figure 3.2. Polyamides for CSI Studies. Hairpin polyamides **1** and **2** targeted to the hypoxia response element (HRE), 5'-TACGTG-3'. Linear *β*-linked polyamides **3** and **4** targeted to GAA repeats in Friedreich's ataxia.

cell culture experiments.[7] Hairpin polyamides **1** and **2** (Figure 3.2), were selected based on results from a project in which a polyamide-fluorescein conjugate, Ct-Py-Py-Im-*(R)*-^{H2N}-γ-Py-Im-Py-Py-Dp-FITC (**1**) displaced hypoxia inducible factor-1α (HIF-1α) from the hypoxia response element (HRE) of the vascular endothelial growth factor (VEGF) gene, downregulating VEGF expression 60% in cell culture experiments.[7a,b] This eight-ring hairpin was programmed to bind the sequence 5'-WTWCGW-3' (W = A,T).[1,3c] In particular, polyamide **1** was shown to bind the HRE sequence, 5'-TACGTG-3' on the VEGF promoter by footprint titration.[7a,b] The Cy3 moiety was conjugated (**2**) at the same position as fluorescein for **1** to best mimic the binding properties between the two polyamides.

As with polyamide **1**, polyamide **3** (Figure 3.2) is known to bind its biologically relevant target. Polyamide **3**, Im-Py-*β*-Im-Py-*β*-Im-*β*-Dp, targets an intronic 5'-(GAA)$_n$-3' repeat hyperexpansion, enabling 2.5-fold upregulation of the frataxin gene, whose deficiency causes the neurodegenerative disorder Friedreich's ataxia.[7c] Limited knowledge about the linear *β*-linked class of polyamides[8] precludes the existence of binding rules. The linear *β*-linked architecture has the added complexity of binding in 1:1 and 2:1 ligand/DNA

stoichiometries, and we would anticipate that this class will be generally less useful due to sequence promiscuity resulting from multiple binding modes. Its 1:1 binding preferences for purine tracts, such as $(GAA)_n$, likely reflect shape selectivity for sequences with narrow DNA minor groove conformations.[8c] In a 2:1 binding stoichiometry, polyamide **3** would be predicted to target 5'-WGCWGCWGCW-3'.[8a] Remarkably, relatively few genes are affected from cell culture studies of **3** suggesting that this polyamide may be specific for 5'-AAGAAGAAG-3'.[7c] The Cy3 fluorophore has been conjugated to the C-terminal 3,3'-diamino-*N*-methyldipropylamine tail (polyamide **4**).

CSI Microarray design and results. CSI microarrays were synthesized using maskless array synthesis (MAS) technology[9] to display all 524,800 unique 10-base pair sites in quadruplicate across six microarrays. Replicates of individual hairpins occur on separate microarrays. Each hairpin on the chip consists of a self complementary palindromic sequence interrupted by a central 5'-GGA-3' sequence to facilitate hairpin formation: 5'-GCGC-$N^1N^2N^3N^4N^5N^6N^7N^8N^9N^{10}$-GCGC-GGA-GCGC-$N^{10'}N^{9'}N^{8'}N^{7'}N^{6'}N^{5'}N^{4'}N^{3'}N^{2'}N^{1'}$-GCGC-3' (N = A,T,C,G). Previous experiments have found that 95% of the oligonucleotides on the array form duplexes.[4c]

Polyamides **2** and **4** were slowly titrated onto the arrays and imaged at each concentration until saturation of the highest intensity binding sites was observed, 10 nM and 175 nM concentrations, respectively for **2** and **4**. After each small addition of polyamide, the arrays were washed prior to imaging. The data for each of the arrays was then normalized as previously described[4c] to give averaged sequence intensities of the 524,800 10-base pair sites for **2** and **4**. As found with previously reported CSI arrays,[4c] histograms of the probe intensities for **2** and **4** display a strong right-handed tail (Figure 3.3). The fractional standard deviations among probe replicates (standard deviation of replicates / average normalized intensity) average 0.15 ± 0.09 (polyamides **2** and **4**), for intensities exceeding 1×10^3 (Figure 3.4).

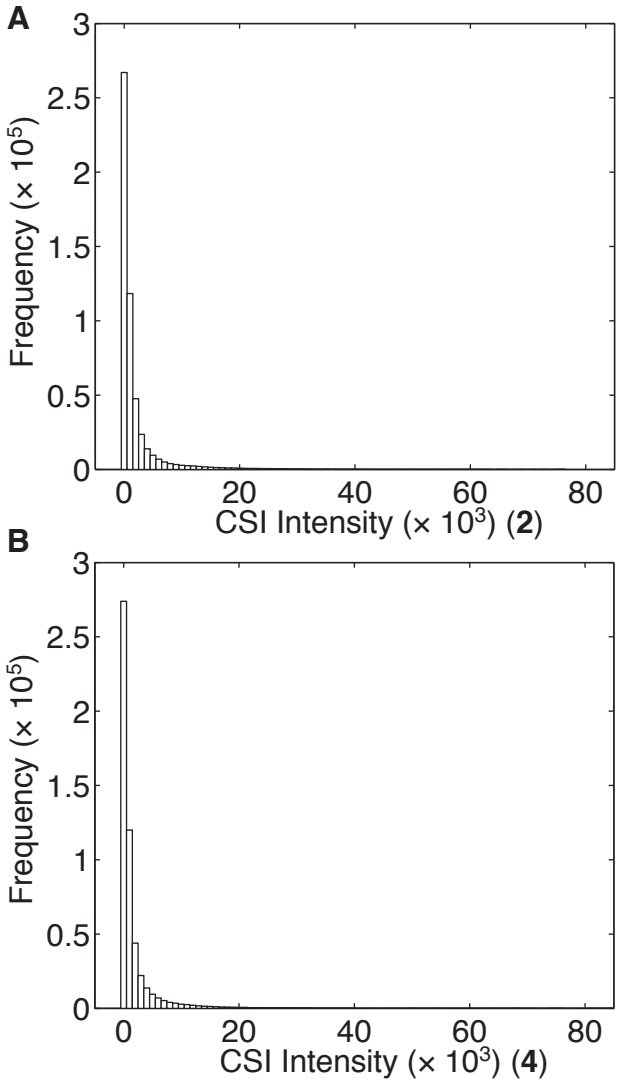

Figure 3.3. Histogram of microarray intensities. a) for polyamide **2**, b) for polyamide **4**

Plasmid Design. Three plasmids have been designed based on output from the CSI microarray intensities (Figure 3.5). Because of our interest in testing the dynamic range of the CSI assay in terms of the representative K_a values measured by a broad range of intensities, plasmids pKAM3 and pJWP17 were constructed to harbor binding sites of equal intensity spacing across a broad portion of each array's intensities, between highest and lowest intensities. The K_a values found using pKAM3 were tightly clustered across the three highest intensities, necessitating further interrogation. Plasmid pKAM4 was designed to probe three additional intensities. A single binding site (**IIIa** and **Ib**) was held constant

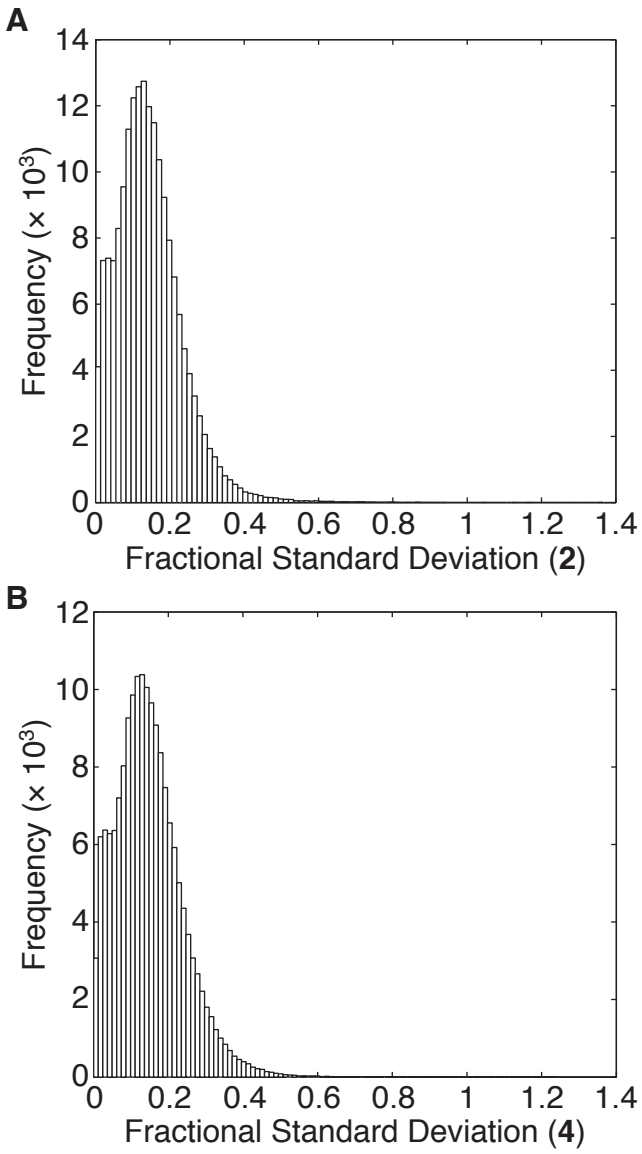

Figure 3.4. Histogram of microarray fractional standard deviations. Fractional standard deviation was calculated as standard deviation of intensities for a specific sequence / average sequence intensity for that specific sequence. a) for polyamide **2**, b) for polyamide **4**

between pKAM3 and pKAM4 to enable interplasmid comparison of binding affinities. Because pJWP17 afforded K_a values broadly spaced across the intensity spectrum, no further study was pursued.

Since we will directly compare footprinting-derived K_a values with CSI-array derived intensities, each plasmid binding site mimics the full 10 base pair binding site from the array in addition to two flanking base pairs on either side of the binding site: 5'-GC-

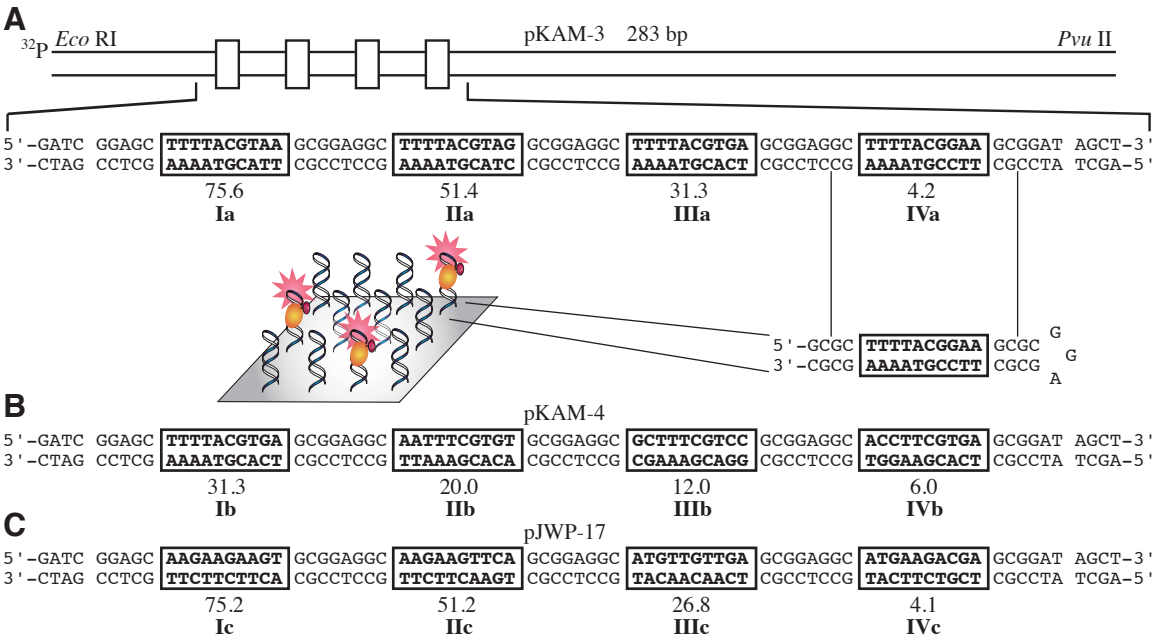

Figure 3.5. Insert sequences utilized in plasmids. Binding sites are boxed, labeled with their corresponding CSI array intensity ($\times 10^3$), and numbered. a) pKAM3 is shown, in addition to a microarray schematic demonstrating the relationship between the plasmid and a selected microarray sequence. b) pKAM4. c) pJWP17

$(N)_{10}$-GC-3' (N = A,T,C,G). Attempts to fully replicate the 5'-GCGC-$(N)_{10}$-GCGC-3' binding site from the array exhibited secondary structure formation when the respective amplicons were sequenced and separated by denaturing gel electrophoresis.

Quantitative DNase I Footprint Titrations: Affinity and Specificity Determination. Hairpin polyamides **1** and **2** were incubated each for 14 h with pKAM3 or pKAM4 prior to DNase I cleavage. These two polyamides were found to bind each of seven unique 10-base pair binding sites in the same rank-order, preferentially binding 5'-TTTTACGTAA-3' with affinities of 7.5×10^9 M^{-1} (**1**) and 4.5×10^9 M^{-1} (**2**) (Figure 3.6 and Table 3.1). Replacing the flourescein dye on polyamide **1** with Cy3 (polyamide **2**) introduced an energetic penalty that ranged from 1.5- to 10-fold, with the minimum penalty occurring at the two highest CSI intensity binding sites (Table 3.1). Polyamide **2** differentiated the highest and lowest affinity binding sites by 70-fold, slightly more than the 50-fold differentiation found for the fluorescein-labeled polyamide **1**.

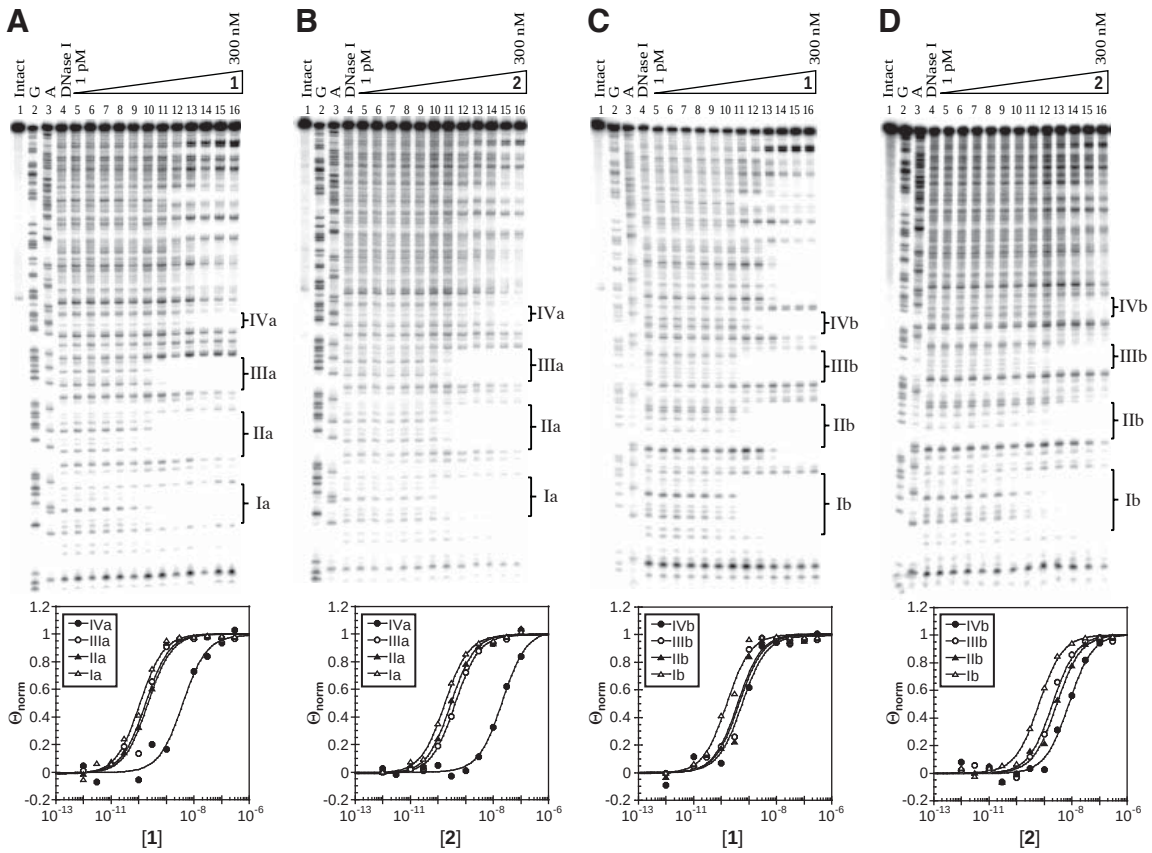

Figure 3.6. DNase I footprinting gels and corresponding isotherms of polyamides **1** and **2** on pKAM3 and pKAM4. a) Polyamide **1** on pKAM3. b) Polyamide **2** on pKAM3. c) Polyamide **1** on pKAM4. d) Polyamide **2** on pKAM4

Table 3.1. Quantitative DNase I Footprinting Derived K_a values (M^{-1}) for Polyamides **1** and **2**. The 10 base pair binding sites and corresponding CSI Microarray intensities are found in each column. All footprinting incubations were conducted at a minimum in triplicate at 23 ºC for 14 h. Standard deviations are shown in parentheses. The bracketed numbers are $K_{a–max}/K_{a–current}$ to compare values within each polyamide series.

pKAM-3		**Ia**	**IIa**	**IIIa**	**IVa**
Polyamide		**TTTTACGTAA**	**TTTTACGTAG**	**TTTTACGTGA**	**TTTTACGGAA**
1	FITC-(+)	$7.5 (\pm1.8) \times 10^9$ **[1]**	$5.1 (\pm0.6) \times 10^9$ **[1.5]**	$4.2 (\pm0.6) \times 10^9$ **[1.8]**	$1.5 (\pm0.8) \times 10^8$ **[50]**
2	Cy3-(+)	$4.5 (\pm1.0) \times 10^9$ **[1]**	$3.0 (\pm0.6) \times 10^9$ **[1.5]**	$2.1 (\pm0.3) \times 10^9$ **[2.1]**	$6.2 (\pm2.0) \times 10^7$ **[73]**
CSI Intensity ($\times 10^3$)		75.6 (±9.9)	51.4 (±7.4)	31.3 (±4.8)	4.2 (±1.4)

pKAM-4		**Ib**	**IIb**	**IIIb**	**IVb**
Polyamide		**TTTTACGTGA**	**AATTTCGTGT**	**GCTTTCGTCC**	**ACCTTCGTGA**
1	FITC-(+)	$5.4 (\pm0.9) \times 10^9$ **[1.3]**	$2.3 (\pm0.1) \times 10^9$ **[3.2]**	$2.8 (\pm0.2) \times 10^9$ **[2.6]**	$1.5 (\pm0.2) \times 10^9$ **[5]**
2	Cy3-(+)	$1.6 (\pm0.2) \times 10^9$ **[2.8]**	$4.0 (\pm0.9) \times 10^8$ **[11]**	$5.8 (\pm0.7) \times 10^8$ **[7.8]**	$1.3 (\pm0.2) \times 10^8$ **[34]**
CSI Intensity ($\times 10^3$)		31.3 (±4.8)	20.0 (±2.8)	12.0 (±1.5)	6.0 (±0.4)

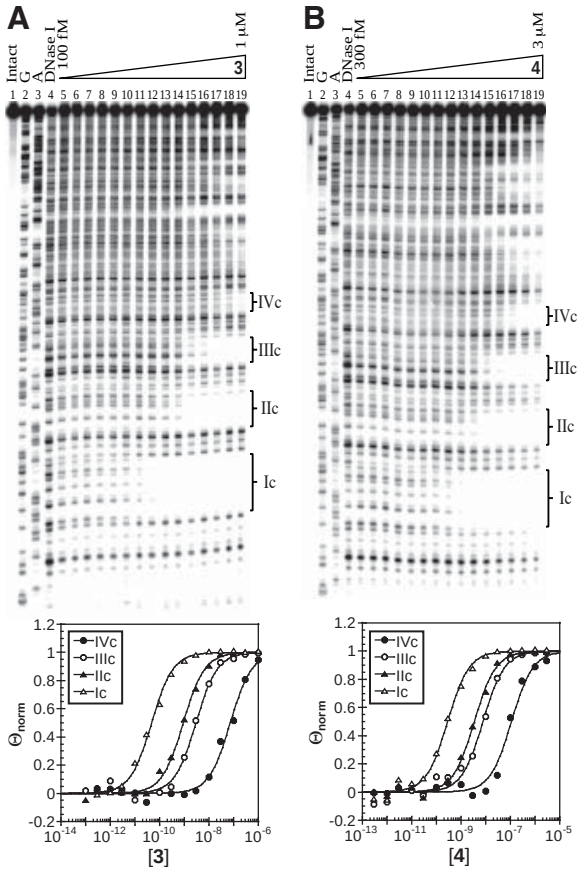

Figure 3.7. DNase I footprinting gels and corresponding isotherms of polyamides **3** and **4** on pJWP17

Table 3.2. Quantitative DNase I Footprinting Derived K_a values (M^{-1}) for Polyamides **3** and **4**. The 10 base pair binding sites and corresponding CSI Microarray intensities are found in each column. All footprinting incubations were conducted at a minimum in triplicate at 23 ºC for 14 h. Standard deviations are shown in parentheses. The bracketed numbers are $K_{a–max}/K_{a–current}$ to compare values within each polyamide series.

pJWP-17	Ic	IIc	IIIc	IVc
Polyamide	**AAGAAGAAGT**	**AAGAAGTTCA**	**ATGTTGTTGA**	**ATGAAGACGA**
3 	2.4 (±0.6) × 10^{10} **[1]**	9.3 (±2.3) × 10^{9} **[3]**	2.9 (±0.7) × 10^{8} **[80]**	1.0 (±0.4) × 10^{7} **[2400]**
4 	3.3 (±0.7) × 10^{9} **[1]**	2.7 (±0.8) × 10^{8} **[10]**	1.1 (±0.4) × 10^{8} **[30]**	1.0 (±0.2) × 10^{7} **[330]**
CSI Intensity (× 10^3)	75.2 (±9.2)	51.2 (±6.2)	26.8 (±7.3)	4.1 (±0.4)

Linear *β*-linked polyamides **3** and **4** were each incubated for 14 h with pJWP17 prior to DNase I cleavage. They bound four unique 10-base pair sites in the same rank-order, preferentially binding 5'-AAGAAGAAGT-3' (Table 3.2 and Figure 3.7).

Appending the Cy3 dye to polyamide **3** either had no effect on affinity or reduced binding affinity as much as 30-fold (Table 3.2). Polyamide **3** bound all four binding sites over a 2400-fold range in affinity, eight times broader than for polyamide **4**.

Calibrating microarrays for K_a prediction. Because DNase I footprinting enables the calculation of K_a and the direct comparison of four binding sites in a single assay, determining energetics data from CSI microarrays is crucial for understanding the global binding specificity of a polyamide. An eight-ring hairpin polyamide targeting 5'-WGWWCW-3' (W = A,T) and characterized by quantitative DNase I footprinting, Im-Py-Py-Py-*γ*-Im-Py-Py-Py-*β*-Dp,[3c,10] has been compared to its Cy3-labeled counterpart studied on the CSI-array platform, demonstrating a linear relationship between intensity and K_a.[4c]

Because microarray intensity at a specific microarray feature should be proportional to the fractional occupancy of DNA at that feature, the relationship between equilibrium association constant (K_a) or dissociation constant (K_d) and background-normalized microarray intensity should be[11]

$$\text{Intensity} = c \times \Theta = c \times \frac{K_a[\text{PA}]}{1 + K_a[\text{PA}]} = c \times \frac{[\text{PA}]}{K_d + [\text{PA}]} \quad . \tag{1}$$

In this relationship, Θ represents the fractional occupancy of DNA at a specific feature, *c* a scalar to reflect that microarray intensity can vary with incident laser intensity, and [PA] the free polyamide concentration on the CSI array. The terms *c* and [PA] are solved for a curve fit to Eq 1 using K_a values derived from DNase I footprint titrations and CSI microarray intensity data. Examining the limiting case where [PA] << K_d being studied one observes a simplification to Eq 1:

$$\text{Intensity} = c \times \frac{[\text{PA}]}{K_d} = c \times [\text{PA}] \times K_a \ . \quad (2)$$

Eq 2 represents the linear subset of the more general CSI intensity – K_a relationship described in Eq 1. Fitting the footprinting data of polyamide **2** to its corresponding microarray intensities (Table 3.1) using Eq 2 fits well ($R^2 = 0.94$). The linearized Eq 2 does not, however, map intensity and K_a with high correlation for polyamide **4**. Fitting the data to Eq 1 affords a better fit ($R^2 = 0.99$), indicating that [PA] is not insignificant relative to the K_d of the highest intensity microarray data (Figure 3.8).[12,13]

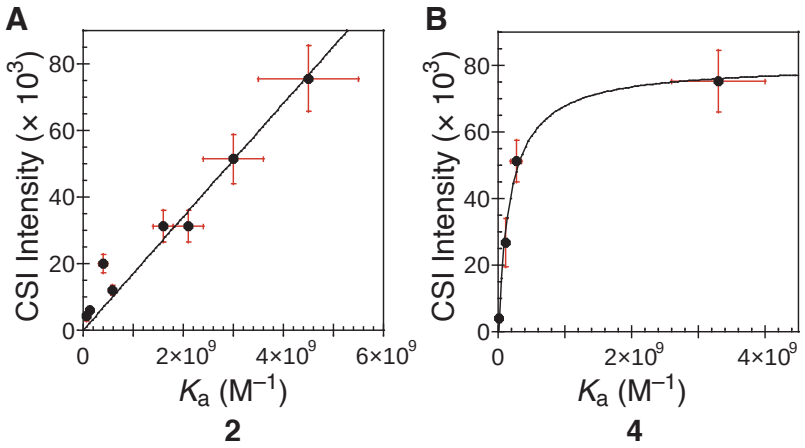

Figure 3.8. CSI array intensities correlate well with DNase I footprinting-determined K_a values. a) Polyamide **2** versus CSI array fit to Eq 2. b) Polyamide **4** versus CSI array fit to Eq 1

The K_a-calibrated microarrays can subsequently be used to interpolate K_a values from normalized sequence intensities. K_a values are derived by rearranging Eq 1 to present K_a as a function of microarray intensity:

$$K_a = \frac{\text{Intensity}}{[\text{PA}] \times (c - \text{Intensity})} \ . \quad (3)$$

In the case where [PA] << K_d, Eq 2 rearranged to

$$K_a = \frac{\text{Intensity}}{[\text{PA}] \times c} \ . \quad (4)$$

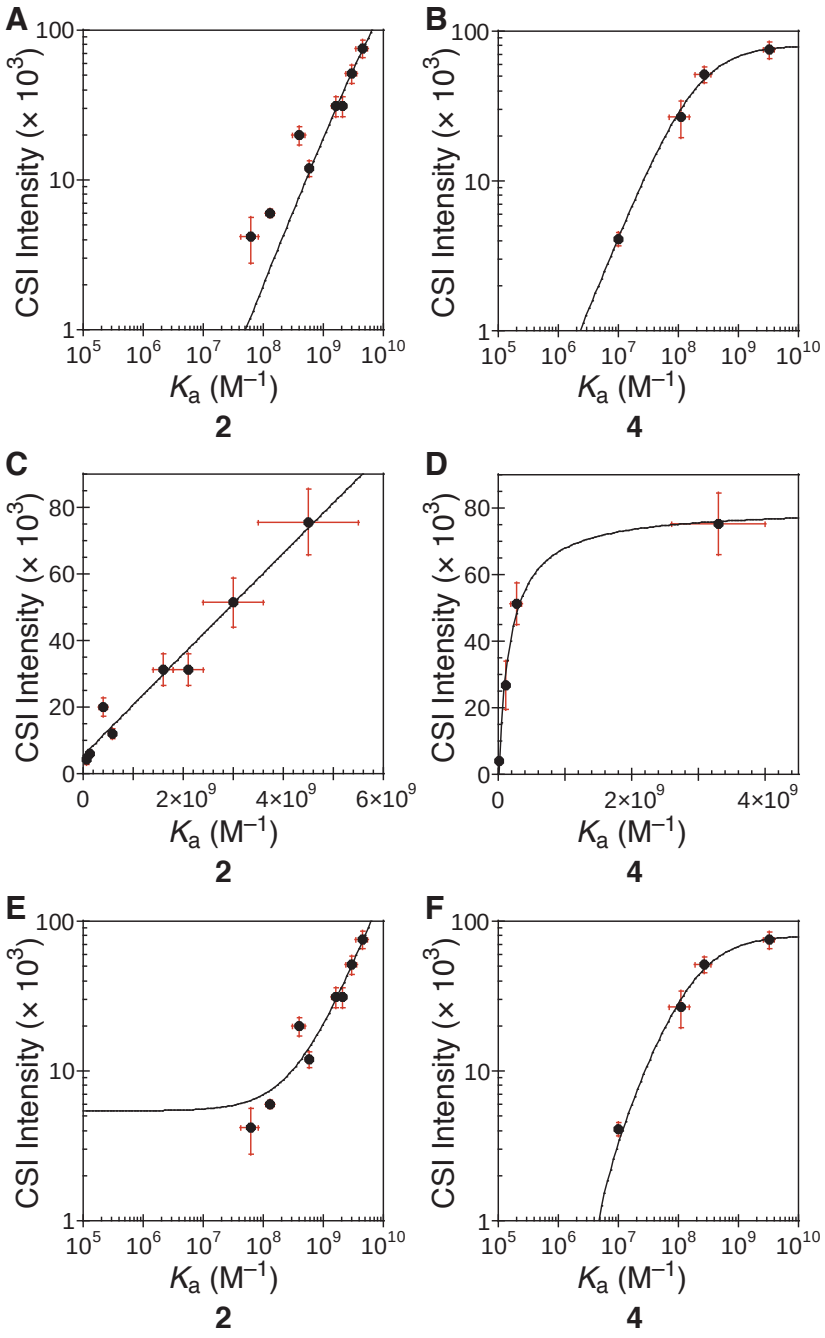

Figure 3.9. Correlation of footprinting data for polyamide **2** and CSI data (a, c, e) and footprinting data for polyamide **4** and CSI data (b, d, f). a) Log-log scale plot of polyamide **2** versus CSI intensity data fit using Eq 2. b) Log-log scale plot of polyamide **4** versus CSI intensity data fit using Eq 1. c) Linear-linear scale plot of polyamide **2** versus CSI data using Eq 2e. d) Linear-linear scale plot of polyamide **4** versus. CSI data using Eq 1e. e) Log-log scale plot of polyamide **2** versus CSI intensity data fit using Eq 2e. f) Log-log scale plot of polyamide **4** versus CSI intensity data fit using Eq 1e

Correlating Binding Between Cy3-labeled and Biologically Relevant Polyamides. While establishing a general K_a – intensity relationship for Cy3-labeled polyamides is a crucial first step towards global sequence interrogation of a core polyamide motif, it is equally important that the biologically relevant polyamide has sequence preferences that correlate with its Cy3-labeled counterpart. Scatter plots of polyamide **1** versus **2** and polyamide **3** versus **4** are best fit by a power relationship of $y = ax^n$, where (x,y) denotes the K_a values for (**1**, **2**) or (**3**, **4**) (Figure 3.10).[14] The R^2 between **1** and **2** is 0.87, and that between **3** and **4** is 0.78.

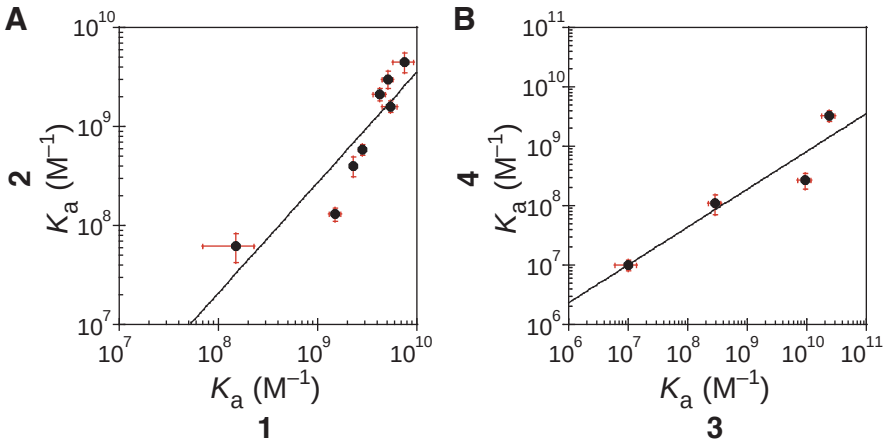

Figure 3.10. Cy3-labeled polyamides and unlabeled polyamides correlate well. a) Correlation of K_a values for polyamide **1** (fluorescein labeled) and polyamide **2** (Cy3 labeled). b) Correlation of K_a values for polyamide **3** (unlabeled) and polyamide **4** (Cy3 labeled)

Sequence Analysis. To graphically represent the binding preferences of polyamides **2** and **4**, sequence logos have been generated (Figures 3.11 and 3.12).

In all cases, the motif finding program MEME[6a] was utilized to extract sequence motifs from the CSI binding intensities. The position specific probability matrices output by MEME were used as inputs to enoLOGOS[15] to generate a sequence logo.[16] The logo for polyamide **2** was created by searching the ~2500 highest sequence intensities of the CSI microarray.[17] These data points span approximately a threefold range in K_a. The logo for polyamide **4** interrogated the 48 highest intensity sequences (a sevenfold range in K_a) of

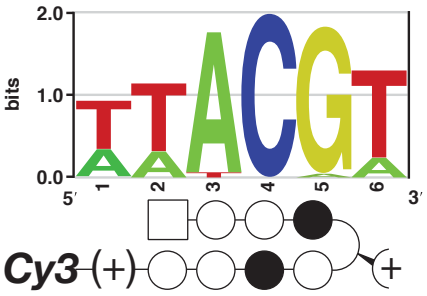

Figure 3.11. Sequence logo for polyamide **2**

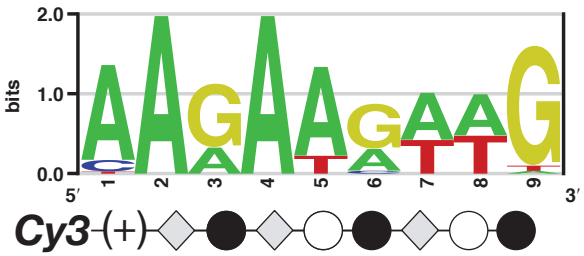

Figure 3.12. Sequence logo for polyamide **4**

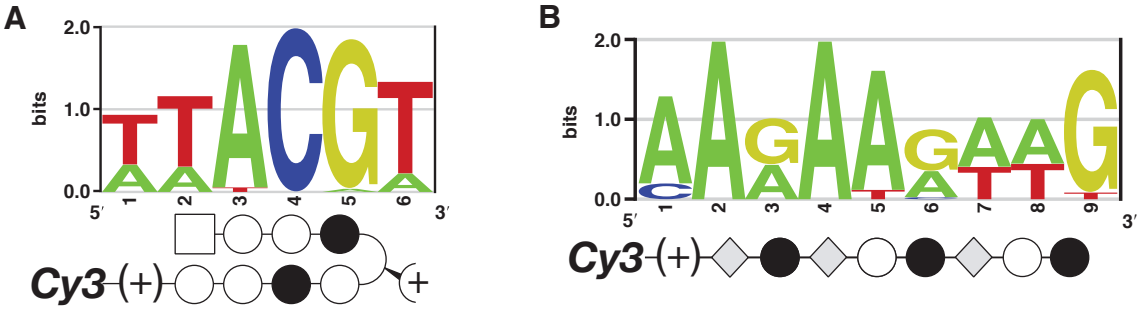

Figure 3.13. K_a-weighting components of individual sequence logos does not alter the sequence logo. Compare a) with Figure 3.11 and b) with Figure 3.12. a) K_a-weighted sequence logo for polyamide **2**. b) K_a-weighted sequence logo for polyamide **4**

the CSI microarray.[18] We examined K_a-weighted sequence logos for both polyamides **2** and **4** and found minimal differences in the resulting logos (compare Figure 3.13 with Figures 3.11 and 3.12).

The motif for polyamide **2** has the most information at a site width of six – 5'-WWACGT-3' (Figure 3.11; W = A,T). The chlorothiophene/pyrrole pair (Ct/Py) specificity cannot be globally elucidated using polyamide **2** because of the palindromic nature of the ACGT binding site core. It is evident that the core does specify 5'-ACG-3' using Py/Py, Py/Im, and Im/Py pairings, respectively. Polyamide **3** specifies 9 base pairs based on MPE footprinting data (Chapter 2B). Polyamide **4** elicits a 9 bp motif that is best represented as 5'-AARAARWWG-3' (Figure 3.12; R = G,A and W = A,T). Previous work would suggest that Im may have no sequence preferences within linear β-linked

polyamides,[8] although this selection of 9 bp high affinity binding sites for **4** suggests at least G·A or A·T specificity, consistent with microarray data from Friedreich's ataxia cell culture work.[7c]

Quantitative Profiling of Single Base Pair Mismatches. While sequence logos provide a visual representation of sequence specificity, traditional studies on polyamides quantitate the specificity of a ring pairing at a selected base pair. We have examined a comprehensive single base pair mutational analysis of both polyamides **2** and **4** using K_a values interpolated from the calibrated CSI microarrays (Tables 3.3 and 3.4).[19] Because the motif finding algorithm MEME found 5'-WWACGT-3' (W = A,T) as a preferred binding sequence for polyamide **2**, we utilized this core sequence for mutational studies.

Table 3.3. Microarray-Derived Binding Affinities and Specificities of All Single Base Pair Mismatch Sites for Polyamide **2**. All K_a values are derived from the geometric average of all CSI binding site intensities on the array containing a specified sequence, converted to a K_a value using Eq 4, corrected to include an error term ε. The values in parentheses are the geometric standard deviations for each K_a value. X·Z entries marked with a superscripted "*" contain averaged intensities below ε. For these entries, an upper bound on the K_a is estimated based on the log–log plot of K_a versus intensity found in Figure 3.9.

Polyamide 2	X·Z	K_a (M^{-1})
5'-W W W W **X** W A C G T-3' *Cy3*-(+) 3'-W W W W **Z** W T G C A-5'	A·T	$2.0\ (1.4) \times 10^9$
	T·A	$2.5\ (1.2) \times 10^9$
	C·G	$6.9\ (1.4) \times 10^8$
	G·C	$6.8\ (1.6) \times 10^8$
5'-W W W W W **X** A C G T-3' *Cy3*-(+) 3'-W W W W W **Z** T G C A-5'	A·T	$1.8\ (1.3) \times 10^9$
	T·A	$2.7\ (1.2) \times 10^9$
	C·G	$1.0\ (2.0) \times 10^8$
	G·C	$1.3\ (2.2) \times 10^8$
5'-W W W W W W **X** C G T-3' *Cy3*-(+) 3'-W W W W W W **Z** G C A-5'	A·T	$2.2\ (1.3) \times 10^9$
	T·A	$1.1\ (1.6) \times 10^9$
	C·G[a]	$\leq 10^8$
	G·C	$1.3\ (2.5) \times 10^8$
5'-W W W W W W A **X** G T-3' *Cy3*-(+) 3'-W W W W W W T **Z** C A-5'	A·T[a]	$\leq 10^8$
	T·A[a]	$\leq 10^8$
	C·G	$2.2\ (1.3) \times 10^9$
	G·C[a]	$\leq 10^8$
5'-W W W W W W A C **X** T-3' *Cy3*-(+) 3'-W W W W W W T G **Z** A-5'	A·T	$1.2\ (1.4) \times 10^9$
	T·A	$2.9\ (1.8) \times 10^8$
	C·G	$2.4\ (1.8) \times 10^8$
	G·C	$2.2\ (1.3) \times 10^9$
5'-W W W W W W A C G **X**-3' *Cy3*-(+) 3'-W W W W W W T G C **Z**-5'	A·T	$1.3\ (1.4) \times 10^9$
	T·A	$2.2\ (1.3) \times 10^9$
	C·G[a]	$\leq 10^8$
	G·C[a]	$\leq 10^8$

Table 3.4. Microarray-Derived Binding Affinities and Specificities of All Single Base Pair Mismatch Sites for Polyamide **4**. All K_a values are derived from the geometric average of all CSI binding site intensities on the array containing a specified sequence, converted to a K_a value using Eq 3, corrected to include an error term ε. The values in parentheses are the geometric standard deviations for each K_a value.

Polyamide 4	X·Z	K_a (M^{-1})
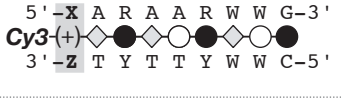	A·T	$1.6\ (2.2) \times 10^8$
	T·A	$8.7\ (2.0) \times 10^7$
	C·G	$4.3\ (1.8) \times 10^7$
	G·C	$4.7\ (1.8) \times 10^7$
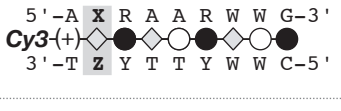	A·T	$1.6\ (2.2) \times 10^8$
	T·A	$7.7\ (2.2) \times 10^7$
	C·G	$2.1\ (1.8) \times 10^7$
	G·C	$3.2\ (1.9) \times 10^7$
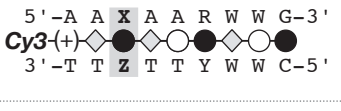	A·T	$1.3\ (2.0) \times 10^8$
	T·A	$3.5\ (1.7) \times 10^7$
	C·G	$8.4\ (1.6) \times 10^7$
	G·C	$2.0\ (2.2) \times 10^8$
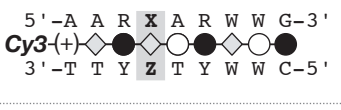	A·T	$1.6\ (2.2) \times 10^8$
	T·A	$4.3\ (1.8) \times 10^7$
	C·G	$9.9\ (1.9) \times 10^6$
	G·C	$7.5\ (2.6) \times 10^6$
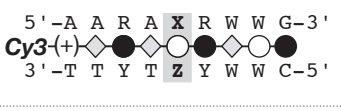	A·T	$1.6\ (2.2) \times 10^8$
	T·A	$8.3\ (2.2) \times 10^7$
	C·G	$9.1\ (2.1) \times 10^6$
	G·C	$1.1\ (2.0) \times 10^7$
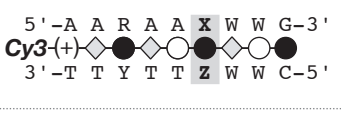	A·T	$1.5\ (2.1) \times 10^8$
	T·A	$5.5\ (1.7) \times 10^7$
	C·G	$8.5\ (1.7) \times 10^7$
	G·C	$1.7\ (2.3) \times 10^8$
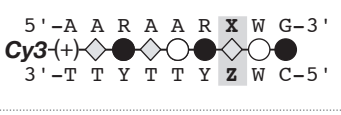	A·T	$1.7\ (2.2) \times 10^8$
	T·A	$1.5\ (2.2) \times 10^8$
	C·G	$2.2\ (2.2) \times 10^7$
	G·C	$2.0\ (2.4) \times 10^7$
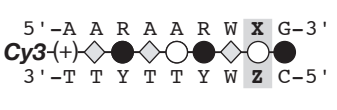	A·T	$1.6\ (2.5) \times 10^8$
	T·A	$1.5\ (2.0) \times 10^8$
	C·G	$3.5\ (2.0) \times 10^7$
	G·C	$3.9\ (2.0) \times 10^7$
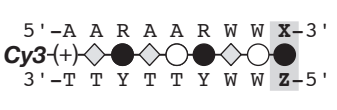	A·T	$1.2\ (1.9) \times 10^8$
	T·A	$1.1\ (2.0) \times 10^8$
	C·G	$1.1\ (1.7) \times 10^8$
	G·C	$1.6\ (2.2) \times 10^8$

Additionally, because of the 5'-ACGT-3' palindromic element of this binding site, we have isolated only binding sites containing 5'-WWWWWWACGT-3' and their mutant counterparts to preclude analyzing variants where the polyamide may be rotated 180º from the presumed orientation. To determine a K_a for 5'-WWWWWWACGT-3' (for example), the geometric mean of all microarray binding site intensities containing this motif was found. Walking from 5' to 3' on 5'-$W^1W^2A^3C^4G^5T^6$-3', we observe that there is threefold

specificity for W versus S (S = C,G) at position 1 (occupied by the linker). At position 2 (Ct/Py pair), there is 20-fold specificity for W versus S, but minimal for T·A versus A·T. The previous study of Ct/Py specificity noted only modest specificity for T·A versus A·T.[3c] Position 3, (a Py/Py pair) confirms the previously observed W over S specificity. At position 4 (a Py/Im pair) the polyamide encodes the greatest specificity with preference for C·G versus A·T, T·A, or G·C. It is likely that this preference is at least 20-fold. At position 5, polyamide **2** appears to exhibit less specificity than would be predicted for an Im/Py ring pair, binding almost as well to A·T as to G·C.[1] The polyamide "turn unit," position 6, confirms a strong preference for W over S.[1] Through this quantitative study, we observe four strongly encoded binding positions, italicized in 5'-W*WWC*G*W*-3'. The discrepancy between the observed sequence logo, as found by MEME, and the suggested specificity by a single base pair mutation study likely stems from (i) the examination of all sequences in the single base pair mutation as compared to only a subset for the sequence logo, (ii) the assumption by the logo of independence of base pair-polyamide interaction at each position, and (iii) the examination in the single base pair mutation of the average K_a of a group of sequences containing a specified motif.

In conjunction with the sequence logo for polyamide **2**, the CSI array analysis validates the sequence specificity programmed by the aromatic amino acid ring pairs. The extensive DNase I footprinting data on eight-ring and six-ring hairpin polyamides, while limited on the scale of a CSI microarray, enabled the creation of pairing rules that are remarkably general.[1] It is evident from the microarray that Im/Py and Py/Im ring pairs offer the greatest specificity for a single base pair, while Py/Py, Ct/Py, and the "turn unit" afford general W specificity. While the Ct/Py ring pair conferred minimal specificity for T·A versus A·T, its W specificity is likely an improvement over the use of a Py/Py ring pair, which at the N-terminus of an eight-ring hairpin polyamide exhibits specificity for A·T, T·A, and G·C versus C·G.[3c] The sequence specificity of **2** correlates remarkably well with the 5'-ACGT-3' specificity of echinomycin,[20] also known to affect VEGF expression

in cell culture.[21]

The examination of polyamide **4** marks the most comprehensive sequence specificity study of a linear *β*-linked polyamide since the original examination of the binding specificity for Im-*β*-Im-Py-*β*-Im-*β*-Im-Py-*β*-Dp.[8a,b] In the 5'-$A^1A^2R^3A^4A^5R^6W^7W^8G^9$-3' sequence (R = G,A; W = A,T), positions 4, 5, and 7, each containing either a Py or a *β*, exhibit the greatest specificity for W over S (S = C,G). Intriguingly, the *β* at position 4 prefers A·T over T·A, an unexpected specificity. The sequence logo for polyamide **4** indicates that Im has modest preference for G·C or A·T over other base pairings—in this mutational study, however, imidazole is generally degenerate. The wide range of K_a values comprising each motif (high geometric standard deviation) make the statistical significance of any specificities under 4 relatively small. In general, the geometric standard deviations for polyamide **4** were higher than those for polyamide **2**, when including only those table entries for polyamide **2** in which each K_a value was composed of all instances of the motif. One potential source of the increased standard deviation in binding affinities is the single variable base flanking the nine base pair binding site for polyamide **4**. Because the minor groove width is a potentially important contributor to binding affinity and specificity for the linear *β*-linked class of polyamides,[8c] a single variable, flanking base is unlikely to enable comprehensive interrogation of the global set of sequence-dependent DNA microstructures. As with polyamide **2**, the discrepancies observed between the sequence logo of polyamide **4** and the comprehensive single base pair mutational analysis likely stem from similar causes.

With the sequence logo (approximated as 5'-AARAARWWG-3') as a snapshot of the highest affinity binding sites for polyamide **4** ($K_a \approx 5 \times 10^8$ to 3.3×10^9 M^{-1}) and the footprint titration binding isotherms for determining DNA binding mode, we confirm a preference for the 1:1 binding stoichiometry. Previous data characterizing the linear *β*-linked polyamide Im-*β*-Im-Py-*β*-Im-*β*-Im-Py-*β*-Dp demonstrated a 30-fold energetic preference for the 1:1 versus 2:1 binding stoichiometry, presumably due to the increased entropic cost of the 2:1 binding mode.[8a] It is remarkable that polyamide **3** exhibited specificity for

upregulation of the frataxin gene in cell culture,[7c] since the sequence preference for **4** was not overwhelmingly 5'-AAGAAGAAG-3'. Two possible explanations for this observation are (i) that multiple binding events in the genome have marginal effects on transcription and that the specificity is amplified by the GAA repeat expansion in Friedreich's ataxia, or (ii) that many of the sequences described by 5'-AARAARWWG-3' exist in higher-order chromosomal structures that cannot be targeted by polyamide **3**.

Suggestions for Microarray Usage. In the case where the free ligand concentration is small relative to the K_d for each binding site on the CSI microarray, a linear K_a – intensity relationship is observed. The binding profiles examined for polyamide **2** and for previously studied molecules are examples of linear K_a – intensity relationships. For the highest intensity sites also studied by DNase I footprinting (Figure 3.8A), the CSI microarray experiment contains greater resolving power and can differentiate K_a values that are indistinguishable by quantitative DNase I footprint titrations. In this example, as CSI intensity data approach ε, small changes in intensity yield large changes in predicted K_a. Because the characterization of DNA-binding ligands is most concerned with defining a perfect match site, this limitation is minor. CSI data for polyamide **2** conservatively enables distinguishing a 50-fold range of K_a values, thus encompassing the majority of single base pair mismatch specificities.

In the case where the free ligand concentration is comparable to the K_d, a non-linear K_a – intensity relationship is observed. The binding profile for polyamide **4** marks an example of a CSI microarray studied compound that occurs outside the linear range of eq 1. In this case, closely clustered high intensity data points can span a broad range of K_a values (Figure 3.8B). The error inherent to the CSI microarray analysis is thus amplified when K_a values in this high CSI intensity region are interpolated.

Because of the gradual polyamide titration onto the array, it should be possible to capture snapshots of both polyamide saturation within the linear K_a–intensity region for the highest affinity binding sites on the microarray and binding site saturation enabling

lower intensity data points to fall within the higher precision linear K_a–intensity region. Such titration may enable high precision K_a data to be extracted from all intensities of the microarray.

The sequence logos presented in this paper represent a snapshot of a binding profile for the highest affinity binding sites by a dye-labeled ligand. The polyamide core dictates the majority of the binding specificity revealed by CSI microarray analysis—the presence of a Cy3 label may reduce affinity to a binding site relative to its unlabeled counterpart but does not alter the rank-order of binding preferences. Complementing the graphical image of a sequence logo, the comprehensive single base pair mutational analysis afforded by the extensive microarray data quantitates one's understanding of the polyamide sequence preferences.

Conclusion.

Correlating the sequence preference landscape present on the CSI microarray to quantitative footprinting enables energetic studies using global binding information. This capacity marks a significant forward step for the field of small molecule·DNA recognition and enables the comprehensive interrogation of DNA binding small molecules to be better understood. The elucidation of 5'-WWACGT-3' as the binding site for **2** confirmed the previously established pairing code for hairpin polyamides, and the determination of 5'-AARAARWWG-3' for **4** helps explain the specificity it exhibited in cell culture. The correlation between a Cy3-labeled polyamide and an unlabeled polyamide of biological interest means that these motifs well approximate the binding profiles for **1** and **3**, respectively. DNase I footprinting-calibrated CSI microarrays have been shown to be an effective technique for determining the binding affinities of DNA-binding ligands for a vastly expanded repertoire of DNA sequences, and we envision them to be a critical tool for reliably determining sequence specificity for other ligands in the future.

Experimental Methods.

Materials. Boc-*β*-Ala-Pam resin (0.81 mmol / g), HBTU, the chiral amino acid Fmoc-D-Dab-Boc-OH, and Boc_2O were purchased from Peptides International. Kaiser oxime resin (0.56 mmol / g) was purchased from Novabiochem. Trifluoroacetic acid (TFA) was purchased from Halocarbon. All solvents were purchased from Aldrich or EMD Biosciences. *rac*-Dithiothreitol (DTT) was purchased from ICN. Cy3-NHS ester was purchased from Invitrogen. RNase-free DEPC water was purchased from US Biochemicals. Water (18.2 MΩ) was purified using a Millipore water purification system.

The pH of buffers was adjusted using a Beckman 340 pH/temp meter. All buffers were sterilized by filtration through either a Nalgene 0.2 μm cellulose nitrate filtration device or a 0.2 μm Whatman cellulose acetate disposable syringe filter. DNA oligonucleotides were ordered PAGE-purified from Integrated DNA Technologies. [γ-^{32}P] adenosine 5'-triphosphate ($\geq$ 7000 Ci/mmol) was obtained from MP Biomedicals. Sonicated, phenol-extracted calf thymus DNA was from Amersham, and all enzymes and molecular biology grade glycogen (20 mg/mL) were purchased from Roche.

Methods. UV spectra were recorded in water using an Agilent 8453 UV-Vis spectrophotometer for polyamide **3**. To solvate polyamides **1**, **2** and **4** in water at sufficiently high concentrations for DNase I footprinting, 5 μL of DMSO was added to a 20 nmol aliquot of polyamide. The solution was then diluted using RNase-free DEPC water. UV spectra of **1**, **2** and **4** were blanked against solutions containing appropriate amounts of DMSO. The concentrations of polyamides **1** and **2** were determined using a local λ_{max} of 313 nm, ε = 69,500 $L \cdot mol^{-1} \cdot cm^{-1}$. The concentrations of polyamides **3** and **4** were determined using a local λ_{max} of 288 nm, ε = 43,125 $L \cdot mol^{-1} \cdot cm^{-1}$. LASER desorption / ionization time-of-flight mass spectrometry (MALDI-TOF MS) was performed using an Applied Biosystems Voyager DE Pro spectrometer. Analytical and preparative high-pressure liquid chromatography (HPLC) were performed with a Beckman Gold system equipped with a diode array (analytical) or single-wavelength (preparative) detector as

previously described.[4c,7]

Synthesis. Polyamides **1** and **2** were synthesized on Kaiser oxime resin[22] and **3** and **4** were synthesized on Boc-*β*-Ala-PAM resin,[23] using previously described methods.[4c,7]

1: (MALDI-TOF) [M+H]+ calcd for $C_{77}H_{80}ClN_{22}O_{14}S_2^+$ 1635.5, observed 1635.9

2: (MALDI-TOF) [M+H]+ calcd for $C_{87}H_{105}ClN_{23}O_{16}S_3^+$ 1858.7, observed 1858.7

3: (MALDI-TOF) [M+H]+ calcd for $C_{41}H_{56}N_{17}O_8^+$ 914.4, observed 914.4

4: (MALDI-TOF) [M+H]+ calcd for $C_{74}HN_{20}O_{15}S_2^+$ 1569.7, observed 1569.6

Plasmid Preparation. Plasmids were constructed by ligating the following hybridized inserts into the BamHI / HindIII polycloning site in pUC19:

pKAM3. 5’-GATCGGAGCTTTTACGTAAGCGGAGGCTTTTACGTAGGCGG
AGGCTTTTACGTGAGCGGAGGCTTTTACGGAAGCGGAT-3’·5’-AGCTATC
CGCTTCCGTAAAAGCCTCCGCTCACGTAAAAGCCTCCGCCTACGTAAA
AGCCTCCGCTTACGTAAAAGCTCC-3’

pKAM4. 5’-GATCGGAGCTTTTACGTGAGCGGAGGCAATTTCGTGTGCGG
AGGCGCTTTCGTCCGCGGAGGCACCTTCGTGAGCGGAT-3’·5’-AGCTATC
CGCTCACGAAGGTGCCTCCGCGGACGAAAGCGCCTCCGCACACGAAAT
TGCCTCCGCTCACGTAAAAGCTCC-3’

pJWP17. 5’-GATCGGAGCAAGAAGAAGTGCGGAGGCAAGAAGTTCAGC
GGAGGCATGTTGTTGAGCGGAGGCATGAAGACGAGCGGAT-3’·5’-AGCTA
TCCGCTCGTCTTCATGCCTCCGCTCAACAACATGCCTCCGCTGAACTTCT
TGCCTCCGCACTTCTTCTTGCTCC-3.’

The ligated plasmid was then transformed into JM109 subcompetent cells. Colonies were selected for α-complementation on agar plates containing 50 mg/L ampicillin, 120 mg/L IPTG, and 40 mg/L X-gal after overnight growth at 37 ºC. Cells were harvested after 16 h growth at 37 ºC in LB medium containing 50 mg/L ampicillin. Plasmids were then purified by mini-prep kits. The presence of the desired inserts was determined by capillary electrophoresis dideoxy sequencing methods.

Preparation of 5'-Labeled DNA for DNase I Footprinting. Two primer oligonucleotides, 5'-AATTCGAGCTCGGTACCCGGG-3' (forward) and 5'-CTGGCACGACAGGTTTCCCGA-3' (reverse) were constructed for PCR amplification. The forward primer was radiolabeled using [γ-^{32}P]-dATP and polynucleotide kinase, followed by purification using ProbeQuant G-50 spin columns. The desired DNA region was amplified as previously described.[2] The labeled fragment was loaded onto a 7% nondenaturing preparatory polyacrylamide gel (5% cross-link), and the desired 283 (pKAM3, pKAM4, pJWP17) base-pair band was visualized by autoradiography and isolated. Chemical sequencing reactions were performed according to published protocols.[2]

Quantitative DNase I Footprint Titrations. All reactions were carried out in a volume of 400 µL according to published protocols. Polyamides were equilibrated with the radiolabeled DNA for 14 h prior to DNase I cleavage at 23 ºC. Quantitation by storage phosphor autoradiography and determination of equilibrium association constants were as previously described.[2]

Microarray Procedures. Microarrays were synthesized by using a Maskless Array Synthesizer (NimbleGen Systems, Madison, WI). Homopolymer (T_{10}) linkers were covalently attached to monohydroxysilane glass slides. Oligonucleotides were then synthesized on the homopolymers to create a high-density oligonucleotide microarray. The array surface was derivatized such that the density of oligonucleotides was sufficiently low within the same feature so that no one oligonucleotide would hybridize with its neighbors. Four copies of each hairpin containing a unique 10 bp site (5'-GCGC-$N^1N^2N^3N^4N^5N^6N^7N^8N^9N^{10}$-GCGC-GGA-GCGC-$N^{10'}N^{9'}N^{8'}N^{7'}N^{6'}N^{5'}N^{4'}N^{3'}N^{2'}N^{1'}$-GCGC-3') required a total of 2,099,200 features, divided among six microarrays.

Binding Assay. Microarray slides were immersed in 1x PBS and placed in a 90 ºC water bath for 30 min to induce hairpin formation of the oligonucleotides. Slides were then transferred to a tube of nonstringent wash buffer (saline/sodium phosphate/EDTA buffer, pH 7.5/0.01% Tween 20) and scanned to check for low background (<200 intensity).

Microarrays were scanned by using an Axon 4000B, and the image files were extracted with GENEPIX PRO Version 3.0 (Axon Instruments, Foster City, CA).

Polyamide Binding. Microarrays prepared as above were placed in the microarray hybridization chamber and washed twice with nonstringent wash buffer. Polyamide was diluted to 10 nM (for **2**) or 175nM (for **4**) in Hyb buffer (100 mM Mes/1 M NaCl/20 mM EDTA, pH 7.5/0.01% Tween 20). Polyamide was then added to the hybridization chamber and incubated at room temperature for 1 h. Finally, the microarrays were washed twice with nonstringent wash buffer and scanned.

Data Processing. For each replicate, global mean normalization was used to ensure the mean intensity of each microarray was the same. Local mean normalization[24] was then used to ensure that the intensity was evenly distributed throughout each sector of the microarray surface. Outliers between replicate features were detected by using the *Q* test at 90% confidence and filtered out. The replicates were then quantile-normalized[25] to account for any possible nonlinearity between arrays. Duplicate features were then averaged together. The median of the averaged features was subtracted to account for background.

Acknowledgment. This work was supported by the National Institutes of Health (GM27681 to P.B.D. and A.Z.A). We thank the Beckman Institute Sequence Analysis Facility for DNA sequencing.

References

(1) Im / Py targets G·C; Py / Py targets A·T and T·A; and Ct / Py targets T·A. (a) Dervan, P. B.; Edelson, B. S. *Curr. Opin. Struct. Biol.* **2003**, *13*, 284–299. (b) Hsu, C. F.; Phillips, J. W.; Trauger, J. W.; Farkas, M. E.; Belitsky, J. M.; Heckel, A.; Olenyuk, B. Z.; Puckett, J. W.; Wang, C. C. C.; Dervan, P. B. *Tetrahedron* **2007**, *63*, 6146–6151.

(2) Trauger, J. W.; Dervan, P. B. *Methods Enzymol.* **2001**, *340*, 450–466.

(3) (a) Doss, R. M.; Marques, M. A.; Foister, S.; Chenoweth, D. M.; Dervan, P. B. *J. Am. Chem. Soc.* **2006**, *128*, 9074–9079. (b) Marques, M. A.; Doss, R. M.; Foister, S.; Dervan, P. B. *J. Am. Chem. Soc.* **2004**, *126*, 10339–10349. (c) Foister, S.; Marques, M. A.; Doss, R. M.; Dervan, P. B. *Bioorg. Med. Chem.* **2003**, *11*, 4333–4340.

(4) (a) For a review on Protein Binding Microarrays (PBMs), see: Bulyk, M. L. *Methods Enzymol.* **2006**, *410*, 279–299. (b) For a review on fluorescence intercalator displacement (FID) assays, see: Tse, W. C.; Boger, D. L. *Acc. Chem. Res.* **2004**, *37*, 61–69. (c) For the initial report of cognate site identifier (CSI) microarrays, see: Warren, C. L.; Kratochvil, N. C. S.; Hauschild, K. E.; Foister, S.; Brezinski, M. L.; Dervan, P. B.; Phillips, G. N.; Ansari, A. Z. *Proc. Natl. Acad. Sci. U. S. A.* **2006**, *103*, 867–872.

(5) Schneider, T. D.; Stephens, R. M. *Nucleic Acids Res.* **1990**, *18*, 6097–6100.

(6) (a) Bailey, T. L.; Elkan, C. In *Proceedings of the Second International Conference on Intelligent Systems for Molecular Biology*; Altman, R., Brutlag, D., Karp, P., Lathrop, R., Searls, D., Eds.; AAAI Press: Menlo Park, 1994, pp 28–36. (b) Liu, X. S.; Brutlag, D. L.; Liu, J. S. *Nat. Biotechnol.* **2002**, *20*, 835–839. (c) Hughes, J. D.; Estep, P. W.; Tavazoie, S.; Church, G. M. *J. Mol. Biol.* **2000**, *296*, 1205–1214.

(7) (a) Olenyuk, B. Z.; Zhang, G. J.; Klco, J. M.; Nickols, N. G.; Kaelin, W. G.; Dervan, P. B. *Proc. Natl. Acad. Sci. U. S. A.* **2004**, *101*, 16768–16773. (b) Nickols, N. G.; Jacobs, C. S.; Farkas, M. E.; Dervan, P. B. *Nucleic Acids Res.* **2007**, *35*, 363–370. (c) Burnett, R.; Melander, C.; Puckett, J. W.; Son, L. S.; Wells, R. D.; Dervan, P. B.;

Gottesfeld, J. M. *Proc. Natl. Acad. Sci. U. S. A.* **2006**, *103*, 11497–11502.

(8) (a) Dervan, P. B.; Urbach, A. R. In *Essays in Contemporary Chemistry*; Quinkert, G., Kisakürek, M. V., Eds.; Verlag Helvetica Chimica Acta: Zurich, 2000, pp 327–339. (b) Urbach, A. R.; Dervan, P. B. *Proc. Natl. Acad. Sci. U. S. A.* **2001**, *98*, 4343–4348. (c) Urbach, A. R.; Love, J. J.; Ross, S. A.; Dervan, P. B. *J. Mol. Biol.* **2002**, *320*, 55–71. (d) Marques, M. A.; Doss, R. M.; Urbach, A. R.; Dervan, P. B. *Helv. Chim. Acta* **2002**, *85*, 4485–4517.

(9) Singh-Gasson, S.; Green, R. D.; Yue, Y. J.; Nelson, C.; Blattner, F.; Sussman, M. R.; Cerrina, F. *Nat. Biotechnol.* **1999**, *17*, 974–978.

(10) (a) Trauger, J. W.; Baird, E. E.; Dervan, P. B. *Nature* **1996**, *382*, 559–561. (b) Trauger, J. W. Ph. D. Thesis, California Institute of Technology, 1999.

(11) For derivation of these equations see the Supporting Information for Bulyk, M. L.; Huang, X. H.; Choo, Y.; Church, G. M. *Proc. Natl. Acad. Sci. U. S. A.* **2001**, *98*, 7158–7163.

(12) (a) $c \times$ [PA] was 1.7×10^{-5} for polyamide **2**. (b) c was 80.2×10^{3} and [PA] was 5.5×10^{-9} M for polyamide **4**. (c) To view plots reflecting the same curve fits of Figure 3.8 on a log–log scale, please see Figure 3.9.

(13) Although the data for polyamide **2** (Figure 3.8A) maps intensity and K_a values using the linearized eq 2, this fit is distinct from that obtained by fitting the data to a line of the form $y = mx + b$, which includes an intensity-axis intercept term. While very small in this case, the differences in the slopes and intercepts of the lines may indicate error both in the background correction of the microarray and in the DNase I footprinting data. To correct for this possibility, we propose the use of an error term, ε, that would modify eqs 1 and 2 to the following: Intensity $= c \times \Theta + \varepsilon = c \times \{K_a[PA]\}/\{1+K_a[PA]\} + \varepsilon = c \times \{[PA]\}/\{K_d+[PA]\} + \varepsilon$ (eq 1e) and Intensity $= c \times [PA]/K_d + \varepsilon = c \times [PA] \times K_a + \varepsilon$ (eq 2e). When fitting the intensity and K_a data for polyamide **2** to the modified equation 2e, one finds a marginally improved fit ($R^2 = 0.97$), although the curve fit for

polyamide **4** using equation 1e is unimproved ($R^2 = 0.99$). For polyamide **2**, $c \times [PA] = 1.5 \times 10^{-5}$ and $\varepsilon = 5.5 \times 10^3$. For polyamide **4**, $c = 81.2 \times 10^3$, $[PA] = 5.7 \times 10^{-9}$ M, and $\varepsilon = -1.1 \times 10^3$.

(14) For the relationship between polyamides **1** and **2**, $a = 0.0253$ and $n = 1.115$. For the relationship between polyamides **3** and **4**, $a = 349.83$ and $n = 0.637$.

(15) Workman, C. T.; Yin, Y. T.; Corcoran, D. L.; Ideker, T.; Stormo, G. D.; Benos, P. V. *Nucleic Acids Res.* **2005**, *33*, W389–W392.

(16) Figure 3.11 utilized 10 variable bases and contained a background GC content of 50%; Figure 3.12 utilized 10 variable bases and two bases, each flanking the 5' and 3' portion of the variable region contained a background GC content of 58%. These background corrections were utilized in the motif searching parameters.

(17) There are 1258 occurrences of a full 6 bp match sequence, TTACGT. Double this number of highest intensity sequences was also searched yielding only modest changes in the data. The sequence logo is reported for the 2516 highest intensity sequences.

(18) There are 24 occurrences of a full 9 bp match sequence, AAGAAGAAG on the microarray. Double this number of highest intensity sequences was searched in addition to searching only the 24 highest intensities, yielding only small changes in the data. The sequence logo reported contains the 48 highest intensity sequences.

(19) To convert intensity to K_a, we have included the error term ε in our calculations. This gives modified versions of Eqs 3 and 4, $K_a = (\text{Intensity} - \varepsilon)/\{[PA] \times (c - \text{Intensity} + \varepsilon)\}$ and $K_a = (\text{Intensity} - \varepsilon)/\{[PA] \times c\}$, respectively.

(20) Van Dyke, M. M.; Dervan, P. B. *Science* **1984**, *225*, 1122–1127.

(21) Kong, D.; Park, E. J.; Stephen, A. G.; Calvani, M.; Cardellina, J. H.; Monks, A.; Fisher, R. J.; Shoemaker, R. H.; Melillo, G. *Cancer Res.* **2005**, *65*, 9047–9055.

(22) Belitsky, J. M.; Nguyen, D. H.; Wurtz, N. R.; Dervan, P. B. *Bioorg. Med. Chem.* **2002**, *10*, 2767–2774.

(23) Baird, E. E.; Dervan, P. B. *J. Am. Chem. Soc.* **1996**, *118*, 6141–6146.

(24) Colantuoni, C.; Henry, G.; Zeger, S.; Pevsner, J. *Bioinformatics* **2002**, *18*, 1540–1541.

(25) Bolstad, B. M.; Irizarry, R. A.; Astrand, M.; Speed, T. P. *Bioinformatics* **2003**, *19*, 185–193.

Chapter 4

Genome-Wide Binding Profile of Androgen Receptor in Dihydrotestosterone-Induced LNCaP Cells

This research has been supervised by Peter B. Dervan (California Institute of Technology) and conducted in conjunction with the Wold lab (California Institute of Technology). Ali Mortazavi, Anthony Kirilusha, Ken McCue, Diane Trout, and Brian Williams have provided valuable help on performing ChIP and assisting with data work-up.

Abstract

The nuclear hormone receptor, androgen receptor, has been mapped genome-wide in LNCaP cells utilizing chromatin immunoprecipitation followed by high throughput sequencing (ChIP-Seq). We observe as many as 7200 androgen receptor binding sites present in 2764 enriched, immunoprecipitated regions. We find a canonical androgen response element in the sequence data that maps to more than half of the immunoprecipitated regions. Furthermore, we define a secondary sequence motif that may be a dimer between an androgen receptor half-site and a forkhead protein. While such interactions are known in the literature, none have observed highly conserved sequence motifs. We observe fourteen other transcription factor motifs to be highly enriched within the binding regions. We characterize the majority of binding regions to be present in gene enhancer regions. Finally, we observe that fewer than 10% of the gene expression changes resulting from DHT-induction correlate with the presence of an androgen receptor binding region.

Introduction

Androgen Receptor Biology

Androgen receptor (AR), one of several nuclear hormone receptors, is a 110 kDa basic helix-loop-helix protein that binds a 5'-GGWACANNNTGTTCT-3' consensus androgen response element (ARE) as a homodimer (Figure 4.1A).[1,2] It resides outside of the nucleus until bound by a steroid, such as dihydroxytestosterone (DHT), which enables translocation into the nucleus, binding to androgen response elements, and modulation of androgen-responsive genes. AR helps to regulate the growth, differentiation, and survival of epithelial cells in the normal prostate.[3] Genotropic actions of AR are responsible for prostate cancer disease progression.[4]

The promoters of several key genes driven by androgen receptor occupancy have been studied in cell culture.[5–10] LNCaP cells have been used primarily because they are most widely available and are one of the oldest established immortalized cell lines.[11–14] The prostate specific androgen (PSA) promoter, a marker gene used to test for the presence of prostate cancer has been well mapped.[8,9] It contains a complex similar to the one drawn in Figure 4.1B. There are several ARE binding events, one in the promoter region, and a handful several kilobases upstream in the enhancer region. Additionally, other transcription factors are known to bind nearby in this promoter and synergistically cooperate in the induction of PSA, such as HIF-1α[15] and CREB.[16] As the complex forms, RNA polymerase II is recruited, and transcription begins. Chromatin immunoprecipitation has validated the presence of AR in both enhancer and promoter regions, as well as the presence of RNA polymerase II in these regions.[8,9]

Mapping the genomic AR-bound loci in LNCaP cells is vital to understand those genes directly regulated by DHT-induced AR binding events. Recent ChIP-chip (ChIP followed by microarray study of immunoprecipitated DNA) analysis has mapped AR occupancy to at most 3% of the contiguous human genome at no better than 500-bp

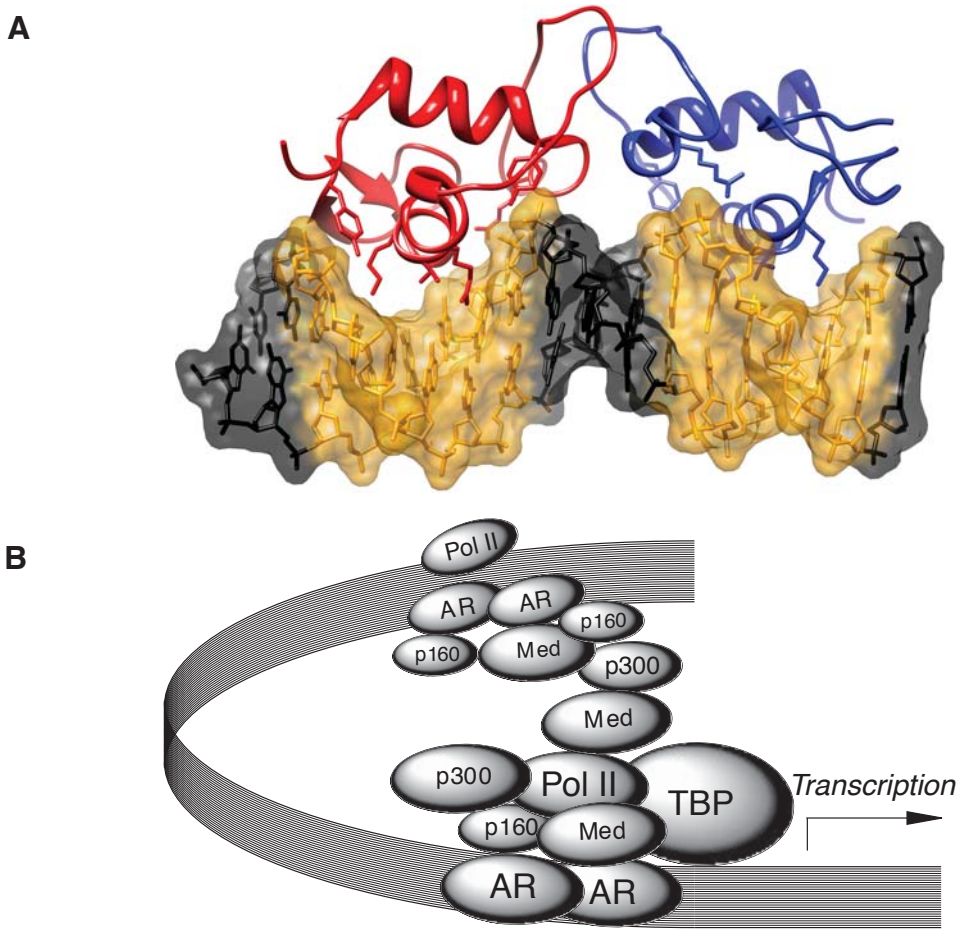

Figure 4.1. Overview of Androgen Receptor Biology. a) Crystal structure of androgen receptor DNA binding domain (PDB 1R4I). b) Example of an androgen receptor promoter / enhancer complex

resolution using either R1881 (1 nM[17,18] or 10 nM[19]) or DHT-induced (10 nM[20] or 100 nM[21]) LNCaP,[18,19,21] C4-2B,[20] or HPr-1AR cells[17] for a variety of time points. These studies have revealed potential new binding partners for androgen receptor, although none has shown a conserved motif of AR and a separate protein. Multiple examples of AR binding near other proteins (within 5–20 base pairs) exist, but a strongly conserved pattern has not emerged.

Disruption of AR binding at the AR-DNA interface may serve as a platform for future therapeutic approaches to mediating prostate cancer disease progression.

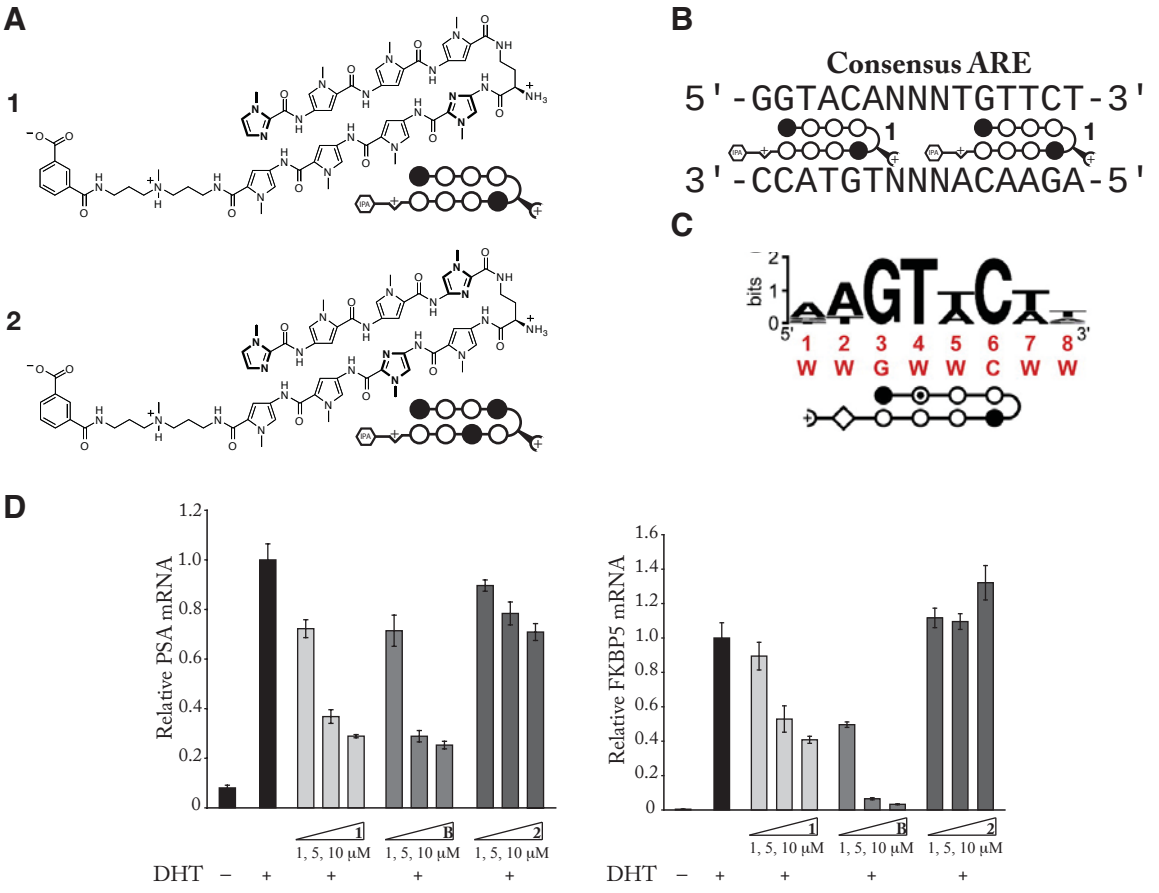

Figure 4.2. Polyamides can target and regulate Androgen Receptor (AR)-driven Gene Transcription. a) Match (1) and mismatch (2) polyamides for AR studies. b) Consensus ARE. c) CSI-derived sequence logo for a polyamide similar to 1. d) Polyamides specifically downregulate expression of PSA and FKBP5, two well characterized genes regulated by AR.

Polyamide Modulation of Androgen Receptor-Driven Gene Expression

We have discovered a polyamide (**1**) that targets the 5'-WGWWCW-3' subset of the androgen response element (ARE) consensus sequence and disrupts the AR-ARE binding event in LNCaP cell culture, resulting in downregulated PSA mRNA transcripts (Figure 4.2). Microarray mRNA transcript analysis demonstrates that polyamide **1** modulates a distinct set of genes from bicalutamide, and from an off-target mismatch polyamide (**2**) that binds to 5'-WGWCGW-3'. These findings suggest that disruption of binding at the protein-DNA interface is empirically distinguishable from protein-small molecule antagonism and that sequence specificity drives observed gene expression changes.[22] It is important to

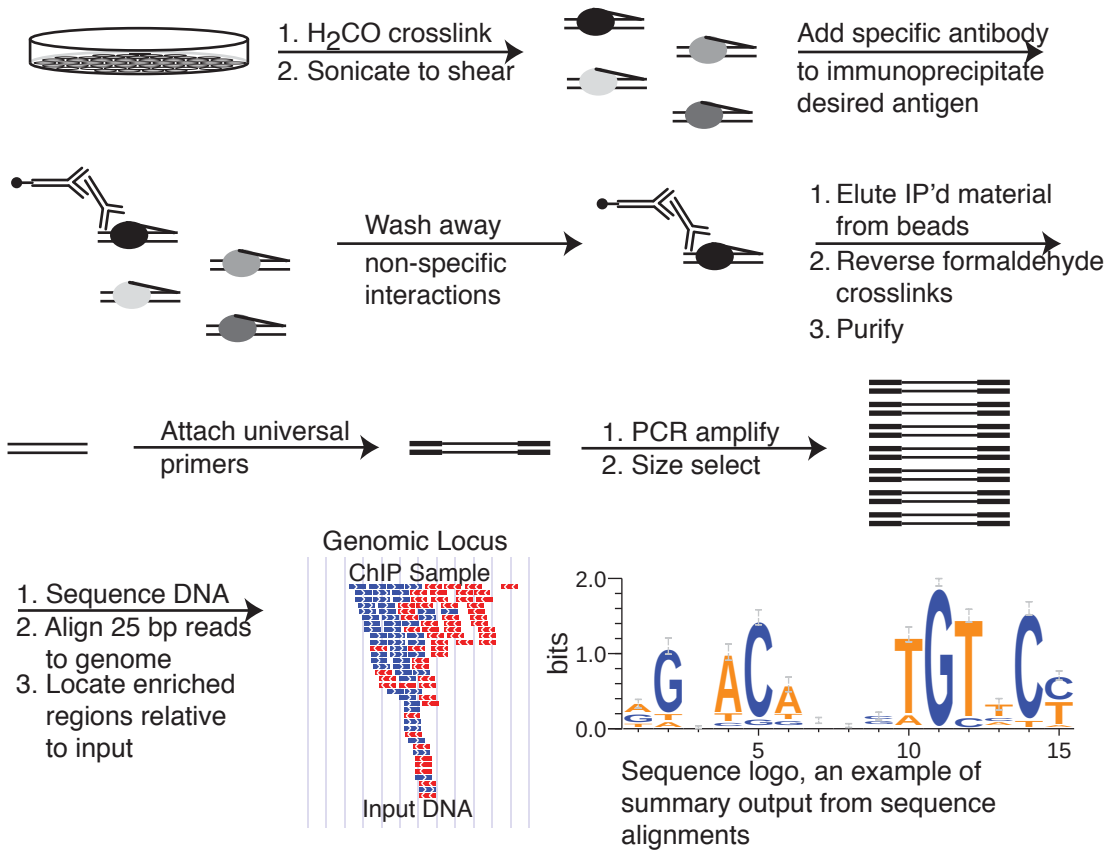

Figure 4.3. Overview of Chromatin Immunoprecipitation followed by High-throughput DNA Sequencing (ChIP-Seq)

understand whether polyamide **1** disrupts the subset of AR-ARE binding events that will be useful for slowing prostate cancer disease development.

Chromatin Immunoprecipitation followed by High Throughput Sequencing

Several new direct ultrahigh-throughput sequencing technologies enable more thorough functional genomics studies to be performed.[23,24] Chromatin immunoprecipitation (ChIP) isolates specific antigen-bound DNA fragments using an antibody bound to an immobilized support, such as magnetic bead, and has been utilized to map DNA occupancy by specific proteins.[25] ChIP-Seq is simply ChIP followed by direct ultra high-throughput DNA sequencing of the antibody-immunoprecipitated sample.[26] Genomic transcription-factor binding events have begun to be measured using ChIP-Seq (Figure 4.3).[26–30] This

technology enables antigen binding events to be resolved at 25 bp resolution, 20-fold better than previous generation ChIP-chip (chromatin immunoprecipitation followed by microarray elucidation of binding regions).[26] It requires no prior knowledge of sequence content. For genome-wide studies, it is substantially less expensive and more efficient—it only sequences material that is immunoprecipitated. It does not probe for other DNA.[24]

Overview of Experiment

This chapter focuses on providing a genome-wide binding baseline for androgen receptor occupancy in DHT-induced LNCaP cell culture. It will resolve the regions occupied by androgen receptor, the frequency of androgen receptor occurrence, binding preferences of androgen receptor, functional locations within nearby genes to binding events, and the correlations between prior microarray data and androgen receptor occupied regions. This data stands as a baseline for future experiments to create a displacement map of polyamide activity.

Results

Androgen receptor (AR)-bound DNA was immunoprecipitated from sonicated, 1 nM dihydrotestosterone (DHT)-induced LNCaP cell lysates using the rabbit polyclonal Santa Cruz Biotech antibody N-20. Real-Time, quantitative PCR (qPCR) revealed 100 (±9)-fold enrichment at the PSA ARE III locus and 48 (±6)-fold enrichment at the FKBP5 intronic locus over the average of two genomic negative loci (Figure 4.4). The immunoprecipitated fragments were then sequenced with an Illumina Genome Sequencer high throughput DNA sequencing machine. A mock sample, which was simply input DNA for the chromatin immunoprecipitation experiment, was sequenced as a control for non-random genomic shearing from the sonication. Sequenced fragments were deconvoluted in ELAND (Solexa), trimmed to 25 base pairs, and aligned to the genome using bowtie.[31] A 1 nM dihydrotestosterone (DHT)-induced sample was examined. Using ERANGE

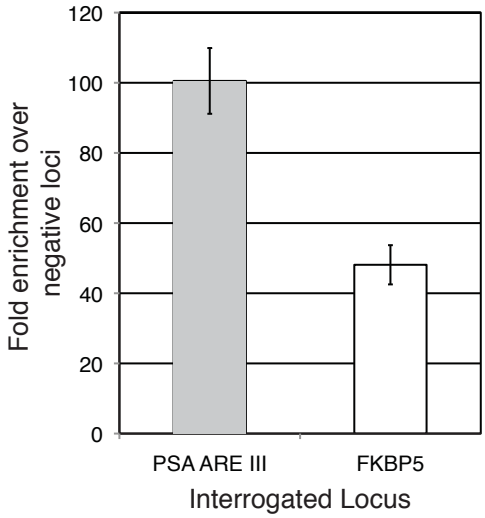

Figure 4.4. Verification of Initial ChIP data for Sequencing Submission. Enrichments are for 1 nM DHT-induced LNCaP cells and are compared relative to other loci in the human genome. An input sample calibrates the relative levels of genomic loci.

Table 4.1. Summary statistics of ChIP-Seq data. Enriched regions were called based on a four-fold enrichment relative to the input sample and a minimum of one read per million reads present in the enriched region.

	Input	ChIP sample
25 base pair reads	24.7 M	20.4 M
Fraction of reads mapped to human genome	69.8% (14.2 M)	43.4% (10.7 M)
Number of uniquely mapped loci	11.9 M	8.9 M
Number of loci mapped to multiple genomic regions	2.3 M	1.8 M
Fraction of reads mapped to enriched regions	1 %	
Number of enriched regions	2764	

3.0alpha,[26,32] 2,764 regions were found to be significantly enriched relative to the input control.

Summary Statistics of Sequenced Samples

While there is no standardized method of reporting data for ChIP-Seq, there are a few summary statistics that should be reported. Table 4.1 summarizes these statistics for both the induced, immunoprecipitated sample and the induced, input sample. There were 24.7 million 25 base pair reads generated for the ChIP'ed sample and 20.4 million 25 base pair reads generated for the input sample. Of these reads 43.4% were mapped to the human genome for the ChIP'ed sample and 69.8% were mapped in the input sample.

Once the reads were mapped to the human genome, regions were characterized as enriched if a given area of the genome was at least fourfold enriched in the ChIP-ed sample relative to the input sample. An additional requirement of one read per million reads was required for each region to be called enriched. With these parameters, roughly 1% of all reads mapped to enriched regions. There were 2,764 regions called enriched relative to the input. Each region spans on average 214 ± 75 base pairs.

Motif Searching

Because AR has been immunoprecipitated, one would expect to find the canonical ARE as a primary motif within the 2,764 enriched regions. The motif searching is computationally faster if highly-enriched events are searched first (Figure 4.5). A motif found from these regions can then be utilized to search all regions. Inevitably some regions will not contain the first motif. These left-over regions can then be submitted for motif searching, and the process can continue iteratively.

Utilizing the 593 most highly-enriched AR binding regions as a seed, motif searching was conducted through the ERANGE 3.0alpha package, using the motif-finding software MEME.[26,32,33] The 15 bp canonical ARE was observed (Figure 4.6). To determine

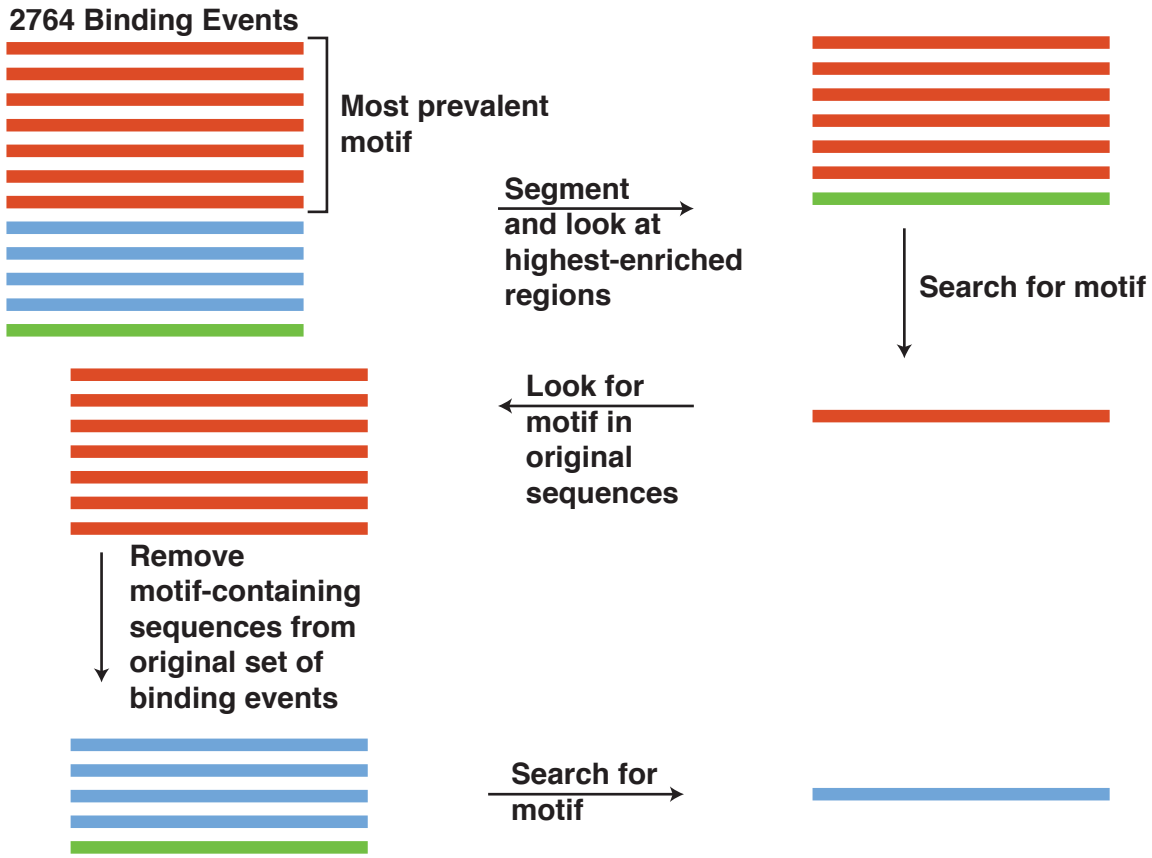

Figure 4.5. Method for finding multiple sequencing motifs using motif-finding algorithms

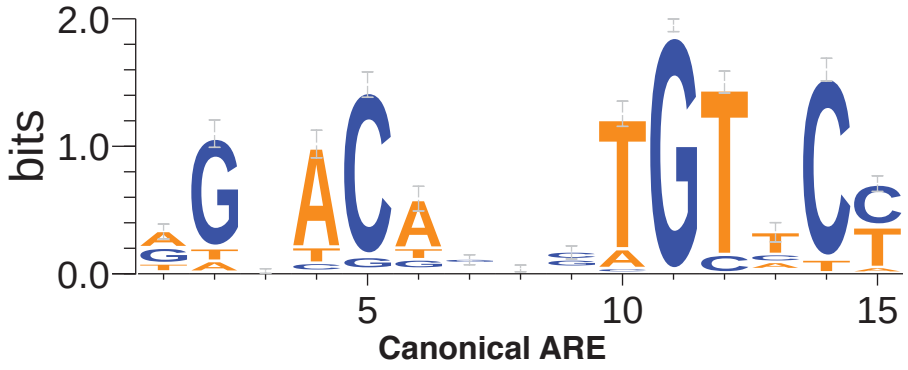

Figure 4.6. The Canonical ARE sequence was found using the 593 most strongly enriched binding regions.

Table 4.2. Prevalence of other ARE Elements in the genome and an upper estimate on the number of ARE binding sites

Motif	Matches within 2,764 Regions
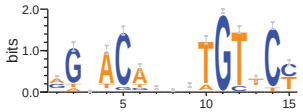	2,752
TGTTCTnnnAGAACA	206
TGTTCTnnnTGTTCT	318
AGAACAnnnTGTTCT	1,074
TGTTCT (half-site)	10,522
Estimated number of Genomic AR Binding Events (Number of half sites – 2 x Number of Canonical Motif – other AR motifs)	7,246

the prevalence of this motif in the 2,764 regions, the frequency matrix for this empirically determined motif was utilized to search the regions and yielded 1,800 regions and 2,752 canonical ARE binding sites.

The ARE binding profiles have been previously segmented to look specifically for ARE half-sites defined as 5'-AGAACA-3,' ARE head-to-head binding 5'-AGAACA$[N]_{0-8}$TGTTCT-3,' ARE tail-to-tail binding 5'-TGTTCT$[N]_{0-8}$AGAACA-3,' and a typical ARE head-to-head binding with three nucleotide spacer 5'-AGAACANNNTGTTCT-3.'[21] In this study, the ARE half-site and ARE dimers were utilized to search the immunoprecipitated regions. For ARE tail-to-tail binding, ARE direct-repeat binding, and ARE head-to-head binding (canonical ARE), a fixed three nucleotide spacer, 5'-NNN-3,' was utilized. Table 4.2 summarizes the findings from these searches.

We can utilize this data to estimate the number of genomic androgen receptor binding events. By counting the ARE half-sites, we have an upper bound on the total number of binding events. Inevitably, two half-sites will be contained within the canonical

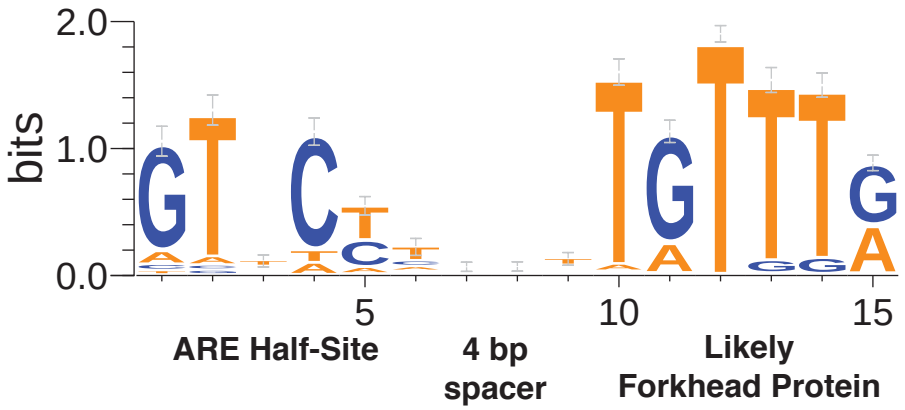

Figure 4.7. Sequence logo of a conserved motif that contains an ARE half-site and a forkhead protein binding site

ARE motif and other ARE dimer motifs. Thus, we can subtract out twice the number of ARE dimer motifs from the number of ARE half-sites. This would give 7,246 putative genomic AR binding events from 2,764 androgen receptor immunoprecipitated regions.

To discover other prominent motifs by the motif-finding software mentioned above, the 964 regions that did not contain the canonical ARE were searched for motifs. This search resulted in a motif containing an ARE half-site and what appears to be a motif for one of the forkhead proteins (Figure 4.7). The frequency matrix of this motif was used to search the entire 2,764 region sample. This motif occurs 1,622 times in 1,275 of the 2,764 regions.

There are several instances in the literature that note potential binding partners with androgen receptor. In previous ChIP-chip work, Brown and co-workers found the ARE half-site close to Oct1, GATA2, and HNF-3α (FOX-A1).[21] A recent ChIP-chip paper from the Coetzee lab noted an overrepresentation of HNF-3α sequences within androgen receptor occupied regions (each region is ~500 bp).[20] LNCaP cells are known to express HNF-3α, and thus it would be a likely candidate for the motif that is observed.[20,21,34] It is also possible that other forkhead proteins may be binding adjacent to the ARE half-site. Because of the forkhead proteins' similar binding preferences, it is not possible to differentiate the occupancy by sequence motif alone. The motif found in these regions

marks *the first instance of a well-conserved motif for the ARE half-site bound with a forkhead protein*.

The ARE-forkhead dimer motif exhibits a strong preference for a four base-pair spacer between the androgen response element and the forkhead binding region (Figure 4.7). Previously published data on AR interactions with HNF-3α showed variable distances of 0 bp to 10 bp between ARE half-site and forkhead binding consensus sequences. The PSA promoter must be bound by HNF-3α to enable transcription.[34]

An alternate approach to searching for motifs involves utilizing public consensus sequence databases such as TRANSFAC[35] or JASPAR[36] to search for overrepresented motifs within the binding regions. A publically available website (the cis-regulatory element annotation system, CEAS) enables such searching by utilizing the enriched immunoprecipitated regions as an input.[37] Eighteen distinct motifs relevant to human cell lines are listed (Figure 4.8). HNF-3α and several other forkhead proteins were most enriched after AR, glucocorticoid receptor, and progesterone receptor. These three nuclear hormone receptors have highly homologous consensus binding sequences, hence it is not surprising to observe their enrichment. Future work will seek to elucidate which of these factors is influential on modulating gene expression in conjunction with AR.

Regions of Genomic Occupancy

In addition to searching for sequence motifs of androgen receptor, we can observe nearby genes to each androgen receptor immunoprecipitated region. These may be suitable targets for androgen receptor regulation. Current algorithms search for the nearest gene within a specified radius of the antigen binding region. By examining different radii mapping with genes, we observe that the number of regions that fail to map to genes decreases rapidly when increasing from a 10 kilobase (kb) radius to a 500 kb radius (Figure 4.9). Six immunoprecipitated regions fail to map to any genes, even within megabase radii. This result is consistent with a 0.14% false discovery rate in the enriched regions.

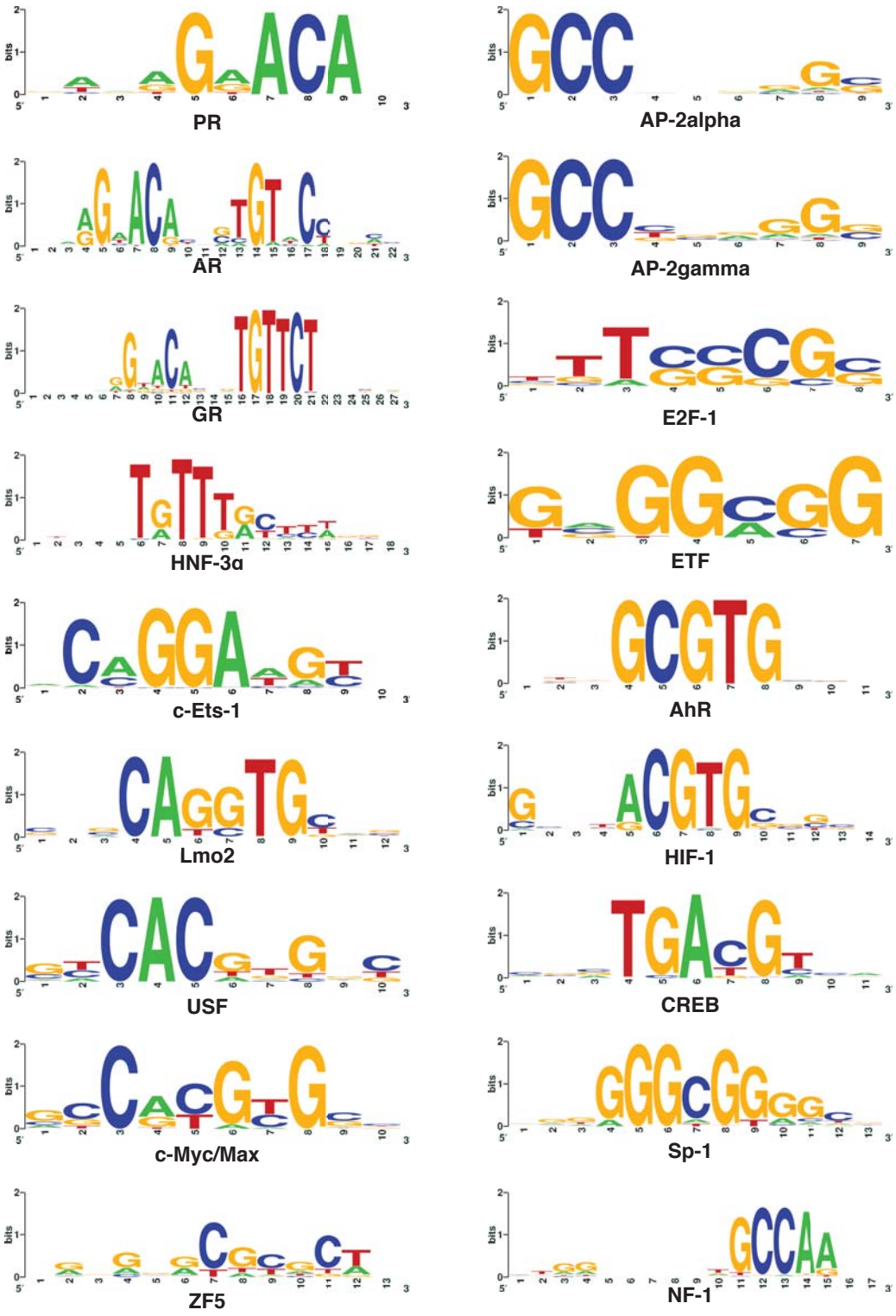

Figure 4.8. Sequence logos of known transcription factor motifs overrepresented within the Androgen Receptor Immunoprecipitated Regions

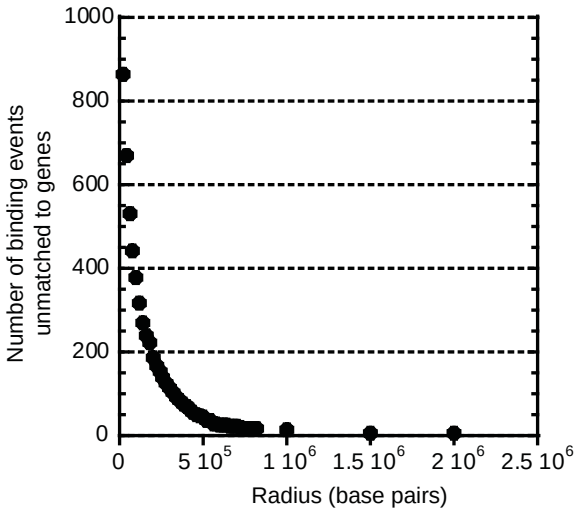

Figure 4.9. An overview of the number of androgen receptor immunoprecipitated regions that fail to map with nearby genes as a function of search radius. 1901 genes map within 20 kb of the androgen receptor binding regions.

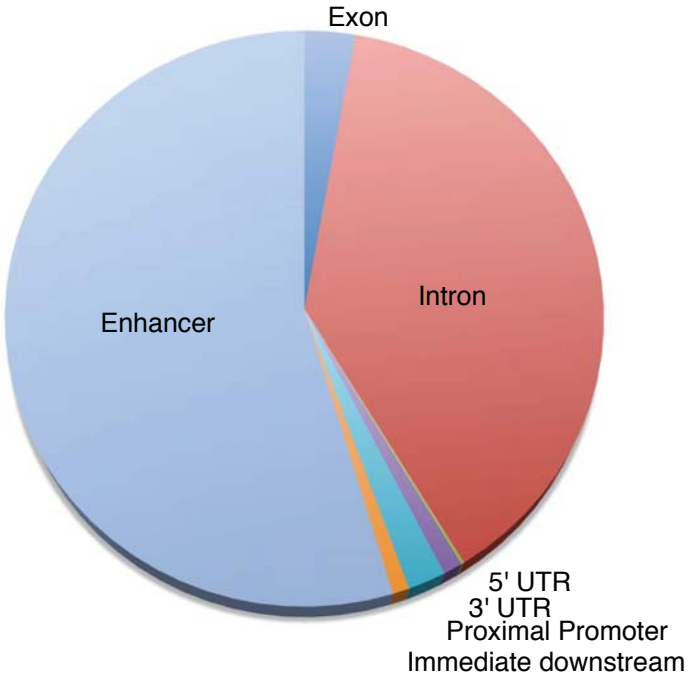

Figure 4.10. The distribution of regions of gene occupancy for androgen receptor binding regions within proximity to genes

Utilizing a 20 kb radius for mapping genes, we observe 1901 regions that map to nearby genes. These regions can be segmented into those located within enhancers (54.6%), exons (2.8%), introns (38.5%), 5'-untranslated regions (0.2%), 3'-untranslated regions (1.0%), proximal promoters (2.0%), and immediate downstream regions (0.9%) of the gene (Figure 4.10).

Correlating Microarray Transcript Analyses with ChIP-Seq Data

We can correlate androgen receptor genomic occupancy nearby genes with changes in mRNA microarray data[22] for vehicle-treated and DHT-induced conditions. Of the 1901 regions associated with genes, 356 regions overlap with 273 genes that change in expression by 1.4-fold or more with a *P* value of less than 0.01 (Figure 4.11). It is intriguing that fewer than 10% of the modulated genes correlate to androgen receptor binding. This could result from long-range (across other genes) androgen receptor transcription modulation via chromosomal looping. It could also be an artifact of androgen receptor-induced genes

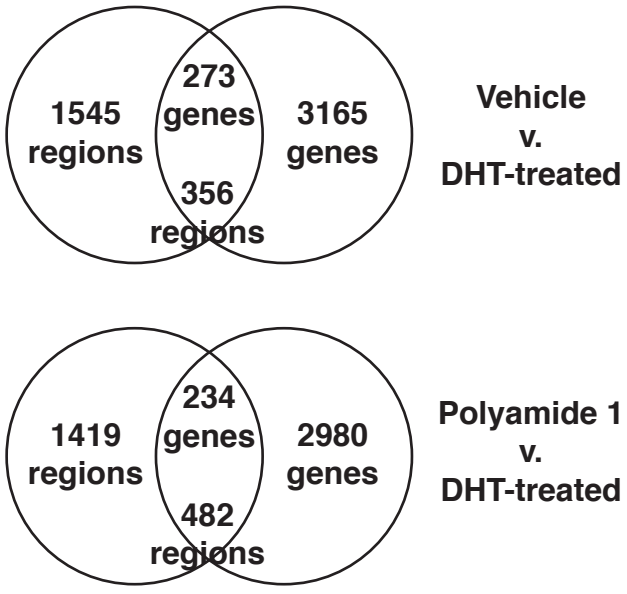

Figure 4.11. Venn diagram correlating AR binding events in proximity to genes with changes in mRNA transcript levels on DNA microarrays. A 1.4-absolute fold change and 0.01 *P* value cut-off were used for microarray values.

activating or repressing the expression of other genes.

Applying the same correlation with androgen receptor occupancy to polyamide **1**-treated microarray data, one observes fewer genes (234) intersecting with more regions (482) as compared with DHT-induced conditions above (Figure 4.11). This observation could signify that polyamides need to interfere with multiple androgen receptor binding events to achieve down- or up-regulation of genes. Future work with ChIP-Seq of polyamide **1**-treated, DHT-induced cells will help to elucidate where the polyamide is acting.

Conclusions

In this initial study of DHT-induced, genome-wide androgen receptor occupancy in LNCaP cells, we have found an upper bound to the number of genomic androgen receptor binding events, roughly 7200. We have observed the canonical ARE to be widely present in the androgen receptor immunoprecipitated regions and have found a defined sequence motif that may be explained by adjacent pairing of AR with HNF-3α. We have defined a set of 1901 regions that occur within 20 kilobases of known genes and observed that the majority of these regions are found within enhancers. By correlating mRNA microarray transcript analyses with androgen receptor immunoprecipitated regions, we observe that fewer than 10% of significantly changed genes can be correlated by androgen receptor occupancy. Herein, we have defined an initial data set of genome-wide binding of androgen receptor.

References

(1) Shaffer, P. L.; Jivan, A.; Dollins, D. E.; Claessens, F.; Gewirth, D. T. *Proc. Natl. Acad. Sci. U. S. A.* **2004**, *101*, 4758–63.

(2) Roche, P. J.; Hoare, S. A.; Parker, M. G. *Mol. Endocrinol.* **1992**, *6*, 2229–35.

(3) Craft, N.; Sawyers, C. L. *Cancer Metastasis Rev.* **1998**, *17*, 421–7.

(4) Scher, H. I.; Sawyers, C. L. *J. Clin. Oncol.* **2005**, *23*, 8253–61.

(5) Jia, L.; Choong, C. S.; Ricciardelli, C.; Kim, J.; Tilley, W. D.; Coetzee, G. A. *Cancer Res.* **2004**, *64*, 2619–26.

(6) Louie, M. C.; Yang, H. Q.; Ma, A. H.; Xu, W.; Zou, J. X.; Kung, H. J.; Chen, H. W. *Proc. Natl. Acad. Sci. U. S. A.* **2003**, *100*, 2226–30.

(7) Kang, Z.; Janne, O. A.; Palvimo, J. J. *Mol. Endocrinol.* **2004**, *18*, 2633–48.

(8) Shang, Y.; Myers, M.; Brown, M. *Mol. Cell* **2002**, *9*, 601–10.

(9) Wang, Q.; Carroll, J. S.; Brown, M. *Mol. Cell* **2005**, *19*, 631–42.

(10) Magee, J. A.; Chang, L. W.; Stormo, G. D.; Milbrandt, J. *Endocrinology* **2006**, *147*, 590–8.

(11) Horoszewicz, J. S.; Leong, S. S.; Chu, T. M.; Wajsman, Z. L.; Friedman, M.; Papsidero, L.; Kim, U.; Chai, L. S.; Kakati, S.; Arya, S. K.; Sandberg, A. A. *Prog. Clin. Biol. Res.* **1980**, *37*, 115–32.

(12) Horoszewicz, J. S.; Leong, S. S.; Kawinski, E.; Karr, J. P.; Rosenthal, H.; Chu, T. M.; Mirand, E. A.; Murphy, G. P. *Cancer Res.* **1983**, *43*, 1809–18.

(13) Sobel, R. E.; Sadar, M. D. *J. Urol.* **2005**, *173*, 342–59.

(14) Sobel, R. E.; Sadar, M. D. *J. Urol.* **2005**, *173*, 360–72.

(15) Horii, K.; Suzuki, Y.; Kondo, Y.; Akimoto, M.; Nishimura, T.; Yamabe, Y.; Sakaue, M.; Sano, T.; Kitagawa, T.; Himeno, S.; Imura, N.; Hara, S. *Mol. Cancer Res.* **2007**, *5*, 383–91.

(16) Kim, J.; Jia, L.; Stallcup, M. R.; Coetzee, G. A. *J. Mol. Endocrinol.* **2005**, *34*,

107–18.

(17) Bolton, E. C.; So, A. Y.; Chaivorapol, C.; Haqq, C. M.; Li, H.; Yamamoto, K. R. *Genes Dev.* **2007**, *21*, 2005–17.

(18) Massie, C. E.; Adryan, B.; Barbosa-Morais, N. L.; Lynch, A. G.; Tran, M. G.; Neal, D. E.; Mills, I. G. *EMBO Reports* **2007**, *8*, 871–878.

(19) Takayama, K.; Kaneshiro, K.; Tsutsumi, S.; Horie-Inoue, K.; Ikeda, K.; Urano, T.; Ijichi, N.; Ouchi, Y.; Shirahige, K.; Aburatani, H.; Inoue, S. *Oncogene* **2007**, *26*, 4453–63.

(20) Jia, L.; Berman, B. P.; Jariwala, U.; Yan, X.; Cogan, J. P.; Walters, A.; Chen, T.; Buchanan, G.; Frenkel, B.; Coetzee, G. A. *PLoS ONE* **2008**, *3*, e3645.

(21) Wang, Q.; Li, W.; Liu, X. S.; Carroll, J. S.; Janne, O. A.; Keeton, E. K.; Chinnaiyan, A. M.; Pienta, K. J.; Brown, M. *Mol. Cell* **2007**, *27*, 380–92.

(22) Nickols, N. G.; Dervan, P. B. *Proc. Natl. Acad. Sci. U. S. A.* **2007**, *104*, 10418–23.

(23) Shendure, J.; Ji, H. *Nat. Biotechnol.* **2008**, *26*, 1135–45.

(24) Wold, B.; Myers, R. M. *Nat. Methods* **2008**, *5*, 19–21.

(25) Solomon, M. J.; Larsen, P. L.; Varshavsky, A. *Cell* **1988**, *53*, 937–947.

(26) Johnson, D. S.; Mortazavi, A.; Myers, R. M.; Wold, B. *Science* **2007**, *316*, 1497–1502.

(27) Chen, X.; Xu, H.; Yuan, P.; Fang, F.; Huss, M.; Vega, V. B.; Wong, E.; Orlov, Y. L.; Zhang, W.; Jiang, J.; Loh, Y. H.; Yeo, H. C.; Yeo, Z. X.; Narang, V.; Govindarajan, K. R.; Leong, B.; Shahab, A.; Ruan, Y.; Bourque, G.; Sung, W. K.; Clarke, N. D.; Wei, C. L.; Ng, H. H. *Cell* **2008**, *133*, 1106–17.

(28) Robertson, G.; Hirst, M.; Bainbridge, M.; Bilenky, M.; Zhao, Y.; Zeng, T.; Euskirchen, G.; Bernier, B.; Varhol, R.; Delaney, A.; Thiessen, N.; Griffith, O. L.; He, A.; Marra, M.; Snyder, M.; Jones, S. *Nat. Methods* **2007**, *4*, 651–7.

(29) Wederell, E. D.; Bilenky, M.; Cullum, R.; Thiessen, N.; Dagpinar, M.; Delaney, A.; Varhol, R.; Zhao, Y.; Zeng, T.; Bernier, B.; Ingham, M.; Hirst, M.; Robertson, G.;

Marra, M. A.; Jones, S.; Hoodless, P. A. *Nucleic Acids Res.* **2008**, *36*, 4549–64.

(30) Nielsen, R.; Pedersen, T. A.; Hagenbeek, D.; Moulos, P.; Siersbaek, R.; Megens, E.; Denissov, S.; Borgesen, M.; Francoijs, K. J.; Mandrup, S.; Stunnenberg, H. G. *Genes Dev.* **2008**, *22*, 2953–67.

(31) Langmead, B.; Trapnell, C.; Pop, M.; Salzberg, S. L. *Genome Biol* **2009**, *10*, R25.

(32) Mortazavi, A.; Williams, B. A.; McCue, K.; Schaeffer, L.; Wold, B. *Nat. Methods* **2008**, *5*, 621–8.

(33) Bailey, T. L.; Elkan, C. In *Proceedings of the Second International Conference on Intelligent Systems for Molecular Biology*; Altman, R., Brutlag, D., Karp, P., Lathrop, R., Searl, D., Eds.; AAAI Press: Menlo Park, 1994, p 28–36.

(34) Gao, N.; Zhang, J.; Rao, M. A.; Case, T. C.; Mirosevich, J.; Wang, Y.; Jin, R.; Gupta, A.; Rennie, P. S.; Matusik, R. J. *Mol. Endocrinol.* **2003**, *17*, 1484–507.

(35) Wingender, E.; Dietze, P.; Karas, H.; Knuppel, R. *Nucleic Acids Res.* **1996**, *24*, 238–41.

(36) Sandelin, A.; Alkema, W.; Engstrom, P.; Wasserman, W. W.; Lenhard, B. *Nucleic Acids Res.* **2004**, *32*, D91–4.

(37) Ji, X.; Li, W.; Song, J.; Wei, L.; Liu, X. S. *Nucleic Acids Res.* **2006**, *34*, W551–4.

Appendix A

X-ray Crystal Structure of methyl 3-chlorothiophene-2-carboxylate

X-ray crystallographic diffraction, data collection and data work-up run by Dr. Michael W. Day at the X-Ray Crystallography Laboratory of the Beckman Institute at the California Institute of Technology.

Methyl 3-chlorothiophene-2-carboxylate (see Figure A.1 for the structure) was synthesized as previously described,[1] in preparation for use in polyamides that target the HIF-1α binding sequence.[2–5] During *in vacuo* concentration of the methyl 3-chlorothiophene-2-carboxylate, a large rectangular crystal formed inside the round bottom flask. The crystal was harvested and submitted for X-ray crystallographic analysis at the X-ray Crystallography Laboratory of the Beckman Institute at the California Institute of Technology. Dr. Michael W. Day performed the analyses. The results are described in Tables A.1–A.5 and Figures A.2 (ORTEP diagram)[6] and A.3 (crystal packing diagram, prepared in Cambridge Crystallographic Data Centre's Mercury software).[7] As of May 2009, no known crystal structures of this compound are in the Cambridge Structural Database.[8]

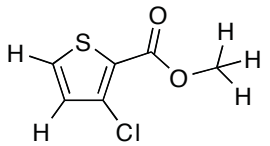

1

Figure A.1. Chemical structure of methyl 3-chlorothiophene-2-carboxylate (**1**)

Table A.1. Crystal data and structure refinement for **1** (CCDC 621056)

Empirical formula	$C_6H_5O_2ClS$
Formula weight	176.61
Crystallization Solvent	Diethylether
Crystal Habit	Block
Crystal size	0.27 x 0.22 x 0.11 mm^3
Crystal color	Colorless

Data Collection

Type of diffractometer	Bruker SMART 1000	
Wavelength	0.71073 Å MoKα	
Data Collection Temperature	100(2) K	
θ range for 4568 reflections used in lattice determination	2.95 to 32.85°	
Unit cell dimensions	a = 3.9030(4) Å b = 7.0415(7) Å c = 14.1389(15) Å	α = 101.291(2)° β = 92.911(2)° γ = 103.851(2)°
Volume	368.03(7) $Å^3$	
Z	2	
Crystal system	Triclinic	
Space group	P-1	
Density (calculated)	1.594 Mg/m^3	
F(000)	180	
Data collection program	Bruker SMART v5.630	
θ range for data collection	2.95 to 33.07°	
Completeness to θ = 33.07°	84.5 %	
Index ranges	$-5 \le h \le 5$, $-10 \le k \le 10$, $-19 \le l \le 19$	
Data collection scan type	ω scans at 7 ϕ settings	
Data reduction program	Bruker SAINT v6.45A	
Reflections collected	7841	
Independent reflections	2339 [R_{int}= 0.0528]	
Absorption coefficient	0.732 mm^{-1}	
Absorption correction	None	
Max. and min. transmission	0.9238 and 0.8268	

Table A.1. **(cont.)**

Structure solution and Refinement

Structure solution program	Bruker XS v6.12
Primary solution method	Direct methods
Secondary solution method	Difference Fourier map
Hydrogen placement	Difference Fourier map
Structure refinement program	Bruker XL v6.12
Refinement method	Full matrix least-squares on F^2
Data / restraints / parameters	2339 / 0 / 111
Treatment of hydrogen atoms	Unrestrained
Goodness-of-fit on F^2	1.548
Final R indices [I>2σ(I), 1821 reflections]	R1 = 0.0335, *w*R2 = 0.0632
R indices (all data)	R1 = 0.0467, *w*R2 = 0.0646
Type of weighting scheme used	Sigma
Weighting scheme used	$w=1/\sigma^2(Fo^2)$
Max shift/error	0.000
Average shift/error	0.000
Largest diff. peak and hole	0.412 and -0.315 e.Å^{-3}

Special Refinement Details

Refinement of F^2 against ALL reflections. The weighted R-factor (*w*R) and goodness of fit (S) are based on F^2, conventional R-factors (R) are based on F, with F set to zero for negative F^2. The threshold expression of $F^2 > 2\sigma(F^2)$ is used only for calculating R-factors(gt), etc. and is not relevant to the choice of reflections for refinement. R-factors based on F^2 are statistically about twice as large as those based on F, and R-factors based on ALL data will be even larger.

All esds (except the esd in the dihedral angle between two l.s. planes) are estimated using the full covariance matrix. The cell esds are taken into account individually in the estimation of esds in distances, angles and torsion angles; correlations between esds in cell parameters are only used when they are defined by crystal symmetry. An approximate (isotropic) treatment of cell esds is used for estimating esds involving l.s. planes.

Table A.2. Atomic coordinates (x 10^4) and equivalent isotropic displacement parameters ($Å^2$x 10^3) for **1** (CCDC 621056). U(eq) is defined as the trace of the orthogonalized U^{ij} tensor

	x	y	z	U_{eq}
S(1)	2592(1)	3029(1)	2079(1)	28(1)
Cl(1)	9437(1)	7820(1)	4119(1)	36(1)
O(1)	7587(3)	8581(2)	2092(1)	41(1)
O(2)	3446(3)	6220(1)	1056(1)	33(1)
C(1)	3599(4)	2345(2)	3129(1)	31(1)
C(2)	5821(4)	3874(2)	3783(1)	30(1)
C(3)	6728(3)	5637(2)	3420(1)	25(1)
C(4)	5223(3)	5433(2)	2496(1)	23(1)
C(5)	5610(4)	6934(2)	1894(1)	25(1)
C(6)	3584(5)	7601(3)	419(1)	39(1)

Table A.3. Bond lengths [Å] and angles [°] for **1** (CCDC 621056)

S(1)-C(1)	1.7041(15)	C(1)-S(1)-C(4)	92.00(7)
S(1)-C(4)	1.7276(12)	C(5)-O(2)-C(6)	115.38(11)
Cl(1)-C(3)	1.7260(12)	C(2)-C(1)-S(1)	112.46(11)
O(1)-C(5)	1.2005(16)	C(2)-C(1)-H(1)	128.8(10)
O(2)-C(5)	1.3531(15)	S(1)-C(1)-H(1)	118.7(10)
O(2)-C(6)	1.4436(18)	C(1)-C(2)-C(3)	111.74(12)
C(1)-C(2)	1.3589(19)	C(1)-C(2)-H(2)	126.3(9)
C(1)-H(1)	0.943(18)	C(3)-C(2)-H(2)	122.0(9)
C(2)-C(3)	1.4100(18)	C(4)-C(3)-C(2)	113.87(11)
C(2)-H(2)	0.928(14)	C(4)-C(3)-Cl(1)	125.06(10)
C(3)-C(4)	1.3720(18)	C(2)-C(3)-Cl(1)	121.06(10)
C(4)-C(5)	1.4670(18)	C(3)-C(4)-C(5)	128.64(11)
C(6)-H(6A)	0.978(16)	C(3)-C(4)-S(1)	109.92(9)
C(6)-H(6B)	0.938(18)	C(5)-C(4)-S(1)	121.44(9)
C(6)-H(6C)	0.96(2)	O(1)-C(5)-O(2)	123.00(12)
		O(1)-C(5)-C(4)	125.90(12)
		O(2)-C(5)-C(4)	111.09(11)
		O(2)-C(6)-H(6A)	111.1(10)
		O(2)-C(6)-H(6B)	108.8(11)
		H(6A)-C(6)-H(6B)	108.0(14)
		O(2)-C(6)-H(6C)	111.2(12)
		H(6A)-C(6)-H(6C)	110.1(15)
		H(6B)-C(6)-H(6C)	107.5(15)

Table A.4. Anisotropic displacement parameters ($Å^2 x\ 10^4$) for **1** (CCDC 621056). The anisotropic displacement factor exponent takes the form: $-2\pi^2[\ h^2a^{*2}U^{11} + ... + 2\ h\ k\ a^*\ b^*\ U^{12}\ ]$

	U^{11}	U^{22}	U^{33}	U^{23}	U^{13}	U^{12}
S(1)	292(2)	213(2)	283(2)	22(1)	-24(1)	-12(1)
Cl(1)	399(2)	280(2)	287(2)	12(1)	-73(1)	-49(2)
O(1)	476(7)	268(5)	394(6)	108(4)	-91(5)	-63(5)
O(2)	391(6)	283(5)	281(5)	73(4)	-76(4)	27(4)
C(1)	338(8)	245(7)	343(7)	97(6)	38(6)	20(6)
C(2)	337(8)	290(7)	250(7)	78(5)	15(6)	44(6)
C(3)	232(7)	215(6)	250(6)	7(5)	14(5)	18(5)
C(4)	210(6)	185(6)	264(6)	19(5)	12(5)	19(5)
C(5)	266(7)	228(6)	254(6)	39(5)	18(5)	58(5)
C(6)	469(10)	402(9)	324(8)	155(7)	-32(7)	107(8)

Table A.5. Hydrogen coordinates ($x\ 10^4$) and isotropic displacement parameters ($Å^2 x\ 10^3$) for **1** (CCDC 621056)

	x	y	z	U_{iso}
H(1)	2630(40)	1010(30)	3186(11)	45(5)
H(2)	6670(40)	3820(20)	4400(10)	30(4)
H(6A)	2860(40)	8790(30)	729(11)	48(5)
H(6B)	2010(50)	6970(30)	-139(13)	56(5)
H(6C)	5910(60)	7980(30)	215(13)	70(6)

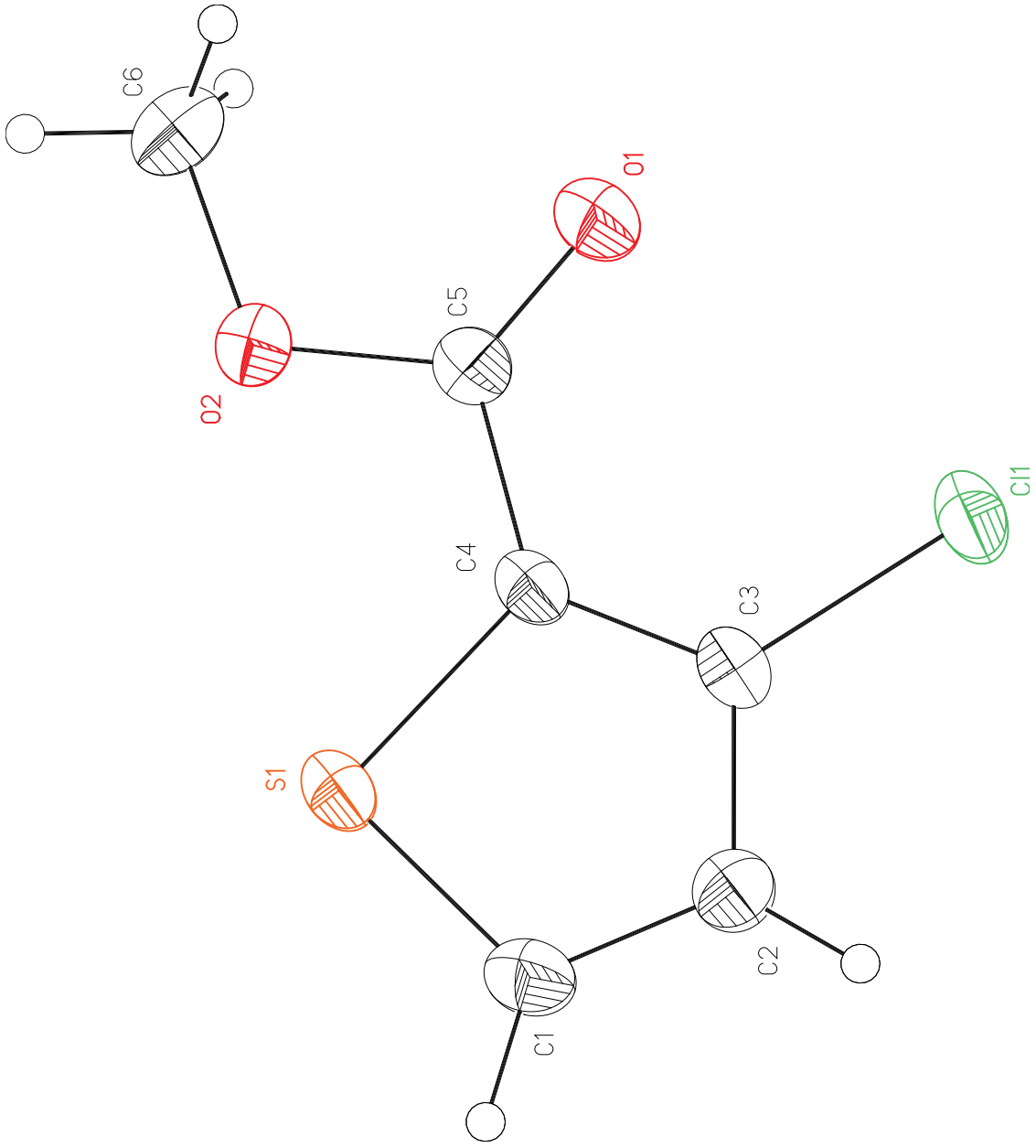

Figure A.2. ORTEP representation of methyl 3-chlorothiophene-2-carboxylate

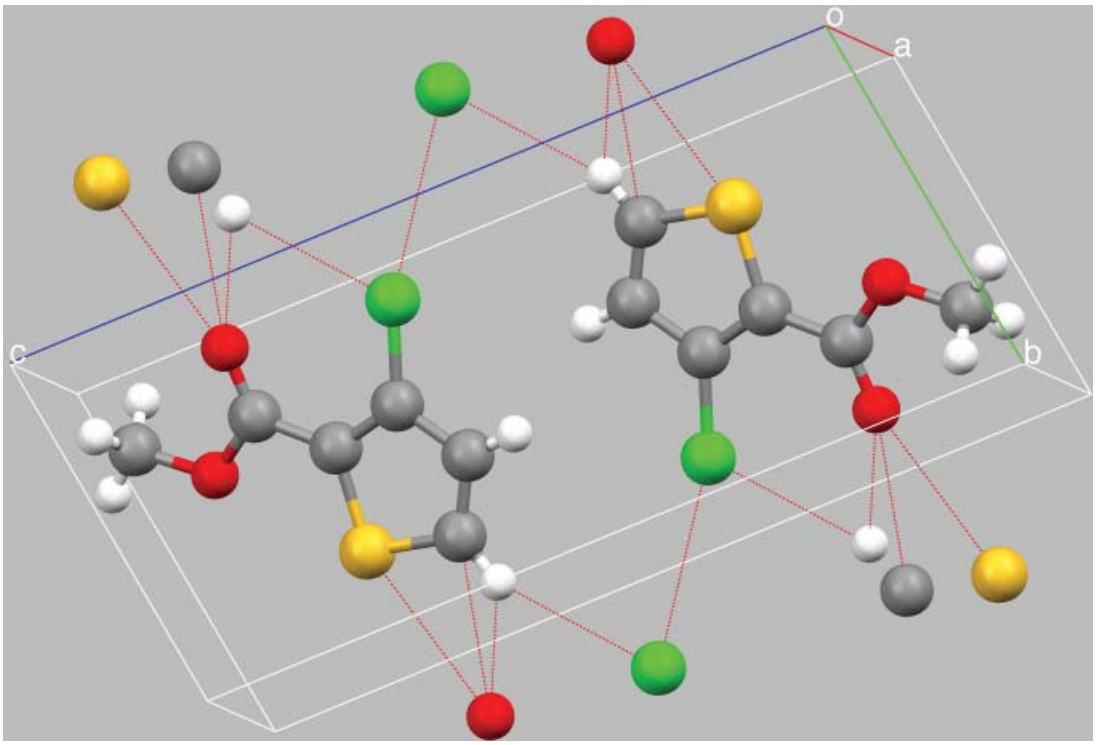

Figure A.3. Crystal packing and van der Waal's contacts for methyl 3-chlorothiophene-2-carboxylate

References

(1) Corral, C.; Lasso, A.; Lissavetzky, J.; Sanchez Alvarez-Insua, A.; Valdeolmillos, A. M. *Heterocycles* **1985**, *23*, 1431–5.

(2) Nickols, N. G.; Jacobs, C. S.; Farkas, M. E.; Dervan, P. B. *ACS Chem. Biol.* **2007**, *2*, 561–71.

(3) Nickols, N. G.; Jacobs, C. S.; Farkas, M. E.; Dervan, P. B. *Nucleic Acids Res.* **2007**, *35*, 363–70.

(4) Olenyuk, B. Z.; Zhang, G. J.; Klco, J. M.; Nickols, N. G.; Kaelin, W. G., Jr.; Dervan, P. B. *Proc. Natl. Acad. Sci. U. S. A.* **2004**, *101*, 16768–73.

(5) Puckett, J. W.; Muzikar, K. A.; Tietjen, J.; Warren, C. L.; Ansari, A. Z.; Dervan, P. B. *J. Am. Chem. Soc.* **2007**, *129*, 12310–9.

(6) Burnett, M. N.; Johnson, C. K. *ORTEP-III: Oak Ridge Thermal Ellipsoid Plot Program for Crystal Structure Illustrations*, Oak Ridge National Laboratory Report ORNL-6895, 1996.

(7) Macrae, C. F.; Bruno, I. J.; Chisholm, J. A.; Edgington, P. R.; McCabe, P.; Pidcock, E.; Rodriguez-Monge, L.; Taylor, R.; van de Streek, J.; Wood, P. A. *J. Appl. Cryst.* **2008**, *41*, 466–470.

(8) Allen, F. H. *Acta Crystallogr.* **2002**, *B58*, 380–8.

Appendix B

DNase I Footprinting and Alkylation Assays of Linear β-linked Compounds and Hairpin Polyamides Targeted to GAA Repeats

Enclosed in this appendix are several footprinting gels of linear *β*-linked polyamides and a single hairpin polyamide (overview in Figure B.1) targeted to $(AAG)_3 \cdot (CTT)_3$ (Figures B.2-B.5). A single thermal cleavage gel of chlorambucil alkylator Im-Py-*β*-Im-Py-*β*-Im-*β*-Dp-Chl (polyamide **7**) alkylating $(GAA)_{33} \cdot (TTC)_{33}$ is shown (Figure B.6). Table B.1 summarizes the findings in Figures B.2–B.5. Table B.2 summarizes MALDI-TOF Mass Spectrometric data collected for the seven compounds used in these studies.

The design of plasmid pJWP12 (Figure B.1B) was based on initial CSI motif data for polyamide **6**, in which 5'-AAGATGTTC-3' was the preferred motif, 5'-AAGAAGTTC-3' an acceptable similar site for the primary motif, and 5'-AAGAAGAAG-3' the binding site for which the polyamide was originally designed. Data from Figure B.2 shows that the affinity of **1** for the principal motif, 5'-AAGATGTTC-3' is less than that for the designed site, 5'-AAGAAGAAG-3.' Chapter 3 probes this discrepancy more in depth. The CSI microarray intensities correlate well with polyamide binding affinities but do not necessarily correlate with the sequence motif generated from the 300 highest affinity binding sites.

Polyamide alkylation studies were undertaken with polyamide **7** due to a collaboration with the Robert D. Wells laboratories at Texas A&M. Preliminary data suggested that polyamide **7** may be able to upregulate frataxin expression in GM15850 cells.

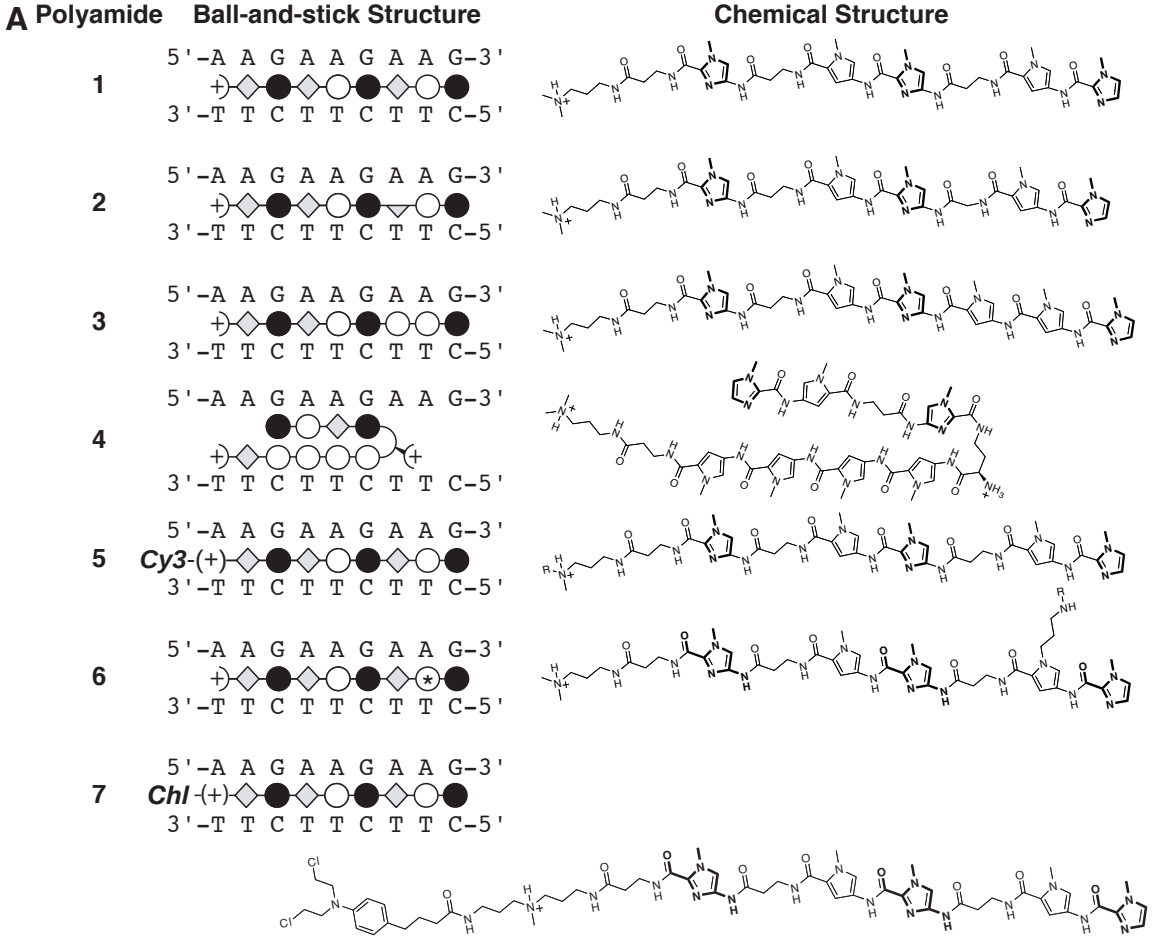

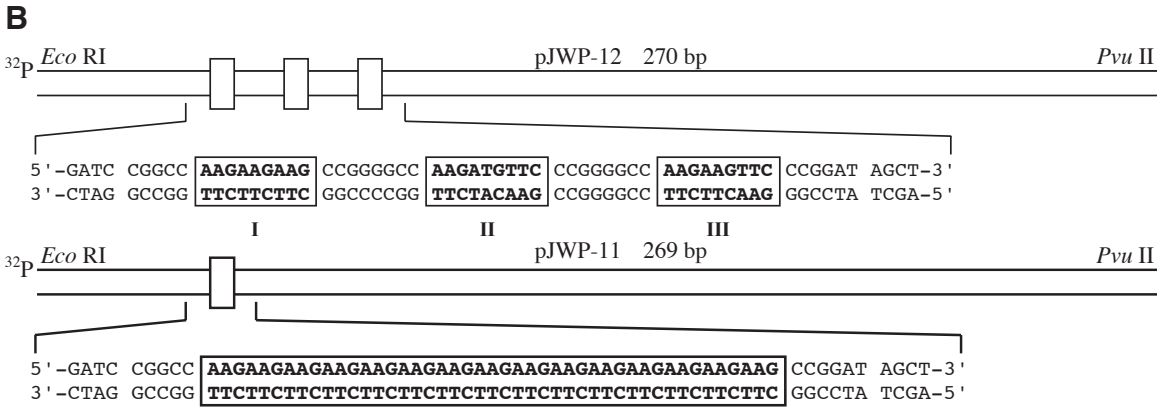

Figure B.1. Overview of Polyamides Studied on pJWP12 and pJWP11 and plasmid sequences of pJWP12 and pJWP11. a) Polyamides studied. b) Plasmid insert sequences

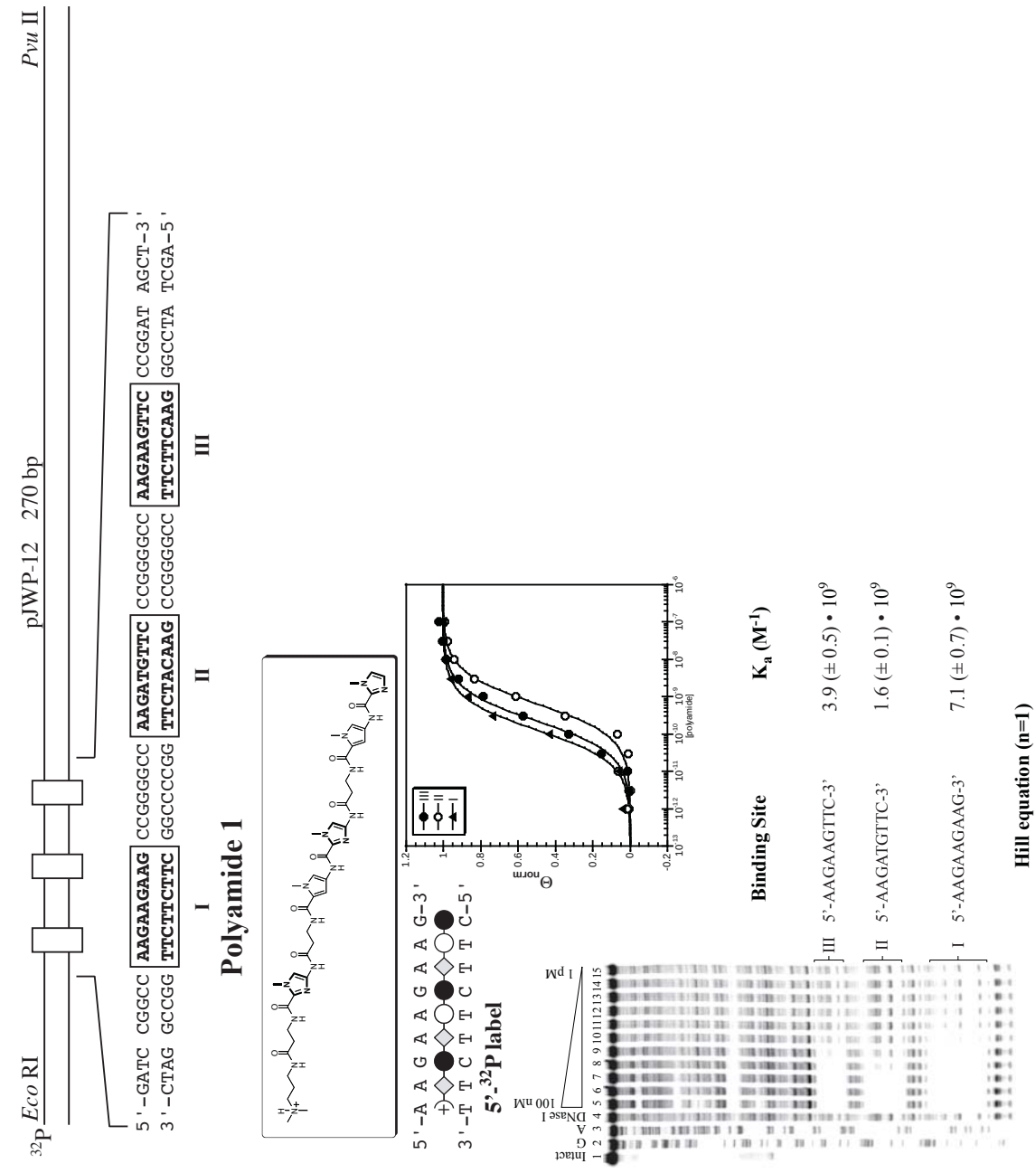

Figure B.2. Quantitative DNase I footprint of a linear *β*-linked polyamide targeting GAA repeats. CSI Motif preferred binding site **III** does not correlate with polyamide preferred binding site **I**.

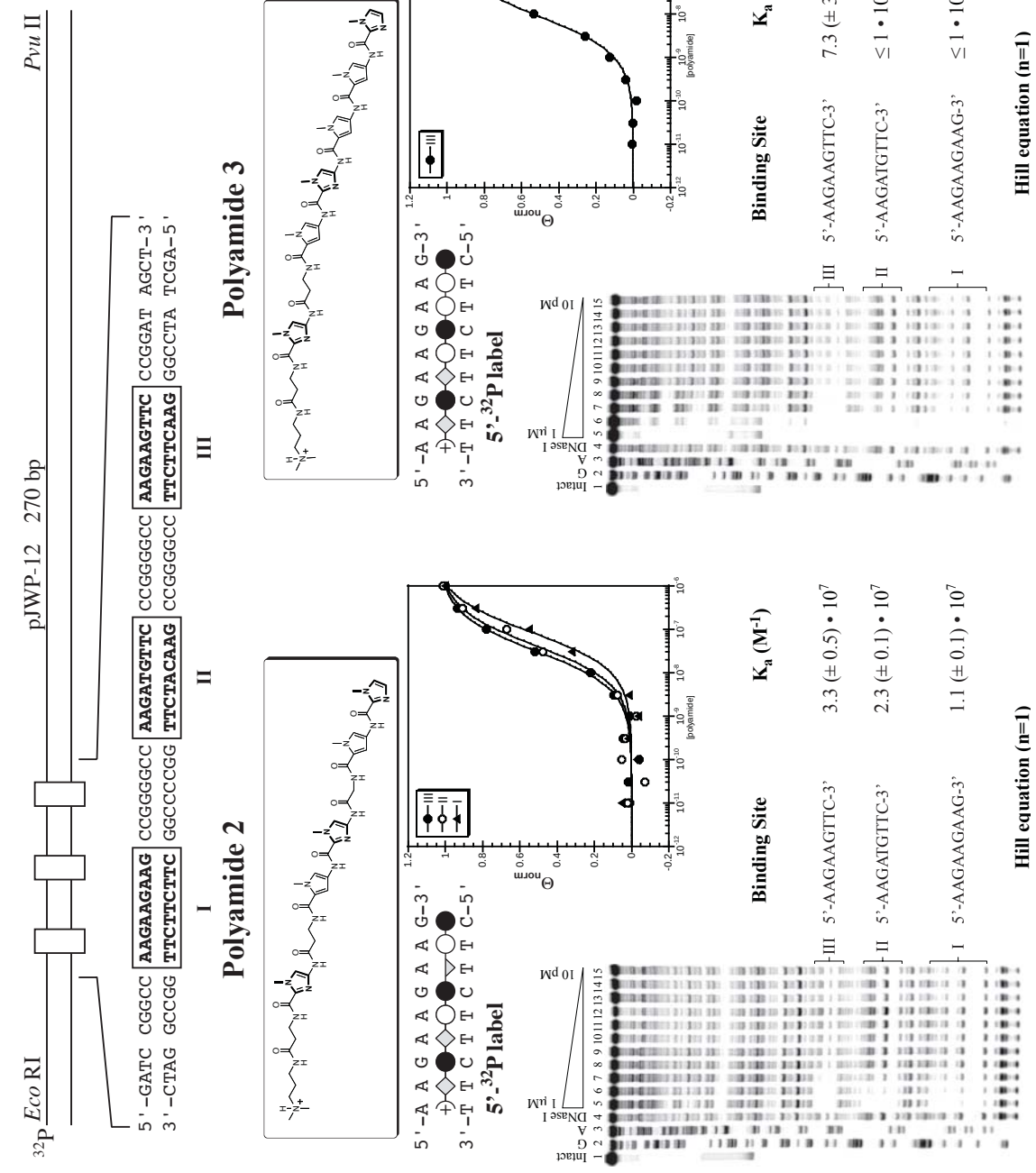

Figure B.3. Quantitative DNase I footprints for two linear *β*-linked polyamides, one containing a *β* → *Gly* point mutation and the other containing a *β* → Py point mutation

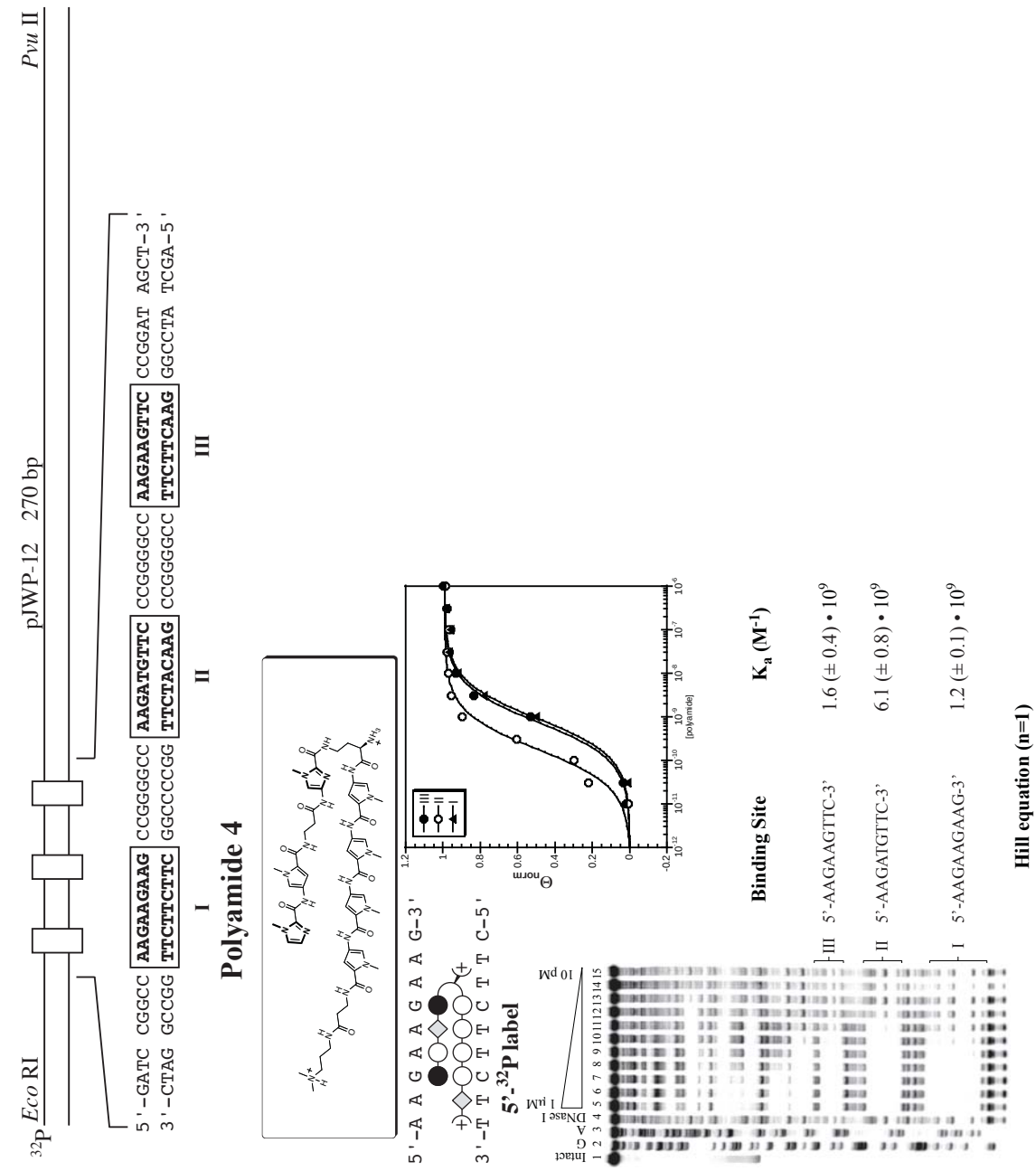

Figure B.4. Quantitative DNase I footprint of a hairpin polyamide targeting GAA repeats

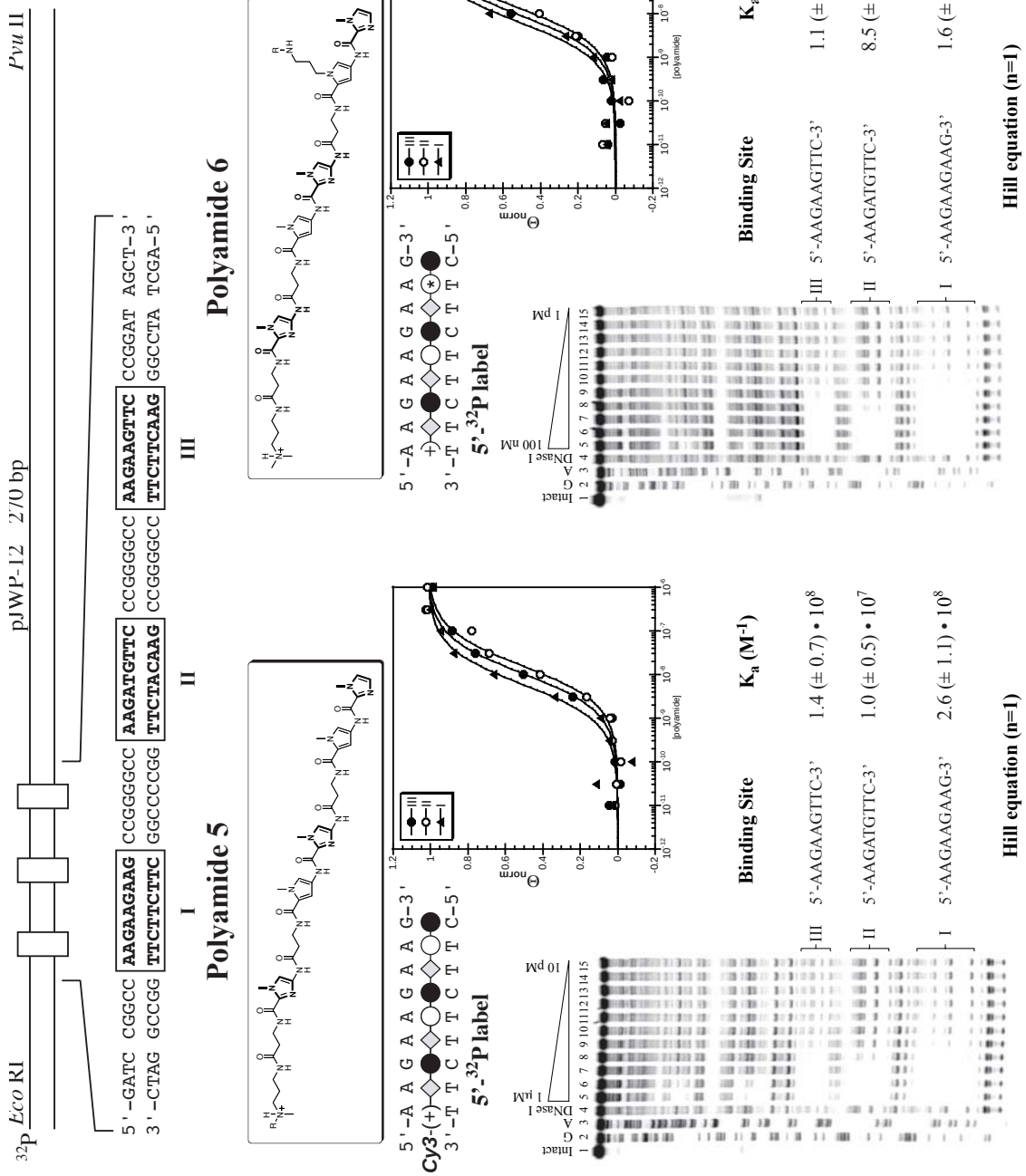

Figure B.5. Quantitative DNase I footprint of two Cy3-labeled, linear *β*-linked polyamides targeting GAA repeats

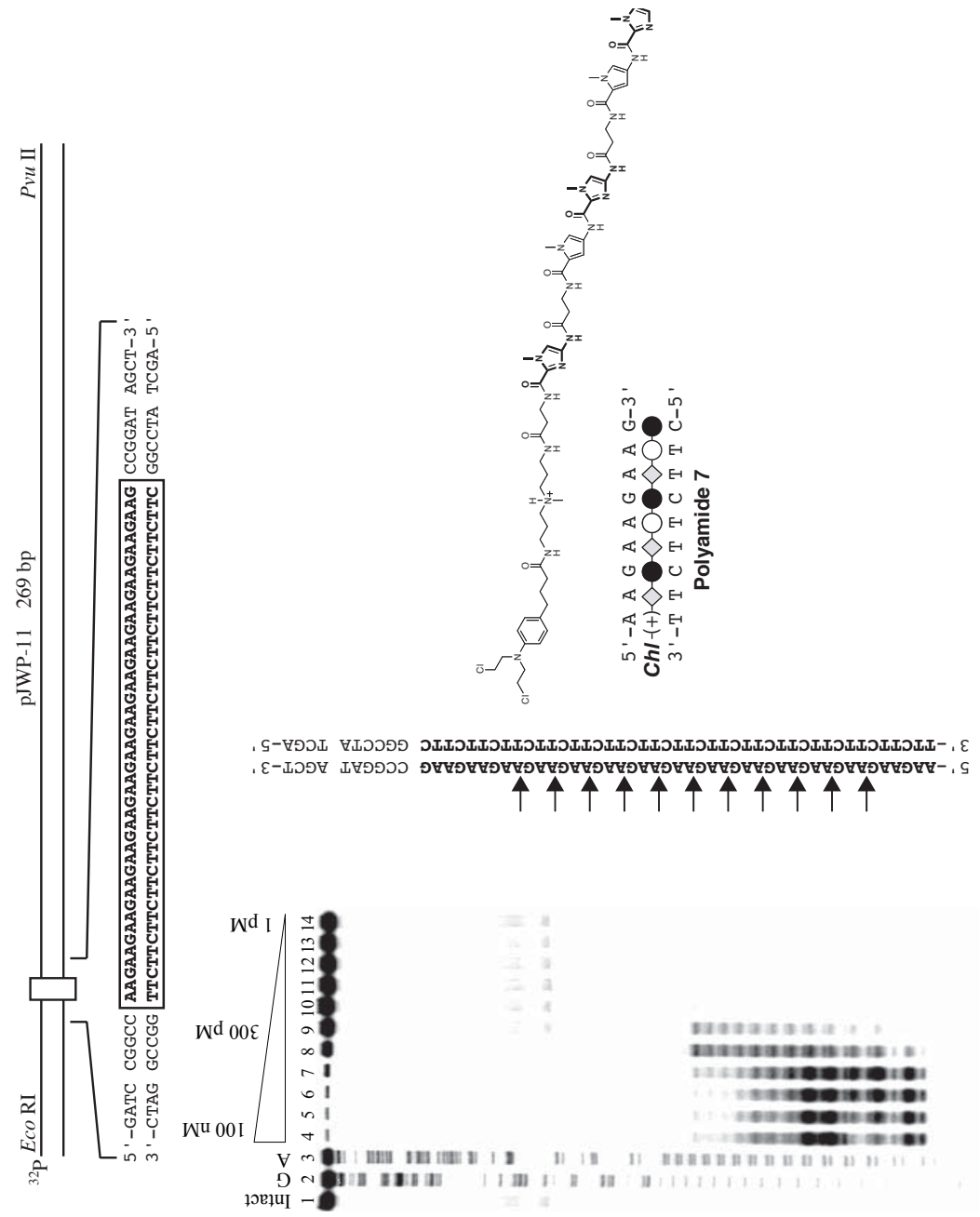

Figure B.6. A Chlorambucil-labeled GAA-targeting β-linked polyamide alkylates $(GAA)_{33}$ repeat sequences

Table B.1. Summary data from Figures B.2–B.5. All values are listed as K_a (M^{-1}) of the polyamide for the specified binding site. Bolded entries represent the highest affinity within a row

Polyamide	Ball-and-stick Structure	AAGAAGAAG	AAGATGTTC	AAGAAGTTC
1		**$7.1 (\pm 0.7) \cdot 10^9$**	$1.6 (\pm 0.1) \cdot 10^9$	$3.9 (\pm 0.5) \cdot 10^9$
2	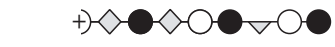	$1.1 (\pm 0.1) \cdot 10^7$	$2.3 (\pm 0.1) \cdot 10^7$	**$3.3 (\pm 0.5) \cdot 10^7$**
3		$\leq 1 \cdot 10^7$	$\leq 1 \cdot 10^7$	**$7.3 (\pm 3.5) \cdot 10^7$**
4		$1.2 (\pm 0.1) \cdot 10^9$	$6.1 (\pm 0.8) \cdot 10^9$	**$1.6 (\pm 0.4) \cdot 10^9$**
5	***Cy3***-(+) 	**$2.6 (\pm 1.1) \cdot 10^8$**	$1.0 (\pm 0.5) \cdot 10^7$	$1.4 (\pm 0.7) \cdot 10^8$
6	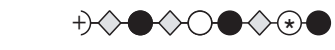	**$1.6 (\pm 0.3) \cdot 10^8$**	$8.5 (\pm 1.5) \cdot 10^7$	$1.1 (\pm 0.1) \cdot 10^8$

Table B.2. MALDI-TOF Mass Spectral Data for polyamides **1–7**

Polyamide	Ball-and-stick Structure	$[M+H]^+$ calc'd	$[M+H]^+$ obsv'd
1		914.4	914.4
2		900.4	900.5
3		965.5	965.4
4	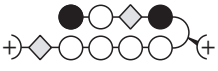	1187.6	1187.6
5	***Cy3***-(+) 	1569.7	1569.6
6		1569.7	1569.7
7	***Chl***-(+) 	1242.6	1242.5

Appendix C

CSI Microarray and Quantitative DNase I Footprinting Data for an Internally Cy3-labeled Linear β-linked Polyamide Targeting GAA Repeats

The experiments in this chapter were performed in collaboration with Christopher L. Warren (University of Wisconsin, Madison), Professor Aseem Z. Ansari (University of Wisconsin, Madison), and Professor Peter B. Dervan (California Institute of Technology).

Abstract

A high-throughput Cognate Site Identity (CSI) microarray platform interrogating all 524,800 10-base pair variable sites is correlated to quantitative DNase I footprinting data of DNA binding pyrrole-imidazole polyamides. Two linear β-linked polyamides programmed to target $(GAA)_3$ repeat sequences and labeled with Cy3 at an internal position within the polyamide and a terminal position are compared with one another. The internally Cy3-labeled polyamide revealed a microarray-derived sequence motif of 5'-AAGAWGWWS-3,' (W = A,T; S = C,G), slightly different from the previously reported terminally labeled sequence motif of 5'-AARAARWWG-3' (R = A,G). Correlation of microarray intensities from the two polyamide experiments revealed a good, positive correlation (R = 0.91) that suggests the polyamide core and not choice of dye placement drives the sequence recognition preferences.

Introduction.

Cell-permeable small molecules which bind specific DNA sequences and are able to interfere with protein-DNA interfaces would be useful in modulating eukaryotic gene expression. For targeting the regulatory elements of eukaryotic genes, knowledge of the preferred binding landscape of the ligand and the energetics of each site would guide gene regulation studies. Pyrrole-imidazole polyamides are a class of cell permeable oligomers which can be programmed, based on simple aromatic amino acid pairing rules, to bind a broad repertoire of DNA sequences.[1,2] Knowledge of polyamide match sites has allowed us to pursue the characterization of the equilibrium association constants and hence, free energies, of hairpin polyamides for cognate DNA sites by quantitative footprint titration methods. Despite the predictive power of simple pairing rules, the sequence dependent variability of DNA minor groove shape affords significant variability in the range of affinities for match as well as all formal single and double base pair mismatch sites.[1,2]

CSI Microarray Platform. Several high-throughput platforms have been developed to characterize the binding properties of ligand-DNA interactions.[3–6] Of these, two have explicitly studied the binding preferences of polyamides. The fluorescence intercalator displacement assay has interrogated polyamide binding to 512 unique 5 bp sequences in a microplate format.[4] The most recently developed cognate site identifier (CSI) microarray platform presents all 524,800 unique ten-mers to fluorescently labeled polyamides, enabling an unbiased interrogation of binding preference.[6] By coupling DNase I footprinting with the CSI microarray data, the binding affinities (K_a values) of a given DNA-binding molecule (such as a polyamide) for any DNA sequence can be determined. We have previously examined and experimentally defined the relationship between Cy3-labeled polyamides and their corresponding CSI Microarray intensity values.[6] In this study, we ask whether the point at which the Cy3 dye has been attached significantly alters sequence specificity.

Two Cy3-labeled polyamides are examined on the CSI microarray that displays all unique 10 base pair sequences, one previously published[6] and one new to this study, both of

core structure Im-Py-*β*-Im-Py-*β*-Im-*β*-Dp. In order to correlate the CSI relative affinities (intensities) to absolute affinities (K_a values), DNase I footprinting was performed on a subset of these sequences for both the Cy3-polyamide conjugate and the related, unlabeled polyamide of known biological activity.

Results and Discussion.

Polyamide Design. The linear *β*-linked polyamide architecture has been chosen to interrogate the effects of Cy3-dye placement on CSI microarray sequence specificity and quantitative DNase I footprint specificity. Polyamide **1**, Im-Py-*β*-Im-Py-*β*-Im-*β*-Dp (Figure C.1), is believed to target the intronic 5'-$(GAA)_n$-3' repeat hyperexpansion in cell culture, enabling 2.5-fold upregulation of the frataxin gene, whose deficiency causes the neurodegenerative disorder Friedreich's Ataxia.[7] Limited knowledge about the linear *β*-linked class of polyamides[6,8–11] precludes the existence of binding rules. The linear *β*-linked architecture has the added complexity of binding in 1:1 and 2:1 ligand/DNA stoichiometries, and we would anticipate that this class will be generally less useful due to sequence promiscuity resulting from multiple binding modes. Its 1:1 binding preferences for purine tracts, such as $(GAA)_n$, likely reflect shape selectivity for sequences with narrow DNA minor groove conformations.[10] In a 2:1 binding stoichiometry, polyamide **1** would

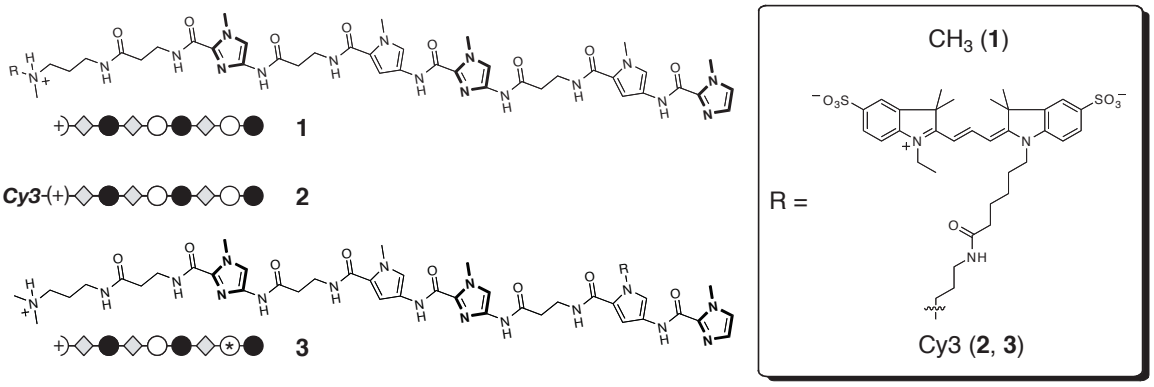

Figure C.1. Polyamides utilized to study the effects of dye placement on CSI microarray determined binding preferences

be predicted to target 5'-WGCWGCWGCW-3'.[8] Remarkably, relatively few genes are affected from cell culture studies of **3** suggesting that this polyamide may be specific for 5'-AAGAAGAAG-3'.[7] The Cy3 fluorophore has been conjugated to the C-terminal 3,3'-diamino-*N*-methyldipropylamine tail (polyamide **2**) in previous work.[6] Current work examines Cy3 fluorophore conjugation to an internal pyrrole, replacing the *N*-methyl moiety with *N*-(propyl-3-amino) as a linker (polyamide **3**).[12]

CSI Microarray design and results. CSI microarrays were synthesized using maskless array synthesis (MAS) technology[13] to display all 524,800 unique 10-base pair sites in quadruplicate across six microarrays. Replicates of individual hairpins occur on separate microarrays. Each hairpin on the chip consists of a self complementary palindromic sequence interrupted by a central 5'-GGA-3' sequence to facilitate hairpin formation: 5'-GCGC-$N^1N^2N^3N^4N^5N^6N^7N^8N^9N^{10}$-GCGC-GGA-GCGC-$N^{10'}N^{9'}N^{8'}N^{7'}N^{6'}N^{5'}N^{4'}N^{3'}N^{2'}N^{1'}$-GCGC-3' (N = A,T,C,G). Previous experiments have found that 95% of the oligonucleotides on the array form duplexes.[5]

Polyamide **3** was slowly titrated onto the arrays and imaged at each concentration until saturation of the highest intensity binding sites was observed, 250 nM concentration for **3**. After each small addition of polyamide, the arrays were washed prior to imaging. The data for each of the arrays was then normalized as previously described[5] to give averaged sequence intensities of the 524,800 10-base pair sites for **3**. As found with previously reported CSI arrays,[5,6] histograms of the probe intensities for **3** display a strong right-handed tail (Figure C.2). The fractional standard deviations among probe replicates (standard deviation of replicates / average normalized intensity) average 0.16 ± 0.10, for intensities exceeding 1×10^3 (Figure C.3).

Plasmid Design. Two plasmids have been designed based on output from the CSI microarray intensities (Figure C.4). Because of our interest in calibrating the CSI microarray to K_a values, we chose a broad range of intensities to interrogate over two plasmids, pJWP16 and pJWP18. A single binding site (**IIa** and **IIIb**) was held constant

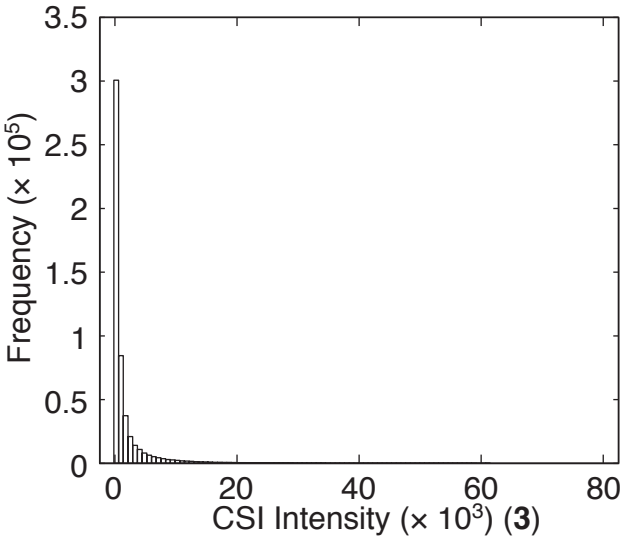

Figure C.2. CSI Intensity Histogram for polyamide **3**

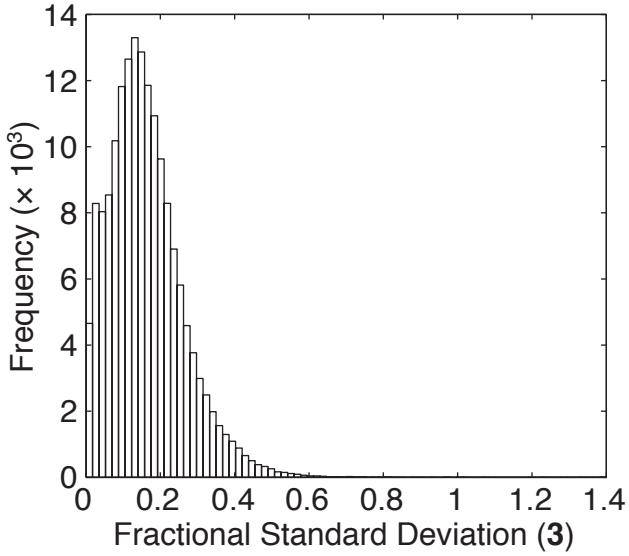

Figure C.3. CSI Fractional Standard Deviation Histogram for polyamide **3**

between pJWP16 and pJWP18 to enable interplasmid comparison of binding affinities.

We designed each plasmid binding site to mimic the full 10 base pair binding site from the array in addition to two flanking base pairs on either side of the binding site: 5'-GC-$(N)_{10}$-GC-3' (N = A,T,C,G). Attempts to fully replicate the 5'-GCGC-$(N)_{10}$-GCGC-3' binding site from the array exhibited secondary structure formation when the

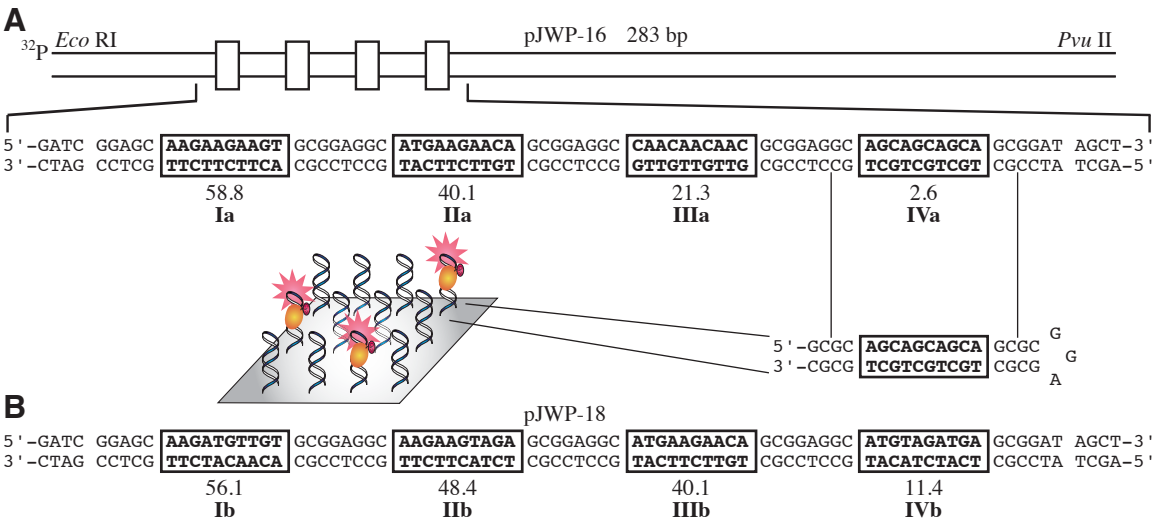

Figure C.4. Plasmids utilized to footprint polyamides **1** and **3**. Designed binding sites are boxed with a rectangle. Beneath each rectangle is the corresponding CSI microarray intensity ($\times 10^3$) and the Roman numeral label for the binding site. a) Structure of pJWP16. b) Structure of pJWP18

respective amplicons were sequenced and separated by denaturing gel electrophoresis.

Quantitative DNase I Footprint Titrations: Affinity and Specificity Determination. Linear β-linked polyamides **1** and **3** were each incubated for 14 h with pJWP16 and pJWP18 prior to DNase I cleavage. They each bound seven unique 10-base pair sites in the same rank-order, preferentially binding 5'-AAGAAGAAGT-3' (Table C.1 and Figure C.5).

Appending the Cy3 dye to polyamide **1** (giving polyamide **3**) typically reduced binding affinity by one order of magnitude (Table C.1). Polyamide **1** bound all four binding sites over an 830-fold range in affinity, 60% broader than for polyamide **3**.

Calibrating microarrays for K_a prediction. The DNase I footprinting data (Table C.1) was mapped to CSI microarray intensities using Eq 1.[6]

$$\text{Intensity} = c \times \Theta = c \times \frac{K_a[\text{PA}]}{1 + K_a[\text{PA}]} = c \times \frac{[\text{PA}]}{K_d + [\text{PA}]} \qquad (1)$$

The line was fit with an R^2 of 0.95, where $c = 59.152$ and $[\text{PA}] = 4.547 \times 10^{-8}$ M. Eq 1 will be rearranged to map CSI microarray intensities to interpolated K_a values.

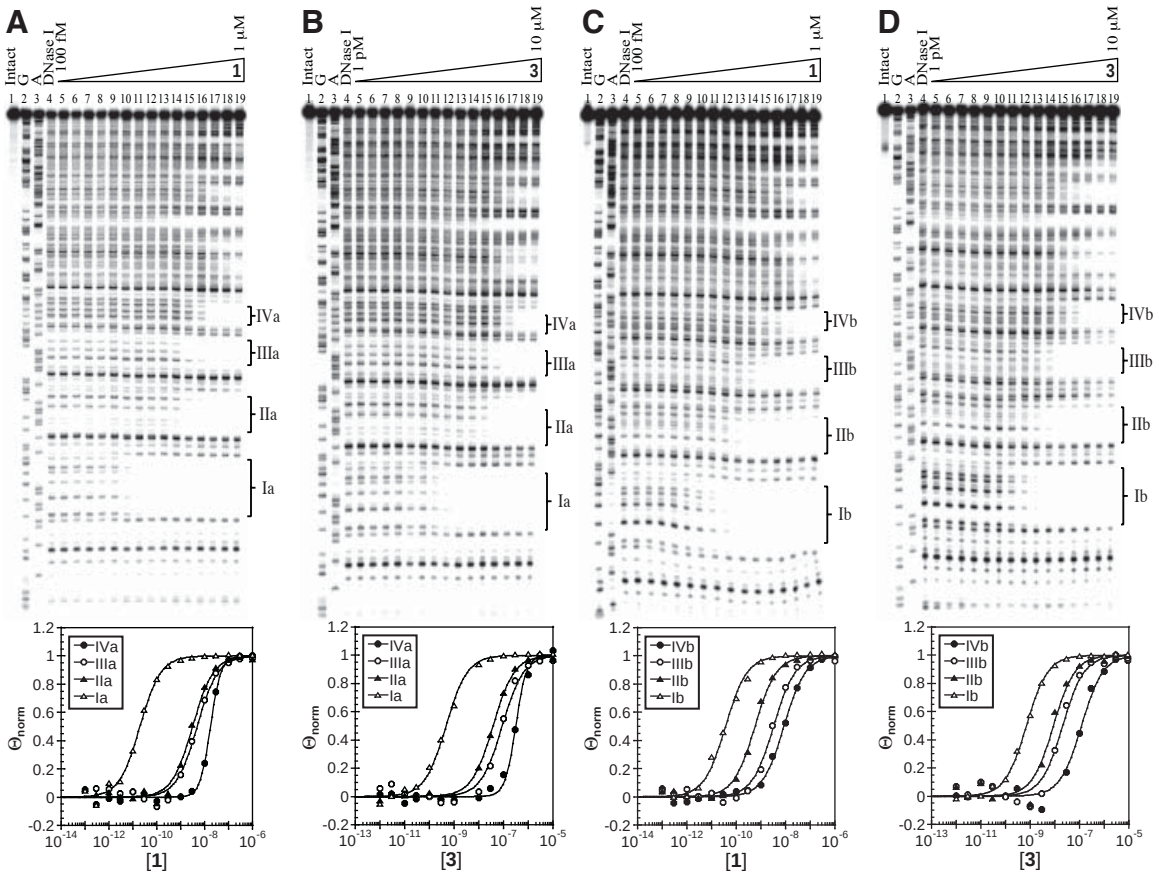

Figure C.5. Quantitative DNase I footprint titrations of polyamides **1** and **3** on plasmids pJWP16 and pJWP18. a) Polyamide **1** on pJWP16. b) Polyamide **3** on pJWP16. c) Polyamide **1** on pJWP18. d) Polyamide **3** on pJWP18

Correlating Binding Between Cy3-labeled Polyamides, Labeled at Different Positions on the Polyamide. Previous work has validated the correlation of Cy3-labeled polyamides with their unlabeled counterparts. A scatter plot of polyamide **1** versus **3** was best fit by a power relationship of $y = ax^n$, where (x,y) denotes the K_a values for (**1**, **3**) (Figure C.7). The R^2 between **1** and **3** is 0.94, and (a,n) were empirically determined as (0.49, 0.90).

To determine the extent which terminally-labeled and internally-labeled Cy3-polyamide conjugates **2** and **3** had correlated CSI Microarray intensity profiles, a scatter plot of all positive microarray intensities was generated (Figure C.8). A line ($y = m\,x + b$) was fit to the data, and a correlation coefficient (R) of 0.91 was observed. The (m, b) pair

Table C.1. Quantitative DNase I Footprinting Derived K_a values (M^{-1}) for Polyamides **1** and **2**. The 10 base pair binding sites and corresponding CSI Microarray intensities are found in each column. All footprinting incubations were conducted at a minimum in triplicate at 23 ºC for 14 h. Standard deviations are shown in parentheses. The bracketed numbers are $K_{a\text{–max}}/K_{a\text{–current}}$ to compare values within each polyamide series (interplasmid comparisons are made).

pJWP-16		**Ia**	**IIa**	**IIIa**	**IVa**
	Polyamide	**AAGAAGAAGT**	**ATGAAGAACA**	**CAACAACAAC**	**AGCAGCAGCA**
1		5.4 (±0.5) × 10^{10} **[1]**	4.6 (±1.7) × 10^{8} **[120]**	2.5 (±0.7) × 10^{8} **[220]**	6.5 (±1.6) × 10^{7} **[830]**
3		1.7 (±0.4) × 10^{9} **[1]**	2.5 (±0.2) × 10^{7} **[68]**	1.3 (±0.1) × 10^{7} **[130]**	3.1 (±0.3) × 10^{6} **[550]**
	CSI Intensity (× 10^3)	58.8 (±2.7)	40.1 (±10.3)	21.3 (±0.3)	2.6 (±1.6)

pJWP-18		**Ib**	**IIb**	**IIIb**	**IVb**
	Polyamide	**AAGATGTTGT**	**AAGAAGTAGA**	**ATGAAGAACA**	**ATGTAGATGA**
1		2.3 (±0.4) × 10^{10} **[2.3]**	1.6 (±0.2) × 10^{9} **[34]**	2.8 (±0.2) × 10^{8} **[190]**	9.8 (±1.4) × 10^{7} **[550]**
3		1.3 (±0.6) × 10^{9} **[1.3]**	1.0 (±0.3) × 10^{8} **[17]**	4.6 (±1.8) × 10^{7} **[37]**	9.8 (±1.8) × 10^{6} **[173]**
	CSI Intensity (× 10^3)	56.1 (±9.3)	48.4 (±19.6)	40.1 (±10.3)	11.4 (±1.6)

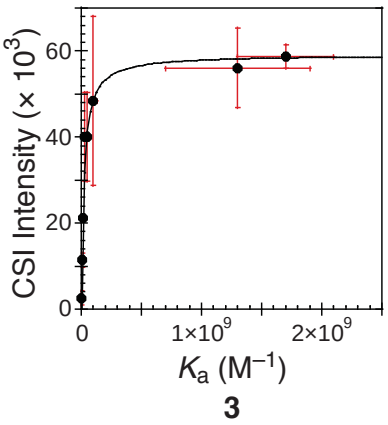

Figure C.6. CSI array intensities correlate well with DNase I footprinting-determined K_a values. Polyamide **3** versus CSI array fit to Eq 1

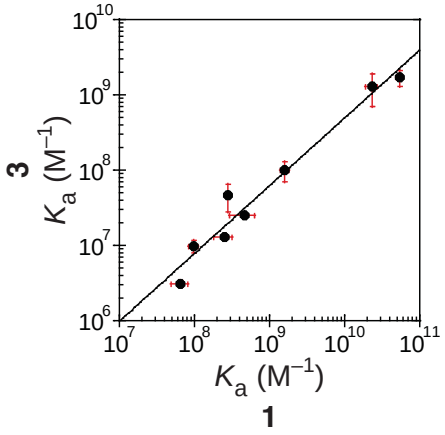

Figure C.7. Cy3-labeled polyamide **3** and unlabeled polyamide **1** correlate well

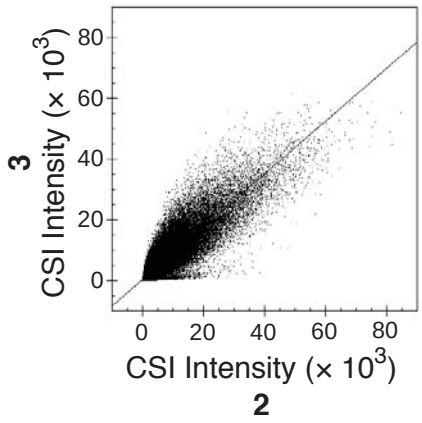

Figure C.8. Scatter Plot Correlation of End-labeled Cy3-polyamide **2** with internally labeled Cy3-polyamide **3**

was empirically determined to be (0.87, 0.25). This high correlation is certainly within the realm of array-to-array technical variability for CSI microarrays, previously reported as an average correlation coefficient of 0.88. This would suggest that Cy3 dye positioning is irrelevant to determining sequence preferences of the polyamide, and that the polyamide amino acid content drives the recognition event's specificity.

Sequence Analysis. To graphically represent the binding preferences of polyamide **3**, a sequence logo has been generated (Figure C.9).

In all cases, the motif finding program MEME[14] was utilized to extract sequence motifs from the CSI binding intensities. The position specific probability matrices output

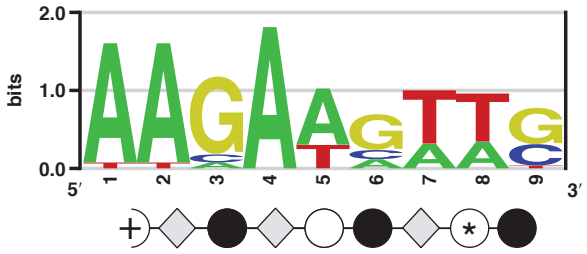

Figure C.9. Sequence logo for polyamide **3**

by MEME were used as inputs to enoLOGOS[15] to generate a sequence logo. The motif search utilized the 10 variable bases of the microarray and two fixed bases, each flanking the variable site 5' and 3.' Because of the change in GC-content, a background GC-content of 58% was utilized in the searches. The logo for polyamide **3** interrogated the 48 highest intensity sequences (a 20-fold range in K_a) of the CSI microarray. We examined the K_a-weighted sequence logo for polyamide **3** and found minimal differences in the resulting logo.

Polyamide **1** specifies 9 base pairs based on MPE footprinting data (Chapter 2B). Polyamide **3** elicits a 9 bp motif that is best represented as 5'-AAGAWGWWS-3' (Figure C.9; S = G,C and W = A,T).

Quantitative Profiling of Single Base Pair Mismatches. While sequence logos provide a visual representation of sequence specificity, traditional studies on polyamides quantitate the specificity of a ring pairing at a selected base pair. We have examined a comprehensive single base pair mutational analysis of polyamide **3** using K_a values interpolated from the calibrated CSI microarrays (Tables C.2 and C.3) using the relationship defined in Eq 1. The examination of polyamide **3** complements the comprehensive sequence specificity study of linear β-linked polyamide **2**. In the 5'-$A^1A^2G^3A^4W^5G^6W^7W^8S^9$-3' sequence (S = G,C; W = A,T), positions 4, 5, and 7, each containing either a Py or a β, exhibit the greatest specificity for W over S (S = C,G). Intriguingly, the β at position 4 prefers A·T over T·A, an unexpected specificity. The sequence logo for polyamide **3** indicates that Im has modest preference for G·C or A·T over other base pairings—in this

Table C.2. Microarray-Derived Binding Affinities and Specificities of All Single Base Pair Mismatch Sites for Polyamide **3** Using 5'-AAGAWGWWS-3' as the Preferred Motif. All K_a values are derived from the geometric average of all CSI binding site intensities on the array containing a specified sequence, converted to a K_a value using eq 3, corrected to include an error term ε. The values in parentheses are the geometric standard deviations for each K_a value.

Polyamide 3	X·Z	K_a (M^{-1})
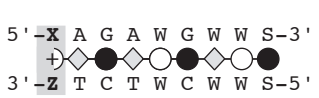	A·T	$4.9\ (3.2) \times 10^7$
	T·A	$2.1\ (2.1) \times 10^7$
	C·G	$7.1\ (2.2) \times 10^6$
	G·C	$6.9\ (2.3) \times 10^6$
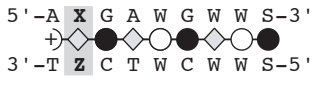	A·T	$4.9\ (3.2) \times 10^7$
	T·A	$2.2\ (2.2) \times 10^7$
	C·G	$2.9\ (2.3) \times 10^6$
	G·C	$4.7\ (2.4) \times 10^6$
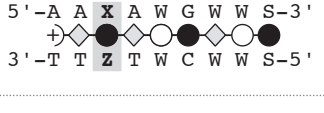	A·T	$1.6\ (1.9) \times 10^7$
	T·A	$5.9\ (2.0) \times 10^6$
	C·G	$2.2\ (2.1) \times 10^7$
	G·C	$4.9\ (3.2) \times 10^7$
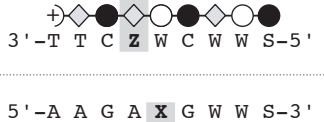	A·T	$4.9\ (3.2) \times 10^7$
	T·A	$1.0\ (2.1) \times 10^7$
	C·G	$6.9\ (1.9) \times 10^5$
	G·C	$3.8\ (2.2) \times 10^5$
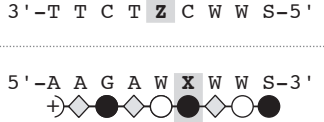	A·T	$6.2\ (3.7) \times 10^7$
	T·A	$3.8\ (2.5) \times 10^7$
	C·G	$5.4\ (1.7) \times 10^5$
	G·C	$1.1\ (2.1) \times 10^6$
	A·T	$1.9\ (2.1) \times 10^7$
	T·A	$1.2\ (1.9) \times 10^7$
	C·G	$2.6\ (2.5) \times 10^7$
	G·C	$4.9\ (3.2) \times 10^7$
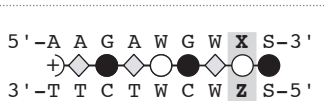	A·T	$3.3\ (2.8) \times 10^7$
	T·A	$7.3\ (3.1) \times 10^7$
	C·G	$9.2\ (1.6) \times 10^5$
	G·C	$1.0\ (1.5) \times 10^6$
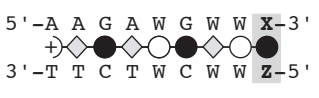	A·T	$5.0\ (3.2) \times 10^7$
	T·A	$4.8\ (3.2) \times 10^7$
	C·G	$3.1\ (1.9) \times 10^6$
	G·C	$5.7\ (2.1) \times 10^6$
	A·T	$2.2\ (1.7) \times 10^7$
	T·A	$1.9\ (2.2) \times 10^7$
	C·G	$6.6\ (3.1) \times 10^7$
	G·C	$3.6\ (2.8) \times 10^7$

Table C.3. Microarray-Derived Binding Affinities and Specificities of All Single Base Pair Mismatch Sites for Polyamide **3** Using 5'-AARAARWWG-3' as the Preferred Motif. All K_a values are derived from the geometric average of all CSI binding site intensities on the array containing a specified sequence, converted to a K_a value using eq 3, corrected to include an error term ε. The values in parentheses are the geometric standard deviations for each K_a value.

Polyamide 3	X·Z	K_a (M^{-1})
	A·T	$2.6\ (2.5) \times 10^7$
	T·A	$1.3\ (2.9) \times 10^7$
	C·G	$4.0\ (1.8) \times 10^6$
	G·C	$4.7\ (1.9) \times 10^6$
	A·T	$2.6\ (2.5) \times 10^7$
	T·A	$1.0\ (2.1) \times 10^7$
	C·G	$2.2\ (2.0) \times 10^6$
	G·C	$3.3\ (2.3) \times 10^6$
	A·T	$1.7\ (2.0) \times 10^7$
	T·A	$4.5\ (1.7) \times 10^6$
	C·G	$1.2\ (1.6) \times 10^7$
	G·C	$3.9\ (2.6) \times 10^7$
	A·T	$2.6\ (2.5) \times 10^7$
	T·A	$5.0\ (1.8) \times 10^6$
	C·G	$1.1\ (2.5) \times 10^6$
	G·C	$9.8\ (3.8) \times 10^5$
	A·T	$2.6\ (2.5) \times 10^7$
	T·A	$1.1\ (2.2) \times 10^7$
	C·G	$1.2\ (2.9) \times 10^6$
	G·C	$1.2\ (2.6) \times 10^6$
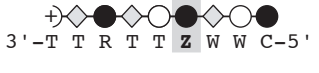	A·T	$2.3\ (2.1) \times 10^7$
	T·A	$8.4\ (1.7) \times 10^6$
	C·G	$1.5\ (2.1) \times 10^7$
	G·C	$2.8\ (2.9) \times 10^7$
	A·T	$2.9\ (2.5) \times 10^7$
	T·A	$2.3\ (2.5) \times 10^7$
	C·G	$2.8\ (2.4) \times 10^6$
	G·C	$2.6\ (2.6) \times 10^6$
	A·T	$2.6\ (2.6) \times 10^7$
	T·A	$2.5\ (2.5) \times 10^7$
	C·G	$5.0\ (2.0) \times 10^6$
	G·C	$4.7\ (1.9) \times 10^6$
	A·T	$2.1\ (1.9) \times 10^7$
	T·A	$1.8\ (1.9) \times 10^7$
	C·G	$3.3\ (2.5) \times 10^7$
	G·C	$2.6\ (2.5) \times 10^7$

mutational study, however, imidazole is generally degenerate. The wide range of K_a values comprising each motif (high geometric standard deviation) make the statistical significance of any specificities under 8 relatively small. In general, the geometric standard deviations for polyamide **3** were higher than those for polyamide **2** within this single base pair mismatch study.

To compare sequence preferences directly with the published mismatch study of polyamide **2**,[6] 5'-$A^1A^2R^3A^4A^5R^6W^7W^8G^9$-3' (R = G,A; Table C.3) was used as a seed from which individual mutations would be studied for polyamide **3**. The results were the same as for 5'-AAGAWGWWS-3,' with positions 4, 5, and 7, showing the greatest specificity for W over S. The *β* at position 4 prefers A·T over T·A.

With the sequence logo (approximated as 5'-AAGAWGWWS-3') as a snapshot of the highest affinity binding sites for polyamide **3** and the footprint titration binding isotherms for determining DNA binding mode, we confirm a preference for the 1:1 binding stoichiometry. Previous data characterizing the linear *β*-linked polyamide Im-*β*-Im-Py-*β*-Im-*β*-Im-Py-*β*-Dp demonstrated a 30-fold energetic preference for the 1:1 versus 2:1 binding stoichiometry, presumably due to the increased entropic cost of the 2:1 binding mode.[8] Here, we have observed a nearly 830-fold preference for the favorable match binding site **Ia** versus the 2:1 stoichiometry binding at binding site **IVa**.

Conclusion.

Correlating the sequence preference landscape present on the CSI microarray to quantitative footprinting enables energetic studies using global binding information. The relationship between Cy3-labeled and unlabeled polyamides have previously been well-correlated, but the question of effects of dye label position has now been addressed. The strong correlation between polyamides labeled at different positions confirms that polyamide core sequence drives sequence preferences. DNase I footprinting-calibrated CSI microarrays will be an effective technique for determining the binding affinities of

DNA-binding ligands for a vastly expanded repertoire of DNA sequences.

Experimental Methods.

Materials. Boc-*β*-Ala-Pam resin (0.81 mmol / g), HBTU, and Boc_2O were purchased from Peptides International. Trifluoroacetic acid (TFA) was purchased from Halocarbon. All solvents were purchased from Aldrich or EMD Biosciences. *rac*-Dithiothreitol (DTT) was purchased from ICN. Cy3-NHS ester was purchased from Invitrogen. RNase-free DEPC water was purchased from US Biochemicals. Water (18.2 MΩ) was purified using a Millipore water purification system.

The pH of buffers was adjusted using a Beckman 340 pH/temp meter. All buffers were sterilized by filtration through either a Nalgene 0.2 μm cellulose nitrate filtration device or a 0.2 μm Whatman cellulose acetate disposable syringe filter. DNA oligonucleotides were ordered PAGE-purified from Integrated DNA Technologies. [γ-^{32}P] adenosine 5'-triphosphate (≥ 7000 Ci/mmol) was obtained from MP Biomedicals. Sonicated, phenol-extracted calf thymus DNA was from Amersham, and all enzymes and molecular biology grade glycogen (20 mg/mL) were purchased from Roche.

Methods. UV spectra were recorded in water using an Agilent 8453 UV-Vis spectrophotometer for polyamide **3**. To solvate polyamide **3** in water at sufficiently high concentrations for DNase I footprinting, 5 μL of DMSO was added to a 20 nmol aliquot of polyamide. The solution was then diluted using RNase-free DEPC water. UV spectra of **3** were blanked against solutions containing appropriate amounts of DMSO. The concentrations of polyamides **1** and **3** were determined using a local λ_{max} of 288 nm, ε = 43,125 $L \cdot mol^{-1} \cdot cm^{-1}$. LASER desorption / ionization time-of-flight mass spectrometry (MALDI-TOF MS) was performed using an Applied Biosystems Voyager DE Pro spectrometer. Analytical and preparative high-pressure liquid chromatography (HPLC) were performed with a Beckman Gold system equipped with a diode array (analytical) or single-wavelength (preparative) detector as previously described.[6]

Synthesis. Polyamides **1, 2,** and **3** were synthesized on Boc-*β*-Ala-PAM resin,[16] using previously described methods.[6]

1: (MALDI-TOF) [M+H]+ calcd for $C_{41}H_{56}N_{17}O_8^+$ 914.4, observed 914.4

2: (MALDI-TOF) [M+H]+ calcd for $C_{41}H_{56}N_{17}O_8^+$ 1569.7, observed 1569.7

3: (MALDI-TOF) [M+H]+ calcd for $C_{74}H\text{-}N_{20}O_{15}S_2^+$ 1569.7, observed 1569.6

Plasmid Preparation. Plasmids were constructed by ligating the following hybridized inserts into the BamHI / HindIII polycloning site in pUC19:

pJWP16. 5'-GATCGGAGCAAGAAGAAGTGCGGAGGCATGAAGAACAGCG
GAGGCCAACAACAACGCGGAGGCAGCAGCAGCAGCGGAT-3'·5'-AGCTA
TCCGCTGCTGCTGCTGCCTCCGCGTTGTTGTTGGCCTCCGCTGTTCTTCA
TGCCTCCGCACTTCTTCTTGCTCC-3'

pJWP18. 5'- GATCGGAGCAAGATGTTGTGCGGAGGCAAGAAGTAGAGCG
GAGGCATGAAGAACAGCGGAGGCATGTAGATGAGCGGAT-3'·5'-AGCTATC
CGCTCATCTACATGCCTCCGCTGTTCTTCATGCCTCCGCTCTACTTCTTGC
CTCCGCACAACATCTTGCTCC-3.'

The ligated plasmid was then transformed into JM109 subcompetent cells. Colonies were selected for α-complementation on agar plates containing 50 mg/L ampicillin, 120 mg/L IPTG, and 40 mg/L X-gal after overnight growth at 37 ºC. Cells were harvested after 16 h growth at 37 ºC in LB medium containing 50 mg/L ampicillin. Plasmids were then purified by mini-prep kits. The presence of the desired inserts was determined by capillary electrophoresis dideoxy sequencing methods.

Preparation of 5'-Labeled DNA for DNase I Footprinting. Two primer oligonucleotides, 5'-AATTCGAGCTCGGTACCCGGG-3' (forward) and 5'-CTGGCACGACAGGTTTCCCGA-3' (reverse) were constructed for PCR amplification. The forward primer was radiolabeled using [γ-^{32}P]-dATP and polynucleotide kinase, followed by purification using ProbeQuant G-50 spin columns. The desired DNA region was amplified as previously described.[17] The labeled fragment was loaded onto

a 7% nondenaturing preparatory polyacrylamide gel (5% cross-link), and the desired 283 (pJWP16, pJWP18) base-pair band was visualized by autoradiography and isolated. Chemical sequencing reactions were performed according to published protocols.[17]

Quantitative DNase I Footprint Titrations. All reactions were carried out in a volume of 400 μL according to published protocols. Polyamides were equilibrated with the radiolabeled DNA for 14 h prior to DNase I cleavage at 23 ºC. Quantitation by storage phosphor autoradiography and determination of equilibrium association constants were as previously described.[17]

Microarray Procedures. Microarrays were synthesized by using a Maskless Array Synthesizer (NimbleGen Systems, Madison, WI). Homopolymer (T_{10}) linkers were covalently attached to monohydroxysilane glass slides. Oligonucleotides were then synthesized on the homopolymers to create a high-density oligonucleotide microarray. The array surface was derivatized such that the density of oligonucleotides was sufficiently low within the same feature so that no one oligonucleotide would hybridize with its neighbors. Four copies of each hairpin containing a unique 10 bp site (5'-GCGC-$N^1N^2N^3N^4N^5N^6N^7N^8N^9N^{10}$-GCGC-GGA-GCGC-$N^{10'}N^{9'}N^{8'}N^{7'}N^{6'}N^{5'}N^{4'}N^{3'}N^{2'}N^{1'}$-GCGC-3') required a total of 2,099,200 features, divided among six microarrays.

Binding Assay. Microarray slides were immersed in 1x PBS and placed in a 90 ºC water bath for 30 min to induce hairpin formation of the oligonucleotides. Slides were then transferred to a tube of nonstringent wash buffer (saline/sodium phosphate/EDTA buffer, pH 7.5/0.01% Tween 20) and scanned to check for low background (<200 intensity). Microarrays were scanned by using an Axon 4000B, and the image files were extracted with GENEPIX PRO Version 3.0 (Axon Instruments, Foster City, CA).

Polyamide Binding. Microarrays prepared as above were placed in the microarray hybridization chamber and washed twice with nonstringent wash buffer. Polyamide was diluted to 250 nM (for **3**) in Hyb buffer (100 mM Mes/1 M NaCl/20 mM EDTA, pH 7.5/0.01% Tween 20). Polyamide was then added to the hybridization chamber and

incubated at room temperature for 1 h. Finally, the microarrays were washed twice with nonstringent wash buffer and scanned.

Data Processing. For each replicate, global mean normalization was used to ensure the mean intensity of each microarray was the same. Local mean normalization[18] was then used to ensure that the intensity was evenly distributed throughout each sector of the microarray surface. Outliers between replicate features were detected by using the *Q* test at 90% confidence and filtered out. The replicates were then quantile-normalized[19] to account for any possible nonlinearity between arrays. Duplicate features were then averaged together. The median of the averaged features was subtracted to account for background.

Acknowledgment. This work was supported by the National Institutes of Health (GM27681 to P.B.D. and A.Z.A). We thank the Beckman Institute Sequence Analysis Facility for DNA sequencing.

References

(1) Dervan, P. B.; Edelson, B. S. *Curr. Opin. Struct. Biol.* **2003**, *13*, 284–99.

(2) Hsu, C. F.; Phillips, J. W.; Trauger, J. W.; Farkas, M. E.; Belitsky, J. M.; Heckel, A.; Olenyuk, B. Z.; Puckett, J. W.; Wang, C. C.; Dervan, P. B. *Tetrahedron* **2007**, *63*, 6146–6151.

(3) Bulyk, M. L. *Methods Enzymol.* **2006**, *410*, 279–99.

(4) Tse, W. C.; Boger, D. L. *Acc. Chem. Res.* **2004**, *37*, 61–9.

(5) Warren, C. L.; Kratochvil, N. C.; Hauschild, K. E.; Foister, S.; Brezinski, M. L.; Dervan, P. B.; Phillips, G. N., Jr.; Ansari, A. Z. *Proc. Natl. Acad. Sci. U. S. A.* **2006**, *103*, 867–72.

(6) Puckett, J. W.; Muzikar, K. A.; Tietjen, J.; Warren, C. L.; Ansari, A. Z.; Dervan, P. B. *J. Am. Chem. Soc.* **2007**, *129*, 12310–9.

(7) Burnett, R.; Melander, C.; Puckett, J. W.; Son, L. S.; Wells, R. D.; Dervan, P. B.; Gottesfeld, J. M. *Proc. Natl. Acad. Sci. U. S. A.* **2006**, *103*, 11497–502.

(8) Dervan, P. B.; Urbach, A. R. In *Essays in Contemporary Chemistry*; Quinkert, G., Kisakürek, M. V., Eds.; Verlag Helvetica Chimica Acta: Zurich, 2000, p 327–339.

(9) Urbach, A. R.; Dervan, P. B. *Proc. Natl. Acad. Sci. U. S. A.* **2001**, *98*, 4343–8.

(10) Urbach, A. R.; Love, J. J.; Ross, S. A.; Dervan, P. B. *J. Mol. Biol.* **2002**, *320*, 55–71.

(11) Marques, M. A.; Doss, R. M.; Urbach, A. R.; Dervan, P. B. *Helv. Chim. Acta* **2002**, *85*, 4485–4517.

(12) Arndt, H.-D.; Hauschild, K. E.; Sullivan, D. P.; Lake, K.; Dervan, P. B.; Ansari, A. Z. *J. Am. Chem. Soc.* **2003**, *125*, 13322–13323.

(13) Singh-Gasson, S.; Green, R. D.; Yue, Y.; Nelson, C.; Blattner, F.; Sussman, M. R.; Cerrina, F. *Nat. Biotechnol.* **1999**, *17*, 974–8.

(14) Bailey, T. L.; Elkan, C. In *Proceedings of the Second International Conference on Intelligent Systems for Molecular Biology*; Altman, R., Brutlag, D., Karp, P.,

Lathrop, R., Searl, D., Eds.; AAAI Press: Menlo Park, 1994, p 28–36.

(15) Workman, C. T.; Yin, Y.; Corcoran, D. L.; Ideker, T.; Stormo, G. D.; Benos, P. V. *Nucleic Acids Res.* **2005**, *33*, W389–92.

(16) Baird, E. E.; Dervan, P. B. *J. Am. Chem. Soc.* **1996**, *118*, 6141–6146.

(17) Trauger, J. W.; Dervan, P. B. *Methods Enzymol.* **2001**, *340*, 450–66.

(18) Colantuoni, C.; Henry, G.; Zeger, S.; Pevsner, J. *Bioinformatics* **2002**, *18*, 1540–1.

(19) Bolstad, B. M.; Irizarry, R. A.; Astrand, M.; Speed, T. P. *Bioinformatics* **2003**, *19*, 185–93.

Appendix D

ChIP-Seq Enriched Regions

The following parameters were reported from the ERANGE 3.0alpha script findall.py for the region enrichment work-up of the ChIP-Seq reads from Chapter 4 that were aligned to the genome using bowtie 0.96. A table listing all of these reads is included in this appendix and follows on the next page.

#enriched sample: AR.N20.VII.171.chip.rds (10.7 M reads)
#control sample: AR.N20.VII.171.input.rds (14.2 M reads)
#enforceDirectionality=True listPeak=True cache=True
#maxSpacing=50 minHits=1.0 minRatio=4.0 minPeak=0.5
#minPlus=0.25 maxPlus=0.75 leftPlus=0.40
#stats: 9298.0 RPM in 2764 regions
23 additional regions failed directionality filter
#4 regions (4.9 RPM) found in background (FDR = 0.14 percent)

Table D.1. Enriched regions from 1 nM DHT-induced LNCaP cells immunoprecipitated by Santa Cruz Biotech SC-816 (N-20). Regions were called enriched relative to an input sample that did not undergo chromatin immunoprecipitation.

regionID	chrom	start	stop	RPM	fold	multi%	plus%	leftPlus%	peakPos	peakHeight
AR.N20.VII.1711	chr1	1778742	1778938	1.60	7.50	0.00	47.10	100.00	1778836	0.8
AR.N20.VII.1712	chr1	2169794	2170037	3.40	6.80	0.00	45.90	88.20	2169943	1.1
AR.N20.VII.1713	chr1	2332149	2332532	6.90	32.70	0.00	45.90	94.10	2332370	1.7
AR.N20.VII.1714	chr1	2375399	2375650	2.50	6.00	0.00	55.60	73.30	2375490	0.7
AR.N20.VII.1715	chr1	3240433	3240763	3.50	6.30	0.00	57.40	50.00	3240481	0.8
AR.N20.VII.1716	chr1	3435928	3436262	6.80	8.80	0.00	58.90	74.40	3436017	2.5
AR.N20.VII.1717	chr1	5709950	5710129	7.40	52.80	0.60	40.90	100.00	5710062	2.4
AR.N20.VII.1718	chr1	6140640	6140833	2.70	12.80	0.00	51.70	100.00	6140734	1
AR.N20.VII.1719	chr1	6395659	6395820	1.00	7.30	0.00	54.50	100.00	6395728	0.6
AR.N20.VII.17110	chr1	7181570	7181719	1.50	7.30	3.00	51.40	100.00	7181633	0.6
AR.N20.VII.17111	chr1	7953800	7953964	1.20	17.30	0.00	69.20	88.90	7953895	0.6
AR.N20.VII.17112	chr1	8241799	8242104	13.10	93.60	0.00	56.00	72.20	8241906	3.4
AR.N20.VII.17113	chr1	8395282	8395426	1.70	23.90	0.00	61.10	63.60	8395348	0.7
AR.N20.VII.17114	chr1	9417873	9418071	2.70	9.60	0.00	58.60	58.80	9417925	0.7
AR.N20.VII.17115	chr1	9419021	9419225	16.80	119.50	0.00	51.60	92.60	9419149	5.9
AR.N20.VII.17116	chr1	9536392	9536635	23.50	83.60	5.80	39.80	99.00	9536515	6.1
AR.N20.VII.17117	chr1	9589612	9589844	1.30	4.60	0.00	57.10	87.50	9589688	0.6
AR.N20.VII.17118	chr1	10618653	10618937	11.80	12.90	0.40	48.30	92.00	10618823	3.9
AR.N20.VII.17119	chr1	11238910	11239177	2.70	19.30	0.00	58.60	88.20	11239036	0.8
AR.N20.VII.17120	chr1	11552401	11552675	2.90	6.90	0.00	38.70	66.70	11552484	1.2
AR.N20.VII.17121	chr1	12171591	12171811	5.40	25.40	0.90	61.70	78.90	12171670	1.6
AR.N20.VII.17122	chr1	12479128	12479325	1.50	10.60	0.00	62.50	100.00	12479262	0.7
AR.N20.VII.17123	chr1	13819049	13819247	1.80	12.60	0.00	52.60	90.00	13819137	0.6
AR.N20.VII.17124	chr1	14937379	14937586	17.60	83.60	0.50	47.60	94.50	14937487	4.7
AR.N20.VII.17125	chr1	16807352	16807644	1.90	9.30	19.10	43.40	88.50	16807555	0.7
AR.N20.VII.17126	chr1	18240299	18240485	2.30	16.60	28.00	50.00	69.20	18240349	0.7
AR.N20.VII.17127	chr1	19188067	19188269	3.80	27.20	0.00	51.20	100.00	19188221	1
AR.N20.VII.17128	chr1	19265494	19265621	1.70	23.90	0.00	55.60	80.00	19265525	0.6
AR.N20.VII.17129	chr1	20231675	20231852	2.80	19.90	0.00	46.70	92.90	20231769	0.7
AR.N20.VII.17130	chr1	21531322	21531512	3.00	42.50	0.00	68.80	68.20	21531402	0.9
AR.N20.VII.17131	chr1	24328408	24328575	3.40	23.90	0.00	52.80	68.40	24328445	1
AR.N20.VII.17132	chr1	24405736	24405939	2.40	8.60	0.00	73.10	100.00	24405861	0.8
AR.N20.VII.17133	chr1	24583858	24584092	4.80	16.90	0.00	60.80	87.10	24583988	1.4
AR.N20.VII.17134	chr1	26999327	26999512	1.50	5.30	0.00	50.00	100.00	26999414	0.6
AR.N20.VII.17135	chr1	27565997	27566285	6.10	21.60	0.00	52.30	97.10	27566216	2
AR.N20.VII.17136	chr1	30747798	30747907	1.10	15.90	0.00	50.00	100.00	30747819	0.7
AR.N20.VII.17137	chr1	30909915	30910094	2.60	18.60	0.00	46.40	76.90	30909971	1.1
AR.N20.VII.17138	chr1	31504063	31504386	3.10	14.80	0.00	50.70	82.90	31504262	0.8
AR.N20.VII.17139	chr1	32462599	32462775	2.00	7.00	4.80	61.90	61.50	32462680	0.7
AR.N20.VII.17140	chr1	32740182	32740437	8.60	40.70	2.20	47.70	88.60	32740323	2.1
AR.N20.VII.17141	chr1	33996956	33997155	1.70	11.90	0.00	50.00	77.80	33997051	0.6
AR.N20.VII.17142	chr1	36399852	36400006	2.10	30.50	0.00	43.50	90.00	36399906	0.9
AR.N20.VII.17143	chr1	36507627	36507901	2.80	12.50	2.80	54.40	100.00	36507820	0.7
AR.N20.VII.17144	chr1	37737463	37737716	3.40	11.90	0.00	51.40	89.50	37737584	0.9
AR.N20.VII.17145	chr1	38381067	38381268	3.60	10.10	0.40	45.00	100.00	38381183	1.1
AR.N20.VII.17146	chr1	39782701	39782898	4.70	33.20	0.00	54.00	74.10	39782768	1.4
AR.N20.VII.17147	chr1	40088961	40089093	1.40	5.00	0.00	62.50	90.00	40089023	0.7
AR.N20.VII.17148	chr1	41734557	41734773	2.40	4.90	0.00	50.00	69.20	41734652	0.8
AR.N20.VII.17149	chr1	42099081	42099323	3.10	44.10	0.80	57.90	67.50	42099152	1
AR.N20.VII.17150	chr1	43479749	43479949	2.10	6.10	0.00	39.10	77.80	43479817	0.5
AR.N20.VII.17151	chr1	43909490	43909683	1.50	21.90	3.00	57.60	78.90	43909601	0.5
AR.N20.VII.17152	chr1	46881674	46881783	1.30	9.30	0.00	42.90	100.00	46881723	0.6
AR.N20.VII.17153	chr1	46920074	46920248	1.50	20.90	4.80	47.60	100.00	46920200	0.7
AR.N20.VII.17154	chr1	48201880	48202103	3.50	25.20	0.00	47.40	94.40	48202017	0.8
AR.N20.VII.17155	chr1	48691204	48691387	3.30	11.60	0.00	44.40	100.00	48691306	0.9
AR.N20.VII.17156	chr1	52187060	52187244	8.20	39.10	0.00	54.00	69.60	52187105	2.6
AR.N20.VII.17157	chr1	55143000	55143243	1.70	8.20	2.70	41.50	76.50	55143132	0.6
AR.N20.VII.17158	chr1	55225805	55226028	2.10	5.10	0.00	64.30	73.30	55225897	0.7
AR.N20.VII.17159	chr1	55845125	55845279	1.30	9.30	0.00	64.30	88.90	55845200	0.5
AR.N20.VII.17160	chr1	57026427	57026692	8.70	30.90	0.00	41.20	84.70	57026565	2.3
AR.N20.VII.17161	chr1	59309621	59309868	9.40	44.70	0.00	46.60	89.60	59309762	2.7
AR.N20.VII.17162	chr1	59683461	59683609	1.40	10.00	0.00	50.00	100.00	59683567	0.6
AR.N20.VII.17163	chr1	59834147	59834395	2.70	12.80	0.00	65.50	68.40	59834209	0.7
AR.N20.VII.17164	chr1	60513078	60513294	2.70	38.50	0.00	56.70	88.20	60513161	0.6
AR.N20.VII.17165	chr1	60666544	60666752	3.30	46.50	0.00	65.70	87.00	60666653	0.8
AR.N20.VII.17166	chr1	61591671	61591852	1.60	22.60	0.00	35.30	100.00	61591757	0.6
AR.N20.VII.17167	chr1	61878968	61879188	8.70	24.70	0.00	43.20	87.80	61879056	2.9
AR.N20.VII.17168	chr1	64026296	64026466	3.40	16.40	0.00	52.60	95.00	64026377	1.2
AR.N20.VII.17169	chr1	64167043	64167272	8.50	48.30	0.00	53.30	100.00	64167184	3
AR.N20.VII.17170	chr1	64281046	64281219	2.10	9.70	0.00	54.50	83.30	64281109	1.1
AR.N20.VII.17171	chr1	66217457	66217743	2.10	9.70	0.00	63.60	92.90	66217651	0.6
AR.N20.VII.17172	chr1	67810958	67811166	2.90	6.90	3.20	46.80	93.10	67811087	1
AR.N20.VII.17173	chr1	68783021	68783245	3.70	53.10	0.00	48.80	85.00	68783085	0.9
AR.N20.VII.17174	chr1	69326836	69327029	1.60	22.60	0.00	70.60	100.00	69326956	0.6
AR.N20.VII.17175	chr1	71112415	71112524	1.10	8.00	0.00	61.50	100.00	71112493	0.7
AR.N20.VII.17176	chr1	74401579	74401739	1.10	15.90	0.00	66.70	100.00	74401655	0.6
AR.N20.VII.17177	chr1	81480964	81481089	1.50	21.20	0.00	37.50	100.00	81481052	0.7
AR.N20.VII.17178	chr1	81756367	81756556	1.70	8.00	0.00	55.60	80.00	81756501	0.7
AR.N20.VII.17179	chr1	84382154	84382314	2.10	29.20	0.00	50.00	100.00	84382252	1.1
AR.N20.VII.17180	chr1	85768387	85768561	2.10	14.60	0.00	52.20	66.70	85768419	0.5
AR.N20.VII.17181	chr1	85772928	85773126	6.00	21.20	0.00	50.80	72.70	85772998	1.4
AR.N20.VII.17182	chr1	87953386	87953577	1.90	26.60	0.00	65.00	84.60	87953492	0.7
AR.N20.VII.17183	chr1	94644696	94644893	1.50	5.20	1.50	59.40	61.00	94644745	0.5
AR.N20.VII.17184	chr1	94982078	94982383	12.40	44.10	0.00	51.90	88.40	94982270	3.3
AR.N20.VII.17185	chr1	95570930	95571236	4.20	13.80	0.30	49.00	77.40	95571061	1.1

regionID	chrom	start	stop	RPM	fold	multi%	plus%	leftPlus%	peakPos	peakHeight
AR.N20.VII.17186	chr1	95608566	95608798	3.20	15.00	0.00	55.90	94.70	95608712	0.7
AR.N20.VII.17187	chr1	96127273	96127559	2.60	37.20	0.00	46.40	100.00	96127511	0.7
AR.N20.VII.17188	chr1	100045066	100045312	2.50	15.90	8.70	47.00	93.50	100045222	1.1
AR.N20.VII.17189	chr1	100724022	100724386	3.50	16.80	0.00	44.70	52.90	100724102	0.8
AR.N20.VII.17190	chr1	100731434	100731592	1.50	5.30	0.00	50.00	87.50	100731501	0.7
AR.N20.VII.17191	chr1	106300705	106300889	2.10	9.70	0.00	50.00	90.90	106300816	0.5
AR.N20.VII.17192	chr1	106620664	106620890	2.00	7.00	0.00	52.10	54.50	106620747	0.6
AR.N20.VII.17193	chr1	108126668	108126907	4.80	33.90	0.00	60.80	77.40	108126796	1.4
AR.N20.VII.17194	chr1	109844025	109844251	2.20	10.60	0.00	58.30	92.90	109844165	0.7
AR.N20.VII.17195	chr1	109976841	109977099	9.60	17.00	0.50	46.40	81.60	109976941	2.5
AR.N20.VII.17196	chr1	110580279	110580449	2.80	19.90	0.00	63.30	84.20	110580351	1
AR.N20.VII.17197	chr1	111143190	111143276	1.20	17.30	0.00	69.20	88.90	111143228	0.7
AR.N20.VII.17198	chr1	111987336	111987522	2.10	10.20	0.00	43.50	100.00	111987454	0.9
AR.N20.VII.17199	chr1	112185485	112185650	2.50	11.90	0.00	40.70	100.00	112185583	0.8
AR.N20.VII.171100	chr1	112292797	112293184	4.10	4.80	1.10	42.50	89.20	112293062	0.9
AR.N20.VII.171101	chr1	112408091	112408227	1.20	5.80	0.00	46.20	100.00	112408134	0.5
AR.N20.VII.171102	chr1	112986166	112986283	1.70	23.90	0.00	50.00	100.00	112986219	0.8
AR.N20.VII.171103	chr1	114779337	114779569	4.70	22.10	0.00	60.00	60.00	114779395	1.3
AR.N20.VII.171104	chr1	115746869	115747108	2.20	15.90	97.90	62.50	76.70	115746965	0.6
AR.N20.VII.171105	chr1	116637145	116637271	1.80	12.60	0.00	26.30	100.00	116637243	0.9
AR.N20.VII.171106	chr1	116820596	116820811	10.00	35.50	0.00	45.80	98.00	116820692	2.9
AR.N20.VII.171107	chr1	116997019	116997252	2.20	8.00	78.10	57.70	57.10	116997084	0.7
AR.N20.VII.171108	chr1	118946612	118946803	1.90	6.80	2.40	63.40	76.90	118946680	0.6
AR.N20.VII.171109	chr1	120376201	120376697	7.40	11.70	98.70	55.10	71.30	120376487	1.6
AR.N20.VII.171110	chr1	120990604	120990919	3.70	52.40	26.60	44.30	94.30	120990828	0.9
AR.N20.VII.171111	chr1	142527141	142527334	1.60	13.50	99.20	66.80	95.00	142527307	0.6
AR.N20.VII.171112	chr1	143043301	143043599	1.50	8.90	98.00	56.30	95.40	143043474	0.7
AR.N20.VII.171113	chr1	143223550	143223848	1.40	10.30	97.70	54.30	94.00	143223723	0.7
AR.N20.VII.171114	chr1	143957614	143958091	8.10	9.60	90.20	50.00	88.50	143957823	1.6
AR.N20.VII.171115	chr1	144106821	144107015	1.70	9.00	18.10	47.70	88.60	144106948	0.8
AR.N20.VII.171116	chr1	144108200	144108379	2.40	13.30	35.90	64.70	40.50	144108217	0.7
AR.N20.VII.171117	chr1	144109181	144109331	1.90	5.80	45.80	58.80	99.10	144109252	0.6
AR.N20.VII.171118	chr1	144110552	144110708	1.70	5.40	46.10	43.50	85.00	144110628	0.6
AR.N20.VII.171119	chr1	145048077	145048269	1.20	8.60	0.00	46.20	100.00	145048184	0.5
AR.N20.VII.171120	chr1	145565296	145565501	3.10	21.90	0.00	55.90	94.70	145565385	0.8
AR.N20.VII.171121	chr1	146389764	146389957	1.60	13.50	99.20	65.30	95.00	146389930	0.6
AR.N20.VII.171122	chr1	146827741	146827947	1.40	4.80	64.90	60.90	100.00	146827916	0.5
AR.N20.VII.171123	chr1	147497171	147497309	2.10	7.80	16.30	46.60	91.00	147497259	0.7
AR.N20.VII.171124	chr1	147565122	147565323	1.60	7.80	32.00	44.50	100.00	147565255	0.6
AR.N20.VII.171125	chr1	147851626	147851953	2.50	7.50	69.30	48.20	78.70	147851756	0.7
AR.N20.VII.171126	chr1	148253306	148253481	2.00	28.50	2.30	39.50	100.00	148253397	0.7
AR.N20.VII.171127	chr1	148800383	148800638	2.40	5.60	2.00	54.90	100.00	148800544	0.8
AR.N20.VII.171128	chr1	148807245	148807442	1.90	26.60	0.00	50.00	80.00	148807338	0.7
AR.N20.VII.171129	chr1	149611687	149611846	1.60	7.50	0.00	64.70	81.80	149611757	0.6
AR.N20.VII.171130	chr1	150286852	150287038	2.00	9.30	0.00	38.10	100.00	150286964	0.7
AR.N20.VII.171131	chr1	150430992	150431261	2.60	12.40	0.00	51.70	73.30	150431105	0.6
AR.N20.VII.171132	chr1	151910302	151910497	1.70	7.40	55.10	47.50	80.10	151910376	0.5
AR.N20.VII.171133	chr1	152590531	152590742	1.60	7.50	0.00	35.30	83.30	152590651	0.5
AR.N20.VII.171134	chr1	152657311	152657680	3.90	11.20	0.00	52.40	100.00	152657615	0.9
AR.N20.VII.171135	chr1	153370456	153370683	9.00	32.20	0.00	40.20	97.40	153370574	3
AR.N20.VII.171136	chr1	154747269	154747494	3.20	9.00	0.00	41.20	85.70	154747371	1.7
AR.N20.VII.171137	chr1	154852963	154853182	14.40	68.20	0.00	53.20	98.80	154853102	3.3
AR.N20.VII.171138	chr1	158368494	158368754	13.30	31.60	0.00	47.60	91.20	158368627	3.1
AR.N20.VII.171139	chr1	158438487	158438646	1.90	13.60	2.40	43.90	100.00	158438552	0.7
AR.N20.VII.171140	chr1	159636053	159636213	1.50	14.10	25.70	54.80	71.60	159636115	0.6
AR.N20.VII.171141	chr1	159767497	159767693	1.70	4.50	51.10	68.80	87.30	159767567	0.6
AR.N20.VII.171142	chr1	159960136	159960344	3.60	10.40	0.00	69.20	77.80	159960233	1.3
AR.N20.VII.171143	chr1	160121017	160121109	1.20	8.60	0.00	53.80	85.70	160121059	0.6
AR.N20.VII.171144	chr1	160969060	160969466	4.80	17.30	0.00	51.90	66.70	160969252	1
AR.N20.VII.171145	chr1	161167076	161167229	1.20	8.60	0.00	46.20	100.00	161167199	0.5
AR.N20.VII.171146	chr1	162252075	162252262	1.60	11.30	0.00	41.20	100.00	162252194	0.7
AR.N20.VII.171147	chr1	162721714	162721899	2.70	9.60	0.00	60.00	100.00	162721835	0.7
AR.N20.VII.171148	chr1	163305744	163305962	4.00	56.90	7.90	43.40	94.60	163305884	1.3
AR.N20.VII.171149	chr1	163517415	163517629	3.30	6.60	0.00	57.10	75.00	163517522	1
AR.N20.VII.171150	chr1	165361488	165361732	2.20	15.90	0.00	50.00	58.30	165361545	0.6
AR.N20.VII.171151	chr1	165780417	165780708	6.70	19.10	0.00	41.70	96.70	165780603	1.6
AR.N20.VII.171152	chr1	165907849	165907992	1.20	8.60	0.00	30.80	50.00	165907889	0.5
AR.N20.VII.171153	chr1	166309958	166310110	1.30	18.60	0.00	42.90	100.00	166310072	0.7
AR.N20.VII.171154	chr1	166867558	166867765	3.20	9.00	0.00	55.90	89.50	166867700	0.8
AR.N20.VII.171155	chr1	169579973	169580238	2.20	15.90	0.00	58.30	71.40	169580093	0.6
AR.N20.VII.171156	chr1	173468166	173468420	3.50	25.20	0.00	36.80	100.00	173468299	1.3
AR.N20.VII.171157	chr1	174766783	174766979	2.40	34.50	0.00	57.70	66.70	174766831	0.8
AR.N20.VII.171158	chr1	175680880	175681060	1.70	6.00	0.00	61.10	100.00	175681008	0.7
AR.N20.VII.171159	chr1	176573198	176573369	2.40	17.30	0.00	51.90	100.00	176573272	0.8
AR.N20.VII.171160	chr1	176926431	176926549	1.00	14.60	0.00	54.50	66.70	176926475	0.5
AR.N20.VII.171161	chr1	178764601	178764851	5.00	71.70	0.00	46.30	88.00	178764719	1.3
AR.N20.VII.171162	chr1	179594841	179595125	4.90	35.20	0.00	52.80	67.90	179594955	0.9
AR.N20.VII.171163	chr1	180453767	180453947	1.50	5.30	0.00	50.00	100.00	180453893	0.6
AR.N20.VII.171164	chr1	180625415	180625616	2.10	9.70	0.00	54.50	66.70	180625453	0.6
AR.N20.VII.171165	chr1	180942984	180943220	3.40	24.10	0.90	42.20	93.50	180943112	0.9
AR.N20.VII.171166	chr1	181038289	181038434	2.10	14.60	0.00	47.80	100.00	181038398	1
AR.N20.VII.171167	chr1	181205066	181205217	1.70	24.30	1.80	72.70	92.50	181205168	0.7
AR.N20.VII.171168	chr1	181324870	181325061	2.70	19.30	0.00	44.80	100.00	181324980	1
AR.N20.VII.171169	chr1	182124306	182124415	1.50	21.20	0.00	25.00	100.00	182124339	0.6
AR.N20.VII.171170	chr1	182658642	182658904	4.30	10.20	0.00	55.30	92.30	182658819	1.4

regionID	chrom	start	stop	RPM	fold	multi%	plus%	leftPlus%	peakPos	peakHeight
AR.N20.VII.171171	chr1	182858015	182858249	1.80	6.30	0.00	68.40	100.00	182858201	0.7
AR.N20.VII.171172	chr1	182868653	182868922	9.60	22.80	0.00	46.20	95.80	182868789	3.5
AR.N20.VII.171173	chr1	183165764	183165935	2.40	17.30	0.00	46.20	75.00	183165787	0.7
AR.N20.VII.171174	chr1	183578705	183578940	4.90	17.40	0.50	40.40	100.00	183578883	1.7
AR.N20.VII.171175	chr1	183770680	183770992	2.90	4.60	1.60	36.50	91.30	183770905	0.7
AR.N20.VII.171176	chr1	185557830	185557962	1.00	9.70	0.00	54.50	100.00	185557912	0.6
AR.N20.VII.171177	chr1	185753447	185753570	1.40	10.00	0.00	26.70	100.00	185753482	0.5
AR.N20.VII.171178	chr1	186073682	186073909	3.60	26.00	0.30	56.50	95.50	186073816	1
AR.N20.VII.171179	chr1	186207769	186207995	2.00	27.90	0.00	42.90	88.90	186207880	0.7
AR.N20.VII.171180	chr1	187810324	187810420	1.00	7.30	0.00	66.70	100.00	187810385	0.6
AR.N20.VII.171181	chr1	188828377	188828591	2.50	17.60	1.90	54.70	93.10	188828482	0.7
AR.N20.VII.171182	chr1	190001123	190001264	1.60	11.30	0.00	52.90	88.90	190001213	0.6
AR.N20.VII.171183	chr1	190732180	190732333	1.10	15.90	0.00	46.20	100.00	190732262	0.6
AR.N20.VII.171184	chr1	191080171	191080384	2.40	28.50	4.90	25.20	100.00	191080307	1
AR.N20.VII.171185	chr1	191097586	191097794	3.90	27.90	0.00	60.50	100.00	191097755	1.1
AR.N20.VII.171186	chr1	191344327	191344528	4.00	14.20	48.00	67.20	66.90	191344393	1.2
AR.N20.VII.171187	chr1	191998005	191998172	1.50	21.20	0.00	68.80	63.60	191998063	0.6
AR.N20.VII.171188	chr1	197073320	197073646	3.80	9.10	0.00	43.90	100.00	197073537	0.7
AR.N20.VII.171189	chr1	199517319	199517533	2.50	9.00	0.00	50.00	64.30	199517426	0.8
AR.N20.VII.171190	chr1	199545211	199545505	2.60	5.30	0.00	50.00	57.10	199545313	0.6
AR.N20.VII.171191	chr1	200011189	200011426	4.20	29.90	0.00	48.90	100.00	200011365	1
AR.N20.VII.171192	chr1	200541030	200541210	1.60	11.40	1.00	33.90	97.30	200541127	0.7
AR.N20.VII.171193	chr1	202212086	202212275	2.00	27.90	0.00	52.40	100.00	202212232	0.6
AR.N20.VII.171194	chr1	202324772	202325028	7.00	33.40	0.70	71.30	73.20	202324899	2.5
AR.N20.VII.171195	chr1	202492361	202492586	2.50	5.50	0.00	60.70	76.50	202492448	0.7
AR.N20.VII.171196	chr1	202652904	202653133	5.30	15.10	0.00	46.60	100.00	202653093	1.6
AR.N20.VII.171197	chr1	203733284	203733438	2.20	5.30	0.00	33.30	87.50	203733314	0.9
AR.N20.VII.171198	chr1	203934648	203935045	5.20	37.20	0.00	46.40	92.30	203934864	1.3
AR.N20.VII.171199	chr1	204780384	204780568	1.60	5.80	2.90	51.40	88.90	204780497	0.7
AR.N20.VII.171200	chr1	205244798	205245032	2.20	15.90	0.00	50.00	83.30	205244880	0.7
AR.N20.VII.171201	chr1	205250015	205250226	2.50	4.50	0.00	42.90	83.30	205250146	1
AR.N20.VII.171202	chr1	205271694	205272177	10.00	28.40	0.00	42.10	100.00	205272063	2.3
AR.N20.VII.171203	chr1	206190766	206191004	2.50	11.90	0.00	44.40	75.00	206190874	0.8
AR.N20.VII.171204	chr1	206538628	206538915	5.20	21.10	0.90	39.60	95.50	206538791	1.5
AR.N20.VII.171205	chr1	207771030	207771189	3.30	15.50	0.00	31.40	100.00	207771103	1
AR.N20.VII.171206	chr1	208025646	208025816	2.00	11.40	46.50	51.20	100.00	208025752	0.6
AR.N20.VII.171207	chr1	209440426	209440537	2.00	13.90	0.00	33.30	71.40	209440461	0.8
AR.N20.VII.171208	chr1	209714515	209714668	6.00	85.00	0.00	41.50	100.00	209714609	2.3
AR.N20.VII.171209	chr1	210137097	210137283	1.90	6.60	0.00	64.40	100.00	210137167	0.7
AR.N20.VII.171210	chr1	210245006	210245137	1.40	10.00	0.00	73.30	72.70	210245042	0.8
AR.N20.VII.171211	chr1	210373305	210373546	1.70	23.70	5.50	46.40	64.00	210373423	0.7
AR.N20.VII.171212	chr1	214768759	214768947	1.80	6.30	0.00	50.00	70.00	214768793	0.6
AR.N20.VII.171213	chr1	215142677	215142982	7.20	25.60	0.00	53.80	97.60	215142882	1.8
AR.N20.VII.171214	chr1	215468772	215468882	1.50	21.90	3.00	45.50	100.00	215468833	0.7
AR.N20.VII.171215	chr1	215766215	215766331	2.60	18.60	0.00	55.20	100.00	215766296	1.1
AR.N20.VII.171216	chr1	217758239	217758398	2.70	19.30	0.00	37.90	90.90	217758332	1.3
AR.N20.VII.171217	chr1	218678533	218678669	1.20	12.30	3.00	58.60	100.00	218678593	0.7
AR.N20.VII.171218	chr1	219052395	219052641	4.20	6.00	0.00	46.70	85.70	219052557	1.1
AR.N20.VII.171219	chr1	219547428	219547540	1.60	23.20	2.90	37.10	100.00	219547472	0.7
AR.N20.VII.171220	chr1	220086045	220086253	2.70	12.90	0.60	58.90	100.00	220086205	0.9
AR.N20.VII.171221	chr1	221988922	221989071	2.10	6.10	0.00	58.30	78.60	221988988	0.9
AR.N20.VII.171222	chr1	222040135	222040373	2.20	30.80	0.90	58.70	84.50	222040277	0.7
AR.N20.VII.171223	chr1	222141041	222141301	2.40	11.50	0.00	38.50	60.00	222141106	0.7
AR.N20.VII.171224	chr1	222427993	222428163	1.40	19.90	0.00	40.00	100.00	222428093	0.5
AR.N20.VII.171225	chr1	222559209	222559395	1.80	8.40	0.00	73.70	92.90	222559299	1
AR.N20.VII.171226	chr1	222894432	222894684	8.30	19.80	0.90	52.00	91.50	222894544	2.6
AR.N20.VII.171227	chr1	223948563	223948774	1.40	6.60	0.00	46.70	100.00	223948682	0.5
AR.N20.VII.171228	chr1	226146070	226146286	2.30	4.70	0.00	60.00	80.00	226146174	0.8
AR.N20.VII.171229	chr1	227056177	227056340	1.50	10.60	0.00	31.20	100.00	227056295	0.5
AR.N20.VII.171230	chr1	227476204	227476401	1.70	8.00	0.00	61.10	100.00	227476358	0.7
AR.N20.VII.171231	chr1	228046429	228046590	2.70	7.70	0.00	31.00	100.00	228046533	1.3
AR.N20.VII.171232	chr1	228047023	228047430	3.70	10.00	0.40	41.30	100.00	228047341	0.9
AR.N20.VII.171233	chr1	228388358	228388588	3.30	11.60	2.90	51.40	73.70	228388499	1
AR.N20.VII.171234	chr1	229064413	229064543	2.30	8.30	0.00	52.00	69.20	229064464	0.9
AR.N20.VII.171235	chr1	229539803	229539962	2.00	13.90	0.00	54.50	91.70	229539858	1.2
AR.N20.VII.171236	chr1	229886850	229887043	6.50	46.50	0.00	51.40	94.40	229886944	1.9
AR.N20.VII.171237	chr1	231891684	231891787	1.00	7.30	0.00	54.50	100.00	231891748	0.7
AR.N20.VII.171238	chr1	232605931	232606044	1.20	8.60	0.00	53.80	71.40	232605976	0.6
AR.N20.VII.171239	chr1	233550662	233550794	1.30	18.60	0.00	64.30	88.90	233550716	0.7
AR.N20.VII.171240	chr1	233638984	233639285	9.20	32.90	0.00	51.50	94.10	233639131	2.4
AR.N20.VII.171241	chr1	234048602	234048831	1.70	4.80	0.00	55.60	90.00	234048732	0.5
AR.N20.VII.171242	chr1	234550642	234550827	2.40	34.50	0.00	65.40	82.40	234550744	0.7
AR.N20.VII.171243	chr1	234619341	234619539	1.70	23.90	0.00	33.30	83.30	234619421	0.6
AR.N20.VII.171244	chr1	236094340	236094574	2.10	4.90	0.00	50.00	45.50	236094410	0.7
AR.N20.VII.171245	chr1	236127006	236127172	1.90	13.30	0.00	50.00	90.00	236127037	0.6
AR.N20.VII.171246	chr1	237286985	237287135	1.70	8.00	0.00	57.90	90.90	237287108	0.6
AR.N20.VII.171247	chr1	238109220	238109443	2.30	6.60	0.00	48.00	75.00	238109295	0.6
AR.N20.VII.171248	chr1	240576303	240576484	1.80	25.20	52.60	50.00	100.00	240576409	0.7
AR.N20.VII.171249	chr1	242892661	242892848	3.40	47.80	0.00	66.70	75.00	242892729	0.9
AR.N20.VII.171250	chr1	243998545	243998801	4.90	23.50	3.80	58.50	66.10	243998643	1.2
AR.N20.VII.171251	chr1	244679506	244679725	2.10	14.90	2.20	53.20	76.00	244679617	0.7
AR.N20.VII.171252	chr1	247134492	247134798	3.70	4.40	10.80	56.30	89.50	247134717	0.8
AR.N20.VII.171253	chr10	1353075	1353197	1.30	4.60	0.00	35.70	80.00	1353132	0.7
AR.N20.VII.171254	chr10	4162073	4162383	2.70	12.80	0.00	48.30	100.00	4162268	0.7
AR.N20.VII.171255	chr10	4672325	4672511	3.40	47.80	0.00	66.70	95.80	4672452	0.9

regionID	chrom	start	stop	RPM	fold	multi%	plus%	leftPlus%	peakPos	peakHeight
AR.N20.VII.171256	chr10	5826872	5827032	1.10	4.00	0.00	49.10	83.30	5826971	0.5
AR.N20.VII.171257	chr10	6337468	6337798	12.20	43.50	0.00	48.90	50.00	6337555	2.5
AR.N20.VII.171258	chr10	8226591	8226791	1.30	9.30	0.00	28.60	100.00	8226663	0.6
AR.N20.VII.171259	chr10	12613382	12613617	2.70	19.30	0.00	58.60	100.00	12613569	0.9
AR.N20.VII.171260	chr10	12771926	12772139	2.10	7.30	0.00	40.90	88.90	12772074	0.6
AR.N20.VII.171261	chr10	13799994	13800178	2.10	5.80	0.00	50.00	100.00	13800109	0.6
AR.N20.VII.171262	chr10	13939609	13939855	2.30	11.10	0.00	60.00	100.00	13939759	0.7
AR.N20.VII.171263	chr10	14654125	14654402	8.30	14.80	0.00	44.90	87.50	14654256	2
AR.N20.VII.171264	chr10	15240575	15240737	1.50	7.10	0.00	56.20	77.80	15240631	0.7
AR.N20.VII.171265	chr10	15685561	15685781	1.80	5.10	1.00	47.90	89.10	15685686	0.7
AR.N20.VII.171266	chr10	15792530	15792789	3.20	9.00	0.00	50.00	82.40	15792624	1
AR.N20.VII.171267	chr10	16684495	16684683	1.90	9.10	2.40	63.40	53.80	16684536	0.5
AR.N20.VII.171268	chr10	21224746	21225095	1.70	4.80	0.00	61.10	54.50	21224766	0.6
AR.N20.VII.171269	chr10	21471198	21471344	1.10	8.00	0.00	50.00	83.30	21471253	0.7
AR.N20.VII.171270	chr10	22017529	22017637	1.20	17.30	0.00	46.20	100.00	22017559	0.9
AR.N20.VII.171271	chr10	22415712	22415879	2.80	19.90	0.00	46.70	85.70	22415781	1.4
AR.N20.VII.171272	chr10	22558408	22558561	1.60	5.50	32.00	56.80	90.00	22558460	0.6
AR.N20.VII.171273	chr10	22795742	22796038	2.60	18.30	1.80	50.90	100.00	22795920	0.6
AR.N20.VII.171274	chr10	24156950	24157118	3.40	47.80	0.00	61.10	95.50	24157080	1
AR.N20.VII.171275	chr10	25491416	25491584	1.40	19.30	3.40	48.30	71.40	25491453	0.6
AR.N20.VII.171276	chr10	25499642	25499824	2.30	33.20	0.00	60.00	100.00	25499724	0.7
AR.N20.VII.171277	chr10	33022442	33022670	1.60	22.60	2.90	41.20	78.60	33022530	0.6
AR.N20.VII.171278	chr10	33523235	33523356	1.30	9.30	0.00	57.10	87.50	33523266	0.5
AR.N20.VII.171279	chr10	34228612	34228826	3.40	47.80	0.00	54.10	95.00	34228741	0.8
AR.N20.VII.171280	chr10	34481427	34481761	3.30	31.70	0.90	51.20	94.50	34481687	0.7
AR.N20.VII.171281	chr10	34955142	34955356	7.30	51.80	1.30	42.30	93.90	34955256	2.1
AR.N20.VII.171282	chr10	36019512	36019873	3.00	21.60	1.50	56.90	81.10	36019680	0.8
AR.N20.VII.171283	chr10	43010294	43010437	2.00	9.30	0.00	72.70	81.20	43010353	0.6
AR.N20.VII.171284	chr10	44489105	44489355	4.00	28.50	0.00	55.80	75.00	44489195	1.1
AR.N20.VII.171285	chr10	44512688	44512861	2.50	11.90	0.00	37.00	90.00	44512771	0.8
AR.N20.VII.171286	chr10	44817345	44817495	2.10	29.50	0.00	49.40	63.60	44817377	0.7
AR.N20.VII.171287	chr10	50383205	50383361	2.60	18.60	0.00	53.60	80.00	50383266	0.8
AR.N20.VII.171288	chr10	52051760	52052066	3.00	4.90	0.00	46.90	93.30	52051841	1.1
AR.N20.VII.171289	chr10	57813718	57813934	3.70	52.30	3.50	45.50	98.60	57813804	1.7
AR.N20.VII.171290	chr10	58388108	58388382	1.80	8.60	0.00	28.20	81.80	58388166	0.8
AR.N20.VII.171291	chr10	59189606	59189870	9.00	42.70	11.90	44.50	97.70	59189735	1.9
AR.N20.VII.171292	chr10	59392671	59392906	2.00	13.90	0.00	57.10	91.70	59392830	0.7
AR.N20.VII.171293	chr10	60966467	60966677	2.40	8.60	0.00	42.30	45.50	60966523	0.6
AR.N20.VII.171294	chr10	61421486	61421697	1.80	12.60	0.00	45.00	77.80	61421566	0.6
AR.N20.VII.171295	chr10	61697615	61697784	2.00	7.10	2.30	48.90	81.80	61697741	0.9
AR.N20.VII.171296	chr10	62397111	62397341	3.10	29.50	4.00	33.50	64.10	62397206	1.2
AR.N20.VII.171297	chr10	62554536	62554730	3.10	22.20	1.50	44.90	80.60	62554620	1
AR.N20.VII.171298	chr10	62676390	62676635	1.50	21.20	0.00	50.00	100.00	62676598	0.5
AR.N20.VII.171299	chr10	62756327	62756482	1.40	19.90	0.00	40.00	83.30	62756427	0.5
AR.N20.VII.171300	chr10	63834706	63835016	1.80	8.40	0.00	52.60	100.00	63834949	0.6
AR.N20.VII.171301	chr10	65142055	65142408	2.80	6.60	0.00	50.00	60.00	65142141	0.5
AR.N20.VII.171302	chr10	65539256	65539486	4.10	29.20	0.00	61.40	100.00	65539397	1.2
AR.N20.VII.171303	chr10	69194123	69194364	3.10	6.70	9.00	54.70	66.60	69194270	0.7
AR.N20.VII.171304	chr10	71341358	71341546	1.80	25.20	0.00	52.60	100.00	71341479	0.7
AR.N20.VII.171305	chr10	72942802	72943038	7.00	16.60	0.00	44.70	88.20	72942916	2
AR.N20.VII.171306	chr10	73019852	73020176	2.30	11.10	0.00	64.00	87.50	73020070	0.7
AR.N20.VII.171307	chr10	73147652	73147832	1.10	8.00	0.00	25.00	100.00	73147785	0.6
AR.N20.VII.171308	chr10	73549339	73549539	1.90	8.00	0.00	44.60	88.90	73549422	0.7
AR.N20.VII.171309	chr10	73678648	73678966	5.00	11.80	0.90	50.50	96.30	73678784	1.4
AR.N20.VII.171310	chr10	73684941	73685183	8.30	17.00	0.60	40.90	86.50	73685031	2.1
AR.N20.VII.171311	chr10	74547714	74547996	1.90	13.30	0.00	40.00	100.00	74547844	0.6
AR.N20.VII.171312	chr10	76251404	76251663	5.30	8.40	0.00	41.70	96.00	76251589	1.6
AR.N20.VII.171313	chr10	76390416	76390650	9.20	43.80	1.00	48.00	89.60	76390558	3
AR.N20.VII.171314	chr10	77163111	77163320	2.10	30.50	0.00	60.90	85.70	77163196	0.6
AR.N20.VII.171315	chr10	77463316	77463621	3.50	12.60	0.00	52.60	85.00	77463411	1.2
AR.N20.VII.171316	chr10	78498939	78499081	2.10	14.60	0.00	50.00	72.70	78499016	0.7
AR.N20.VII.171317	chr10	78672948	78673057	1.60	5.70	0.70	35.00	100.00	78673009	0.9
AR.N20.VII.171318	chr10	78717454	78717810	3.40	6.80	0.00	52.80	78.90	78717704	0.6
AR.N20.VII.171319	chr10	78928110	78928339	28.10	99.90	0.30	44.50	94.90	78928205	8.6
AR.N20.VII.171320	chr10	78928743	78928908	3.80	10.90	0.00	39.00	100.00	78928850	1.4
AR.N20.VII.171321	chr10	78937147	78937445	5.20	9.30	0.00	50.90	82.80	78937296	1.4
AR.N20.VII.171322	chr10	79317364	79317517	2.20	30.80	0.70	69.80	75.30	79317440	0.7
AR.N20.VII.171323	chr10	79596602	79596790	2.40	34.50	0.00	53.80	78.60	79596698	0.8
AR.N20.VII.171324	chr10	80159762	80159843	3.00	42.50	0.00	40.50	100.00	80159816	1.8
AR.N20.VII.171325	chr10	80172522	80172810	3.10	7.40	1.50	41.80	78.60	80172610	0.9
AR.N20.VII.171326	chr10	82600261	82600445	4.40	62.40	0.00	57.40	96.30	82600360	1.4
AR.N20.VII.171327	chr10	88414740	88414900	2.30	32.50	2.00	49.00	91.70	88414827	0.8
AR.N20.VII.171328	chr10	89397822	89397988	1.30	18.60	0.00	33.30	100.00	89397927	0.6
AR.N20.VII.171329	chr10	92773241	92773401	1.00	7.30	0.00	58.30	71.40	92773301	0.6
AR.N20.VII.171330	chr10	93553993	93554150	1.20	5.80	0.00	30.80	100.00	93554068	0.5
AR.N20.VII.171331	chr10	93778897	93779036	1.20	17.30	0.00	53.80	100.00	93778943	0.7
AR.N20.VII.171332	chr10	94481252	94481414	2.00	27.90	0.00	47.60	100.00	94481314	0.9
AR.N20.VII.171333	chr10	95512946	95513134	1.00	4.60	0.00	45.50	80.00	95513064	0.5
AR.N20.VII.171334	chr10	98608517	98608681	1.50	21.20	0.00	41.20	100.00	98608626	0.6
AR.N20.VII.171335	chr10	99653094	99653222	1.20	17.30	0.00	71.40	100.00	99653186	0.6
AR.N20.VII.171336	chr10	100830082	100830243	1.40	6.60	0.00	53.30	100.00	100830212	0.5
AR.N20.VII.171337	chr10	101088802	101088997	2.80	13.30	0.00	53.30	93.80	101088953	0.8
AR.N20.VII.171338	chr10	101562082	101562271	2.10	29.20	0.00	54.50	100.00	101562202	0.7
AR.N20.VII.171339	chr10	102530231	102530373	1.40	10.30	3.20	32.30	100.00	102530319	0.6
AR.N20.VII.171340	chr10	106038305	106038467	2.70	12.80	0.00	62.10	66.70	106038341	0.9

regionID	chrom	start	stop	RPM	fold	multi%	plus%	leftPlus%	peakPos	peakHeight
AR.N20.VII.171341	chr10	106059792	106059929	1.70	6.00	0.00	33.30	100.00	106059818	0.7
AR.N20.VII.171342	chr10	106118259	106118443	1.70	23.90	0.00	44.40	75.00	106118327	0.8
AR.N20.VII.171343	chr10	106571882	106572189	4.20	20.10	1.10	50.50	73.90	106572001	1.2
AR.N20.VII.171344	chr10	110471755	110471934	2.50	11.90	48.10	50.70	75.60	110471839	0.9
AR.N20.VII.171345	chr10	112534076	112534253	1.60	7.50	0.00	35.30	66.70	112534150	0.5
AR.N20.VII.171346	chr10	113331263	113331482	2.60	7.40	3.00	40.70	100.00	113331404	0.7
AR.N20.VII.171347	chr10	113456135	113456239	1.70	8.00	72.20	49.10	100.00	113456211	1.4
AR.N20.VII.171348	chr10	113537721	113537911	3.50	50.50	0.00	47.40	100.00	113537828	1
AR.N20.VII.171349	chr10	113560209	113560421	1.70	23.90	0.00	50.00	100.00	113560347	0.7
AR.N20.VII.171350	chr10	115912391	115912569	1.20	16.60	4.00	52.00	100.00	115912478	0.5
AR.N20.VII.171351	chr10	117051360	117051480	1.20	8.60	0.00	46.20	100.00	117051445	0.5
AR.N20.VII.171352	chr10	117191715	117191917	1.60	11.30	0.00	52.90	77.80	117191760	0.5
AR.N20.VII.171353	chr10	118178861	118179041	1.90	26.60	1.70	71.40	93.30	118178990	0.9
AR.N20.VII.171354	chr10	118302929	118303115	4.70	67.30	11.20	65.50	78.40	118302980	2.1
AR.N20.VII.171355	chr10	119513493	119513653	1.80	25.20	0.00	60.00	83.30	119513560	0.7
AR.N20.VII.171356	chr10	119554328	119554485	2.30	33.20	0.00	40.00	90.00	119554376	0.9
AR.N20.VII.171357	chr10	121034476	121034582	1.50	7.10	0.00	62.50	100.00	121034526	0.7
AR.N20.VII.171358	chr10	122826380	122826564	2.50	9.00	0.00	48.10	100.00	122826488	0.8
AR.N20.VII.171359	chr10	123870608	123870861	53.60	152.80	0.40	45.50	95.40	123870736	12.4
AR.N20.VII.171360	chr10	124977369	124977598	2.60	18.80	1.20	57.10	100.00	124977511	1
AR.N20.VII.171361	chr10	126043353	126043557	4.70	13.40	1.00	56.40	73.70	126043414	1.6
AR.N20.VII.171362	chr10	127270461	127270715	5.70	27.00	0.00	49.20	76.70	127270566	1.5
AR.N20.VII.171363	chr10	127362518	127362654	4.30	61.10	0.00	52.20	100.00	127362572	1.8
AR.N20.VII.171364	chr10	128237501	128237743	1.60	22.60	0.00	52.90	77.80	128237659	0.5
AR.N20.VII.171365	chr10	128259576	128259803	9.10	43.10	0.50	43.10	97.60	128259673	3.3
AR.N20.VII.171366	chr10	128732523	128732785	4.80	13.80	0.00	46.20	91.70	128732634	1.2
AR.N20.VII.171367	chr10	129656446	129656575	2.40	11.50	0.00	59.30	93.80	129656540	1
AR.N20.VII.171368	chr10	129798000	129798259	3.40	24.60	0.00	51.40	73.70	129798099	1
AR.N20.VII.171369	chr10	131267422	131267642	2.80	10.00	0.00	66.70	85.00	131267499	1.2
AR.N20.VII.171370	chr10	132833352	132833495	1.90	26.60	0.00	65.00	76.90	132833399	0.7
AR.N20.VII.171371	chr10	132870138	132870356	3.40	8.20	0.00	56.80	85.70	132870275	1.2
AR.N20.VII.171372	chr10	134298277	134298437	1.90	6.80	2.40	51.20	72.70	134298328	0.8
AR.N20.VII.171373	chr10	134349130	134349376	5.50	13.10	0.00	49.20	100.00	134349248	1.6
AR.N20.VII.171374	chr10	134732748	134733014	9.20	16.40	1.00	58.20	59.00	134732827	2.1
AR.N20.VII.171375	chr11	226264	226392	1.60	5.00	0.00	29.40	100.00	226318	0.7
AR.N20.VII.171376	chr11	809659	809896	2.10	5.10	0.00	39.10	77.80	809757	1
AR.N20.VII.171377	chr11	2756998	2757189	2.10	6.10	0.00	65.20	53.30	2757056	0.6
AR.N20.VII.171378	chr11	2868484	2868752	4.30	8.70	0.00	47.80	95.50	2868626	1.6
AR.N20.VII.171379	chr11	3137139	3137396	5.00	14.30	0.00	55.60	96.70	3137270	1.7
AR.N20.VII.171380	chr11	4584180	4584348	1.20	8.60	7.70	46.20	100.00	4584247	0.6
AR.N20.VII.171381	chr11	4934328	4934529	3.90	55.40	13.80	40.10	94.00	4934447	1.6
AR.N20.VII.171382	chr11	7511102	7511277	1.70	23.90	0.00	38.90	100.00	7511229	0.7
AR.N20.VII.171383	chr11	7516535	7516883	5.50	15.70	0.00	52.50	77.40	7516712	1.5
AR.N20.VII.171384	chr11	7520531	7520711	1.80	25.20	0.00	73.70	64.30	7520563	0.7
AR.N20.VII.171385	chr11	7533579	7533714	1.40	6.60	0.00	53.30	75.00	7533630	0.6
AR.N20.VII.171386	chr11	7600721	7600900	2.40	34.50	0.00	46.20	91.70	7600775	0.7
AR.N20.VII.171387	chr11	7613685	7613820	1.70	11.90	0.00	55.60	50.00	7613702	0.7
AR.N20.VII.171388	chr11	10909952	10910102	1.20	8.60	0.00	61.50	100.00	10910038	0.6
AR.N20.VII.171389	chr11	11562331	11562551	2.40	33.90	2.00	52.80	71.40	11562430	0.5
AR.N20.VII.171390	chr11	12048560	12048820	5.00	23.90	0.00	59.30	96.90	12048710	1.3
AR.N20.VII.171391	chr11	12178534	12178708	1.60	22.60	0.00	29.40	100.00	12178634	0.7
AR.N20.VII.171392	chr11	12226510	12226786	11.10	52.70	1.70	43.70	89.40	12226635	2.7
AR.N20.VII.171393	chr11	12831750	12832000	2.90	20.60	0.00	51.60	93.80	12831878	0.6
AR.N20.VII.171394	chr11	12975427	12975563	1.60	11.30	0.00	64.70	81.80	12975481	0.7
AR.N20.VII.171395	chr11	13764862	13765016	1.90	5.30	0.00	60.00	91.70	13764914	1.1
AR.N20.VII.171396	chr11	14598345	14598526	1.80	8.40	0.00	42.10	100.00	14598438	0.5
AR.N20.VII.171397	chr11	15472129	15472354	1.70	6.10	1.40	39.70	96.60	15472237	0.5
AR.N20.VII.171398	chr11	16204479	16204637	3.40	16.40	0.00	67.60	60.00	16204506	1.2
AR.N20.VII.171399	chr11	17383859	17384084	3.90	18.60	0.00	57.10	62.50	17383952	1
AR.N20.VII.171400	chr11	20489000	20489246	2.50	35.80	0.00	55.60	100.00	20489132	0.8
AR.N20.VII.171401	chr11	22652964	22653109	1.10	5.30	0.00	50.00	100.00	22653007	0.6
AR.N20.VII.171402	chr11	25368819	25369026	1.90	26.60	0.00	50.00	60.00	25368874	0.6
AR.N20.VII.171403	chr11	25968206	25968457	2.50	11.90	0.00	55.60	100.00	25968367	0.8
AR.N20.VII.171404	chr11	26198003	26198144	1.30	9.50	0.00	43.90	100.00	26198054	0.6
AR.N20.VII.171405	chr11	26888885	26889006	3.40	47.70	0.00	33.30	91.60	26888936	1.9
AR.N20.VII.171406	chr11	27097347	27097541	2.80	13.30	0.00	36.70	90.90	27097441	0.8
AR.N20.VII.171407	chr11	27155473	27155703	4.50	21.20	0.00	41.70	95.00	27155612	1.1
AR.N20.VII.171408	chr11	27492858	27493090	1.90	8.90	0.00	70.00	57.10	27492945	0.6
AR.N20.VII.171409	chr11	27694455	27694635	1.40	17.70	0.00	46.70	100.00	27694542	0.7
AR.N20.VII.171410	chr11	30348387	30348597	2.20	15.60	2.10	44.70	90.50	30348540	0.7
AR.N20.VII.171411	chr11	31485707	31485858	2.10	9.70	0.00	36.40	100.00	31485771	1
AR.N20.VII.171412	chr11	32282793	32283017	1.80	25.90	2.60	43.90	77.80	32282876	0.7
AR.N20.VII.171413	chr11	32307636	32307748	1.20	10.10	4.00	48.00	100.00	32307700	0.7
AR.N20.VII.171414	chr11	32891704	32891904	1.90	26.60	0.00	50.00	90.00	32891827	1
AR.N20.VII.171415	chr11	34618164	34618359	3.70	52.40	1.30	41.80	81.80	34618298	1
AR.N20.VII.171416	chr11	34728495	34728669	2.10	7.30	0.00	54.50	91.70	34728572	0.6
AR.N20.VII.171417	chr11	34889260	34889513	3.60	51.80	0.00	66.70	57.70	34889321	1.1
AR.N20.VII.171418	chr11	35039747	35039953	2.60	18.80	1.20	50.60	93.00	35039853	0.9
AR.N20.VII.171419	chr11	35136809	35137035	5.30	18.90	0.00	65.50	86.80	35136936	1.6
AR.N20.VII.171420	chr11	35233722	35233915	6.20	44.10	0.80	54.10	91.70	35233804	1.9
AR.N20.VII.171421	chr11	35282656	35282873	3.10	8.90	1.50	50.70	100.00	35282816	1.1
AR.N20.VII.171422	chr11	35316173	35316383	2.00	28.50	2.30	39.50	100.00	35316244	0.8
AR.N20.VII.171423	chr11	35886196	35886481	4.10	11.30	1.40	57.30	80.00	35886321	0.9
AR.N20.VII.171424	chr11	35928246	35928477	2.20	6.40	0.00	58.30	100.00	35928412	0.9
AR.N20.VII.171425	chr11	36296225	36296441	2.70	19.00	5.70	51.00	85.60	36296308	0.9

regionID	chrom	start	stop	RPM	fold	multi%	plus%	leftPlus%	peakPos	peakHeight
AR.N20.VII.171426	chr11	36446111	36446404	4.90	69.70	1.00	50.50	84.90	36446219	1.4
AR.N20.VII.171427	chr11	38511637	38511812	1.70	4.30	5.50	62.50	100.00	38511775	0.7
AR.N20.VII.171428	chr11	42734808	42735055	2.30	33.20	0.00	56.00	57.10	42734896	0.6
AR.N20.VII.171429	chr11	42802296	42802427	1.10	12.70	0.00	41.70	100.00	42802382	0.7
AR.N20.VII.171430	chr11	42822102	42822377	2.30	8.10	2.00	44.90	100.00	42822293	0.8
AR.N20.VII.171431	chr11	44637859	44638035	2.00	5.60	0.00	50.00	72.70	44637936	0.6
AR.N20.VII.171432	chr11	44844200	44844444	2.10	4.20	0.00	47.80	90.90	44844366	0.8
AR.N20.VII.171433	chr11	45744103	45744290	1.50	7.30	9.10	39.40	84.60	45744167	0.5
AR.N20.VII.171434	chr11	46252110	46252255	1.20	4.30	0.00	50.00	100.00	46252216	0.6
AR.N20.VII.171435	chr11	48020034	48020311	4.90	60.40	2.10	49.20	88.90	48020181	1.6
AR.N20.VII.171436	chr11	48033945	48034244	3.40	9.60	0.00	44.40	81.20	48034067	1.2
AR.N20.VII.171437	chr11	48971590	48971781	1.90	12.60	93.60	41.40	91.60	48971613	0.9
AR.N20.VII.171438	chr11	50704868	50704969	1.00	7.00	8.90	40.70	78.00	50704882	0.9
AR.N20.VII.171439	chr11	54787192	54787401	2.50	28.90	47.40	72.20	73.30	54787269	1
AR.N20.VII.171440	chr11	54966859	54967050	1.70	11.90	0.00	72.20	92.30	54966953	0.7
AR.N20.VII.171441	chr11	56849866	56850035	1.30	9.30	0.00	50.00	71.40	56849912	0.7
AR.N20.VII.171442	chr11	57027061	57027247	8.10	38.50	0.00	44.90	95.00	57027182	2.6
AR.N20.VII.171443	chr11	57709498	57709643	1.40	19.90	0.00	73.30	100.00	57709614	0.6
AR.N20.VII.171444	chr11	59075012	59075130	1.40	8.80	29.00	58.10	62.60	59075040	0.6
AR.N20.VII.171445	chr11	60417552	60417680	1.60	23.20	0.00	54.10	80.00	60417583	0.8
AR.N20.VII.171446	chr11	61125740	61125984	4.80	8.50	0.00	58.80	66.70	61125810	1.3
AR.N20.VII.171447	chr11	61219575	61219769	8.60	24.60	0.50	49.20	95.60	61219689	2.3
AR.N20.VII.171448	chr11	61847927	61848084	1.00	7.30	0.00	45.50	100.00	61848036	0.5
AR.N20.VII.171449	chr11	62032424	62032611	2.30	16.60	0.00	52.00	53.80	62032474	0.6
AR.N20.VII.171450	chr11	62079024	62079185	1.30	6.20	0.00	42.90	100.00	62079083	0.7
AR.N20.VII.171451	chr11	62111841	62112096	5.30	25.20	0.00	49.10	100.00	62111987	1.3
AR.N20.VII.171452	chr11	63158695	63158928	2.00	28.60	16.50	58.00	64.00	63158757	0.6
AR.N20.VII.171453	chr11	65713438	65713700	16.40	46.90	0.30	51.20	80.60	65713562	5
AR.N20.VII.171454	chr11	65872106	65872308	2.90	11.20	22.00	53.20	85.50	65872217	1.1
AR.N20.VII.171455	chr11	65897307	65897564	2.80	10.00	0.00	63.30	68.40	65897431	0.8
AR.N20.VII.171456	chr11	66242300	66242460	2.40	5.80	0.00	53.80	92.90	66242403	1
AR.N20.VII.171457	chr11	66325911	66326042	1.40	19.90	0.00	46.70	85.70	66325923	0.6
AR.N20.VII.171458	chr11	67037022	67037205	1.80	6.30	0.00	52.60	100.00	67037137	0.9
AR.N20.VII.171459	chr11	67984184	67984336	1.80	5.00	0.00	26.30	100.00	67984290	0.7
AR.N20.VII.171460	chr11	68062188	68062378	3.50	49.60	0.90	57.10	100.00	68062276	1.1
AR.N20.VII.171461	chr11	68175910	68176064	2.70	19.30	0.00	44.80	100.00	68176017	1.1
AR.N20.VII.171462	chr11	68371607	68371810	2.10	9.70	0.00	40.90	88.90	68371699	1
AR.N20.VII.171463	chr11	68630193	68630401	2.40	4.90	0.00	34.60	66.70	68630289	0.8
AR.N20.VII.171464	chr11	70263767	70264023	17.50	31.10	64.20	49.70	85.60	70263904	3
AR.N20.VII.171465	chr11	70501832	70502063	45.20	91.90	0.10	44.90	90.00	70501956	12.4
AR.N20.VII.171466	chr11	74194980	74195224	4.90	69.70	1.00	53.30	85.70	74195138	1.2
AR.N20.VII.171467	chr11	74961430	74961782	2.40	11.50	0.00	38.50	80.00	74961658	0.6
AR.N20.VII.171468	chr11	75031213	75031445	2.70	39.20	1.70	47.50	85.70	75031336	0.7
AR.N20.VII.171469	chr11	76162789	76162930	2.00	9.30	0.00	50.00	45.50	76162809	0.7
AR.N20.VII.171470	chr11	77489163	77489266	2.00	27.90	0.00	42.90	88.90	77489183	1.1
AR.N20.VII.171471	chr11	77557384	77557565	1.30	4.60	0.00	50.00	100.00	77557468	0.7
AR.N20.VII.171472	chr11	80171406	80171613	24.10	114.60	0.00	51.10	94.10	80171505	7.2
AR.N20.VII.171473	chr11	82799599	82799875	8.50	24.20	0.00	51.60	85.40	82799755	2.4
AR.N20.VII.171474	chr11	89215834	89216027	2.10	19.60	99.30	52.90	100.00	89215980	0.9
AR.N20.VII.171475	chr11	89292039	89292298	6.70	35.20	99.30	43.70	95.40	89292188	1.8
AR.N20.VII.171476	chr11	89297830	89298089	6.70	35.20	98.70	55.90	71.30	89297916	1.8
AR.N20.VII.171477	chr11	89374071	89374325	2.20	20.40	97.90	45.70	79.60	89374157	0.9
AR.N20.VII.171478	chr11	90981520	90981787	2.80	19.90	0.00	53.30	87.50	90981695	0.7
AR.N20.VII.171479	chr11	92562360	92562630	6.00	28.50	0.80	49.60	90.60	92562474	2.2
AR.N20.VII.171480	chr11	92729438	92729612	1.10	8.00	0.00	50.00	100.00	92729548	0.6
AR.N20.VII.171481	chr11	94081651	94081861	2.50	11.70	1.90	37.70	90.00	94081733	0.7
AR.N20.VII.171482	chr11	94167066	94167292	2.80	10.00	0.00	46.70	85.70	94167148	1
AR.N20.VII.171483	chr11	94218445	94218732	2.70	7.70	0.00	55.20	75.00	94218598	0.5
AR.N20.VII.171484	chr11	95566192	95566384	2.00	13.90	0.00	57.10	100.00	95566323	0.5
AR.N20.VII.171485	chr11	96986170	96986317	1.40	9.10	3.20	57.00	88.90	96986206	0.6
AR.N20.VII.171486	chr11	100008949	100009125	3.50	25.20	0.00	55.00	90.90	100009030	1.1
AR.N20.VII.171487	chr11	100266770	100266962	1.60	11.30	0.00	50.00	77.80	100266843	0.6
AR.N20.VII.171488	chr11	103699881	103700045	1.10	7.60	4.30	52.20	83.30	103699971	0.6
AR.N20.VII.171489	chr11	104844217	104844404	1.70	8.00	0.00	42.10	87.50	104844265	0.7
AR.N20.VII.171490	chr11	106537696	106537923	2.00	28.30	10.90	36.50	100.00	106537825	0.7
AR.N20.VII.171491	chr11	106600897	106601081	1.60	11.30	0.00	70.60	83.30	106600950	0.7
AR.N20.VII.171492	chr11	108447608	108447773	2.70	19.30	0.00	71.00	95.50	108447725	1.5
AR.N20.VII.171493	chr11	110513885	110514104	2.50	35.80	0.00	50.00	100.00	110514027	0.7
AR.N20.VII.171494	chr11	110681471	110681649	1.70	23.90	0.00	38.90	100.00	110681564	0.7
AR.N20.VII.171495	chr11	112715924	112716158	2.00	9.30	0.00	28.60	100.00	112716020	0.5
AR.N20.VII.171496	chr11	113505984	113506165	2.30	11.10	0.00	48.00	100.00	113506120	0.6
AR.N20.VII.171497	chr11	113535945	113536260	4.40	15.80	1.10	34.70	100.00	113536170	1
AR.N20.VII.171498	chr11	113538746	113539043	13.60	32.30	0.00	45.60	88.20	113538941	3
AR.N20.VII.171499	chr11	113539940	113540213	4.30	20.40	0.00	54.30	100.00	113540059	1.1
AR.N20.VII.171500	chr11	113555220	113555530	42.50	151.50	0.20	52.10	85.10	113555394	8.5
AR.N20.VII.171501	chr11	113854096	113854325	1.60	7.10	2.00	57.70	100.00	113854209	0.6
AR.N20.VII.171502	chr11	114596444	114596623	2.90	13.70	0.00	51.60	93.80	114596540	0.8
AR.N20.VII.171503	chr11	116447282	116447481	4.70	33.60	1.30	62.60	77.30	116447396	1.4
AR.N20.VII.171504	chr11	119899080	119899299	3.40	23.90	0.00	47.20	76.50	119899208	1
AR.N20.VII.171505	chr11	120417057	120417329	5.80	20.70	0.80	51.20	84.40	120417186	1.6
AR.N20.VII.171506	chr11	120676281	120676511	3.30	23.20	0.00	52.80	100.00	120676422	1
AR.N20.VII.171507	chr11	121025821	121025940	1.00	14.60	0.00	27.30	100.00	121025895	0.6
AR.N20.VII.171508	chr11	124257713	124257889	1.40	5.00	0.00	46.70	71.40	124257785	0.6
AR.N20.VII.171509	chr11	124414924	124415055	1.10	15.90	0.00	41.70	100.00	124415009	0.5
AR.N20.VII.171510	chr11	124649538	124649782	2.40	11.50	0.00	69.20	88.90	124649710	0.9

regionID	chrom	start	stop	RPM	fold	multi%	plus%	leftPlus%	peakPos	peakHeight
AR.N20.VII.171511	chr11	125919453	125919668	1.70	23.90	0.00	50.00	100.00	125919569	0.5
AR.N20.VII.171512	chr11	128256503	128256732	9.50	67.40	0.50	52.70	87.20	128256595	2.4
AR.N20.VII.171513	chr11	128292348	128292572	1.80	6.30	0.00	45.50	80.00	128292393	0.6
AR.N20.VII.171514	chr11	128739384	128739550	2.10	7.60	0.00	33.30	100.00	128739467	0.6
AR.N20.VII.171515	chr11	128913523	128913739	4.80	9.70	0.00	47.10	54.20	128913573	1.3
AR.N20.VII.171516	chr11	129400559	129400742	14.60	207.40	0.00	42.90	100.00	129400643	4.7
AR.N20.VII.171517	chr11	129805196	129805395	4.80	17.30	0.00	48.10	76.00	129805265	1.8
AR.N20.VII.171518	chr11	130013814	130014001	2.00	7.00	0.00	54.50	75.00	130013894	0.7
AR.N20.VII.171519	chr11	130790930	130791164	4.50	64.40	1.00	46.50	69.60	130790999	1.3
AR.N20.VII.171520	chr11	132758788	132759085	4.90	23.50	0.00	50.00	92.60	132758971	0.9
AR.N20.VII.171521	chr11	133633849	133634036	1.70	8.00	0.00	44.40	100.00	133633991	0.7
AR.N20.VII.171522	chr11	133872756	133872968	13.40	95.30	0.30	58.70	83.70	133872839	5.1
AR.N20.VII.171523	chr11	133902508	133902781	3.80	27.20	2.50	50.40	95.30	133902673	0.9
AR.N20.VII.171524	chr12	808581	808753	2.40	34.30	3.20	60.00	58.10	808628	0.6
AR.N20.VII.171525	chr12	1915937	1916177	5.60	11.50	0.80	36.40	100.00	1916052	2.2
AR.N20.VII.171526	chr12	2642071	2642197	1.60	22.60	0.00	58.80	100.00	2642127	1
AR.N20.VII.171527	chr12	2754914	2755241	7.50	15.20	0.00	48.10	97.40	2755121	2.4
AR.N20.VII.171528	chr12	4836995	4837150	1.70	8.00	5.60	55.60	100.00	4837103	0.5
AR.N20.VII.171529	chr12	5327588	5327816	1.50	7.10	0.00	56.20	100.00	5327740	0.6
AR.N20.VII.171530	chr12	6000499	6000754	1.90	13.60	22.00	58.50	75.00	6000551	0.6
AR.N20.VII.171531	chr12	6246593	6246799	1.60	7.50	0.00	70.60	83.30	6246714	0.6
AR.N20.VII.171532	chr12	6355551	6355817	2.00	4.60	0.00	57.10	100.00	6355778	0.6
AR.N20.VII.171533	chr12	6629967	6630163	1.20	17.30	0.00	30.80	100.00	6630010	0.6
AR.N20.VII.171534	chr12	7838562	7838860	2.40	10.60	96.20	52.20	82.90	7838694	0.5
AR.N20.VII.171535	chr12	7940585	7940817	2.10	9.20	86.20	52.00	98.60	7940749	0.6
AR.N20.VII.171536	chr12	7942372	7942668	2.40	10.30	98.70	51.00	82.10	7942502	0.5
AR.N20.VII.171537	chr12	8034841	8034983	1.10	8.00	0.00	25.00	100.00	8034935	0.6
AR.N20.VII.171538	chr12	8309734	8309790	8.00	114.20	0.00	32.30	100.00	8309743	8
AR.N20.VII.171539	chr12	11667657	11667885	1.60	5.60	0.00	64.70	90.90	11667779	0.6
AR.N20.VII.171540	chr12	11728349	11728503	1.10	8.00	0.00	41.70	80.00	11728376	0.6
AR.N20.VII.171541	chr12	13179959	13180336	3.40	4.80	0.00	58.60	95.30	13180263	0.7
AR.N20.VII.171542	chr12	13774557	13774749	2.00	9.50	2.30	60.50	84.60	13774589	0.8
AR.N20.VII.171543	chr12	13998219	13998380	1.20	17.30	0.00	38.50	100.00	13998287	0.6
AR.N20.VII.171544	chr12	15319015	15319173	1.60	22.60	0.00	64.70	90.90	15319089	0.7
AR.N20.VII.171545	chr12	15864299	15864540	2.00	13.90	0.00	47.60	80.00	15864411	0.6
AR.N20.VII.171546	chr12	16518184	16518423	2.40	17.30	0.00	46.20	91.70	16518310	0.6
AR.N20.VII.171547	chr12	17238456	17238681	2.10	29.20	0.00	45.50	100.00	17238595	0.7
AR.N20.VII.171548	chr12	20745018	20745161	2.20	15.90	0.00	58.30	92.90	20745089	0.8
AR.N20.VII.171549	chr12	21395223	21395509	3.60	51.80	0.00	56.40	68.20	21395311	1.1
AR.N20.VII.171550	chr12	22804545	22804761	1.70	8.00	0.00	72.20	69.20	22804650	0.6
AR.N20.VII.171551	chr12	22808003	22808174	1.40	19.90	0.00	73.30	100.00	22808140	0.6
AR.N20.VII.171552	chr12	23231191	23231517	4.10	19.30	1.50	50.80	82.00	23231331	1
AR.N20.VII.171553	chr12	26840202	26840373	3.60	17.30	0.00	59.00	91.30	26840286	0.9
AR.N20.VII.171554	chr12	27583399	27583585	2.30	32.50	2.00	63.30	93.50	27583509	0.7
AR.N20.VII.171555	chr12	27694761	27695018	1.40	9.60	3.40	58.60	100.00	27694886	0.5
AR.N20.VII.171556	chr12	27909433	27909663	1.90	26.60	0.00	55.00	100.00	27909565	0.6
AR.N20.VII.171557	chr12	28275494	28275737	2.70	19.60	1.70	52.50	100.00	28275653	0.7
AR.N20.VII.171558	chr12	28549969	28550174	1.50	5.30	0.00	43.80	85.70	28550019	0.6
AR.N20.VII.171559	chr12	29607846	29608086	2.50	17.90	0.00	51.90	100.00	29607972	0.8
AR.N20.VII.171560	chr12	29779052	29779253	2.00	27.90	0.00	54.50	100.00	29779188	0.5
AR.N20.VII.171561	chr12	30380303	30380514	2.40	16.90	2.00	56.90	72.40	30380388	0.7
AR.N20.VII.171562	chr12	31504284	31504525	2.80	10.00	0.00	46.70	85.70	31504463	1.1
AR.N20.VII.171563	chr12	32312231	32312529	3.00	24.80	8.70	63.00	85.00	32312439	1.1
AR.N20.VII.171564	chr12	32724579	32724801	2.80	13.30	0.00	50.00	100.00	32724707	1
AR.N20.VII.171565	chr12	33626056	33626197	1.30	9.30	0.00	57.10	100.00	33626141	0.6
AR.N20.VII.171566	chr12	33809916	33810046	1.50	7.10	0.00	62.50	80.00	33810008	0.7
AR.N20.VII.171567	chr12	37235762	37235944	1.60	11.30	5.90	51.00	100.00	37235846	0.7
AR.N20.VII.171568	chr12	39315135	39315266	1.10	5.30	0.00	58.30	57.10	39315148	0.6
AR.N20.VII.171569	chr12	39575492	39575658	6.70	21.90	2.30	44.00	96.80	39575592	2.6
AR.N20.VII.171570	chr12	39741338	39741511	2.10	19.50	0.00	54.50	66.70	39741431	0.6
AR.N20.VII.171571	chr12	40692234	40692420	8.90	31.90	0.00	48.00	89.40	40692304	2.7
AR.N20.VII.171572	chr12	41545521	41545704	1.70	11.90	0.00	44.40	100.00	41545607	0.7
AR.N20.VII.171573	chr12	41595564	41595862	3.70	26.60	0.00	57.50	69.60	41595711	0.8
AR.N20.VII.171574	chr12	45173991	45174259	5.70	81.30	0.40	49.00	76.70	45174116	1.5
AR.N20.VII.171575	chr12	45473025	45473283	5.10	24.30	0.00	56.40	96.80	45473186	1.8
AR.N20.VII.171576	chr12	45713171	45713327	1.80	8.40	0.00	57.90	90.90	45713251	0.8
AR.N20.VII.171577	chr12	49393494	49393681	11.60	82.60	0.40	50.20	81.60	49393535	3.8
AR.N20.VII.171578	chr12	50806537	50807154	17.20	24.60	0.00	53.20	73.70	50806663	3.2
AR.N20.VII.171579	chr12	51363098	51363301	2.00	27.90	0.00	61.90	61.50	51363149	0.6
AR.N20.VII.171580	chr12	51854957	51855193	2.30	16.60	0.00	48.00	91.70	51855054	0.5
AR.N20.VII.171581	chr12	52696714	52696909	2.70	9.60	0.00	41.40	91.70	52696787	1.2
AR.N20.VII.171582	chr12	53136253	53136407	3.20	45.10	0.00	55.90	100.00	53136329	1.2
AR.N20.VII.171583	chr12	53476837	53477001	3.40	23.90	0.00	54.10	85.00	53476898	1.2
AR.N20.VII.171584	chr12	54383417	54383592	1.40	5.10	3.20	48.40	86.70	54383511	0.6
AR.N20.VII.171585	chr12	54589285	54589495	1.70	11.90	0.00	72.20	69.20	54589354	0.6
AR.N20.VII.171586	chr12	55958605	55958828	4.00	57.10	0.00	44.20	89.50	55958738	1.3
AR.N20.VII.171587	chr12	56800303	56800474	1.40	10.00	0.00	53.30	100.00	56800379	0.6
AR.N20.VII.171588	chr12	57710537	57710786	2.40	8.60	0.00	57.70	100.00	57710704	0.8
AR.N20.VII.171589	chr12	63109104	63109304	3.20	15.00	0.00	55.90	84.20	63109159	1
AR.N20.VII.171590	chr12	63270341	63270573	5.00	35.50	0.90	47.70	84.30	63270425	1.5
AR.N20.VII.171591	chr12	63314117	63314241	1.40	9.20	5.80	27.80	97.00	63314188	0.7
AR.N20.VII.171592	chr12	64247987	64248254	6.40	15.10	0.50	53.20	100.00	64248157	1.9
AR.N20.VII.171593	chr12	65251896	65252044	1.40	6.60	0.00	53.30	100.00	65251947	0.6
AR.N20.VII.171594	chr12	69080299	69080465	1.40	6.60	0.00	53.30	100.00	69080382	0.5
AR.N20.VII.171595	chr12	69843343	69843488	1.30	9.30	0.00	42.90	83.30	69843420	0.5

regionID	chrom	start	stop	RPM	fold	multi%	plus%	leftPlus%	peakPos	peakHeight
AR.N20.VII.171596	chr12	70401935	70402116	1.40	6.60	0.00	73.30	81.80	70402069	0.5
AR.N20.VII.171597	chr12	70467001	70467260	2.20	31.90	0.00	54.20	100.00	70467154	0.9
AR.N20.VII.171598	chr12	71733987	71734227	11.00	156.70	0.00	50.40	100.00	71734143	2.8
AR.N20.VII.171599	chr12	72515352	72515480	1.10	15.90	0.00	66.70	75.00	72515370	0.7
AR.N20.VII.171600	chr12	72997247	72997411	1.80	25.20	0.00	57.90	72.70	72997290	0.6
AR.N20.VII.171601	chr12	73660787	73661023	2.30	33.20	0.00	40.00	90.00	73660918	0.6
AR.N20.VII.171602	chr12	73722365	73722461	1.10	15.90	0.00	50.00	83.30	73722393	0.6
AR.N20.VII.171603	chr12	73809417	73809630	2.10	29.90	2.20	53.30	83.30	73809497	0.7
AR.N20.VII.171604	chr12	75338160	75338413	2.00	13.90	0.00	52.40	81.80	75338290	0.5
AR.N20.VII.171605	chr12	77717652	77717847	6.90	24.60	0.00	62.20	78.30	77717724	2.2
AR.N20.VII.171606	chr12	78949772	78949973	1.80	25.60	1.30	46.80	100.00	78949875	0.8
AR.N20.VII.171607	chr12	79238153	79238533	3.30	15.50	0.00	45.70	56.20	79238232	0.7
AR.N20.VII.171608	chr12	79503237	79503412	3.60	25.90	0.00	37.50	100.00	79503328	1.4
AR.N20.VII.171609	chr12	80544419	80544635	2.60	18.60	3.60	53.60	90.00	80544512	0.7
AR.N20.VII.171610	chr12	80917435	80917631	2.40	17.30	3.80	69.20	94.40	80917517	0.8
AR.N20.VII.171611	chr12	85183083	85183235	1.70	6.10	2.70	42.90	50.00	85183107	0.7
AR.N20.VII.171612	chr12	87440952	87441146	5.20	37.20	0.00	46.40	100.00	87441047	1.7
AR.N20.VII.171613	chr12	87719250	87719402	1.30	18.60	0.00	42.90	100.00	87719332	0.6
AR.N20.VII.171614	chr12	88945172	88945311	2.60	13.60	2.30	33.10	89.10	88945205	1.2
AR.N20.VII.171615	chr12	89084759	89084909	1.00	14.60	0.00	45.50	100.00	89084826	0.6
AR.N20.VII.171616	chr12	89795754	89795966	3.00	27.00	11.40	42.10	72.80	89795817	1.3
AR.N20.VII.171617	chr12	90636299	90636555	2.20	31.90	0.00	45.80	100.00	90636489	0.6
AR.N20.VII.171618	chr12	90948631	90948851	4.30	15.30	0.00	37.00	94.10	90948755	1.3
AR.N20.VII.171619	chr12	92470369	92470631	1.80	4.30	2.60	66.70	76.90	92470487	0.5
AR.N20.VII.171620	chr12	92731896	92732234	11.20	53.30	0.40	61.00	94.60	92732132	2.6
AR.N20.VII.171621	chr12	92861619	92861852	3.00	21.40	0.00	53.10	88.30	92861728	0.7
AR.N20.VII.171622	chr12	93070706	93070855	1.20	8.60	0.00	42.90	100.00	93070803	0.5
AR.N20.VII.171623	chr12	93480016	93480246	2.10	14.60	0.00	59.10	84.60	93480104	0.6
AR.N20.VII.171624	chr12	93510021	93510312	6.00	85.10	0.20	45.30	82.40	93510114	1.3
AR.N20.VII.171625	chr12	93807567	93807732	2.40	17.30	0.00	42.30	90.90	93807668	0.6
AR.N20.VII.171626	chr12	94496756	94496833	1.00	14.60	0.00	54.50	100.00	94496778	0.7
AR.N20.VII.171627	chr12	94635868	94636027	1.20	4.30	0.00	46.20	83.30	94635957	0.6
AR.N20.VII.171628	chr12	94656115	94656378	1.80	12.60	0.00	52.60	100.00	94656288	0.6
AR.N20.VII.171629	chr12	96486652	96486926	3.60	17.30	0.00	46.20	72.20	96486715	0.9
AR.N20.VII.171630	chr12	97422073	97422236	2.10	4.40	20.20	40.30	96.40	97422171	0.8
AR.N20.VII.171631	chr12	98650099	98650315	1.60	7.80	3.00	60.10	90.50	98650194	0.5
AR.N20.VII.171632	chr12	99892720	99892960	10.00	35.50	0.00	48.60	87.00	99892808	2.5
AR.N20.VII.171633	chr12	100534114	100534242	1.80	25.20	0.00	57.90	81.80	100534184	0.6
AR.N20.VII.171634	chr12	101260600	101260759	4.20	29.90	0.00	46.70	100.00	101260667	1.4
AR.N20.VII.171635	chr12	101421010	101421298	3.50	25.20	0.00	57.90	95.50	101421177	1.1
AR.N20.VII.171636	chr12	102291058	102291230	1.70	6.00	0.00	50.00	55.60	102291110	0.6
AR.N20.VII.171637	chr12	103543030	103543208	2.70	38.50	0.00	56.70	64.70	103543111	0.7
AR.N20.VII.171638	chr12	105700636	105700789	1.70	11.90	0.00	50.00	100.00	105700744	0.7
AR.N20.VII.171639	chr12	109712685	109712809	1.00	14.60	0.00	50.00	100.00	109712747	0.6
AR.N20.VII.171640	chr12	109989833	109990103	39.70	80.70	0.10	50.90	78.40	109989928	10.4
AR.N20.VII.171641	chr12	111174508	111174651	2.10	29.20	0.00	34.80	100.00	111174608	0.8
AR.N20.VII.171642	chr12	111228177	111228432	3.70	6.60	1.30	50.60	80.00	111228292	1.1
AR.N20.VII.171643	chr12	113833538	113833718	1.30	9.30	7.00	27.10	100.00	113833653	0.5
AR.N20.VII.171644	chr12	114414178	114414337	1.20	8.60	0.00	46.20	100.00	114414290	0.6
AR.N20.VII.171645	chr12	114739707	114740036	4.00	11.40	0.00	53.50	91.30	114739840	1
AR.N20.VII.171646	chr12	115327607	115327728	1.50	10.60	0.00	50.00	87.50	115327653	0.7
AR.N20.VII.171647	chr12	115559121	115559418	2.90	13.70	0.00	61.30	73.70	115559263	0.7
AR.N20.VII.171648	chr12	115960587	115960741	1.90	26.60	0.00	33.30	100.00	115960639	0.6
AR.N20.VII.171649	chr12	118638828	118639074	4.50	31.90	0.00	58.30	85.70	118638972	1.3
AR.N20.VII.171650	chr12	122448987	122449219	5.70	27.00	0.00	60.70	86.50	122449105	1.7
AR.N20.VII.171651	chr12	123181211	123181503	2.80	6.60	0.00	46.70	85.70	123181360	0.9
AR.N20.VII.171652	chr12	123570756	123571090	5.30	9.50	0.00	52.60	63.30	123570874	1.3
AR.N20.VII.171653	chr12	130563847	130564090	1.90	8.90	0.00	45.00	55.60	130563958	0.5
AR.N20.VII.171654	chr12	130947099	130947268	1.80	6.30	0.00	31.60	100.00	130947219	0.8
AR.N20.VII.171655	chr12	131430258	131430443	1.90	13.30	0.00	55.00	90.90	131430381	0.7
AR.N20.VII.171656	chr12	131437991	131438150	1.30	6.20	0.00	42.90	83.30	131438099	0.6
AR.N20.VII.171657	chr12	131581011	131581160	1.50	4.20	0.00	70.60	75.00	131581090	0.6
AR.N20.VII.171658	chr12	131914916	131915236	4.10	5.30	0.00	52.30	69.60	131915069	1.1
AR.N20.VII.171659	chr13	20505672	20505846	1.60	7.50	0.00	70.60	100.00	20505814	0.7
AR.N20.VII.171660	chr13	23194834	23195047	3.40	47.80	0.00	52.80	100.00	23194976	0.9
AR.N20.VII.171661	chr13	23674459	23674685	10.00	142.10	0.00	48.60	98.10	23674553	3
AR.N20.VII.171662	chr13	24968672	24968990	3.40	47.80	0.00	52.80	100.00	24968910	1
AR.N20.VII.171663	chr13	25450438	25450699	2.20	15.90	0.00	37.50	88.90	25450566	0.6
AR.N20.VII.171664	chr13	26107892	26108080	2.60	12.40	14.10	53.30	100.00	26108004	0.8
AR.N20.VII.171665	chr13	26383092	26383233	1.20	17.30	0.00	46.70	100.00	26383206	0.5
AR.N20.VII.171666	chr13	27438184	27438354	1.50	21.20	0.00	37.50	100.00	27438268	0.6
AR.N20.VII.171667	chr13	29719866	29720049	2.20	31.90	0.00	50.00	100.00	29719968	1.1
AR.N20.VII.171668	chr13	30565108	30565394	1.90	6.60	0.00	55.00	90.90	30565271	0.5
AR.N20.VII.171669	chr13	31085286	31085441	1.30	6.30	2.30	37.20	100.00	31085387	0.7
AR.N20.VII.171670	chr13	32700079	32700322	1.90	13.30	0.00	65.00	76.90	32700133	0.6
AR.N20.VII.171671	chr13	33807823	33808035	9.00	128.80	0.00	43.90	74.40	33807898	2.2
AR.N20.VII.171672	chr13	34299500	34299591	1.00	7.30	0.00	54.50	100.00	34299564	0.6
AR.N20.VII.171673	chr13	35774417	35774701	2.40	17.30	0.00	55.60	100.00	35774655	0.7
AR.N20.VII.171674	chr13	38415424	38415601	2.30	16.60	4.00	57.70	100.00	38415570	0.8
AR.N20.VII.171675	chr13	39948847	39948943	1.20	17.30	0.00	53.80	57.10	39948867	0.6
AR.N20.VII.171676	chr13	40532270	40532490	2.70	6.40	0.00	51.70	80.00	40532343	0.9
AR.N20.VII.171677	chr13	42025881	42026088	2.40	34.50	0.00	57.70	86.70	42025974	0.7
AR.N20.VII.171678	chr13	42396529	42396739	17.90	84.80	0.30	51.60	91.10	42396614	6
AR.N20.VII.171679	chr13	43691153	43691336	8.20	58.40	0.00	53.40	100.00	43691242	2.6
AR.N20.VII.171680	chr13	44326736	44327068	3.40	9.60	0.00	25.00	88.90	44326971	0.7

regionID	chrom	start	stop	RPM	fold	multi%	plus%	leftPlus%	peakPos	peakHeight
AR.N20.VII.171681	chr13	44394696	44394916	9.10	130.10	1.00	58.90	94.10	44394816	2.9
AR.N20.VII.171682	chr13	44540262	44540462	2.00	9.30	0.00	57.10	91.70	44540340	0.8
AR.N20.VII.171683	chr13	44812531	44812735	2.00	13.90	0.00	71.40	60.00	44812574	0.6
AR.N20.VII.171684	chr13	49330804	49330983	2.70	38.50	0.00	41.40	100.00	49330893	1.1
AR.N20.VII.171685	chr13	49838420	49838602	2.00	13.90	0.00	66.70	100.00	49838516	0.6
AR.N20.VII.171686	chr13	50796461	50796598	2.00	7.00	0.00	66.70	57.10	50796504	0.7
AR.N20.VII.171687	chr13	50869555	50869766	1.30	9.30	0.00	35.70	100.00	50869693	0.6
AR.N20.VII.171688	chr13	50992091	50992356	2.50	17.90	0.00	44.40	91.70	50992297	0.7
AR.N20.VII.171689	chr13	51590171	51590413	2.70	19.30	0.00	55.20	100.00	51590276	0.7
AR.N20.VII.171690	chr13	51724972	51725153	2.20	10.20	51.30	49.80	82.60	51725079	0.8
AR.N20.VII.171691	chr13	51846640	51846782	1.90	13.30	32.50	57.50	100.00	51846725	0.7
AR.N20.VII.171692	chr13	52025602	52025772	2.60	18.80	41.40	31.20	88.70	52025687	1.2
AR.N20.VII.171693	chr13	52669712	52669835	1.70	23.90	0.00	66.70	58.30	52669732	0.7
AR.N20.VII.171694	chr13	59481705	59481876	1.30	6.20	0.00	64.30	88.90	59481760	0.6
AR.N20.VII.171695	chr13	62194210	62194318	1.50	10.60	0.00	52.90	77.80	62194246	0.7
AR.N20.VII.171696	chr13	63728985	63729171	2.50	35.80	0.00	35.70	70.00	63729050	0.7
AR.N20.VII.171697	chr13	75112883	75113060	1.70	11.90	0.00	44.40	100.00	75112996	0.6
AR.N20.VII.171698	chr13	75308705	75308894	2.40	8.60	0.00	46.20	100.00	75308831	0.7
AR.N20.VII.171699	chr13	76527417	76527593	1.70	11.90	0.00	55.60	70.00	76527471	0.5
AR.N20.VII.171700	chr13	76615781	76616021	1.70	12.10	12.30	50.70	100.00	76615939	0.6
AR.N20.VII.171701	chr13	82537401	82537623	2.40	8.60	0.00	53.80	92.90	82537521	0.9
AR.N20.VII.171702	chr13	87640090	87640280	1.50	10.60	0.00	35.30	100.00	87640241	0.6
AR.N20.VII.171703	chr13	88398864	88399085	7.70	110.20	0.00	46.40	100.00	88399035	2
AR.N20.VII.171704	chr13	90691541	90691735	1.20	17.30	0.00	53.80	85.70	90691641	0.6
AR.N20.VII.171705	chr13	93391696	93391796	1.50	5.50	3.00	57.60	100.00	93391737	0.8
AR.N20.VII.171706	chr13	94718424	94718611	2.30	32.30	20.60	44.90	100.00	94718511	0.9
AR.N20.VII.171707	chr13	98544346	98544561	2.90	41.20	0.00	45.20	71.40	98544426	0.8
AR.N20.VII.171708	chr13	101917286	101917459	3.30	23.20	0.00	60.00	90.50	101917356	1
AR.N20.VII.171709	chr13	101953792	101954040	3.20	45.10	0.00	47.10	93.80	101953907	0.9
AR.N20.VII.171710	chr13	102845164	102845322	2.00	13.90	0.00	42.90	100.00	102845259	0.9
AR.N20.VII.171711	chr13	103824916	103825071	2.90	41.20	0.00	35.50	100.00	103824995	1
AR.N20.VII.171712	chr13	105266955	105267195	2.90	41.80	1.60	60.30	89.50	105267110	0.8
AR.N20.VII.171713	chr13	105546992	105547179	1.50	10.60	0.00	50.00	87.50	105547090	0.6
AR.N20.VII.171714	chr13	106187463	106187694	7.50	26.90	0.00	42.60	94.20	106187577	2.1
AR.N20.VII.171715	chr13	106717255	106717466	2.70	12.80	0.00	36.70	100.00	106717388	0.7
AR.N20.VII.171716	chr13	108846751	108846907	1.40	10.00	0.00	40.00	50.00	108846772	0.6
AR.N20.VII.171717	chr13	108959967	108960213	21.50	102.20	18.20	49.80	91.40	108960070	5.3
AR.N20.VII.171718	chr13	109465292	109465514	3.40	23.90	0.00	52.80	68.40	109465354	0.7
AR.N20.VII.171719	chr13	110076066	110076236	1.30	9.30	0.00	42.90	100.00	110076172	0.5
AR.N20.VII.171720	chr13	110698053	110698282	1.80	8.40	0.00	36.80	57.10	110698088	0.7
AR.N20.VII.171721	chr13	111076846	111077007	1.80	10.10	0.00	52.60	80.00	111076923	0.5
AR.N20.VII.171722	chr13	111109098	111109354	3.00	42.50	0.00	37.50	83.30	111109180	0.7
AR.N20.VII.171723	chr13	112100165	112100349	1.40	8.20	45.20	41.90	84.60	112100272	0.6
AR.N20.VII.171724	chr14	20221253	20221370	1.30	5.10	22.20	31.00	100.00	20221333	0.6
AR.N20.VII.171725	chr14	21141709	21141913	1.30	9.30	0.00	50.00	85.70	21141733	0.6
AR.N20.VII.171726	chr14	21206605	21206739	1.10	8.00	0.00	58.30	100.00	21206682	0.6
AR.N20.VII.171727	chr14	22099827	22100093	1.90	4.40	0.00	55.00	81.80	22099994	0.6
AR.N20.VII.171728	chr14	23434150	23434315	1.10	15.00	0.00	64.70	72.70	23434220	0.6
AR.N20.VII.171729	chr14	23516362	23516524	2.00	6.30	97.70	67.40	89.70	23516409	0.8
AR.N20.VII.171730	chr14	23559136	23559298	2.40	6.20	82.40	56.90	89.70	23559183	0.8
AR.N20.VII.171731	chr14	24493414	24493620	7.10	33.90	0.70	36.30	96.50	24493491	2.3
AR.N20.VII.171732	chr14	25161903	25162086	1.60	7.70	0.00	71.40	100.00	25161969	0.8
AR.N20.VII.171733	chr14	26638683	26638986	2.90	8.40	1.60	52.40	63.60	26638785	0.5
AR.N20.VII.171734	chr14	28491739	28492085	2.60	10.60	0.00	39.30	81.80	28491985	0.5
AR.N20.VII.171735	chr14	30525953	30526180	1.70	23.90	0.00	50.00	100.00	30526076	0.6
AR.N20.VII.171736	chr14	33029594	33029798	1.80	5.00	0.00	42.10	75.00	33029679	0.6
AR.N20.VII.171737	chr14	33793092	33793244	3.20	22.60	0.00	61.80	81.00	33793127	1.3
AR.N20.VII.171738	chr14	34918292	34918487	2.10	29.20	0.00	40.90	88.90	34918384	0.6
AR.N20.VII.171739	chr14	34942890	34943184	4.40	12.60	1.10	50.50	54.20	34942977	1
AR.N20.VII.171740	chr14	35468190	35468473	6.10	43.20	3.10	50.70	84.80	35468323	1.4
AR.N20.VII.171741	chr14	35969834	35970044	2.20	10.60	0.00	36.00	100.00	35969973	0.8
AR.N20.VII.171742	chr14	36906735	36906903	2.10	9.70	0.00	54.50	100.00	36906781	0.7
AR.N20.VII.171743	chr14	48404945	48405098	3.00	43.10	1.50	46.20	86.70	48405054	0.9
AR.N20.VII.171744	chr14	49178353	49178584	3.90	11.20	0.00	50.00	85.70	49178492	1.3
AR.N20.VII.171745	chr14	50300209	50300389	2.00	13.90	0.00	66.70	100.00	50300275	0.8
AR.N20.VII.171746	chr14	50631457	50631615	1.10	5.30	0.00	58.30	71.40	50631521	0.6
AR.N20.VII.171747	chr14	50919042	50919192	1.60	7.50	0.00	52.90	100.00	50919124	0.6
AR.N20.VII.171748	chr14	52082209	52082406	3.80	18.10	2.40	47.60	94.90	52082289	1.1
AR.N20.VII.171749	chr14	54074627	54074771	1.70	8.00	0.00	66.70	75.00	54074669	0.6
AR.N20.VII.171750	chr14	54351576	54351858	2.40	5.80	0.00	57.00	66.70	54351731	0.6
AR.N20.VII.171751	chr14	55593542	55593754	1.80	6.30	0.00	47.40	100.00	55593654	0.6
AR.N20.VII.171752	chr14	56390944	56391113	4.20	59.70	0.00	55.60	88.00	56391006	1.5
AR.N20.VII.171753	chr14	57355111	57355336	2.60	18.60	0.00	39.30	90.90	57355194	0.7
AR.N20.VII.171754	chr14	58012870	58013059	2.90	41.20	0.00	45.20	100.00	58012960	0.7
AR.N20.VII.171755	chr14	60975407	60975569	1.50	10.60	0.00	43.80	100.00	60975446	0.7
AR.N20.VII.171756	chr14	61082305	61082485	3.30	15.50	0.00	51.40	100.00	61082402	0.8
AR.N20.VII.171757	chr14	64051666	64051933	2.50	35.80	0.00	55.60	53.30	64051767	0.6
AR.N20.VII.171758	chr14	64058259	64058389	1.20	17.30	0.00	46.20	83.30	64058317	0.7
AR.N20.VII.171759	chr14	64286485	64286698	4.80	22.60	0.00	47.10	91.70	64286629	1.5
AR.N20.VII.171760	chr14	64654906	64655116	5.20	12.40	0.00	64.90	97.30	64655009	1.8
AR.N20.VII.171761	chr14	67087677	67087827	2.70	19.30	0.00	58.60	100.00	67087761	1.2
AR.N20.VII.171762	chr14	69526903	69527049	1.90	13.30	0.00	50.00	100.00	69526980	0.7
AR.N20.VII.171763	chr14	69604384	69604539	1.10	8.00	0.00	75.00	88.90	69604477	0.6
AR.N20.VII.171764	chr14	70491381	70491539	2.00	13.90	0.00	61.90	76.90	70491452	0.6
AR.N20.VII.171765	chr14	70599337	70599622	2.40	23.00	7.60	66.10	76.70	70599444	0.9

regionID	chrom	start	stop	RPM	fold	multi%	plus%	leftPlus%	peakPos	peakHeight
AR.N20.VII.171766	chr14	72673980	72674140	2.00	7.10	2.30	32.60	100.00	72674047	0.7
AR.N20.VII.171767	chr14	72823485	72823629	1.70	8.00	0.00	42.10	100.00	72823600	0.7
AR.N20.VII.171768	chr14	73197001	73197265	8.00	114.20	0.00	51.20	97.70	73197161	2.5
AR.N20.VII.171769	chr14	73291521	73291782	2.10	7.30	0.00	50.00	72.70	73291616	0.7
AR.N20.VII.171770	chr14	74790994	74791161	1.10	5.30	0.00	41.70	80.00	74791078	0.5
AR.N20.VII.171771	chr14	75072051	75072284	9.90	140.70	0.00	48.10	98.10	75072164	2.8
AR.N20.VII.171772	chr14	75102359	75102714	5.00	14.30	0.00	44.30	62.50	75102524	1
AR.N20.VII.171773	chr14	75253877	75254129	2.70	19.30	0.00	48.30	64.30	75253987	0.8
AR.N20.VII.171774	chr14	76612530	76612683	1.80	8.40	5.30	34.20	84.60	76612558	0.6
AR.N20.VII.171775	chr14	78610622	78610883	1.40	10.00	6.70	46.70	85.70	78610750	0.7
AR.N20.VII.171776	chr14	78861304	78861511	2.70	7.70	0.00	44.80	100.00	78861419	0.9
AR.N20.VII.171777	chr14	79590164	79590469	2.70	8.40	8.50	47.50	57.10	79590259	0.6
AR.N20.VII.171778	chr14	80124290	80124516	4.60	32.50	0.00	42.90	100.00	80124426	1.5
AR.N20.VII.171779	chr14	80902364	80902678	3.70	7.60	0.00	47.10	100.00	80902544	1.6
AR.N20.VII.171780	chr14	80937014	80937205	2.90	13.70	0.00	35.50	63.60	80937056	0.8
AR.N20.VII.171781	chr14	83790372	83790585	3.40	12.30	0.00	43.20	100.00	83790497	1.4
AR.N20.VII.171782	chr14	85407138	85407348	2.40	16.90	2.00	34.80	77.80	85407197	0.9
AR.N20.VII.171783	chr14	90827195	90827357	3.30	23.20	0.00	57.10	90.00	90827250	1.4
AR.N20.VII.171784	chr14	90903641	90903811	2.20	10.40	2.10	36.20	100.00	90903730	0.8
AR.N20.VII.171785	chr14	91140637	91140895	3.20	22.00	79.60	53.00	86.80	91140734	1
AR.N20.VII.171786	chr14	91624729	91624862	2.20	31.90	0.00	33.30	100.00	91624821	0.9
AR.N20.VII.171787	chr14	91845026	91845150	1.20	5.80	0.00	38.50	100.00	91845106	0.7
AR.N20.VII.171788	chr14	92255970	92256180	2.00	5.60	0.00	47.60	90.00	92256072	0.6
AR.N20.VII.171789	chr14	92523557	92523764	2.10	15.30	0.00	41.70	100.00	92523709	1.2
AR.N20.VII.171790	chr14	92579568	92579826	2.00	4.80	2.30	51.20	72.70	92579693	0.6
AR.N20.VII.171791	chr14	93932172	93932371	1.90	8.90	0.00	50.00	100.00	93932249	0.6
AR.N20.VII.171792	chr14	94101027	94101190	3.40	49.10	0.00	32.40	91.70	94101095	1.4
AR.N20.VII.171793	chr14	94135367	94135524	1.60	22.60	0.00	64.70	90.90	94135467	0.7
AR.N20.VII.171794	chr14	95423465	95423698	4.80	17.30	0.00	50.00	100.00	95423639	1.3
AR.N20.VII.171795	chr14	97840719	97841012	3.80	54.40	0.00	56.10	100.00	97840865	1.2
AR.N20.VII.171796	chr14	98728259	98728422	1.70	6.00	0.00	38.90	100.00	98728336	0.6
AR.N20.VII.171797	chr14	98894003	98894110	1.60	11.30	0.00	61.10	81.80	98894051	0.7
AR.N20.VII.171798	chr14	99011384	99011586	2.10	7.30	0.00	39.10	100.00	99011503	0.8
AR.N20.VII.171799	chr14	99115263	99115537	10.30	24.40	0.30	54.70	91.20	99115412	3.2
AR.N20.VII.171800	chr14	99221510	99221724	2.40	11.50	0.00	53.80	71.40	99221618	0.6
AR.N20.VII.171801	chr14	99503002	99503225	6.90	23.40	0.70	52.10	73.00	99503079	1.9
AR.N20.VII.171802	chr14	99576125	99576320	3.70	14.10	5.60	33.00	100.00	99576251	0.9
AR.N20.VII.171803	chr14	101041748	101041987	13.50	38.40	0.30	47.10	92.70	101041850	3.7
AR.N20.VII.171804	chr14	102941066	102941203	1.00	14.60	0.00	54.50	100.00	102941158	0.5
AR.N20.VII.171805	chr14	103061655	103061851	2.10	5.30	16.00	54.90	96.70	103061787	0.8
AR.N20.VII.171806	chr14	103156948	103157088	1.20	16.80	5.10	44.20	100.00	103157015	0.7
AR.N20.VII.171807	chr14	104120199	104120337	2.10	14.60	0.00	54.50	83.30	104120250	0.7
AR.N20.VII.171808	chr14	106325548	106325779	2.50	17.60	1.90	43.40	100.00	106325676	0.6
AR.N20.VII.171809	chr15	18897813	18898219	3.10	8.30	98.50	46.70	75.00	18898023	0.8
AR.N20.VII.171810	chr15	19146490	19146642	1.30	4.10	14.30	57.10	68.80	19146545	0.5
AR.N20.VII.171811	chr15	20390234	20390495	1.70	11.90	0.00	50.00	88.90	20390401	0.5
AR.N20.VII.171812	chr15	20856381	20857107	3.00	4.60	95.50	50.40	86.70	20856911	0.8
AR.N20.VII.171813	chr15	21200203	21200519	10.30	22.70	37.80	52.00	86.60	21200372	2.9
AR.N20.VII.171814	chr15	21342445	21342792	6.30	29.90	2.20	52.80	97.20	21342629	1.4
AR.N20.VII.171815	chr15	21395442	21395621	2.40	11.00	4.60	30.50	100.00	21395510	0.7
AR.N20.VII.171816	chr15	24424425	24424614	2.10	30.40	8.40	44.40	80.30	24424506	0.9
AR.N20.VII.171817	chr15	24425574	24425820	9.80	27.90	0.00	43.80	100.00	24425745	2.7
AR.N20.VII.171818	chr15	25317449	25317717	2.00	7.00	0.00	57.10	58.30	25317511	0.6
AR.N20.VII.171819	chr15	26126388	26126807	2.90	5.80	70.40	56.10	87.30	26126675	0.6
AR.N20.VII.171820	chr15	26705889	26706278	3.10	8.10	74.40	60.80	88.00	26706047	0.9
AR.N20.VII.171821	chr15	28361291	28361556	3.80	9.90	98.80	50.00	97.60	28361426	0.9
AR.N20.VII.171822	chr15	29579823	29579928	1.00	14.60	0.00	72.70	62.50	29579843	0.5
AR.N20.VII.171823	chr15	29583974	29584267	2.90	4.60	0.00	51.60	68.80	29584130	0.6
AR.N20.VII.171824	chr15	29891204	29891419	1.80	5.00	0.00	26.30	80.00	29891318	0.6
AR.N20.VII.171825	chr15	30055278	30055654	34.50	23.40	0.10	55.10	91.80	30055501	8
AR.N20.VII.171826	chr15	30336089	30336354	4.60	10.00	82.70	59.20	82.80	30336219	0.9
AR.N20.VII.171827	chr15	30903348	30903619	13.00	46.10	0.00	42.60	95.00	30903457	3.6
AR.N20.VII.171828	chr15	31109901	31110096	1.60	22.60	0.00	61.10	90.90	31109992	0.6
AR.N20.VII.171829	chr15	33163793	33164079	2.30	10.80	95.00	50.40	92.60	33163950	0.5
AR.N20.VII.171830	chr15	33388249	33388490	3.10	43.80	0.00	55.90	89.50	33388379	1.2
AR.N20.VII.171831	chr15	34886612	34886779	1.50	5.30	0.00	50.00	87.50	34886673	0.6
AR.N20.VII.171832	chr15	36974797	36975040	11.40	81.00	0.80	47.60	96.60	36974904	3.6
AR.N20.VII.171833	chr15	37529338	37529567	2.30	16.30	2.00	71.40	91.40	37529443	0.6
AR.N20.VII.171834	chr15	37654851	37654990	2.10	29.20	0.00	56.50	92.30	37654946	0.9
AR.N20.VII.171835	chr15	38469583	38469815	2.00	28.50	2.30	55.30	100.00	38469738	0.5
AR.N20.VII.171836	chr15	38673270	38673465	2.10	6.60	51.60	43.90	100.00	38673394	0.6
AR.N20.VII.171837	chr15	40866642	40866733	1.10	8.00	0.00	50.00	50.00	40866664	0.7
AR.N20.VII.171838	chr15	41939173	41939360	1.00	7.30	0.00	36.40	100.00	41939227	0.6
AR.N20.VII.171839	chr15	42929616	42929752	1.00	7.30	0.00	45.50	100.00	42929683	0.5
AR.N20.VII.171840	chr15	42978949	42979316	3.90	15.90	73.80	43.50	75.70	42979174	1.1
AR.N20.VII.171841	chr15	43067470	43067856	3.30	8.40	90.00	61.40	67.40	43067608	0.8
AR.N20.VII.171842	chr15	43219254	43219537	3.30	9.40	1.40	54.90	76.90	43219410	0.8
AR.N20.VII.171843	chr15	43278038	43278228	2.90	5.90	41.40	63.30	67.00	43278105	0.7
AR.N20.VII.171844	chr15	43279803	43280044	3.40	5.40	33.70	63.30	56.70	43279885	0.8
AR.N20.VII.171845	chr15	43280518	43280750	4.30	4.70	27.80	55.30	67.20	43280617	1.4
AR.N20.VII.171846	chr15	43602678	43602912	2.30	16.60	0.00	48.00	100.00	43602823	0.7
AR.N20.VII.171847	chr15	43891459	43891622	2.60	36.90	6.60	49.80	90.40	43891549	1
AR.N20.VII.171848	chr15	45256629	45256862	1.20	17.30	0.00	46.20	100.00	45256784	0.6
AR.N20.VII.171849	chr15	45853902	45854026	1.00	14.60	0.00	72.70	100.00	45853943	0.6
AR.N20.VII.171850	chr15	45980301	45980491	2.20	31.20	2.10	63.80	60.00	45980355	0.7

regionID	chrom	start	stop	RPM	fold	multi%	plus%	leftPlus%	peakPos	peakHeight
AR.N20.VII.171851	chr15	46097306	46097510	2.70	9.60	0.00	62.10	100.00	46097438	1
AR.N20.VII.171852	chr15	46586948	46587085	1.00	14.60	0.00	72.70	100.00	46587023	0.5
AR.N20.VII.171853	chr15	46861085	46861255	1.70	11.90	0.00	63.20	100.00	46861187	0.6
AR.N20.VII.171854	chr15	47155263	47155450	1.30	18.60	0.00	71.40	90.00	47155357	0.5
AR.N20.VII.171855	chr15	48324564	48324833	2.90	8.30	1.10	40.20	92.30	48324726	0.9
AR.N20.VII.171856	chr15	48581290	48581544	2.00	28.50	6.90	61.80	80.30	48581405	0.8
AR.N20.VII.171857	chr15	48751284	48751485	1.50	19.30	2.00	67.30	90.90	48751350	0.6
AR.N20.VII.171858	chr15	49574016	49574253	2.20	21.20	0.00	66.70	68.80	49574088	0.7
AR.N20.VII.171859	chr15	50150765	50150986	3.10	43.80	0.00	60.60	90.00	50150838	1
AR.N20.VII.171860	chr15	50330056	50330327	2.10	5.10	0.00	60.90	57.10	50330198	0.5
AR.N20.VII.171861	chr15	50369379	50369597	2.20	5.30	0.00	50.00	91.70	50369484	0.6
AR.N20.VII.171862	chr15	50733145	50733357	2.80	13.50	1.60	50.80	61.30	50733199	0.6
AR.N20.VII.171863	chr15	52176549	52176793	4.80	68.40	1.00	55.30	96.50	52176712	1.2
AR.N20.VII.171864	chr15	53020956	53021249	2.00	27.90	0.00	42.90	88.90	53021100	0.6
AR.N20.VII.171865	chr15	53024337	53024488	1.80	21.20	26.20	37.10	78.80	53024372	1.2
AR.N20.VII.171866	chr15	53336867	53336979	1.00	7.30	0.00	41.70	60.00	53336910	0.6
AR.N20.VII.171867	chr15	55197555	55197718	1.60	11.30	0.00	70.60	75.00	55197632	0.5
AR.N20.VII.171868	chr15	55608488	55608723	2.60	36.50	1.80	58.20	62.50	55608569	0.8
AR.N20.VII.171869	chr15	57633711	57633847	1.20	17.30	0.00	53.80	100.00	57633784	0.5
AR.N20.VII.171870	chr15	58801826	58802149	5.20	37.20	0.00	49.10	89.30	58801934	2
AR.N20.VII.171871	chr15	58993499	58993768	2.40	5.80	0.00	46.20	83.30	58993602	0.8
AR.N20.VII.171872	chr15	59279318	59279466	4.60	16.30	0.00	62.00	96.80	59279373	2
AR.N20.VII.171873	chr15	59782350	59782593	17.40	49.50	0.10	48.20	92.20	59782460	4.5
AR.N20.VII.171874	chr15	60593507	60593680	4.20	19.90	0.00	63.00	89.70	60593580	1.4
AR.N20.VII.171875	chr15	60820120	60820390	4.80	9.70	0.00	49.00	80.00	60820268	1.4
AR.N20.VII.171876	chr15	60978363	60978548	2.20	15.90	0.00	41.70	70.00	60978444	0.7
AR.N20.VII.171877	chr15	61132465	61132679	3.00	14.20	0.00	52.90	88.90	61132622	1.3
AR.N20.VII.171878	chr15	61145172	61145392	1.40	10.00	0.00	60.00	88.90	61145262	0.6
AR.N20.VII.171879	chr15	62152143	62152318	2.20	15.90	0.00	41.70	100.00	62152233	0.7
AR.N20.VII.171880	chr15	63153476	63153527	3.60	51.80	28.20	39.20	100.00	63153487	3.6
AR.N20.VII.171881	chr15	63948430	63948639	1.80	8.50	13.90	57.50	91.60	63948532	0.6
AR.N20.VII.171882	chr15	64468583	64468805	2.20	31.20	0.00	58.90	100.00	64468711	0.7
AR.N20.VII.171883	chr15	64661690	64661954	3.50	16.50	0.00	40.00	47.80	64661757	0.7
AR.N20.VII.171884	chr15	64729078	64729183	1.00	14.60	0.00	27.30	66.70	64729108	0.6
AR.N20.VII.171885	chr15	64729805	64730031	3.30	9.30	0.00	68.60	87.50	64729922	0.8
AR.N20.VII.171886	chr15	66672083	66672237	2.10	12.80	2.20	46.70	90.50	66672151	0.7
AR.N20.VII.171887	chr15	67114652	67114919	2.90	4.60	0.00	62.50	95.00	67114853	0.8
AR.N20.VII.171888	chr15	67554454	67554817	2.70	11.50	2.90	53.20	87.00	67554685	0.7
AR.N20.VII.171889	chr15	67683391	67683678	2.20	15.90	0.00	45.80	100.00	67683572	0.6
AR.N20.VII.171890	chr15	67771750	67772000	1.40	6.60	0.00	60.00	88.90	67771865	0.6
AR.N20.VII.171891	chr15	69226209	69226383	1.80	25.20	0.00	47.40	88.90	69226321	0.6
AR.N20.VII.171892	chr15	70234720	70234955	7.70	15.70	0.00	44.60	86.50	70234844	2.4
AR.N20.VII.171893	chr15	70253356	70253485	1.60	22.60	0.00	58.80	100.00	70253382	0.8
AR.N20.VII.171894	chr15	71081948	71082133	1.40	19.90	0.00	33.30	100.00	71082055	0.5
AR.N20.VII.171895	chr15	72743781	72744095	4.60	32.50	0.00	32.70	100.00	72743892	1.2
AR.N20.VII.171896	chr15	72858576	72858863	1.50	20.80	2.10	34.00	100.00	72858718	0.6
AR.N20.VII.171897	chr15	72877960	72878101	2.70	6.40	0.00	37.90	81.80	72878027	1
AR.N20.VII.171898	chr15	74652138	74652327	2.10	14.60	0.00	70.50	94.10	74652265	1
AR.N20.VII.171899	chr15	75195706	75195864	1.10	15.90	0.00	58.30	100.00	75195738	0.6
AR.N20.VII.171900	chr15	75896984	75897209	3.40	15.90	0.00	52.80	78.90	75897087	1.2
AR.N20.VII.171901	chr15	76509055	76509165	1.00	14.60	0.00	27.30	100.00	76509137	0.6
AR.N20.VII.171902	chr15	76683908	76684105	2.40	8.60	0.00	50.00	100.00	76684036	0.6
AR.N20.VII.171903	chr15	77857873	77858077	8.60	40.90	0.40	47.10	59.10	77857938	2
AR.N20.VII.171904	chr15	78985953	78986056	1.10	8.00	0.00	30.80	100.00	78986029	0.5
AR.N20.VII.171905	chr15	79467776	79468020	12.80	30.30	0.00	50.00	76.80	79467856	3.2
AR.N20.VII.171906	chr15	79484254	79484390	1.70	23.90	0.00	55.60	80.00	79484290	0.6
AR.N20.VII.171907	chr15	82123144	82123399	4.60	32.50	0.00	38.00	100.00	82123274	1.2
AR.N20.VII.171908	chr15	83637712	83637833	1.20	8.60	0.00	46.20	100.00	83637768	0.7
AR.N20.VII.171909	chr15	83675540	83675726	5.30	15.10	0.00	50.00	96.60	83675619	1.9
AR.N20.VII.171910	chr15	83876980	83877180	2.80	5.80	1.60	63.90	94.90	83877102	0.8
AR.N20.VII.171911	chr15	84359360	84359577	1.90	6.80	2.40	61.00	68.00	84359442	0.6
AR.N20.VII.171912	chr15	87462206	87462358	2.00	13.90	0.00	61.90	100.00	87462315	1.1
AR.N20.VII.171913	chr15	87474126	87474327	9.60	136.10	0.50	46.90	90.70	87474175	2.7
AR.N20.VII.171914	chr15	88156525	88156682	1.40	5.00	0.00	33.30	100.00	88156602	0.6
AR.N20.VII.171915	chr15	89204794	89204935	1.20	7.90	1.00	67.30	100.00	89204908	0.6
AR.N20.VII.171916	chr15	89386231	89386553	3.80	26.90	13.60	49.00	84.90	89386377	1
AR.N20.VII.171917	chr15	90871440	90871712	7.40	26.40	0.60	53.50	85.90	90871582	2.3
AR.N20.VII.171918	chr15	90983441	90983651	2.60	18.60	0.00	64.30	72.20	90983517	0.7
AR.N20.VII.171919	chr15	90998444	90998688	36.20	103.00	0.30	50.80	79.20	90998536	8.6
AR.N20.VII.171920	chr15	91497255	91497431	2.10	7.50	2.20	34.00	100.00	91497383	0.7
AR.N20.VII.171921	chr15	94558246	94558413	2.30	16.60	0.00	44.00	100.00	94558347	0.8
AR.N20.VII.171922	chr15	96889134	96889428	3.30	15.50	0.00	54.30	63.20	96889247	0.6
AR.N20.VII.171923	chr15	97149957	97150077	1.30	18.60	0.00	71.40	90.00	97150001	0.7
AR.N20.VII.171924	chr15	97164542	97164826	3.40	22.30	12.10	39.30	82.50	97164684	1.1
AR.N20.VII.171925	chr15	97313416	97313559	1.90	13.60	2.40	32.60	100.00	97313483	0.8
AR.N20.VII.171926	chr15	97947582	97947753	1.50	21.20	0.00	56.20	88.90	97947672	0.6
AR.N20.VII.171927	chr15	98026963	98027190	2.10	30.50	0.00	60.90	85.70	98027109	0.7
AR.N20.VII.171928	chr15	98991481	98991675	2.30	16.30	2.00	60.80	80.60	98991584	0.7
AR.N20.VII.171929	chr15	99129582	99129846	2.20	4.50	2.10	55.30	92.30	99129737	0.8
AR.N20.VII.171930	chr15	99248169	99248445	3.50	16.60	1.60	58.50	95.50	99248314	1.1
AR.N20.VII.171931	chr15	99251661	99252014	3.40	8.20	0.00	56.80	76.20	99251760	1
AR.N20.VII.171932	chr15	99255588	99256116	10.30	11.30	0.50	56.10	79.20	99255723	2.4
AR.N20.VII.171933	chr15	99635176	99635458	3.00	4.20	0.00	65.60	90.50	99635355	0.7
AR.N20.VII.171934	chr16	378481	378683	2.30	6.90	15.00	44.20	81.70	378607	0.8
AR.N20.VII.171935	chr16	680371	680529	1.20	5.80	0.00	53.80	85.70	680476	0.6

regionID	chrom	start	stop	RPM	fold	multi%	plus%	leftPlus%	peakPos	peakHeight
AR.N20.VII.171936	chr16	727733	727909	3.60	17.30	0.00	40.00	87.50	727856	1.2
AR.N20.VII.171937	chr16	1522516	1522725	2.50	6.00	0.00	44.40	100.00	1522630	0.7
AR.N20.VII.171938	chr16	1620899	1621238	5.20	10.50	0.90	43.20	50.00	1620972	0.9
AR.N20.VII.171939	chr16	1635992	1636252	2.20	5.30	0.00	62.50	73.30	1636073	0.6
AR.N20.VII.171940	chr16	2029638	2029834	2.10	7.30	0.00	27.30	100.00	2029688	0.7
AR.N20.VII.171941	chr16	2076160	2076484	6.50	6.20	0.00	42.90	56.70	2076263	1.4
AR.N20.VII.171942	chr16	2378907	2379169	6.80	10.80	12.30	61.60	91.10	2379048	1.6
AR.N20.VII.171943	chr16	3140623	3140800	1.80	5.80	43.90	55.30	85.40	3140701	0.5
AR.N20.VII.171944	chr16	3172470	3172801	2.00	6.40	14.40	48.20	100.00	3172712	0.8
AR.N20.VII.171945	chr16	3543195	3543420	3.00	12.70	3.10	68.80	100.00	3543363	1.1
AR.N20.VII.171946	chr16	3636353	3636532	1.30	4.60	0.00	50.00	85.70	3636417	0.6
AR.N20.VII.171947	chr16	3686971	3687227	2.90	8.20	0.00	54.80	76.50	3687077	0.9
AR.N20.VII.171948	chr16	4476189	4476465	2.50	7.20	0.00	37.00	80.00	4476334	0.7
AR.N20.VII.171949	chr16	4659410	4659693	3.30	9.40	0.00	43.80	81.20	4659551	0.7
AR.N20.VII.171950	chr16	4902654	4902809	1.80	8.40	0.00	31.60	100.00	4902759	0.7
AR.N20.VII.171951	chr16	6619258	6619413	2.60	18.60	0.00	67.90	100.00	6619340	1.2
AR.N20.VII.171952	chr16	8045952	8046049	1.00	14.60	0.00	45.50	80.00	8045972	0.5
AR.N20.VII.171953	chr16	8988814	8989075	3.60	10.40	0.40	46.00	88.90	8989016	1.1
AR.N20.VII.171954	chr16	9366778	9367014	5.80	20.60	0.00	53.20	78.80	9366882	1.8
AR.N20.VII.171955	chr16	10521896	10522179	10.40	37.00	0.30	47.50	90.60	10522031	3.6
AR.N20.VII.171956	chr16	14287209	14287427	3.40	5.10	15.10	39.70	48.30	14287249	1
AR.N20.VII.171957	chr16	14420167	14420534	9.10	86.30	44.10	46.20	88.00	14420335	2.6
AR.N20.VII.171958	chr16	14657864	14658068	2.80	19.90	0.00	70.00	85.70	14657934	0.9
AR.N20.VII.171959	chr16	14983983	14984222	2.40	10.50	88.30	44.10	82.60	14984085	0.6
AR.N20.VII.171960	chr16	17386576	17386842	7.40	35.00	0.10	30.50	58.50	17386680	3.4
AR.N20.VII.171961	chr16	19022719	19022887	2.20	8.00	0.00	62.50	100.00	19022798	0.8
AR.N20.VII.171962	chr16	19050370	19050558	1.70	8.00	0.00	33.30	83.30	19050452	0.6
AR.N20.VII.171963	chr16	19779201	19779482	2.80	39.80	0.00	56.70	82.40	19779375	0.7
AR.N20.VII.171964	chr16	20358669	20359098	3.40	7.50	64.70	47.10	91.30	20358951	0.7
AR.N20.VII.171965	chr16	20506433	20506816	3.70	8.00	58.10	45.80	72.20	20506583	0.8
AR.N20.VII.171966	chr16	21516689	21516900	2.00	13.90	0.00	38.10	87.50	21516814	0.5
AR.N20.VII.171967	chr16	22108852	22109101	2.10	4.20	0.00	27.30	66.70	22108938	0.6
AR.N20.VII.171968	chr16	22114506	22114687	2.60	4.80	9.60	57.80	76.00	22114568	0.8
AR.N20.VII.171969	chr16	22130969	22131150	2.50	35.80	0.00	48.10	92.30	22131037	0.7
AR.N20.VII.171970	chr16	23121945	23122065	1.30	9.30	0.00	35.70	100.00	23122011	0.6
AR.N20.VII.171971	chr16	23281449	23281731	4.00	5.70	0.00	53.50	87.00	23281620	1.4
AR.N20.VII.171972	chr16	23483879	23484058	2.50	35.80	0.00	66.70	83.30	23483960	0.8
AR.N20.VII.171973	chr16	25608043	25608302	2.80	5.70	0.00	46.70	85.70	25608164	0.7
AR.N20.VII.171974	chr16	31036756	31036950	2.50	9.00	0.00	59.30	93.80	31036855	0.9
AR.N20.VII.171975	chr16	34615927	34616265	3.70	15.00	9.00	45.90	94.60	34616120	1.1
AR.N20.VII.171976	chr16	45467956	45468171	2.10	9.70	0.00	54.50	91.70	45468080	0.8
AR.N20.VII.171977	chr16	46488993	46489137	1.50	10.90	2.80	31.10	58.50	46489064	0.9
AR.N20.VII.171978	chr16	46626509	46626746	2.70	19.30	0.00	51.70	73.30	46626583	0.6
AR.N20.VII.171979	chr16	48528700	48528901	4.20	10.00	0.50	42.40	100.00	48528834	1.3
AR.N20.VII.171980	chr16	50249310	50249560	4.60	32.50	0.00	57.10	89.30	50249442	1.8
AR.N20.VII.171981	chr16	51093469	51093640	3.90	27.90	0.00	47.60	100.00	51093582	1.4
AR.N20.VII.171982	chr16	51136765	51136939	1.80	5.00	0.00	36.80	100.00	51136902	0.6
AR.N20.VII.171983	chr16	51454444	51454684	1.90	6.60	0.00	40.00	87.50	51454597	0.8
AR.N20.VII.171984	chr16	52371528	52371745	1.40	5.10	0.00	58.10	77.80	52371664	0.5
AR.N20.VII.171985	chr16	53132302	53132431	1.70	6.00	0.00	44.40	87.50	53132323	0.9
AR.N20.VII.171986	chr16	53330887	53331031	1.70	23.90	0.00	61.90	100.00	53330964	1
AR.N20.VII.171987	chr16	55199589	55199840	3.80	4.50	0.00	50.00	85.70	55199714	1
AR.N20.VII.171988	chr16	55273578	55273763	5.00	11.80	0.90	42.30	91.50	55273677	1.6
AR.N20.VII.171989	chr16	55857601	55857765	1.90	8.90	0.00	55.00	45.50	55857636	0.6
AR.N20.VII.171990	chr16	56123670	56123924	1.50	4.20	0.00	58.80	70.00	56123708	0.5
AR.N20.VII.171991	chr16	57928943	57929144	4.00	28.20	1.20	50.60	90.70	57929040	1
AR.N20.VII.171992	chr16	62055012	62055220	3.40	24.60	0.00	56.80	81.00	62055109	1
AR.N20.VII.171993	chr16	65094525	65094783	3.30	6.70	1.40	35.20	100.00	65094699	1
AR.N20.VII.171994	chr16	65528685	65528859	12.70	90.30	0.00	46.00	96.80	65528764	4.5
AR.N20.VII.171995	chr16	66053244	66053500	2.60	6.10	1.80	61.80	70.60	66053344	0.6
AR.N20.VII.171996	chr16	66351713	66351892	1.80	25.20	0.00	31.60	83.30	66351847	0.6
AR.N20.VII.171997	chr16	66998281	66998493	2.00	7.00	0.00	52.40	100.00	66998411	0.6
AR.N20.VII.171998	chr16	67774286	67774404	1.00	14.60	0.00	63.60	85.70	67774307	0.6
AR.N20.VII.171999	chr16	67774513	67774719	1.60	7.70	2.90	51.40	100.00	67774636	0.7
AR.N20.VII.1711000	chr16	67845271	67845451	1.80	12.60	0.00	47.40	100.00	67845335	0.8
AR.N20.VII.1711001	chr16	68009409	68009596	2.10	10.20	0.00	39.10	66.70	68009455	0.8
AR.N20.VII.1711002	chr16	68649574	68649813	2.50	11.00	83.50	48.20	92.30	68649708	0.6
AR.N20.VII.1711003	chr16	69174139	69174276	1.90	6.80	2.40	58.50	91.70	69174198	0.9
AR.N20.VII.1711004	chr16	69757773	69757970	4.60	21.70	0.00	46.90	91.30	69757875	1.3
AR.N20.VII.1711005	chr16	70048259	70048410	1.90	6.60	0.00	65.00	100.00	70048369	0.9
AR.N20.VII.1711006	chr16	70185427	70185619	3.40	49.10	0.00	43.20	100.00	70185512	1.4
AR.N20.VII.1711007	chr16	70349710	70350023	2.10	9.70	0.00	43.50	90.00	70349850	0.7
AR.N20.VII.1711008	chr16	70615349	70615646	6.30	12.90	0.00	50.00	76.50	70615492	1.7
AR.N20.VII.1711009	chr16	70779942	70780134	2.90	10.30	0.00	51.60	93.80	70780034	1
AR.N20.VII.1711010	chr16	71269352	71269675	3.00	19.90	19.90	56.00	89.00	71269433	1.4
AR.N20.VII.1711011	chr16	71581532	71581819	3.30	9.30	0.00	45.70	87.50	71581704	0.8
AR.N20.VII.1711012	chr16	72055595	72055775	1.80	25.90	0.00	59.00	100.00	72055702	0.7
AR.N20.VII.1711013	chr16	74901385	74901662	4.60	13.00	0.00	51.00	96.00	74901598	1.3
AR.N20.VII.1711014	chr16	76006257	76006418	2.20	10.60	0.00	52.00	84.60	76006309	0.7
AR.N20.VII.1711015	chr16	76027082	76027278	2.30	33.20	0.00	40.00	100.00	76027198	1
AR.N20.VII.1711016	chr16	76714552	76714764	29.90	426.20	0.30	48.10	100.00	76714670	8.7
AR.N20.VII.1711017	chr16	77280550	77280762	3.10	6.30	0.00	48.50	100.00	77280682	1.1
AR.N20.VII.1711018	chr16	78479655	78479764	1.30	18.60	0.00	50.00	71.40	78479697	0.5
AR.N20.VII.1711019	chr16	79467070	79467300	3.60	17.30	0.00	53.80	76.20	79467155	1
AR.N20.VII.1711020	chr16	79572320	79572476	1.50	10.60	0.00	56.20	88.90	79572402	0.6

regionID	chrom	start	stop	RPM	fold	multi%	plus%	leftPlus%	peakPos	peakHeight
AR.N20.VII.1711021	chr16	82687867	82688038	2.40	33.90	0.00	52.90	92.60	82687941	0.9
AR.N20.VII.1711022	chr16	83041047	83041460	2.70	7.70	0.00	55.20	75.00	83041218	0.8
AR.N20.VII.1711023	chr16	83504412	83504770	6.10	23.10	1.90	57.70	78.90	83504572	1.9
AR.N20.VII.1711024	chr16	83728576	83728769	2.10	10.20	0.00	47.80	90.90	83728668	0.7
AR.N20.VII.1711025	chr16	83740771	83741075	1.30	5.70	3.30	71.40	80.60	83740931	0.6
AR.N20.VII.1711026	chr16	83940662	83940879	2.10	6.00	2.20	57.80	84.60	83940807	0.7
AR.N20.VII.1711027	chr16	84115669	84115829	4.10	11.80	1.10	56.20	88.00	84115756	1.2
AR.N20.VII.1711028	chr16	84272420	84272631	2.20	8.00	0.00	62.50	93.30	84272499	0.6
AR.N20.VII.1711029	chr16	86668451	86668708	5.70	11.60	0.00	42.60	73.10	86668600	1.5
AR.N20.VII.1711030	chr16	87143249	87143357	1.40	5.00	0.00	46.70	100.00	87143262	0.7
AR.N20.VII.1711031	chr16	87855710	87855845	1.50	10.60	0.00	50.00	100.00	87855793	0.5
AR.N20.VII.1711032	chr16	87939555	87939779	11.60	55.30	0.00	58.70	87.80	87939671	3.4
AR.N20.VII.1711033	chr17	198478	198637	6.20	29.40	0.80	57.80	97.40	198552	2.7
AR.N20.VII.1711034	chr17	284744	284904	4.70	22.10	0.00	48.00	95.80	284837	1.6
AR.N20.VII.1711035	chr17	1410692	1410883	1.70	11.90	0.00	44.40	100.00	1410772	0.7
AR.N20.VII.1711036	chr17	2986285	2986475	2.80	39.80	20.00	55.00	93.90	2986410	1.1
AR.N20.VII.1711037	chr17	3510307	3510555	10.00	35.50	0.00	51.40	87.30	3510423	3.7
AR.N20.VII.1711038	chr17	3740745	3740865	1.30	4.60	0.00	50.00	71.40	3740781	0.6
AR.N20.VII.1711039	chr17	4160300	4160470	1.90	26.60	0.00	45.00	77.80	4160324	0.7
AR.N20.VII.1711040	chr17	7072167	7072402	2.60	12.20	1.80	63.60	54.30	7072265	0.6
AR.N20.VII.1711041	chr17	7099130	7099304	17.10	121.60	0.70	59.30	80.00	7099216	4.8
AR.N20.VII.1711042	chr17	7747741	7748004	3.10	8.80	0.00	48.50	81.20	7747887	0.7
AR.N20.VII.1711043	chr17	7803650	7803875	2.40	17.30	0.00	46.20	100.00	7803766	0.7
AR.N20.VII.1711044	chr17	7876076	7876257	1.10	8.10	1.40	57.50	100.00	7876163	0.7
AR.N20.VII.1711045	chr17	7900597	7900954	6.10	14.40	1.50	43.80	66.70	7900672	1.6
AR.N20.VII.1711046	chr17	7964288	7964482	1.50	9.40	36.10	51.50	100.00	7964434	0.6
AR.N20.VII.1711047	chr17	7995881	7996066	3.30	6.60	0.00	62.90	77.30	7995930	1.2
AR.N20.VII.1711048	chr17	7998365	7998623	21.60	34.20	0.40	48.30	89.50	7998503	5.4
AR.N20.VII.1711049	chr17	8030355	8030492	1.70	4.60	46.30	48.50	77.50	8030385	0.7
AR.N20.VII.1711050	chr17	8030844	8031134	3.70	6.40	30.40	46.60	76.10	8030913	1
AR.N20.VII.1711051	chr17	8064874	8065052	2.30	7.50	35.00	38.90	100.00	8064981	1.1
AR.N20.VII.1711052	chr17	8065518	8065684	2.00	4.10	39.00	60.20	94.30	8065629	0.6
AR.N20.VII.1711053	chr17	8070632	8070791	1.20	7.60	29.70	56.70	100.00	8070733	0.6
AR.N20.VII.1711054	chr17	9529042	9529257	3.90	18.60	0.00	41.90	100.00	9529210	1.4
AR.N20.VII.1711055	chr17	9781099	9781520	17.60	20.90	0.00	57.10	80.70	9781346	4.5
AR.N20.VII.1711056	chr17	10068277	10068429	1.90	13.30	0.00	55.00	72.70	10068309	0.7
AR.N20.VII.1711057	chr17	11373952	11374138	1.90	26.60	0.00	59.10	61.50	11374044	0.7
AR.N20.VII.1711058	chr17	11830668	11830865	1.20	8.60	0.00	71.40	80.00	11830728	0.7
AR.N20.VII.1711059	chr17	11938476	11938658	2.60	37.20	0.00	53.60	73.30	11938576	0.8
AR.N20.VII.1711060	chr17	13003976	13004144	1.80	25.20	0.00	57.90	100.00	13004090	0.7
AR.N20.VII.1711061	chr17	13834172	13834326	3.80	18.10	0.00	65.90	66.70	13834249	1.3
AR.N20.VII.1711062	chr17	13897307	13897489	2.00	27.90	0.00	54.50	100.00	13897443	0.7
AR.N20.VII.1711063	chr17	14050129	14050385	3.10	4.90	0.00	45.50	80.00	14050213	0.7
AR.N20.VII.1711064	chr17	14763363	14763551	5.50	15.50	0.90	52.90	87.30	14763439	2.4
AR.N20.VII.1711065	chr17	15259194	15259346	1.10	8.00	0.00	50.00	83.30	15259247	0.7
AR.N20.VII.1711066	chr17	15975735	15975981	6.50	23.10	0.70	46.80	100.00	15975895	1.6
AR.N20.VII.1711067	chr17	16312565	16312738	2.00	9.30	0.00	47.60	100.00	16312668	0.7
AR.N20.VII.1711068	chr17	16862677	16862953	11.10	17.60	0.00	37.50	82.20	16862790	2.6
AR.N20.VII.1711069	chr17	17045372	17045703	3.10	4.90	1.00	30.00	90.00	17045486	0.7
AR.N20.VII.1711070	chr17	17250357	17250591	5.40	8.60	0.00	56.90	75.80	17250474	1.7
AR.N20.VII.1711071	chr17	17335790	17336079	5.20	21.20	0.00	33.90	94.70	17335977	1.8
AR.N20.VII.1711072	chr17	17827547	17827809	6.20	14.80	0.00	46.30	80.60	17827708	1.6
AR.N20.VII.1711073	chr17	19352028	19352173	3.40	7.80	9.10	50.30	100.00	19352146	1.1
AR.N20.VII.1711074	chr17	19474180	19474343	2.30	33.20	0.00	56.00	92.90	19474254	1.1
AR.N20.VII.1711075	chr17	19781619	19781710	1.30	9.00	3.70	33.30	100.00	19781653	0.6
AR.N20.VII.1711076	chr17	20135766	20136106	3.40	11.90	0.00	58.30	61.90	20135904	0.9
AR.N20.VII.1711077	chr17	20844116	20844321	1.90	8.90	0.00	52.40	72.70	20844223	0.8
AR.N20.VII.1711078	chr17	22598502	22598847	2.70	4.30	0.00	55.20	75.00	22598711	0.7
AR.N20.VII.1711079	chr17	22672813	22673007	2.50	35.80	0.00	59.30	100.00	22672868	0.7
AR.N20.VII.1711080	chr17	22766254	22766478	2.00	27.90	9.50	54.80	69.60	22766359	0.5
AR.N20.VII.1711081	chr17	23426547	23426707	2.20	8.00	0.00	70.80	82.40	23426615	0.8
AR.N20.VII.1711082	chr17	24979238	24979350	1.70	23.90	0.00	42.10	87.50	24979304	0.7
AR.N20.VII.1711083	chr17	26901067	26901498	3.80	5.70	14.60	50.00	70.70	26901270	1
AR.N20.VII.1711084	chr17	27979371	27979549	1.30	9.30	0.00	50.00	85.70	27979473	0.7
AR.N20.VII.1711085	chr17	32705572	32705732	1.50	11.00	3.00	66.70	63.60	32705590	0.7
AR.N20.VII.1711086	chr17	34161551	34161715	1.70	6.10	30.50	36.70	100.00	34161629	0.7
AR.N20.VII.1711087	chr17	35484971	35485176	4.60	11.20	0.00	67.30	87.90	35485059	1.2
AR.N20.VII.1711088	chr17	35920075	35920328	4.30	7.60	0.00	56.50	92.30	35920237	1.3
AR.N20.VII.1711089	chr17	36674381	36674681	3.40	12.10	1.40	39.70	100.00	36674569	1
AR.N20.VII.1711090	chr17	37946674	37947020	2.90	5.10	0.00	48.40	80.00	37946843	0.9
AR.N20.VII.1711091	chr17	38390062	38390297	3.40	24.20	0.00	54.80	60.00	38390141	0.9
AR.N20.VII.1711092	chr17	39509749	39509975	11.80	55.90	0.30	50.70	98.40	39509904	3.1
AR.N20.VII.1711093	chr17	41542944	41543173	1.70	11.90	0.00	55.60	90.00	41543085	0.6
AR.N20.VII.1711094	chr17	42227036	42227167	1.90	13.30	0.00	70.00	85.70	42227093	0.9
AR.N20.VII.1711095	chr17	43387966	43388197	5.60	16.10	2.50	48.00	72.90	43388061	1.1
AR.N20.VII.1711096	chr17	43916293	43916470	2.60	36.50	0.00	35.10	100.00	43916413	1
AR.N20.VII.1711097	chr17	44251062	44251379	6.00	12.10	0.00	45.30	82.80	44251146	1.6
AR.N20.VII.1711098	chr17	44823520	44823750	4.00	57.10	0.00	58.10	96.00	44823645	1.3
AR.N20.VII.1711099	chr17	44836241	44836403	1.50	7.10	0.00	56.20	88.90	44836376	0.6
AR.N20.VII.1711100	chr17	46196486	46196706	2.40	11.50	0.00	50.00	61.50	46196545	0.6
AR.N20.VII.1711101	chr17	46341748	46341917	4.00	57.10	0.00	37.20	75.00	46341794	1.1
AR.N20.VII.1711102	chr17	51040067	51040303	6.70	19.10	0.00	44.40	87.50	51040186	2
AR.N20.VII.1711103	chr17	51163315	51163475	2.00	13.90	0.00	42.90	88.90	51163366	0.7
AR.N20.VII.1711104	chr17	51605097	51605395	2.60	7.40	0.00	35.70	50.00	51605170	0.6
AR.N20.VII.1711105	chr17	52240946	52241194	10.80	154.00	0.00	54.30	98.40	52241080	4.4

regionID	chrom	start	stop	RPM	fold	multi%	plus%	leftPlus%	peakPos	peakHeight
AR.N20.VII.1711106	chr17	52508289	52508473	3.00	21.20	0.00	43.80	85.70	52508332	1.1
AR.N20.VII.1711107	chr17	52647803	52647944	1.30	8.50	8.00	59.70	100.00	52647869	0.7
AR.N20.VII.1711108	chr17	53333816	53334083	1.70	6.00	0.00	38.90	57.10	53333941	0.5
AR.N20.VII.1711109	chr17	53455468	53455750	3.10	14.60	0.00	69.70	73.90	53455591	0.7
AR.N20.VII.1711110	chr17	55301667	55301832	2.10	29.20	0.00	66.70	87.50	55301719	0.7
AR.N20.VII.1711111	chr17	56723751	56723960	2.10	15.30	0.00	47.80	72.70	56723829	0.6
AR.N20.VII.1711112	chr17	56864141	56864456	2.60	18.80	1.20	50.60	48.80	56864243	0.7
AR.N20.VII.1711113	chr17	56943660	56943870	4.70	33.20	2.00	66.00	90.90	56943755	1.8
AR.N20.VII.1711114	chr17	58156959	58157212	16.10	38.10	0.20	48.90	85.90	58157072	4
AR.N20.VII.1711115	chr17	58470600	58470780	4.10	9.80	1.10	44.90	85.00	58470705	1.3
AR.N20.VII.1711116	chr17	59269690	59269939	11.00	31.40	0.10	44.00	90.40	59269796	3.6
AR.N20.VII.1711117	chr17	62102672	62102908	3.30	7.70	0.00	45.70	100.00	62102790	0.8
AR.N20.VII.1711118	chr17	62199192	62199290	1.40	19.90	0.00	33.30	100.00	62199237	0.9
AR.N20.VII.1711119	chr17	62395569	62395862	4.90	35.20	0.00	50.90	81.50	62395712	1.2
AR.N20.VII.1711120	chr17	63886365	63886687	3.60	8.60	0.00	64.10	80.00	63886584	0.7
AR.N20.VII.1711121	chr17	63937886	63938150	1.80	25.20	0.00	36.80	71.40	63938014	0.6
AR.N20.VII.1711122	chr17	64747712	64747973	1.30	9.30	0.00	64.30	88.90	64747869	0.6
AR.N20.VII.1711123	chr17	64969927	64970183	2.10	15.30	0.00	56.50	100.00	64970144	0.5
AR.N20.VII.1711124	chr17	64987919	64988176	3.90	18.60	0.00	31.00	76.90	64988058	1
AR.N20.VII.1711125	chr17	65068761	65068992	1.40	10.30	3.20	32.30	80.00	65068864	0.5
AR.N20.VII.1711126	chr17	67417883	67418117	3.10	43.80	1.50	59.10	79.50	67417961	1
AR.N20.VII.1711127	chr17	67659274	67659502	1.40	10.00	0.00	53.30	100.00	67659375	0.6
AR.N20.VII.1711128	chr17	68723294	68723557	5.70	13.60	0.00	53.90	57.80	68723375	1.7
AR.N20.VII.1711129	chr17	68867733	68867944	3.20	6.40	0.00	47.10	68.80	68867799	1
AR.N20.VII.1711130	chr17	68934983	68935242	3.50	14.90	1.30	44.00	100.00	68935141	0.8
AR.N20.VII.1711131	chr17	69041003	69041323	3.50	7.20	0.00	47.40	72.20	69041166	1
AR.N20.VII.1711132	chr17	70266122	70266334	11.10	26.40	0.40	46.40	100.00	70266221	4.1
AR.N20.VII.1711133	chr17	71507644	71507959	5.20	6.20	0.00	44.60	72.00	71507779	1.1
AR.N20.VII.1711134	chr17	71665248	71665462	2.40	17.30	0.00	42.30	100.00	71665354	0.8
AR.N20.VII.1711135	chr17	71681795	71682065	2.40	17.30	0.00	50.00	53.80	71681900	0.5
AR.N20.VII.1711136	chr17	71704419	71704677	7.60	27.20	0.00	50.00	90.20	71704550	1.7
AR.N20.VII.1711137	chr17	73622719	73622987	21.80	38.80	0.60	53.10	84.00	73622801	6.5
AR.N20.VII.1711138	chr17	74506487	74506742	2.60	4.60	1.80	56.40	87.10	74506572	0.7
AR.N20.VII.1711139	chr17	75657135	75657455	9.80	17.40	0.00	50.90	77.80	75657243	2.2
AR.N20.VII.1711140	chr17	76887409	76887594	1.90	13.40	0.70	55.30	100.00	76887540	0.6
AR.N20.VII.1711141	chr17	77657570	77657840	2.10	4.40	0.00	56.50	53.80	77657696	0.5
AR.N20.VII.1711142	chr17	77665214	77665408	5.10	14.60	0.00	42.90	95.80	77665335	1.7
AR.N20.VII.1711143	chr17	77703801	77704053	11.60	13.80	0.00	45.20	94.70	77703923	3.7
AR.N20.VII.1711144	chr17	77977418	77977619	1.80	5.00	0.00	57.90	81.80	77977506	0.7
AR.N20.VII.1711145	chr17	78045779	78046091	2.50	6.90	36.60	57.30	57.80	78045894	0.6
AR.N20.VII.1711146	chr18	1454476	1454609	1.10	15.90	0.00	50.00	100.00	1454530	0.6
AR.N20.VII.1711147	chr18	2523176	2523326	2.70	38.50	0.00	51.70	66.70	2523196	0.9
AR.N20.VII.1711148	chr18	2938265	2938459	2.10	7.30	0.00	27.30	100.00	2938357	0.7
AR.N20.VII.1711149	chr18	5236152	5236377	2.00	9.50	2.30	74.40	93.80	5236316	0.6
AR.N20.VII.1711150	chr18	7626131	7626234	1.10	5.30	0.00	66.70	100.00	7626179	0.7
AR.N20.VII.1711151	chr18	8130207	8130381	1.40	6.60	0.00	40.00	100.00	8130299	0.5
AR.N20.VII.1711152	chr18	8324058	8324256	1.80	12.60	0.00	45.00	77.80	8324157	0.7
AR.N20.VII.1711153	chr18	8331723	8331918	1.40	10.00	0.00	60.00	77.80	8331788	0.6
AR.N20.VII.1711154	chr18	8694033	8694411	4.70	16.60	0.00	56.00	85.70	8694262	1.2
AR.N20.VII.1711155	chr18	9707686	9707849	2.80	13.40	0.80	40.50	75.50	9707753	0.9
AR.N20.VII.1711156	chr18	10031240	10031505	1.50	7.70	16.80	26.70	72.00	10031293	0.5
AR.N20.VII.1711157	chr18	10716622	10716791	4.00	12.70	2.30	50.60	81.80	10716692	1.4
AR.N20.VII.1711158	chr18	11742741	11742892	2.50	35.80	0.00	66.70	94.40	11742826	1.1
AR.N20.VII.1711159	chr18	11846510	11846653	1.20	8.60	0.00	35.70	100.00	11846609	0.5
AR.N20.VII.1711160	chr18	11966577	11966889	3.20	12.80	1.00	57.30	100.00	11966848	0.6
AR.N20.VII.1711161	chr18	12579515	12579617	1.00	7.30	0.00	36.40	75.00	12579575	0.5
AR.N20.VII.1711162	chr18	13117263	13117563	6.90	9.40	0.00	58.70	68.20	13117359	1.7
AR.N20.VII.1711163	chr18	13816696	13816849	2.10	29.20	0.00	63.60	57.10	13816722	0.7
AR.N20.VII.1711164	chr18	14079797	14080009	6.20	22.20	0.00	65.70	68.20	14079891	2.1
AR.N20.VII.1711165	chr18	14925664	14925945	4.00	9.30	21.40	41.00	66.20	14925773	0.9
AR.N20.VII.1711166	chr18	17855702	17855977	3.20	6.40	0.00	52.90	88.90	17855791	1.1
AR.N20.VII.1711167	chr18	17881543	17881776	3.20	15.00	0.00	41.20	92.90	17881689	1
AR.N20.VII.1711168	chr18	18289550	18289715	1.80	12.60	0.00	42.10	100.00	18289662	0.7
AR.N20.VII.1711169	chr18	18319772	18320039	9.10	21.70	0.00	56.10	90.90	18319932	2.6
AR.N20.VII.1711170	chr18	19072125	19072358	2.40	34.50	0.00	61.50	68.80	19072207	0.6
AR.N20.VII.1711171	chr18	19446430	19446573	2.10	30.50	0.00	60.90	92.90	19446516	0.9
AR.N20.VII.1711172	chr18	19518645	19519084	3.50	25.20	0.00	39.50	60.00	19518789	0.5
AR.N20.VII.1711173	chr18	19559879	19560105	2.50	11.90	0.00	55.60	86.70	19559967	1
AR.N20.VII.1711174	chr18	19660108	19660335	2.40	17.30	0.00	38.50	80.00	19660131	0.7
AR.N20.VII.1711175	chr18	20097197	20097355	1.30	18.60	0.00	57.10	87.50	20097231	0.6
AR.N20.VII.1711176	chr18	20470859	20471047	3.20	11.30	0.00	61.80	100.00	20470960	1
AR.N20.VII.1711177	chr18	22579328	22579598	7.80	37.20	0.00	59.50	62.00	22579438	1.8
AR.N20.VII.1711178	chr18	22891399	22891724	3.00	10.60	0.00	62.50	70.00	22891558	0.8
AR.N20.VII.1711179	chr18	26845486	26845655	1.10	7.60	4.30	56.00	100.00	26845574	0.5
AR.N20.VII.1711180	chr18	27203575	27203694	1.80	26.00	2.50	27.20	82.20	27203592	0.7
AR.N20.VII.1711181	chr18	29761386	29761524	1.20	8.60	0.00	46.20	100.00	29761441	0.6
AR.N20.VII.1711182	chr18	31304494	31304791	7.80	18.60	0.00	47.60	87.50	31304667	1.6
AR.N20.VII.1711183	chr18	31931115	31931351	1.80	25.70	1.70	36.20	100.00	31931210	0.5
AR.N20.VII.1711184	chr18	34630841	34631014	2.80	39.80	0.00	30.00	88.90	34630900	0.9
AR.N20.VII.1711185	chr18	36996260	36996463	2.40	6.90	0.00	66.70	83.30	36996373	0.8
AR.N20.VII.1711186	chr18	37172294	37172628	3.10	44.50	1.50	55.20	100.00	37172573	0.8
AR.N20.VII.1711187	chr18	40404959	40405085	1.40	6.60	0.00	53.30	100.00	40405054	0.7
AR.N20.VII.1711188	chr18	40530959	40531173	1.80	8.40	0.00	52.60	60.00	40531011	0.7
AR.N20.VII.1711189	chr18	41554838	41554936	1.20	8.60	0.00	57.10	87.50	41554870	0.7
AR.N20.VII.1711190	chr18	43299756	43300045	2.60	9.30	0.00	60.70	88.20	43299929	0.8

regionID	chrom	start	stop	RPM	fold	multi%	plus%	leftPlus%	peakPos	peakHeight
AR.N20.VII.1711191	chr18	43364882	43365062	3.70	6.60	0.00	52.50	95.20	43364964	1.1
AR.N20.VII.1711192	chr18	43842277	43842445	3.60	17.30	0.00	43.60	100.00	43842366	1.4
AR.N20.VII.1711193	chr18	43982998	43983219	2.20	4.60	0.00	50.00	58.30	43983067	0.6
AR.N20.VII.1711194	chr18	44137600	44137779	6.00	42.50	0.00	57.60	92.10	44137689	2.1
AR.N20.VII.1711195	chr18	44451260	44451364	1.00	7.30	0.00	36.40	100.00	44451332	0.6
AR.N20.VII.1711196	chr18	44514322	44514516	3.40	23.90	0.00	55.60	100.00	44514422	1.1
AR.N20.VII.1711197	chr18	50206516	50206682	5.60	40.20	0.80	36.60	100.00	50206603	2.2
AR.N20.VII.1711198	chr18	50775655	50775843	1.30	9.30	0.00	49.60	85.70	50775751	0.6
AR.N20.VII.1711199	chr18	53895682	53895773	1.10	15.90	0.00	66.70	100.00	53895699	0.7
AR.N20.VII.1711200	chr18	54104047	54104211	2.00	27.90	0.00	57.10	83.30	54104104	0.9
AR.N20.VII.1711201	chr18	54368146	54368482	9.20	21.80	0.50	44.20	79.50	54368248	3.1
AR.N20.VII.1711202	chr18	54370502	54370657	1.20	5.50	4.00	40.00	100.00	54370601	0.5
AR.N20.VII.1711203	chr18	54873212	54873513	4.40	15.60	0.00	52.10	52.00	54873322	0.9
AR.N20.VII.1711204	chr18	55790402	55790570	2.00	8.00	19.00	47.70	100.00	55790510	0.8
AR.N20.VII.1711205	chr18	57741034	57741215	3.40	8.20	13.50	54.10	100.00	57741138	0.7
AR.N20.VII.1711206	chr18	58319233	58319424	4.70	66.40	0.00	41.20	100.00	58319319	1.9
AR.N20.VII.1711207	chr18	66595814	66595989	1.20	6.90	0.00	53.80	100.00	66595896	0.7
AR.N20.VII.1711208	chr18	68006790	68007003	2.80	20.20	4.90	56.60	81.20	68006837	1
AR.N20.VII.1711209	chr18	69008086	69008262	2.40	17.30	0.00	38.50	90.00	69008149	0.9
AR.N20.VII.1711210	chr18	69551764	69551877	1.20	17.30	0.00	46.20	66.70	69551783	0.6
AR.N20.VII.1711211	chr18	69574484	69574920	4.30	61.70	1.10	53.80	76.00	69574724	0.7
AR.N20.VII.1711212	chr18	70100889	70101081	7.40	35.00	0.00	46.80	100.00	70100991	2.6
AR.N20.VII.1711213	chr18	70360596	70360782	1.90	13.30	0.00	35.00	100.00	70360708	0.6
AR.N20.VII.1711214	chr18	74872528	74872702	3.00	10.60	0.00	43.10	92.90	74872599	0.8
AR.N20.VII.1711215	chr18	75352270	75352473	1.60	4.60	1.40	42.00	100.00	75352383	0.6
AR.N20.VII.1711216	chr19	1334323	1334653	3.10	4.70	25.60	59.40	87.60	1334561	0.9
AR.N20.VII.1711217	chr19	1824789	1825031	2.00	4.80	0.00	58.10	76.00	1824883	0.6
AR.N20.VII.1711218	chr19	1983343	1983601	2.10	7.50	2.20	71.10	75.00	1983488	0.6
AR.N20.VII.1711219	chr19	2044408	2044539	2.40	11.90	51.00	72.50	94.60	2044507	1.1
AR.N20.VII.1711220	chr19	2097053	2097232	1.50	10.60	0.00	50.00	100.00	2097171	0.6
AR.N20.VII.1711221	chr19	2479825	2480083	2.50	7.20	0.00	63.00	76.50	2479916	0.7
AR.N20.VII.1711222	chr19	2495045	2495353	5.00	9.00	0.00	37.00	80.00	2495126	1.3
AR.N20.VII.1711223	chr19	3287781	3287979	3.60	5.80	0.00	41.00	81.20	3287908	1.2
AR.N20.VII.1711224	chr19	3380769	3380947	6.10	28.90	0.40	39.80	69.20	3380835	1.7
AR.N20.VII.1711225	chr19	4942647	4942875	18.80	66.90	1.80	51.60	96.30	4942763	5.7
AR.N20.VII.1711226	chr19	4942998	4943394	16.20	37.40	0.30	45.50	96.20	4943160	3.4
AR.N20.VII.1711227	chr19	5220173	5220493	5.20	7.40	1.80	44.60	76.00	5220357	1.6
AR.N20.VII.1711228	chr19	5572317	5572575	1.90	13.30	0.00	55.00	90.90	5572447	0.6
AR.N20.VII.1711229	chr19	5756884	5757058	2.10	6.10	0.00	60.90	92.90	5756978	0.9
AR.N20.VII.1711230	chr19	6744597	6744798	2.40	11.30	5.90	60.80	74.20	6744696	0.6
AR.N20.VII.1711231	chr19	7279472	7279821	4.50	32.30	94.90	41.70	74.20	7279682	1
AR.N20.VII.1711232	chr19	8345064	8345489	2.90	5.50	3.60	49.70	71.20	8345264	0.5
AR.N20.VII.1711233	chr19	10737153	10737380	2.40	8.60	0.00	42.30	81.80	10737243	0.9
AR.N20.VII.1711234	chr19	12963049	12963431	18.30	15.30	0.70	50.20	84.90	12963277	3.8
AR.N20.VII.1711235	chr19	15467062	15467314	4.00	18.80	1.20	43.50	100.00	15467196	1.4
AR.N20.VII.1711236	chr19	16335068	16335226	2.60	12.40	0.00	42.90	83.30	16335169	1.1
AR.N20.VII.1711237	chr19	16705828	16706049	3.40	8.20	0.00	45.90	100.00	16705974	1
AR.N20.VII.1711238	chr19	16834455	16834695	2.30	6.60	0.00	68.00	82.40	16834553	0.9
AR.N20.VII.1711239	chr19	16958191	16958380	3.40	23.90	0.00	55.60	60.00	16958273	0.9
AR.N20.VII.1711240	chr19	18669591	18670961	24.90	4.90	16.50	44.60	73.90	18670644	1.8
AR.N20.VII.1711241	chr19	23797542	23797738	1.50	21.90	3.00	45.50	100.00	23797667	0.6
AR.N20.VII.1711242	chr19	35335402	35335677	4.40	12.50	0.00	46.30	77.30	35335530	1.5
AR.N20.VII.1711243	chr19	35488392	35488472	1.30	17.80	62.70	62.70	100.00	35488441	1.2
AR.N20.VII.1711244	chr19	38093687	38093870	1.50	10.70	6.90	64.90	80.20	38093773	0.7
AR.N20.VII.1711245	chr19	39493364	39493648	5.30	12.60	0.00	49.10	82.10	39493479	1.1
AR.N20.VII.1711246	chr19	39640761	39640966	1.90	8.90	0.00	50.00	100.00	39640877	0.6
AR.N20.VII.1711247	chr19	39654853	39655030	1.20	8.70	1.30	53.20	85.70	39654918	0.6
AR.N20.VII.1711248	chr19	40613309	40613446	1.20	17.70	15.20	53.60	100.00	40613412	0.8
AR.N20.VII.1711249	chr19	43473341	43473549	1.30	9.30	0.00	57.10	100.00	43473522	0.5
AR.N20.VII.1711250	chr19	43558291	43558504	4.20	59.70	0.00	53.30	100.00	43558393	1.4
AR.N20.VII.1711251	chr19	43632280	43632399	1.60	22.80	1.00	70.90	98.60	43632319	1.1
AR.N20.VII.1711252	chr19	45447580	45447707	1.50	4.20	0.00	56.20	44.40	45447600	0.6
AR.N20.VII.1711253	chr19	45659706	45659999	4.70	9.50	2.00	33.00	84.80	45659802	1.5
AR.N20.VII.1711254	chr19	45832227	45832393	1.80	5.00	0.00	68.40	76.90	45832316	0.6
AR.N20.VII.1711255	chr19	48890691	48890931	5.00	35.50	0.90	54.20	79.30	48890758	1.7
AR.N20.VII.1711256	chr19	50938142	50938431	7.00	49.80	0.00	57.30	76.70	50938268	1.3
AR.N20.VII.1711257	chr19	51496054	51496236	2.60	12.40	3.60	64.30	77.80	51496150	1
AR.N20.VII.1711258	chr19	52171644	52171868	1.80	8.40	0.00	50.00	100.00	52171787	0.7
AR.N20.VII.1711259	chr19	54311756	54312033	2.20	10.60	0.00	45.80	100.00	54311947	0.7
AR.N20.VII.1711260	chr19	55205354	55205548	1.40	6.60	0.00	73.30	100.00	55205457	0.6
AR.N20.VII.1711261	chr19	56045855	56046158	3.00	14.20	3.10	48.50	87.50	56046095	0.7
AR.N20.VII.1711262	chr19	56068199	56068406	1.80	5.00	5.30	73.70	100.00	56068339	0.7
AR.N20.VII.1711263	chr19	56084739	56085045	3.80	18.00	1.80	44.80	54.80	56084865	0.7
AR.N20.VII.1711264	chr19	56266160	56266437	2.20	15.00	11.20	65.30	100.00	56266390	0.7
AR.N20.VII.1711265	chr19	57155598	57155853	1.90	8.30	18.60	44.10	50.40	57155621	0.8
AR.N20.VII.1711266	chr19	60879696	60879898	7.50	35.80	0.00	44.40	83.30	60879758	2.3
AR.N20.VII.1711267	chr19	61159697	61159877	1.40	19.30	0.00	37.90	45.50	61159710	0.5
AR.N20.VII.1711268	chr19	62565688	62565875	1.30	18.60	0.00	50.00	100.00	62565837	0.6
AR.N20.VII.1711269	chr19	62708111	62708599	4.10	7.30	71.50	55.50	77.40	62708365	1.1
AR.N20.VII.1711270	chr19	63518137	63518285	1.30	17.90	40.70	48.10	84.60	63518163	0.5
AR.N20.VII.1711271	chr19_random	256643	256748	2.30	32.30	0.00	42.10	80.60	256691	1
AR.N20.VII.1711272	chr1_random	1237434	1237673	2.20	15.90	97.90	39.60	94.70	1237577	0.6
AR.N20.VII.1711273	chr2	548944	549139	1.50	21.20	0.00	37.50	100.00	549031	0.7
AR.N20.VII.1711274	chr2	1614756	1614919	1.50	21.20	0.00	43.80	100.00	1614839	0.6
AR.N20.VII.1711275	chr2	1669567	1669903	5.00	17.90	0.00	51.90	75.00	1669768	1.3

regionID	chrom	start	stop	RPM	fold	multi%	plus%	leftPlus%	peakPos	peakHeight
AR.N20.VII.1711276	chr2	3452967	3453340	12.90	18.30	0.00	51.40	81.70	3453073	3.6
AR.N20.VII.1711277	chr2	3849309	3849562	6.40	22.90	1.40	57.90	46.90	3849418	1.7
AR.N20.VII.1711278	chr2	5169340	5169533	3.60	51.10	1.30	64.60	88.20	5169434	1.2
AR.N20.VII.1711279	chr2	7089387	7089946	4.50	4.80	6.40	50.40	100.00	7089681	0.7
AR.N20.VII.1711280	chr2	8283141	8283283	1.30	9.30	0.00	53.30	100.00	8283256	0.7
AR.N20.VII.1711281	chr2	9058633	9059068	9.20	23.30	4.80	48.80	91.00	9058941	2.5
AR.N20.VII.1711282	chr2	10328305	10328533	1.90	6.60	0.00	52.40	54.50	10328394	0.6
AR.N20.VII.1711283	chr2	10463744	10463908	1.40	19.90	0.00	53.30	62.50	10463820	0.5
AR.N20.VII.1711284	chr2	10509968	10510149	1.70	4.80	0.00	61.10	54.50	10510039	0.7
AR.N20.VII.1711285	chr2	11597008	11597334	4.60	10.80	0.00	38.80	68.40	11597147	0.9
AR.N20.VII.1711286	chr2	16784938	16785134	2.20	4.60	0.00	44.00	81.80	16785052	0.8
AR.N20.VII.1711287	chr2	16988404	16988602	1.60	7.50	0.00	41.20	85.70	16988534	0.7
AR.N20.VII.1711288	chr2	17381286	17381491	2.00	13.90	0.00	42.90	88.90	17381418	0.6
AR.N20.VII.1711289	chr2	17840206	17840435	1.80	25.20	0.00	63.20	91.70	17840318	0.7
AR.N20.VII.1711290	chr2	17917757	17917939	1.60	7.50	0.00	44.40	100.00	17917885	0.6
AR.N20.VII.1711291	chr2	18845236	18845491	3.10	43.80	0.00	39.40	69.20	18845339	0.7
AR.N20.VII.1711292	chr2	19189993	19190163	2.10	9.70	0.00	50.00	90.90	19190094	0.7
AR.N20.VII.1711293	chr2	19539683	19539946	1.60	11.30	0.00	41.20	57.10	19539750	0.7
AR.N20.VII.1711294	chr2	20918756	20918987	2.30	11.10	0.00	50.00	84.60	20918866	1.1
AR.N20.VII.1711295	chr2	23015848	23015997	2.10	30.50	0.00	52.20	91.70	23015905	1
AR.N20.VII.1711296	chr2	23484740	23485035	2.50	11.90	0.00	48.10	84.60	23484933	0.7
AR.N20.VII.1711297	chr2	23822136	23822407	2.40	11.50	0.00	46.20	75.00	23822245	0.6
AR.N20.VII.1711298	chr2	26848788	26848996	3.10	21.90	0.00	45.50	100.00	26848929	0.8
AR.N20.VII.1711299	chr2	27127083	27127291	2.20	4.70	19.00	57.10	63.40	27127149	0.6
AR.N20.VII.1711300	chr2	27127562	27127684	1.80	9.00	41.80	47.60	100.00	27127644	0.7
AR.N20.VII.1711301	chr2	28147658	28147884	3.10	44.50	1.50	28.40	100.00	28147752	1.1
AR.N20.VII.1711302	chr2	28822979	28823121	2.70	38.50	0.00	50.00	100.00	28823083	1.1
AR.N20.VII.1711303	chr2	30294315	30294618	3.10	11.00	0.00	57.60	57.90	30294447	0.7
AR.N20.VII.1711304	chr2	30716308	30716467	1.90	26.60	0.00	45.00	77.80	30716331	0.6
AR.N20.VII.1711305	chr2	31396211	31396440	2.90	41.20	0.00	58.10	83.30	31396264	0.7
AR.N20.VII.1711306	chr2	33652889	33653073	1.10	15.30	4.30	30.40	100.00	33652965	0.6
AR.N20.VII.1711307	chr2	35877861	35878011	1.70	11.90	0.00	55.60	90.00	35877940	0.7
AR.N20.VII.1711308	chr2	38219699	38219987	3.50	12.60	0.00	42.10	93.80	38219867	0.9
AR.N20.VII.1711309	chr2	42957013	42957210	3.60	17.00	1.30	49.40	100.00	42957172	0.8
AR.N20.VII.1711310	chr2	46105876	46106005	1.50	10.60	0.00	50.00	100.00	46105978	0.5
AR.N20.VII.1711311	chr2	46947574	46947764	2.70	19.30	0.00	58.60	76.50	46947665	1.1
AR.N20.VII.1711312	chr2	58161845	58162001	2.20	31.90	0.00	50.00	91.70	58161889	0.7
AR.N20.VII.1711313	chr2	62505643	62505884	1.90	5.30	0.00	55.00	63.60	62505760	0.7
AR.N20.VII.1711314	chr2	64987615	64987796	1.20	6.20	3.80	48.10	68.40	64987644	0.5
AR.N20.VII.1711315	chr2	67400097	67400260	1.40	19.90	0.00	60.00	100.00	67400227	0.6
AR.N20.VII.1711316	chr2	67527360	67527562	2.60	18.60	0.00	50.00	71.40	67527432	0.9
AR.N20.VII.1711317	chr2	67642279	67642486	2.90	20.60	0.00	51.60	87.50	67642363	1
AR.N20.VII.1711318	chr2	70595423	70595628	4.30	8.70	0.00	45.70	81.00	70595501	1.1
AR.N20.VII.1711319	chr2	71780932	71781090	3.40	49.10	0.00	51.40	78.90	71780990	1.3
AR.N20.VII.1711320	chr2	73811537	73811695	1.80	25.20	0.00	42.10	100.00	73811660	0.6
AR.N20.VII.1711321	chr2	74064354	74064469	1.20	17.30	0.00	30.80	75.00	74064412	0.6
AR.N20.VII.1711322	chr2	75116264	75116455	1.80	25.20	0.00	36.80	100.00	75116406	0.7
AR.N20.VII.1711323	chr2	75562038	75562231	2.60	12.20	1.80	50.90	92.90	75562169	0.9
AR.N20.VII.1711324	chr2	75574026	75574188	1.30	4.60	0.00	57.10	87.50	75574068	0.6
AR.N20.VII.1711325	chr2	75868918	75869127	2.00	5.60	0.00	56.20	75.00	75869045	0.7
AR.N20.VII.1711326	chr2	76931624	76931810	2.10	30.50	0.00	52.20	100.00	76931726	0.7
AR.N20.VII.1711327	chr2	77319135	77319268	1.50	21.20	0.00	56.20	100.00	77319208	0.5
AR.N20.VII.1711328	chr2	79346680	79346852	2.10	29.20	0.00	68.20	80.00	79346743	0.8
AR.N20.VII.1711329	chr2	79872744	79873017	4.10	19.70	1.10	50.60	84.40	79872875	1.1
AR.N20.VII.1711330	chr2	82775591	82775792	1.60	5.60	0.00	64.70	72.70	82775669	0.6
AR.N20.VII.1711331	chr2	83974764	83975007	2.20	7.00	7.30	56.20	82.40	83974864	0.7
AR.N20.VII.1711332	chr2	85039273	85039421	2.00	14.30	2.30	72.10	80.60	85039337	0.8
AR.N20.VII.1711333	chr2	85629864	85629997	1.70	6.00	0.00	44.40	100.00	85629946	0.9
AR.N20.VII.1711334	chr2	85789341	85789593	28.80	410.50	0.70	49.20	90.20	85789445	7.4
AR.N20.VII.1711335	chr2	96367724	96367871	1.40	20.10	0.00	60.30	67.10	96367782	0.6
AR.N20.VII.1711336	chr2	98257839	98258000	1.10	8.00	0.00	50.00	100.00	98257970	0.5
AR.N20.VII.1711337	chr2	99847885	99848103	2.80	39.80	0.00	36.70	100.00	99847981	0.9
AR.N20.VII.1711338	chr2	99981891	99982140	12.50	59.30	0.00	54.80	95.90	99982030	4.3
AR.N20.VII.1711339	chr2	100050687	100051111	5.70	40.80	0.80	59.30	86.30	100050940	1.7
AR.N20.VII.1711340	chr2	101063147	101063582	3.70	7.60	0.00	51.20	90.50	101063451	0.6
AR.N20.VII.1711341	chr2	101103538	101103804	2.30	5.50	0.00	64.00	68.80	101103612	0.6
AR.N20.VII.1711342	chr2	101878799	101879099	14.30	101.70	0.10	53.10	85.50	101878897	4.8
AR.N20.VII.1711343	chr2	102103648	102103860	2.30	16.60	0.00	40.00	80.00	102103725	0.8
AR.N20.VII.1711344	chr2	105232825	105233076	3.40	11.90	0.00	35.10	92.30	105232971	1
AR.N20.VII.1711345	chr2	105299014	105299130	1.30	17.90	3.70	63.00	88.20	105299058	0.6
AR.N20.VII.1711346	chr2	107694149	107694373	2.70	19.30	0.00	27.60	100.00	107694265	1.1
AR.N20.VII.1711347	chr2	107694913	107695198	2.90	10.30	0.00	41.90	92.30	107695071	0.8
AR.N20.VII.1711348	chr2	108203081	108203286	6.40	18.30	0.00	51.40	94.40	108203151	2
AR.N20.VII.1711349	chr2	108615323	108615545	3.10	21.90	0.00	51.50	88.20	108615426	1
AR.N20.VII.1711350	chr2	110081787	110082036	1.70	4.50	97.30	40.50	93.30	110081920	0.5
AR.N20.VII.1711351	chr2	110596434	110596683	1.70	4.50	97.30	62.20	73.90	110596546	0.5
AR.N20.VII.1711352	chr2	111458778	111459013	4.20	14.90	0.00	51.10	73.90	111458835	1
AR.N20.VII.1711353	chr2	113062654	113062827	6.10	17.30	0.00	48.60	91.20	113062730	2.7
AR.N20.VII.1711354	chr2	118452694	118452843	1.60	19.70	11.40	39.10	90.80	118452785	1.1
AR.N20.VII.1711355	chr2	119811832	119812158	8.40	29.90	0.00	42.20	97.40	119812056	1.9
AR.N20.VII.1711356	chr2	119840311	119840475	1.80	10.10	0.00	36.80	85.70	119840401	1
AR.N20.VII.1711357	chr2	121291690	121291875	1.80	12.80	1.70	34.40	100.00	121291802	0.6
AR.N20.VII.1711358	chr2	121429629	121429823	3.00	14.40	1.50	29.20	100.00	121429735	1.1
AR.N20.VII.1711359	chr2	121734813	121734990	2.60	12.20	1.80	47.30	84.60	121734875	0.9
AR.N20.VII.1711360	chr2	122101357	122101493	1.70	23.90	0.00	61.10	90.90	122101455	0.5

regionID	chrom	start	stop	RPM	fold	multi%	plus%	leftPlus%	peakPos	peakHeight
AR.N20.VII.1711361	chr2	122840562	122840714	1.30	9.30	0.00	57.10	87.50	122840648	0.5
AR.N20.VII.1711362	chr2	129575310	129575479	3.30	47.10	1.40	49.30	62.90	129575338	1
AR.N20.VII.1711363	chr2	129808887	129809083	2.30	4.10	0.00	44.00	81.80	129808987	0.6
AR.N20.VII.1711364	chr2	131098791	131099054	1.30	15.80	63.00	46.80	84.50	131098927	0.5
AR.N20.VII.1711365	chr2	131594869	131595255	2.20	6.40	0.00	62.50	53.30	131595036	0.6
AR.N20.VII.1711366	chr2	134931996	134932123	3.50	16.60	1.30	68.00	80.40	134932063	0.9
AR.N20.VII.1711367	chr2	135313778	135313991	5.00	14.30	0.00	47.70	100.00	135313914	1.1
AR.N20.VII.1711368	chr2	135637431	135637622	1.40	20.60	3.20	51.60	75.00	135637535	0.7
AR.N20.VII.1711369	chr2	136546772	136546937	1.40	9.30	32.70	31.90	100.00	136546890	0.7
AR.N20.VII.1711370	chr2	138500192	138500392	1.40	19.90	0.00	66.70	100.00	138500364	0.5
AR.N20.VII.1711371	chr2	139367896	139368086	5.30	75.70	0.00	62.10	94.40	139367980	2.1
AR.N20.VII.1711372	chr2	146348603	146348737	1.10	15.90	0.00	50.00	66.70	146348659	0.6
AR.N20.VII.1711373	chr2	147759138	147759265	2.40	34.50	0.00	53.80	57.10	147759160	0.8
AR.N20.VII.1711374	chr2	147961910	147962189	3.70	53.10	0.00	60.00	91.70	147962082	0.9
AR.N20.VII.1711375	chr2	150731082	150731318	3.90	27.90	0.00	57.10	83.30	150731200	1.4
AR.N20.VII.1711376	chr2	150892906	150893150	3.30	46.50	0.00	74.30	73.10	150893031	0.9
AR.N20.VII.1711377	chr2	150927586	150927648	1.20	6.90	87.10	34.80	87.00	150927621	1
AR.N20.VII.1711378	chr2	151059464	151059614	2.10	15.30	0.00	52.20	91.70	151059516	0.7
AR.N20.VII.1711379	chr2	151170499	151170717	1.80	6.60	3.80	58.90	70.10	151170576	0.7
AR.N20.VII.1711380	chr2	151177813	151178022	8.90	126.10	0.00	44.20	97.60	151177940	2.1
AR.N20.VII.1711381	chr2	155152768	155152870	1.20	12.90	0.00	38.50	100.00	155152841	0.7
AR.N20.VII.1711382	chr2	157063180	157063301	1.30	18.20	5.10	62.00	100.00	157063255	0.6
AR.N20.VII.1711383	chr2	159658259	159658509	2.10	30.50	0.00	69.60	100.00	159658437	0.7
AR.N20.VII.1711384	chr2	160472741	160472959	3.50	20.20	0.00	55.30	76.20	160472828	1.3
AR.N20.VII.1711385	chr2	160785308	160785500	1.20	17.30	0.00	46.20	83.30	160785418	0.5
AR.N20.VII.1711386	chr2	162649459	162649707	2.10	29.20	0.00	40.90	100.00	162649587	0.5
AR.N20.VII.1711387	chr2	162654101	162654326	3.00	14.30	1.00	40.20	76.90	162654153	1.1
AR.N20.VII.1711388	chr2	163932684	163932881	1.50	21.20	0.00	50.00	50.00	163932737	0.6
AR.N20.VII.1711389	chr2	164241773	164241942	2.40	17.30	0.00	57.70	46.70	164241823	0.6
AR.N20.VII.1711390	chr2	168651692	168651968	6.70	19.10	0.00	54.10	87.50	168651828	1.9
AR.N20.VII.1711391	chr2	168843211	168843549	3.70	26.70	1.50	48.00	89.70	168843458	0.9
AR.N20.VII.1711392	chr2	169091629	169091782	1.60	22.60	0.00	70.60	66.70	169091665	0.7
AR.N20.VII.1711393	chr2	172661827	172662018	2.70	9.60	0.00	48.30	100.00	172661897	1.6
AR.N20.VII.1711394	chr2	172728431	172728667	2.80	13.30	0.00	36.70	100.00	172728579	0.8
AR.N20.VII.1711395	chr2	174424411	174424650	2.00	13.90	0.00	60.90	100.00	174424559	0.6
AR.N20.VII.1711396	chr2	176179547	176179752	5.00	35.80	0.00	46.30	100.00	176179649	1.4
AR.N20.VII.1711397	chr2	177057818	177058037	2.20	15.90	0.00	50.00	58.30	177057860	0.6
AR.N20.VII.1711398	chr2	177129410	177129605	2.10	29.20	0.00	68.20	100.00	177129549	0.8
AR.N20.VII.1711399	chr2	178171433	178171512	1.40	19.90	0.00	62.50	100.00	178171478	0.7
AR.N20.VII.1711400	chr2	179482657	179482858	2.10	30.50	0.00	47.80	63.60	179482697	0.6
AR.N20.VII.1711401	chr2	180147283	180147500	1.60	22.60	0.00	64.70	81.80	180147384	0.5
AR.N20.VII.1711402	chr2	181372222	181372425	2.30	11.10	0.00	66.70	94.40	181372316	0.8
AR.N20.VII.1711403	chr2	188114763	188115017	4.50	63.70	0.00	50.00	100.00	188114910	1.4
AR.N20.VII.1711404	chr2	188559382	188559660	7.70	55.10	0.00	60.20	96.00	188559511	2.3
AR.N20.VII.1711405	chr2	189146427	189146747	10.20	144.70	0.00	54.10	84.70	189146546	2.8
AR.N20.VII.1711406	chr2	192505281	192505473	4.70	33.20	0.00	43.10	100.00	192505364	1.4
AR.N20.VII.1711407	chr2	193023695	193023869	2.30	16.60	0.00	42.30	100.00	193023803	0.7
AR.N20.VII.1711408	chr2	194048091	194048386	4.60	65.10	0.00	51.00	80.00	194048244	1
AR.N20.VII.1711409	chr2	195611250	195611407	2.10	29.20	0.00	40.90	100.00	195611332	1
AR.N20.VII.1711410	chr2	195936634	195936734	1.00	4.90	0.00	54.50	100.00	195936680	0.7
AR.N20.VII.1711411	chr2	196779906	196780041	1.80	8.40	0.00	63.20	100.00	196780005	0.7
AR.N20.VII.1711412	chr2	198186456	198186658	1.70	8.00	0.00	66.70	91.70	198186600	0.7
AR.N20.VII.1711413	chr2	203129293	203129461	2.20	6.40	0.00	54.20	84.60	203129368	0.7
AR.N20.VII.1711414	chr2	207396246	207396484	10.50	50.00	0.00	45.20	71.20	207396319	2.8
AR.N20.VII.1711415	chr2	209125909	209126089	1.40	10.00	0.00	66.70	70.00	209125949	0.5
AR.N20.VII.1711416	chr2	210806590	210806827	10.30	73.50	2.40	45.50	92.10	210806727	3
AR.N20.VII.1711417	chr2	211754775	211754982	2.00	27.90	0.00	57.10	91.70	211754882	0.7
AR.N20.VII.1711418	chr2	211981507	211981779	3.30	23.20	0.00	48.60	94.10	211981627	0.7
AR.N20.VII.1711419	chr2	213889484	213889676	2.80	13.30	0.00	46.70	100.00	213889631	1
AR.N20.VII.1711420	chr2	214951669	214951902	2.20	15.90	0.00	37.50	88.90	214951781	0.7
AR.N20.VII.1711421	chr2	217451079	217451362	2.50	11.90	0.00	44.40	58.30	217451167	0.6
AR.N20.VII.1711422	chr2	217913241	217913425	2.10	14.90	2.20	51.10	100.00	217913378	0.6
AR.N20.VII.1711423	chr2	218438408	218438668	2.30	11.10	0.00	52.00	69.20	218438512	0.7
AR.N20.VII.1711424	chr2	219017765	219017823	2.10	10.20	0.00	66.70	93.80	219017775	2.1
AR.N20.VII.1711425	chr2	222183696	222183901	9.10	26.00	0.00	57.00	77.20	222183785	2.6
AR.N20.VII.1711426	chr2	223369692	223370006	2.80	19.70	2.40	55.60	87.90	223369910	0.7
AR.N20.VII.1711427	chr2	223793296	223793513	5.70	81.00	1.60	57.90	91.80	223793400	2.3
AR.N20.VII.1711428	chr2	226414181	226414622	3.90	18.70	3.00	61.50	76.90	226414450	0.9
AR.N20.VII.1711429	chr2	227250160	227250323	2.40	34.50	0.00	30.80	100.00	227250250	1.2
AR.N20.VII.1711430	chr2	227311796	227312016	5.60	79.70	0.00	60.00	77.80	227311909	1.5
AR.N20.VII.1711431	chr2	228150664	228150828	1.50	7.10	0.00	56.20	66.70	228150684	0.7
AR.N20.VII.1711432	chr2	230258673	230258786	1.10	15.90	0.00	50.00	100.00	230258745	0.7
AR.N20.VII.1711433	chr2	234141146	234141398	2.60	6.60	3.50	46.50	92.30	234141271	0.8
AR.N20.VII.1711434	chr2	234942386	234942643	3.70	10.60	0.00	37.50	100.00	234942550	1.3
AR.N20.VII.1711435	chr2	235626359	235626642	4.20	29.90	0.00	56.50	69.20	235626510	1
AR.N20.VII.1711436	chr2	236237391	236237587	2.30	8.30	0.00	44.00	100.00	236237528	0.9
AR.N20.VII.1711437	chr2	237151540	237151753	1.90	5.30	0.00	40.00	87.50	237151588	0.6
AR.N20.VII.1711438	chr2	237253416	237253604	5.60	26.60	0.00	39.30	100.00	237253511	2
AR.N20.VII.1711439	chr2	238023038	238023180	1.30	15.50	0.00	28.60	50.00	238023103	0.6
AR.N20.VII.1711440	chr2	238076015	238076152	2.00	9.30	0.00	42.90	100.00	238076111	0.7
AR.N20.VII.1711441	chr2	238603830	238603990	1.20	16.60	4.00	52.00	92.30	238603851	0.5
AR.N20.VII.1711442	chr2	238817564	238817882	4.50	32.20	1.00	37.10	100.00	238817761	1.4
AR.N20.VII.1711443	chr2	239738553	239738652	1.20	17.30	0.00	69.20	77.80	239738587	0.7
AR.N20.VII.1711444	chr2	239903762	239903973	1.60	4.50	0.00	58.80	60.00	239903809	0.5
AR.N20.VII.1711445	chr2	239983471	239983594	1.00	7.30	0.00	36.40	75.00	239983544	0.6

regionID	chrom	start	stop	RPM	fold	multi%	plus%	leftPlus%	peakPos	peakHeight
AR.N20.VII.1711446	chr2	241681501	241681790	3.80	9.10	87.80	46.30	50.90	241681594	0.7
AR.N20.VII.1711447	chr2	241690440	241690580	1.30	9.30	0.00	28.60	50.00	241690492	0.6
AR.N20.VII.1711448	chr2	242050008	242050338	1.50	7.10	0.00	41.20	57.10	242050219	0.6
AR.N20.VII.1711449	chr2	242138511	242138654	1.90	7.60	0.00	60.00	100.00	242138626	0.8
AR.N20.VII.1711450	chr2	242689004	242689183	1.20	17.30	0.00	46.20	100.00	242689093	0.6
AR.N20.VII.1711451	chr20	630482	630689	4.60	21.70	0.00	42.90	95.20	630602	1.4
AR.N20.VII.1711452	chr20	819972	820204	5.60	26.60	1.70	53.30	78.50	820097	1.2
AR.N20.VII.1711453	chr20	4099696	4099912	2.80	13.50	1.60	42.60	92.30	4099783	1.1
AR.N20.VII.1711454	chr20	8023065	8023271	2.70	38.50	0.00	48.30	100.00	8023180	1
AR.N20.VII.1711455	chr20	8744680	8744861	1.90	26.60	0.00	47.60	100.00	8744802	0.7
AR.N20.VII.1711456	chr20	9235326	9235534	3.20	11.30	0.00	47.10	75.00	9235401	1.1
AR.N20.VII.1711457	chr20	9263668	9263823	1.60	22.60	0.00	50.00	100.00	9263741	0.6
AR.N20.VII.1711458	chr20	10587431	10587654	2.50	35.20	0.00	39.60	100.00	10587572	0.8
AR.N20.VII.1711459	chr20	10790233	10790531	1.80	12.60	0.00	36.80	85.70	10790392	0.5
AR.N20.VII.1711460	chr20	11086202	11086431	1.90	4.40	0.00	75.00	100.00	11086381	0.8
AR.N20.VII.1711461	chr20	11218282	11218415	1.10	15.90	0.00	58.30	71.40	11218317	0.6
AR.N20.VII.1711462	chr20	11338302	11338484	2.20	15.90	0.00	45.80	81.80	11338390	0.6
AR.N20.VII.1711463	chr20	11959179	11959370	2.20	6.40	0.00	50.00	91.70	11959329	0.8
AR.N20.VII.1711464	chr20	14137730	14137859	1.70	23.90	0.00	52.60	100.00	14137808	0.7
AR.N20.VII.1711465	chr20	17934825	17935014	2.90	8.40	1.60	55.60	100.00	17934956	0.9
AR.N20.VII.1711466	chr20	19893326	19893515	2.40	4.30	0.00	42.30	45.50	19893355	0.8
AR.N20.VII.1711467	chr20	19895629	19895950	4.20	14.90	0.00	51.10	95.70	19895833	1.3
AR.N20.VII.1711468	chr20	20014561	20014771	2.10	29.20	0.00	63.60	71.40	20014637	0.6
AR.N20.VII.1711469	chr20	21207666	21207764	1.00	4.90	0.00	63.60	85.70	21207707	0.6
AR.N20.VII.1711470	chr20	21918253	21918447	4.30	61.10	0.00	63.00	96.60	21918338	1.6
AR.N20.VII.1711471	chr20	21922991	21923146	3.70	13.30	0.00	52.50	52.40	21923012	1.1
AR.N20.VII.1711472	chr20	22224804	22224928	2.80	19.90	0.00	63.30	89.50	22224885	1.3
AR.N20.VII.1711473	chr20	24968417	24968717	2.50	6.00	0.00	55.60	100.00	24968641	0.8
AR.N20.VII.1711474	chr20	25202287	25202471	2.70	12.60	1.80	54.20	87.50	25202387	1
AR.N20.VII.1711475	chr20	25208795	25209119	6.30	5.60	0.00	46.40	75.00	25208929	1.3
AR.N20.VII.1711476	chr20	25239053	25239280	1.40	5.00	0.00	40.00	100.00	25239181	0.6
AR.N20.VII.1711477	chr20	30119062	30119285	10.50	25.00	0.90	52.20	96.60	30119197	3.9
AR.N20.VII.1711478	chr20	30796497	30796797	2.00	7.00	0.00	66.70	78.60	30796722	0.5
AR.N20.VII.1711479	chr20	31783873	31784329	12.30	17.60	0.40	45.30	90.00	31784163	3.3
AR.N20.VII.1711480	chr20	32304262	32304412	4.70	50.60	13.30	47.00	83.10	32304290	2.5
AR.N20.VII.1711481	chr20	32315636	32315869	11.30	24.80	2.10	52.30	100.00	32315800	3
AR.N20.VII.1711482	chr20	33259527	33259754	4.10	19.50	0.00	43.20	100.00	33259688	1.3
AR.N20.VII.1711483	chr20	33958740	33958979	1.70	8.00	0.00	38.90	100.00	33958930	0.6
AR.N20.VII.1711484	chr20	34218583	34218626	13.10	46.80	0.00	47.20	100.00	34218590	13.1
AR.N20.VII.1711485	chr20	34686116	34686334	2.50	9.00	0.00	59.30	50.00	34686171	0.7
AR.N20.VII.1711486	chr20	34875652	34875940	3.00	5.30	0.00	53.10	88.20	34875812	0.8
AR.N20.VII.1711487	chr20	35365609	35365797	3.60	15.50	0.00	51.30	90.00	35365735	1.2
AR.N20.VII.1711488	chr20	36051546	36051798	1.50	10.60	0.00	43.80	100.00	36051723	0.6
AR.N20.VII.1711489	chr20	36171044	36171268	3.50	25.20	0.00	51.30	80.00	36171164	1.3
AR.N20.VII.1711490	chr20	36667003	36667261	4.00	19.00	0.00	44.20	73.70	36667056	1
AR.N20.VII.1711491	chr20	37062356	37062514	1.40	10.00	0.00	66.70	80.00	37062403	0.7
AR.N20.VII.1711492	chr20	38530956	38531147	2.30	33.20	0.00	36.00	100.00	38531086	0.8
AR.N20.VII.1711493	chr20	39712650	39712914	3.20	45.10	0.00	44.10	93.30	39712786	1
AR.N20.VII.1711494	chr20	41911928	41912219	2.90	6.90	0.00	35.50	100.00	41912119	0.9
AR.N20.VII.1711495	chr20	42776345	42776479	1.30	9.50	1.80	47.80	84.80	42776411	0.6
AR.N20.VII.1711496	chr20	43062040	43062288	1.70	12.30	2.70	51.40	84.20	43062141	0.5
AR.N20.VII.1711497	chr20	43577714	43577951	10.60	75.20	1.20	48.10	77.10	43577785	2.5
AR.N20.VII.1711498	chr20	45039001	45039238	2.30	16.30	2.00	38.80	73.70	45039137	0.8
AR.N20.VII.1711499	chr20	45380980	45381157	2.30	4.70	0.00	72.00	77.80	45381035	0.8
AR.N20.VII.1711500	chr20	45526645	45526835	1.40	10.00	0.00	68.80	81.80	45526736	0.6
AR.N20.VII.1711501	chr20	45773247	45773393	1.70	11.90	0.00	50.00	100.00	45773342	0.8
AR.N20.VII.1711502	chr20	47565660	47565834	1.60	7.30	0.00	64.70	90.90	47565728	0.6
AR.N20.VII.1711503	chr20	47633721	47633972	11.20	39.80	0.00	53.70	93.80	47633834	3.7
AR.N20.VII.1711504	chr20	48445281	48445580	2.20	15.60	19.10	51.10	87.50	48445428	0.8
AR.N20.VII.1711505	chr20	48465397	48465846	5.80	5.20	4.00	57.60	87.50	48465748	1.4
AR.N20.VII.1711506	chr20	48588342	48588522	1.80	8.40	0.00	36.80	100.00	48588416	0.7
AR.N20.VII.1711507	chr20	49171801	49171998	3.40	16.40	0.00	44.70	100.00	49171950	1.3
AR.N20.VII.1711508	chr20	50656468	50656651	2.90	8.20	0.00	48.40	80.00	50656513	1.3
AR.N20.VII.1711509	chr20	53035092	53035316	3.00	42.50	0.00	62.50	90.00	53035205	0.9
AR.N20.VII.1711510	chr20	54613220	54613349	2.10	14.60	0.00	63.60	71.40	54613254	0.8
AR.N20.VII.1711511	chr20	55694101	55694291	1.30	9.30	0.00	57.10	100.00	55694193	0.6
AR.N20.VII.1711512	chr20	55766422	55766598	1.10	15.90	0.00	25.00	66.70	55766468	0.6
AR.N20.VII.1711513	chr20	55771768	55772006	5.50	78.30	0.00	45.80	92.60	55771868	1.8
AR.N20.VII.1711514	chr20	55781787	55782004	8.20	58.70	0.60	49.70	95.50	55781904	2.2
AR.N20.VII.1711515	chr20	57308482	57308673	2.30	10.80	2.00	56.90	86.20	57308576	0.8
AR.N20.VII.1711516	chr20	57834661	57835255	6.20	4.50	0.00	59.10	53.80	57834971	1.3
AR.N20.VII.1711517	chr20	58061852	58062152	2.00	13.90	0.00	63.60	64.30	58062045	0.5
AR.N20.VII.1711518	chr20	60223643	60223850	1.30	9.30	0.00	50.00	100.00	60223819	0.6
AR.N20.VII.1711519	chr21	16374185	16374384	5.30	75.70	0.00	67.20	76.90	16374296	1.5
AR.N20.VII.1711520	chr21	25235872	25236066	2.80	13.50	1.60	36.10	63.60	25235950	0.7
AR.N20.VII.1711521	chr21	26418824	26419042	2.30	16.60	0.00	44.00	100.00	26418946	0.7
AR.N20.VII.1711522	chr21	26432909	26433129	1.60	22.60	0.00	47.10	87.50	26433009	0.6
AR.N20.VII.1711523	chr21	27449457	27449567	1.60	11.30	0.00	35.30	83.30	27449477	0.7
AR.N20.VII.1711524	chr21	28432129	28432246	1.20	17.30	0.00	46.20	100.00	28432189	0.7
AR.N20.VII.1711525	chr21	28734191	28734393	12.20	57.80	0.40	39.80	100.00	28734297	4
AR.N20.VII.1711526	chr21	29252027	29252254	6.00	28.30	0.00	45.30	100.00	29252140	1.4
AR.N20.VII.1711527	chr21	29440368	29440552	1.90	13.30	0.00	50.00	100.00	29440457	0.6
AR.N20.VII.1711528	chr21	29730388	29730597	1.80	8.40	0.00	31.60	100.00	29730498	0.6
AR.N20.VII.1711529	chr21	31036556	31036695	1.00	8.80	27.70	58.00	69.20	31036605	0.7
AR.N20.VII.1711530	chr21	31561959	31562130	3.30	46.50	0.00	38.90	100.00	31562037	1.1

regionID	chrom	start	stop	RPM	fold	multi%	plus%	leftPlus%	peakPos	peakHeight
AR.N20.VII.1711531	chr21	32705838	32706011	6.70	23.70	0.70	39.50	93.10	32705910	2.4
AR.N20.VII.1711532	chr21	33598894	33599117	2.10	30.50	0.00	52.20	75.00	33598966	0.6
AR.N20.VII.1711533	chr21	36800356	36800504	2.00	13.30	0.00	57.10	91.70	36800457	1
AR.N20.VII.1711534	chr21	37940621	37940834	1.90	6.60	0.00	42.90	100.00	37940805	0.6
AR.N20.VII.1711535	chr21	38374932	38375154	5.20	36.80	0.90	47.80	85.20	38375002	1.6
AR.N20.VII.1711536	chr21	40739156	40739301	1.20	16.60	4.00	40.00	100.00	40739223	0.5
AR.N20.VII.1711537	chr21	40876988	40877077	1.10	8.00	0.00	50.00	100.00	40877015	0.6
AR.N20.VII.1711538	chr21	40935877	40936051	3.80	54.40	0.00	58.50	100.00	40935956	2
AR.N20.VII.1711539	chr21	41339748	41339933	2.70	18.90	1.80	54.40	100.00	41339861	1.2
AR.N20.VII.1711540	chr21	41459144	41459330	1.10	5.30	0.00	66.70	100.00	41459254	0.6
AR.N20.VII.1711541	chr21	41815526	41815698	2.50	17.90	0.00	70.40	73.70	41815591	0.7
AR.N20.VII.1711542	chr21	41877211	41877335	1.20	8.60	0.00	64.30	77.80	41877283	0.6
AR.N20.VII.1711543	chr21	42278229	42278363	1.00	14.60	0.00	54.50	100.00	42278281	0.6
AR.N20.VII.1711544	chr21	42523578	42523689	1.20	17.30	0.00	57.10	100.00	42523622	0.7
AR.N20.VII.1711545	chr21	42965265	42965569	8.90	63.10	0.00	57.30	80.00	42965364	2.6
AR.N20.VII.1711546	chr21	43024695	43024909	10.10	35.80	0.00	52.70	72.40	43024781	2.4
AR.N20.VII.1711547	chr21	43587557	43587692	1.20	4.30	0.00	38.50	100.00	43587648	0.6
AR.N20.VII.1711548	chr21	44432886	44433164	3.90	13.90	0.00	40.50	94.10	44433049	1.3
AR.N20.VII.1711549	chr21	44981044	44981259	5.70	8.20	0.80	53.70	87.90	44981141	1.8
AR.N20.VII.1711550	chr21	45350327	45350470	1.60	7.50	0.00	61.10	54.50	45350355	0.6
AR.N20.VII.1711551	chr21	45470370	45470591	4.80	34.50	0.00	51.90	96.30	45470510	1
AR.N20.VII.1711552	chr21	45665967	45666103	1.50	4.20	0.00	35.30	83.30	45666017	0.6
AR.N20.VII.1711553	chr21	46406774	46406859	1.60	11.30	0.00	52.60	70.00	46406795	0.9
AR.N20.VII.1711554	chr21	46866363	46866492	1.30	18.60	0.00	28.60	100.00	46866465	0.5
AR.N20.VII.1711555	chr22	14487670	14487910	1.40	4.80	64.00	34.20	100.00	14487829	0.6
AR.N20.VII.1711556	chr22	17198389	17198675	5.80	21.10	98.90	46.80	82.50	17198520	1.6
AR.N20.VII.1711557	chr22	17975019	17975210	3.40	6.10	0.00	40.50	73.30	17975076	0.8
AR.N20.VII.1711558	chr22	18096176	18096324	1.40	20.60	3.20	54.80	88.20	18096227	0.6
AR.N20.VII.1711559	chr22	19829206	19829504	5.80	19.90	98.90	50.60	86.90	19829349	1.6
AR.N20.VII.1711560	chr22	19949630	19949916	5.80	21.10	98.90	46.80	82.50	19949761	1.6
AR.N20.VII.1711561	chr22	20392044	20392245	1.80	25.20	0.00	57.90	81.80	20392145	0.5
AR.N20.VII.1711562	chr22	21232358	21232590	2.70	9.70	1.10	38.60	91.20	21232487	1.3
AR.N20.VII.1711563	chr22	22140205	22140401	1.40	9.40	25.50	38.60	100.00	22140321	0.6
AR.N20.VII.1711564	chr22	22611023	22611263	3.20	12.90	97.10	55.90	76.30	22611159	0.9
AR.N20.VII.1711565	chr22	22693855	22694095	3.20	12.90	97.10	55.90	76.30	22693991	0.9
AR.N20.VII.1711566	chr22	23321924	23322108	2.30	16.60	0.00	48.00	75.00	23321986	0.7
AR.N20.VII.1711567	chr22	28243674	28243938	5.90	83.60	0.00	58.70	91.90	28243825	1.9
AR.N20.VII.1711568	chr22	28289694	28289819	2.00	9.30	0.00	66.70	85.70	28289729	0.7
AR.N20.VII.1711569	chr22	29017022	29017319	3.40	6.80	0.00	41.70	100.00	29017210	1
AR.N20.VII.1711570	chr22	31505887	31505995	1.20	17.30	0.00	61.50	62.50	31505898	0.6
AR.N20.VII.1711571	chr22	33791756	33791934	2.00	7.00	0.00	54.50	66.70	33791809	0.6
AR.N20.VII.1711572	chr22	33917516	33917777	3.30	31.60	4.80	61.60	52.30	33917602	1.1
AR.N20.VII.1711573	chr22	37481305	37481435	1.50	7.10	0.00	56.20	66.70	37481362	0.6
AR.N20.VII.1711574	chr22	38694640	38694809	2.10	9.70	0.00	63.60	57.10	38694686	0.6
AR.N20.VII.1711575	chr22	39458717	39458895	2.80	13.30	0.00	50.00	93.30	39458826	1
AR.N20.VII.1711576	chr22	39988013	39988256	1.90	5.30	0.00	55.00	63.60	39988076	0.6
AR.N20.VII.1711577	chr22	40143952	40144235	10.70	21.80	0.00	47.40	94.50	40144121	2.3
AR.N20.VII.1711578	chr22	40959297	40959502	3.90	18.60	0.00	42.90	100.00	40959402	1.2
AR.N20.VII.1711579	chr22	41652061	41652273	1.70	4.80	0.00	55.60	100.00	41652192	0.7
AR.N20.VII.1711580	chr22	43419658	43419847	2.70	38.50	0.00	37.90	100.00	43419786	1.1
AR.N20.VII.1711581	chr22	43633459	43633637	2.00	9.20	69.60	50.30	50.00	43633499	0.6
AR.N20.VII.1711582	chr22	43641109	43641287	1.60	7.50	94.30	48.70	89.80	43641248	0.6
AR.N20.VII.1711583	chr22	43893223	43893421	4.00	56.50	5.90	68.30	89.70	43893324	1.8
AR.N20.VII.1711584	chr22	43965137	43965323	3.90	27.90	0.00	44.20	100.00	43965229	1.2
AR.N20.VII.1711585	chr22	44584046	44584235	3.90	13.90	2.00	68.90	96.50	44584170	1.3
AR.N20.VII.1711586	chr22	44749815	44750062	7.50	26.60	0.00	43.90	88.90	44749934	2.4
AR.N20.VII.1711587	chr22	44842366	44842560	1.50	10.60	0.00	35.30	100.00	44842496	0.5
AR.N20.VII.1711588	chr22	45844132	45845534	12.60	8.50	71.00	56.20	66.80	45845088	0.9
AR.N20.VII.1711589	chr22	46066970	46067161	4.60	32.50	0.00	56.00	92.90	46067068	1.2
AR.N20.VII.1711590	chr22	48577487	48577705	3.00	4.70	0.00	50.00	87.50	48577586	1.1
AR.N20.VII.1711591	chr22	48611650	48611793	2.60	7.40	0.00	67.90	94.70	48611750	0.9
AR.N20.VII.1711592	chr22	48729041	48729292	7.40	21.00	0.00	48.80	94.90	48729143	2.3
AR.N20.VII.1711593	chr22	48993972	48994146	2.60	37.20	17.90	65.50	73.70	48994045	1
AR.N20.VII.1711594	chr3	2886657	2886939	4.10	11.80	0.80	63.90	100.00	2886833	1.8
AR.N20.VII.1711595	chr3	3503467	3503658	2.10	30.50	0.00	56.00	100.00	3503579	0.9
AR.N20.VII.1711596	chr3	4339410	4339591	2.20	31.10	1.70	61.50	100.00	4339497	0.7
AR.N20.VII.1711597	chr3	4705265	4705435	1.40	19.90	0.00	46.70	100.00	4705381	0.6
AR.N20.VII.1711598	chr3	5005741	5005959	1.50	10.60	0.00	31.20	100.00	5005907	0.6
AR.N20.VII.1711599	chr3	7177518	7177703	5.00	20.40	24.80	51.10	100.00	7177618	1.9
AR.N20.VII.1711600	chr3	7399154	7399340	2.30	33.20	0.00	56.00	100.00	7399293	0.7
AR.N20.VII.1711601	chr3	9211465	9211619	1.30	6.20	0.00	42.90	100.00	9211550	0.9
AR.N20.VII.1711602	chr3	9791213	9791431	1.90	27.20	2.40	61.00	92.00	9791347	0.7
AR.N20.VII.1711603	chr3	12995972	12996122	2.10	7.60	0.00	56.50	100.00	12996071	0.9
AR.N20.VII.1711604	chr3	14245637	14245860	2.20	17.90	16.90	46.10	90.80	14245742	0.7
AR.N20.VII.1711605	chr3	14265646	14265853	2.40	17.30	0.00	38.50	90.00	14265747	0.6
AR.N20.VII.1711606	chr3	14312372	14312569	2.80	39.80	0.00	56.70	100.00	14312490	0.9
AR.N20.VII.1711607	chr3	14640214	14640439	1.90	5.30	0.00	50.00	90.00	14640278	0.8
AR.N20.VII.1711608	chr3	15690189	15690321	1.80	12.60	0.00	50.00	100.00	15690254	0.6
AR.N20.VII.1711609	chr3	15798637	15798806	1.00	7.30	0.00	54.50	100.00	15798732	0.5
AR.N20.VII.1711610	chr3	17822195	17822387	2.30	33.20	0.00	68.00	58.80	17822241	0.7
AR.N20.VII.1711611	chr3	18163100	18163262	1.30	6.20	0.00	50.00	100.00	18163160	0.5
AR.N20.VII.1711612	chr3	21660371	21660615	5.90	21.10	0.80	46.50	96.60	21660508	1.9
AR.N20.VII.1711613	chr3	23859643	23859870	2.10	7.30	0.00	63.60	100.00	23859766	0.8
AR.N20.VII.1711614	chr3	23975875	23976143	3.70	26.60	0.00	60.00	87.50	23976001	1.2
AR.N20.VII.1711615	chr3	24150504	24150679	2.60	18.60	0.00	42.90	100.00	24150591	0.9

regionID	chrom	start	stop	RPM	fold	multi%	plus%	leftPlus%	peakPos	peakHeight
AR.N20.VII.1711616	chr3	24156611	24156816	7.80	55.80	0.00	45.30	92.30	24156698	2.7
AR.N20.VII.1711617	chr3	24157875	24158111	2.20	10.40	2.10	59.60	100.00	24158050	0.7
AR.N20.VII.1711618	chr3	25278908	25279132	5.40	25.40	1.70	60.90	82.90	25278973	1.8
AR.N20.VII.1711619	chr3	26752852	26753042	2.10	15.30	0.00	52.20	83.30	26752918	0.8
AR.N20.VII.1711620	chr3	29929403	29929602	2.00	14.30	2.30	37.20	100.00	29929476	0.7
AR.N20.VII.1711621	chr3	32150428	32150631	4.50	32.20	1.00	50.50	95.90	32150486	1.7
AR.N20.VII.1711622	chr3	33219485	33219673	4.90	17.60	0.00	66.00	54.30	33219545	1.2
AR.N20.VII.1711623	chr3	37098864	37099018	1.70	12.30	0.00	73.00	85.20	37098945	0.8
AR.N20.VII.1711624	chr3	37310229	37310512	2.50	36.30	4.80	53.10	41.40	37310304	0.7
AR.N20.VII.1711625	chr3	37534107	37534394	3.10	5.50	0.00	45.50	80.00	37534340	0.9
AR.N20.VII.1711626	chr3	37986487	37986539	11.30	160.60	0.00	46.30	100.00	37986496	11.3
AR.N20.VII.1711627	chr3	38017966	38018175	2.70	5.50	0.00	62.10	88.90	38018064	0.8
AR.N20.VII.1711628	chr3	39158217	39158479	6.10	43.10	0.00	56.10	100.00	39158414	1.9
AR.N20.VII.1711629	chr3	40647847	40648083	2.40	17.10	6.80	40.80	100.00	40648002	0.7
AR.N20.VII.1711630	chr3	40903574	40903770	1.60	11.30	0.00	64.70	100.00	40903680	0.7
AR.N20.VII.1711631	chr3	41549579	41549754	2.10	7.30	4.50	50.00	81.80	41549663	0.8
AR.N20.VII.1711632	chr3	42440653	42441016	4.30	23.60	45.90	51.30	62.00	42440786	1
AR.N20.VII.1711633	chr3	42561218	42561669	5.70	16.30	0.80	43.20	70.40	42561483	1
AR.N20.VII.1711634	chr3	42579037	42579265	4.50	31.90	0.00	45.80	95.50	42579196	1.3
AR.N20.VII.1711635	chr3	42858015	42858192	4.40	15.60	0.00	61.70	89.70	42858116	1.7
AR.N20.VII.1711636	chr3	43898404	43898568	1.10	15.90	0.00	58.30	85.70	43898425	0.5
AR.N20.VII.1711637	chr3	44886943	44887202	2.20	4.60	0.00	37.50	88.90	44887078	0.6
AR.N20.VII.1711638	chr3	45555162	45555410	2.40	17.30	0.00	61.50	81.20	45555291	0.8
AR.N20.VII.1711639	chr3	45563662	45563920	3.30	15.50	0.00	57.10	85.00	45563778	1
AR.N20.VII.1711640	chr3	45633956	45634274	5.20	10.50	0.90	55.80	68.30	45634142	1.4
AR.N20.VII.1711641	chr3	45878032	45878197	1.00	7.30	0.00	45.50	100.00	45878152	0.6
AR.N20.VII.1711642	chr3	46020182	46020412	2.50	8.70	82.90	57.00	75.90	46020247	0.7
AR.N20.VII.1711643	chr3	46020849	46021046	2.10	15.20	95.60	38.30	100.00	46020982	0.7
AR.N20.VII.1711644	chr3	46220319	46220561	1.90	6.60	5.00	45.00	100.00	46220390	0.7
AR.N20.VII.1711645	chr3	46368957	46369196	2.20	20.80	97.90	55.30	88.50	46369077	0.5
AR.N20.VII.1711646	chr3	46683170	46683361	3.30	15.70	1.40	39.40	85.70	46683251	1.2
AR.N20.VII.1711647	chr3	48248815	48249041	3.70	53.10	0.00	60.00	45.80	48248836	1
AR.N20.VII.1711648	chr3	48253237	48253430	2.90	10.30	0.00	29.00	100.00	48253371	1
AR.N20.VII.1711649	chr3	50458360	50458635	2.40	6.90	0.00	51.90	100.00	50458591	0.7
AR.N20.VII.1711650	chr3	52820259	52820428	2.10	4.20	0.00	43.50	100.00	52820370	0.7
AR.N20.VII.1711651	chr3	52839040	52839241	1.50	7.10	0.00	37.50	100.00	52839163	0.6
AR.N20.VII.1711652	chr3	52878720	52878879	2.30	33.20	0.00	64.00	87.50	52878810	1.1
AR.N20.VII.1711653	chr3	53173735	53174026	4.10	11.70	0.00	52.30	100.00	53173939	1.5
AR.N20.VII.1711654	chr3	54959799	54959937	2.10	30.50	0.00	43.50	100.00	54959879	0.9
AR.N20.VII.1711655	chr3	55624167	55624322	2.50	35.80	0.00	66.70	50.00	55624187	0.8
AR.N20.VII.1711656	chr3	56015488	56015694	1.40	10.00	0.00	60.00	100.00	56015584	0.7
AR.N20.VII.1711657	chr3	56794677	56794895	3.20	15.10	0.60	44.40	86.80	56794790	1.2
AR.N20.VII.1711658	chr3	57933621	57933799	2.10	7.60	0.00	56.50	92.30	57933704	0.7
AR.N20.VII.1711659	chr3	58081276	58081425	1.30	9.30	0.00	35.70	80.00	58081363	0.6
AR.N20.VII.1711660	chr3	58110970	58111256	4.00	11.30	1.20	41.20	80.00	58111098	1.1
AR.N20.VII.1711661	chr3	59274269	59274483	2.30	5.50	0.00	60.00	73.30	59274355	0.7
AR.N20.VII.1711662	chr3	59502204	59502431	5.10	36.50	0.00	41.80	78.30	59502326	1.4
AR.N20.VII.1711663	chr3	59566772	59567085	8.50	40.30	0.00	52.70	97.90	59566929	2.1
AR.N20.VII.1711664	chr3	62057925	62058144	5.90	83.60	0.00	50.80	90.60	62058050	1.2
AR.N20.VII.1711665	chr3	62376952	62377195	2.20	15.90	0.00	37.50	100.00	62377118	0.8
AR.N20.VII.1711666	chr3	63936629	63936823	1.60	11.30	0.00	52.90	66.70	63936650	0.5
AR.N20.VII.1711667	chr3	64329304	64329506	4.50	15.90	0.00	50.00	95.80	64329434	1.2
AR.N20.VII.1711668	chr3	64494364	64494597	3.30	11.60	0.00	52.80	47.40	64494423	0.8
AR.N20.VII.1711669	chr3	65581895	65582085	4.10	29.20	0.00	54.50	83.30	65581962	1.6
AR.N20.VII.1711670	chr3	65850605	65850727	1.20	5.80	0.00	30.80	100.00	65850675	0.6
AR.N20.VII.1711671	chr3	67840069	67840229	1.90	26.60	0.00	60.00	91.70	67840172	0.6
AR.N20.VII.1711672	chr3	69068662	69069111	5.00	17.90	0.00	51.90	85.70	69068885	1.1
AR.N20.VII.1711673	chr3	72123656	72123851	3.20	45.80	1.40	54.90	89.70	72123778	1
AR.N20.VII.1711674	chr3	72430122	72430355	3.40	8.20	0.00	43.20	100.00	72430273	1.1
AR.N20.VII.1711675	chr3	72438763	72438989	5.00	23.90	0.00	42.60	95.70	72438880	1.6
AR.N20.VII.1711676	chr3	72468937	72469209	8.20	6.50	0.70	44.00	87.20	72469082	2.6
AR.N20.VII.1711677	chr3	73936142	73936404	10.50	49.90	4.10	50.30	89.60	73936263	2.5
AR.N20.VII.1711678	chr3	74696477	74696685	3.20	15.00	0.00	50.00	100.00	74696584	1
AR.N20.VII.1711679	chr3	74775629	74775824	12.20	58.00	0.00	43.90	100.00	74775768	3.4
AR.N20.VII.1711680	chr3	74836739	74837031	1.40	10.00	0.00	53.30	100.00	74836955	0.6
AR.N20.VII.1711681	chr3	76561662	76561951	2.70	9.60	0.00	44.80	100.00	76561872	0.7
AR.N20.VII.1711682	chr3	81686181	81686452	6.20	29.70	0.00	46.30	64.50	81686325	1.6
AR.N20.VII.1711683	chr3	82188218	82188421	4.80	68.40	1.00	55.30	96.50	82188325	1.5
AR.N20.VII.1711684	chr3	84238070	84238197	1.30	9.30	0.00	60.00	100.00	84238140	0.6
AR.N20.VII.1711685	chr3	85103477	85103606	1.60	22.60	0.00	47.10	75.00	85103498	0.9
AR.N20.VII.1711686	chr3	87727865	87727955	1.10	15.90	0.00	75.00	88.90	87727885	0.8
AR.N20.VII.1711687	chr3	99985711	99985921	3.70	52.40	1.30	55.60	82.20	99985797	1.2
AR.N20.VII.1711688	chr3	101058754	101059019	6.90	98.20	0.00	54.10	85.00	101058906	1.8
AR.N20.VII.1711689	chr3	102142684	102142855	4.40	31.20	0.00	61.70	89.70	102142759	1.4
AR.N20.VII.1711690	chr3	102512278	102512446	1.80	12.60	0.00	47.40	77.80	102512345	0.7
AR.N20.VII.1711691	chr3	103439906	103440057	1.30	4.60	0.00	28.60	100.00	103440007	0.6
AR.N20.VII.1711692	chr3	103731181	103731374	2.70	12.80	0.00	58.60	94.10	103731259	1.1
AR.N20.VII.1711693	chr3	103779013	103779306	3.00	14.20	0.00	43.80	92.90	103779155	1
AR.N20.VII.1711694	chr3	103872670	103872862	1.60	17.40	2.90	62.90	81.80	103872755	0.7
AR.N20.VII.1711695	chr3	105800788	105800978	2.40	34.50	0.00	57.70	86.70	105800909	1.1
AR.N20.VII.1711696	chr3	105812911	105813109	5.70	27.00	0.00	45.90	92.90	105812994	1.8
AR.N20.VII.1711697	chr3	106012533	106012724	1.80	4.20	0.00	42.10	87.50	106012637	0.7
AR.N20.VII.1711698	chr3	106342556	106342895	2.60	37.20	0.00	39.30	72.70	106342651	0.7
AR.N20.VII.1711699	chr3	107775234	107775378	1.60	22.60	0.00	41.20	100.00	107775266	0.6
AR.N20.VII.1711700	chr3	107880221	107880427	1.50	15.10	18.40	41.70	100.00	107880351	0.7

regionID	chrom	start	stop	RPM	fold	multi%	plus%	leftPlus%	peakPos	peakHeight
AR.N20.VII.1711701	chr3	108640309	108640556	10.60	21.60	0.00	50.90	94.80	108640426	2.7
AR.N20.VII.1711702	chr3	108919052	108919187	1.30	12.40	0.00	64.30	100.00	108919103	0.6
AR.N20.VII.1711703	chr3	109254604	109254756	2.20	15.90	0.00	58.30	100.00	109254700	1
AR.N20.VII.1711704	chr3	109444790	109445017	1.70	23.90	0.00	55.60	100.00	109444941	0.6
AR.N20.VII.1711705	chr3	113336439	113336634	1.70	12.30	2.70	43.20	75.00	113336482	0.5
AR.N20.VII.1711706	chr3	115291341	115291538	2.60	12.40	0.00	64.30	88.90	115291448	0.9
AR.N20.VII.1711707	chr3	118811686	118811980	5.40	25.40	0.90	45.30	88.70	118811866	1.3
AR.N20.VII.1711708	chr3	120988035	120988244	5.80	27.40	0.00	54.00	76.50	120988125	1.3
AR.N20.VII.1711709	chr3	123600544	123600745	2.60	36.80	24.20	65.00	97.20	123600660	0.9
AR.N20.VII.1711710	chr3	123853225	123853392	3.20	45.30	42.80	72.60	58.20	123853265	1
AR.N20.VII.1711711	chr3	123954127	123954320	2.30	11.10	0.00	48.00	100.00	123954229	0.8
AR.N20.VII.1711712	chr3	124270279	124270425	1.30	6.20	0.00	42.90	100.00	124270375	0.6
AR.N20.VII.1711713	chr3	124829296	124829507	2.60	37.20	0.00	55.20	50.00	124829364	0.7
AR.N20.VII.1711714	chr3	125302493	125302765	2.20	10.40	2.10	48.90	91.30	125302592	0.8
AR.N20.VII.1711715	chr3	127467846	127468060	6.60	23.40	0.70	67.40	97.90	127467985	1.7
AR.N20.VII.1711716	chr3	127557413	127557739	5.70	16.20	0.00	54.10	87.90	127557624	1.3
AR.N20.VII.1711717	chr3	127803848	127804035	1.90	9.10	17.10	29.30	100.00	127803908	0.5
AR.N20.VII.1711718	chr3	128150652	128150798	1.20	8.60	0.00	46.20	66.70	128150704	0.5
AR.N20.VII.1711719	chr3	128275858	128276029	1.80	8.40	5.30	50.00	80.00	128275899	0.8
AR.N20.VII.1711720	chr3	128505705	128506260	3.90	4.60	4.80	51.20	81.80	128505968	0.6
AR.N20.VII.1711721	chr3	129286306	129286557	3.30	7.70	0.00	60.00	81.00	129286464	1
AR.N20.VII.1711722	chr3	129548236	129548380	1.80	7.20	10.30	53.40	89.00	129548292	0.7
AR.N20.VII.1711723	chr3	130625634	130625928	2.70	39.20	5.10	39.30	50.00	130625704	0.7
AR.N20.VII.1711724	chr3	132050702	132050900	2.60	7.40	0.00	42.90	50.00	132050761	0.7
AR.N20.VII.1711725	chr3	133469264	133469468	1.80	12.60	0.00	57.90	100.00	133469377	0.7
AR.N20.VII.1711726	chr3	135146647	135147021	9.30	18.90	0.50	51.80	54.40	135146742	2
AR.N20.VII.1711727	chr3	139484456	139484722	5.00	14.30	0.00	57.40	93.50	139484592	1.3
AR.N20.VII.1711728	chr3	140518909	140519047	1.20	4.30	0.00	38.50	60.00	140518953	0.6
AR.N20.VII.1711729	chr3	141796923	141797072	2.80	10.00	0.00	64.50	100.00	141797043	1
AR.N20.VII.1711730	chr3	142429989	142430236	2.10	7.30	0.00	54.50	91.70	142430132	0.6
AR.N20.VII.1711731	chr3	142998961	142999331	3.10	11.00	0.00	45.50	86.70	142999136	0.8
AR.N20.VII.1711732	chr3	144598402	144598649	2.20	31.00	1.40	51.40	91.70	144598567	0.5
AR.N20.VII.1711733	chr3	145307102	145307307	4.10	14.40	0.00	70.10	70.50	145307183	1
AR.N20.VII.1711734	chr3	149825827	149826126	2.20	31.90	0.00	45.80	100.00	149826039	0.6
AR.N20.VII.1711735	chr3	151928407	151928547	1.40	5.00	0.00	66.70	90.00	151928458	0.6
AR.N20.VII.1711736	chr3	152313374	152313482	1.40	6.60	0.00	37.50	100.00	152313438	1
AR.N20.VII.1711737	chr3	153470782	153470956	1.30	9.30	0.00	64.30	88.90	153470855	0.7
AR.N20.VII.1711738	chr3	153586364	153586534	2.50	17.90	0.00	33.30	100.00	153586427	0.7
AR.N20.VII.1711739	chr3	155281787	155281970	1.70	11.90	0.00	50.00	100.00	155281907	0.6
AR.N20.VII.1711740	chr3	155545943	155546170	1.90	26.60	0.00	45.00	100.00	155546140	0.7
AR.N20.VII.1711741	chr3	155893725	155893892	1.90	8.90	0.00	45.00	100.00	155893810	0.8
AR.N20.VII.1711742	chr3	155992194	155992426	2.20	15.90	0.00	41.70	70.00	155992255	0.7
AR.N20.VII.1711743	chr3	156433774	156434039	3.40	7.00	0.00	62.20	91.30	156433921	1
AR.N20.VII.1711744	chr3	156504963	156505097	2.20	8.00	0.00	50.00	66.70	156504992	0.7
AR.N20.VII.1711745	chr3	157714167	157714351	1.20	8.60	0.00	69.20	88.90	157714274	0.6
AR.N20.VII.1711746	chr3	158321006	158321373	3.10	7.30	0.00	45.50	86.70	158321148	1.1
AR.N20.VII.1711747	chr3	158741191	158741385	2.30	11.10	0.00	40.00	100.00	158741311	1
AR.N20.VII.1711748	chr3	161997380	161997553	2.90	41.20	0.00	48.40	93.30	161997488	0.9
AR.N20.VII.1711749	chr3	162787468	162787636	3.50	16.80	0.00	44.70	100.00	162787576	1.4
AR.N20.VII.1711750	chr3	170158722	170158915	1.60	11.60	0.00	48.60	88.20	170158817	0.6
AR.N20.VII.1711751	chr3	172428752	172428949	6.00	21.20	0.00	51.60	100.00	172428846	2.2
AR.N20.VII.1711752	chr3	172926785	172926973	1.50	21.60	1.50	56.90	100.00	172926872	0.6
AR.N20.VII.1711753	chr3	173326538	173326744	2.40	17.30	0.00	50.00	84.60	173326662	0.7
AR.N20.VII.1711754	chr3	173404400	173404756	3.00	6.10	0.00	43.80	85.70	173404557	0.9
AR.N20.VII.1711755	chr3	173809132	173809333	2.30	16.60	0.00	36.00	100.00	173809240	0.7
AR.N20.VII.1711756	chr3	173892513	173892651	1.40	10.00	0.00	53.30	87.50	173892581	0.6
AR.N20.VII.1711757	chr3	175541555	175541779	3.70	53.10	0.00	55.00	95.50	175541663	0.9
AR.N20.VII.1711758	chr3	175875945	175876143	1.90	13.30	0.00	60.00	100.00	175876097	0.7
AR.N20.VII.1711759	chr3	176685239	176685502	6.40	30.50	0.00	48.60	94.10	176685386	1.7
AR.N20.VII.1711760	chr3	176978777	176978921	2.50	35.80	0.00	48.10	92.30	176978869	0.6
AR.N20.VII.1711761	chr3	178500583	178500958	2.50	5.10	0.00	51.90	85.70	178500758	0.6
AR.N20.VII.1711762	chr3	178665829	178666032	2.30	10.80	2.00	57.10	71.40	178665873	0.8
AR.N20.VII.1711763	chr3	179286191	179286494	2.70	12.80	0.00	51.70	46.70	179286271	0.8
AR.N20.VII.1711764	chr3	181108367	181108578	1.40	10.00	0.00	40.00	50.00	181108401	0.7
AR.N20.VII.1711765	chr3	183485322	183485604	2.30	16.10	1.00	56.40	86.00	183485511	0.7
AR.N20.VII.1711766	chr3	184025545	184025763	1.90	8.90	0.00	45.00	88.90	184025618	0.6
AR.N20.VII.1711767	chr3	184090491	184090747	2.10	10.20	0.00	39.10	100.00	184090657	0.6
AR.N20.VII.1711768	chr3	184571342	184571609	1.90	5.30	0.00	50.00	80.00	184571460	0.6
AR.N20.VII.1711769	chr3	184965954	184966175	10.80	76.70	0.40	51.10	93.20	184966106	3.2
AR.N20.VII.1711770	chr3	185494965	185495055	2.40	16.90	1.60	40.70	86.50	185494986	2.2
AR.N20.VII.1711771	chr3	185572087	185572350	1.70	6.00	0.00	44.40	87.50	185572261	0.6
AR.N20.VII.1711772	chr3	188822241	188822406	1.00	14.60	0.00	63.60	85.70	188822311	0.7
AR.N20.VII.1711773	chr3	188939899	188940247	4.80	13.50	0.00	56.90	58.60	188940010	1.3
AR.N20.VII.1711774	chr3	189001998	189002103	1.40	10.00	0.00	26.70	100.00	189002076	0.6
AR.N20.VII.1711775	chr3	189147609	189147780	2.00	7.00	0.00	38.10	87.50	189147701	0.7
AR.N20.VII.1711776	chr3	189276838	189276980	1.40	19.90	0.00	62.50	100.00	189276910	0.6
AR.N20.VII.1711777	chr3	189277607	189277853	2.90	8.20	0.00	45.20	85.70	189277693	0.9
AR.N20.VII.1711778	chr3	189772146	189772264	1.40	10.00	0.00	73.30	81.80	189772192	0.7
AR.N20.VII.1711779	chr3	189892679	189892977	2.50	4.50	0.00	63.00	94.10	189892839	0.7
AR.N20.VII.1711780	chr3	190148521	190148760	15.50	36.80	0.30	46.30	97.50	190148618	4.3
AR.N20.VII.1711781	chr3	190650550	190650756	4.80	33.90	0.00	51.00	100.00	190650667	1.3
AR.N20.VII.1711782	chr3	191150665	191150912	2.10	29.20	0.00	47.80	100.00	191150809	0.5
AR.N20.VII.1711783	chr3	192008241	192008532	7.70	36.70	0.00	56.60	97.90	192008410	2.2
AR.N20.VII.1711784	chr3	194021440	194021671	2.20	10.10	0.00	45.80	90.90	194021616	0.6
AR.N20.VII.1711785	chr3	195064583	195064726	3.70	53.10	0.00	47.50	89.50	195064657	1.2

regionID	chrom	start	stop	RPM	fold	multi%	plus%	leftPlus%	peakPos	peakHeight
AR.N20.VII.1711786	chr3	195122882	195123109	5.70	16.20	0.00	54.10	90.90	195122997	1.4
AR.N20.VII.1711787	chr3	196073312	196073478	3.30	23.20	0.00	62.90	90.90	196073375	1.2
AR.N20.VII.1711788	chr3	196940210	196940617	4.70	4.60	48.80	51.20	85.30	196940411	1.1
AR.N20.VII.1711789	chr3	198182108	198182221	1.10	15.90	0.00	58.30	85.70	198182175	0.6
AR.N20.VII.1711790	chr3	198606376	198606592	2.60	12.40	0.00	39.30	90.90	198606487	0.8
AR.N20.VII.1711791	chr3_random	145007	145462	4.80	16.90	99.00	56.90	96.60	145311	0.8
AR.N20.VII.1711792	chr3_random	647229	647468	2.20	20.80	97.90	55.30	88.50	647349	0.5
AR.N20.VII.1711793	chr4	31188	31420	1.90	4.60	26.50	32.50	100.00	31365	1
AR.N20.VII.1711794	chr4	677025	677319	2.10	4.40	4.30	43.50	70.00	677187	0.6
AR.N20.VII.1711795	chr4	1195775	1195929	2.70	6.50	1.10	48.90	100.00	1195880	1
AR.N20.VII.1711796	chr4	1513957	1514196	2.10	7.60	0.00	52.20	83.30	1514105	0.6
AR.N20.VII.1711797	chr4	1526826	1527028	2.50	4.50	0.00	66.70	72.20	1526941	0.7
AR.N20.VII.1711798	chr4	1871284	1871621	2.60	7.40	0.00	57.10	68.80	1871418	0.5
AR.N20.VII.1711799	chr4	2586650	2586837	2.30	11.10	4.00	60.00	86.70	2586727	1
AR.N20.VII.1711800	chr4	3151061	3151474	10.80	8.20	47.30	53.10	42.80	3151168	1.6
AR.N20.VII.1711801	chr4	4579160	4579381	4.50	21.20	0.00	58.30	53.60	4579231	1.3
AR.N20.VII.1711802	chr4	6748932	6749155	1.70	8.00	0.00	57.90	45.50	6749016	0.6
AR.N20.VII.1711803	chr4	6799754	6799928	2.00	4.60	0.00	52.40	100.00	6799878	0.6
AR.N20.VII.1711804	chr4	6833765	6833951	1.60	11.30	0.00	33.30	100.00	6833879	0.7
AR.N20.VII.1711805	chr4	6911748	6911903	5.80	82.30	0.00	51.30	81.20	6911785	1.9
AR.N20.VII.1711806	chr4	7009890	7010149	8.80	31.20	0.00	40.40	89.50	7010002	2.4
AR.N20.VII.1711807	chr4	8404583	8404976	4.90	35.20	0.00	43.40	78.30	8404737	1
AR.N20.VII.1711808	chr4	10108505	10108630	1.40	10.30	0.00	33.30	100.00	10108527	0.6
AR.N20.VII.1711809	chr4	10141024	10141400	4.50	12.70	0.00	56.20	70.40	10141236	0.9
AR.N20.VII.1711810	chr4	12472213	12472441	4.80	69.00	0.00	48.10	68.00	12472299	1.5
AR.N20.VII.1711811	chr4	14760761	14760991	2.70	7.70	0.00	51.70	86.70	14760864	0.7
AR.N20.VII.1711812	chr4	14780287	14780490	3.40	23.90	0.00	63.90	100.00	14780424	1.3
AR.N20.VII.1711813	chr4	20250145	20250389	5.60	79.40	1.40	51.50	93.50	20250283	1.8
AR.N20.VII.1711814	chr4	20293742	20293935	2.20	5.30	0.00	58.30	57.10	20293796	0.6
AR.N20.VII.1711815	chr4	24107421	24107644	8.30	23.60	0.00	55.10	85.70	24107540	1.9
AR.N20.VII.1711816	chr4	24415909	24416102	3.20	11.30	0.00	48.60	82.40	24416009	0.9
AR.N20.VII.1711817	chr4	25218188	25218444	1.80	4.20	2.40	55.10	100.00	25218417	0.7
AR.N20.VII.1711818	chr4	25735406	25735658	2.20	15.90	8.30	56.20	85.20	25735536	0.8
AR.N20.VII.1711819	chr4	25752653	25752883	5.30	75.70	0.00	57.90	75.80	25752741	1.6
AR.N20.VII.1711820	chr4	31002834	31003033	1.50	21.20	0.00	56.20	100.00	31002947	0.6
AR.N20.VII.1711821	chr4	37100229	37100374	1.50	7.10	0.00	68.80	100.00	37100345	0.8
AR.N20.VII.1711822	chr4	37551496	37551692	1.80	25.20	0.00	52.60	90.00	37551617	0.7
AR.N20.VII.1711823	chr4	38299950	38300110	2.10	29.20	0.00	40.30	100.00	38300023	0.7
AR.N20.VII.1711824	chr4	40284705	40284956	3.40	49.10	0.00	48.60	88.90	40284855	1
AR.N20.VII.1711825	chr4	40503947	40504116	3.20	22.60	0.00	68.60	83.30	40504039	1.1
AR.N20.VII.1711826	chr4	40774540	40774741	8.40	59.70	1.10	46.10	100.00	40774679	2.1
AR.N20.VII.1711827	chr4	42028896	42029107	2.70	19.30	0.00	36.70	81.80	42028971	0.7
AR.N20.VII.1711828	chr4	42604777	42605071	5.40	15.40	0.00	53.40	80.60	42604909	1.6
AR.N20.VII.1711829	chr4	47548985	47549182	3.30	47.40	1.90	65.40	60.00	47549046	1.1
AR.N20.VII.1711830	chr4	54214392	54214658	3.70	17.70	0.00	47.50	57.90	54214440	1.1
AR.N20.VII.1711831	chr4	54237330	54237450	1.00	7.30	0.00	63.60	100.00	54237386	0.6
AR.N20.VII.1711832	chr4	57289549	57289805	8.10	57.80	0.00	59.80	86.50	57289666	2.3
AR.N20.VII.1711833	chr4	57794460	57794635	1.70	23.90	0.00	44.40	87.50	57794521	0.6
AR.N20.VII.1711834	chr4	61420882	61421061	2.40	34.50	0.00	42.30	100.00	61420991	0.9
AR.N20.VII.1711835	chr4	65013742	65013875	1.60	7.70	1.90	48.10	100.00	65013814	0.6
AR.N20.VII.1711836	chr4	66584002	66584197	1.60	11.30	0.00	41.20	57.10	66584020	0.7
AR.N20.VII.1711837	chr4	68260474	68260845	2.80	39.80	0.00	53.30	87.50	68260753	0.7
AR.N20.VII.1711838	chr4	70221660	70221820	2.00	7.60	8.10	46.00	95.00	70221749	0.9
AR.N20.VII.1711839	chr4	72235697	72235884	2.30	16.60	0.00	56.00	92.90	72235769	0.7
AR.N20.VII.1711840	chr4	73978016	73978302	3.00	21.20	0.00	59.40	94.70	73978157	0.8
AR.N20.VII.1711841	chr4	74059400	74059605	3.50	25.20	0.00	42.10	81.20	74059456	1.3
AR.N20.VII.1711842	chr4	74132475	74132719	1.90	6.70	6.40	62.50	85.00	74132631	0.5
AR.N20.VII.1711843	chr4	74360017	74360241	3.20	22.60	0.00	44.10	66.70	74360067	0.8
AR.N20.VII.1711844	chr4	74980163	74980367	6.60	23.60	0.00	40.30	100.00	74980250	2.5
AR.N20.VII.1711845	chr4	76088488	76088754	2.10	14.60	0.00	50.00	72.70	76088600	0.6
AR.N20.VII.1711846	chr4	76816640	76816948	8.50	13.40	0.00	58.20	77.40	76816764	2.1
AR.N20.VII.1711847	chr4	77666661	77666897	2.50	11.90	0.00	48.10	92.30	77666813	0.7
AR.N20.VII.1711848	chr4	77711505	77711800	2.90	13.70	0.00	54.80	88.20	77711609	0.9
AR.N20.VII.1711849	chr4	77751689	77752126	3.50	7.20	0.00	57.90	68.20	77751928	0.8
AR.N20.VII.1711850	chr4	77844375	77844515	2.20	15.90	0.00	41.70	100.00	77844433	0.9
AR.N20.VII.1711851	chr4	78704378	78704722	15.40	27.40	0.60	54.50	82.30	78704532	3.3
AR.N20.VII.1711852	chr4	79061975	79062127	3.00	14.20	0.00	63.60	90.50	79062043	1.3
AR.N20.VII.1711853	chr4	80739098	80739261	1.00	4.90	0.00	45.50	100.00	80739156	0.6
AR.N20.VII.1711854	chr4	81243896	81244111	1.90	26.60	0.00	40.00	75.00	81243962	0.8
AR.N20.VII.1711855	chr4	83388760	83388934	1.70	24.60	3.80	60.70	91.30	83388862	0.7
AR.N20.VII.1711856	chr4	87524508	87524619	1.20	4.30	0.00	30.80	100.00	87524572	0.7
AR.N20.VII.1711857	chr4	87727657	87727917	2.20	31.90	0.00	70.80	82.40	87727781	0.9
AR.N20.VII.1711858	chr4	87978392	87978576	1.80	25.20	0.00	57.90	90.90	87978482	0.7
AR.N20.VII.1711859	chr4	89181799	89182140	2.60	15.70	2.10	55.30	72.10	89181915	0.7
AR.N20.VII.1711860	chr4	89655138	89655465	8.70	74.50	5.40	52.70	91.90	89655299	1.9
AR.N20.VII.1711861	chr4	89724755	89724940	1.60	11.30	0.00	64.70	63.60	89724791	0.6
AR.N20.VII.1711862	chr4	90385698	90385935	3.90	9.30	0.00	59.50	76.00	90385781	0.9
AR.N20.VII.1711863	chr4	92102333	92102414	1.00	14.60	0.00	33.30	100.00	92102354	0.5
AR.N20.VII.1711864	chr4	92178257	92178424	2.70	19.30	0.00	51.70	100.00	92178350	0.9
AR.N20.VII.1711865	chr4	95479017	95479232	5.30	75.70	8.80	39.70	95.70	95479166	1.9
AR.N20.VII.1711866	chr4	95656262	95656419	1.10	15.90	0.00	61.50	87.50	95656349	0.5
AR.N20.VII.1711867	chr4	95820325	95820607	5.90	16.70	0.00	55.60	88.60	95820521	1.4
AR.N20.VII.1711868	chr4	96477067	96477266	1.70	23.90	0.00	38.90	100.00	96477171	0.6
AR.N20.VII.1711869	chr4	101158362	101158484	1.90	26.60	0.00	60.00	91.70	101158416	0.8
AR.N20.VII.1711870	chr4	101223299	101223445	2.30	16.60	0.00	56.00	71.40	101223329	0.8

regionID	chrom	start	stop	RPM	fold	multi%	plus%	leftPlus%	peakPos	peakHeight
AR.N20.VII.1711871	chr4	101770440	101770640	1.30	9.00	3.70	51.90	100.00	101770550	0.7
AR.N20.VII.1711872	chr4	102351551	102351741	2.90	41.20	0.00	65.60	81.00	102351646	1
AR.N20.VII.1711873	chr4	103084951	103085113	1.50	5.30	0.00	50.00	87.50	103085010	0.5
AR.N20.VII.1711874	chr4	108823045	108823127	1.10	15.90	0.00	41.70	100.00	108823096	0.8
AR.N20.VII.1711875	chr4	108824591	108824824	1.60	11.30	0.00	52.90	100.00	108824741	0.7
AR.N20.VII.1711876	chr4	109199409	109199551	1.70	11.90	0.00	66.70	91.70	109199507	0.8
AR.N20.VII.1711877	chr4	111199379	111199566	1.50	11.00	3.00	33.30	100.00	111199455	0.7
AR.N20.VII.1711878	chr4	114757185	114757312	1.40	19.90	0.00	50.00	87.50	114757258	0.7
AR.N20.VII.1711879	chr4	115607075	115607191	1.50	21.20	0.00	25.00	75.00	115607094	0.7
AR.N20.VII.1711880	chr4	115703237	115703434	4.00	57.10	0.00	55.80	83.30	115703311	1.4
AR.N20.VII.1711881	chr4	123840809	123841065	4.30	6.50	2.50	49.50	95.60	123840964	1.2
AR.N20.VII.1711882	chr4	125578623	125578774	1.20	8.60	0.00	28.60	100.00	125578669	0.5
AR.N20.VII.1711883	chr4	129985501	129985692	1.80	8.40	0.00	63.20	91.70	129985604	0.5
AR.N20.VII.1711884	chr4	132803124	132803442	9.20	22.20	83.40	47.50	90.20	132803215	2.6
AR.N20.VII.1711885	chr4	139539074	139539356	3.70	26.60	0.00	50.00	45.00	139539128	0.8
AR.N20.VII.1711886	chr4	140267515	140267815	10.10	144.00	0.50	54.40	88.10	140267680	3
AR.N20.VII.1711887	chr4	140649499	140649773	1.90	26.60	0.00	47.60	60.00	140649615	0.5
AR.N20.VII.1711888	chr4	140837208	140837436	3.00	38.70	0.30	40.80	100.00	140837304	1.1
AR.N20.VII.1711889	chr4	141591083	141591230	1.70	23.90	0.00	61.10	72.70	141591130	0.5
AR.N20.VII.1711890	chr4	141698706	141698868	1.90	26.50	4.90	37.50	100.00	141698766	0.5
AR.N20.VII.1711891	chr4	144053718	144053935	6.20	29.70	0.00	38.80	84.60	144053823	1.8
AR.N20.VII.1711892	chr4	144922179	144922308	1.70	23.90	0.00	50.00	88.90	144922200	0.9
AR.N20.VII.1711893	chr4	147383245	147383379	1.80	12.60	0.00	57.90	90.90	147383312	1
AR.N20.VII.1711894	chr4	148257985	148258387	3.40	16.40	2.70	40.50	86.70	148258223	0.7
AR.N20.VII.1711895	chr4	149080921	149081118	1.30	18.60	0.00	35.70	100.00	149081013	0.7
AR.N20.VII.1711896	chr4	149196472	149196707	2.60	7.50	1.20	56.50	93.80	149196659	0.8
AR.N20.VII.1711897	chr4	149832882	149833100	15.60	55.60	0.30	42.70	94.40	149832991	5.2
AR.N20.VII.1711898	chr4	151863549	151863849	2.40	12.50	1.30	63.20	68.80	151863680	0.7
AR.N20.VII.1711899	chr4	152294310	152294446	1.60	11.30	0.00	35.30	100.00	152294392	0.6
AR.N20.VII.1711900	chr4	154078916	154079016	1.40	10.00	0.00	60.00	77.80	154078945	0.9
AR.N20.VII.1711901	chr4	154130121	154130318	2.90	20.90	1.60	61.50	80.00	154130202	1
AR.N20.VII.1711902	chr4	154142776	154142916	1.10	8.00	0.00	66.70	87.50	154142828	0.6
AR.N20.VII.1711903	chr4	154410312	154410525	7.50	53.80	0.00	52.40	90.70	154410441	2.3
AR.N20.VII.1711904	chr4	155507606	155507747	1.60	11.30	0.00	47.10	62.50	155507686	0.7
AR.N20.VII.1711905	chr4	155710216	155710395	2.10	4.40	0.00	60.90	78.60	155710298	1
AR.N20.VII.1711906	chr4	159937066	159937349	4.20	59.70	0.00	40.00	72.20	159937173	0.9
AR.N20.VII.1711907	chr4	160154437	160154612	1.90	26.80	10.70	56.20	79.40	160154523	0.6
AR.N20.VII.1711908	chr4	161150382	161150529	1.50	7.10	0.00	75.00	100.00	161150479	0.5
AR.N20.VII.1711909	chr4	161364486	161364657	1.30	6.30	15.60	61.80	100.00	161364576	0.6
AR.N20.VII.1711910	chr4	163256064	163256272	1.50	21.20	0.00	43.80	100.00	163256185	0.6
AR.N20.VII.1711911	chr4	164250580	164250838	2.60	18.60	0.00	53.60	46.70	164250630	0.7
AR.N20.VII.1711912	chr4	166526262	166526479	2.30	16.60	0.00	40.00	80.00	166526310	0.7
AR.N20.VII.1711913	chr4	166850899	166851032	1.20	16.60	4.00	40.00	80.00	166850972	0.6
AR.N20.VII.1711914	chr4	170077705	170077897	2.20	10.60	0.00	58.30	71.40	170077774	0.7
AR.N20.VII.1711915	chr4	170261875	170262184	1.90	6.60	0.00	65.00	92.30	170262091	0.5
AR.N20.VII.1711916	chr4	171238246	171238547	4.60	22.10	1.70	48.20	75.00	171238419	1.5
AR.N20.VII.1711917	chr4	174194948	174195220	1.90	6.60	0.00	65.00	100.00	174195177	0.6
AR.N20.VII.1711918	chr4	174605966	174606163	1.90	5.30	0.00	57.10	100.00	174606057	0.6
AR.N20.VII.1711919	chr4	183114043	183114239	2.20	31.30	2.60	48.70	100.00	183114097	0.6
AR.N20.VII.1711920	chr4	183115209	183115489	4.60	21.70	0.00	51.00	88.00	183115336	1.2
AR.N20.VII.1711921	chr4	184418712	184418956	2.90	8.00	10.70	49.90	93.60	184418864	0.8
AR.N20.VII.1711922	chr4	184575655	184575841	2.80	6.60	0.00	46.70	85.70	184575722	0.9
AR.N20.VII.1711923	chr4	187704717	187705727	20.60	4.40	47.40	50.10	88.70	187705579	2.4
AR.N20.VII.1711924	chr4	190807308	190807503	2.10	7.60	0.00	52.20	58.30	190807330	0.8
AR.N20.VII.1711925	chr4	190828597	190828773	2.00	5.60	0.00	42.90	55.60	190828639	0.5
AR.N20.VII.1711926	chr4_random	111358	111728	16.00	19.00	64.70	48.30	57.70	111453	2.6
AR.N20.VII.1711927	chr5	1417377	1417543	2.50	11.90	0.00	58.60	88.20	1417468	1.1
AR.N20.VII.1711928	chr5	5863725	5863866	1.50	21.20	0.00	50.00	100.00	5863800	0.6
AR.N20.VII.1711929	chr5	10275575	10275739	1.40	6.60	0.00	33.30	80.00	10275633	0.6
AR.N20.VII.1711930	chr5	10609502	10609655	1.00	4.90	0.00	54.50	100.00	10609622	0.6
AR.N20.VII.1711931	chr5	10757049	10757179	1.20	5.80	0.00	53.80	100.00	10757135	0.7
AR.N20.VII.1711932	chr5	11614626	11614791	2.10	14.60	0.00	59.10	84.60	11614660	1
AR.N20.VII.1711933	chr5	11765142	11765311	1.80	25.20	0.00	63.20	66.70	11765206	0.8
AR.N20.VII.1711934	chr5	12163360	12163540	1.40	15.40	3.20	58.10	100.00	12163452	0.5
AR.N20.VII.1711935	chr5	13784550	13784667	1.10	15.90	0.00	33.30	100.00	13784612	0.6
AR.N20.VII.1711936	chr5	13998538	13998800	1.90	6.40	0.80	60.30	98.60	13998700	0.5
AR.N20.VII.1711937	chr5	14642224	14642421	3.60	25.90	0.00	48.70	100.00	14642330	0.9
AR.N20.VII.1711938	chr5	14769984	14770152	1.10	5.30	0.00	46.20	100.00	14770032	0.5
AR.N20.VII.1711939	chr5	14770214	14770481	3.00	14.20	0.00	37.50	91.70	14770356	0.8
AR.N20.VII.1711940	chr5	14982542	14982691	2.70	12.80	6.90	51.70	100.00	14982663	0.8
AR.N20.VII.1711941	chr5	15036883	15037140	2.30	8.30	0.00	52.00	76.90	15036946	0.6
AR.N20.VII.1711942	chr5	15409820	15410185	2.50	8.40	44.50	71.50	94.00	15410015	0.9
AR.N20.VII.1711943	chr5	16600645	16600917	4.80	69.00	0.00	44.20	65.20	16600759	1.1
AR.N20.VII.1711944	chr5	16829723	16830022	4.20	11.90	0.00	46.70	76.20	16829860	1
AR.N20.VII.1711945	chr5	20533322	20533586	1.40	13.70	16.10	38.70	83.30	20533429	0.5
AR.N20.VII.1711946	chr5	23763196	23763438	2.50	11.90	0.00	59.30	81.20	23763255	0.7
AR.N20.VII.1711947	chr5	28229443	28229612	1.80	25.20	0.00	52.60	100.00	28229547	0.6
AR.N20.VII.1711948	chr5	28916913	28917113	2.10	14.60	0.00	68.20	80.00	28916998	0.6
AR.N20.VII.1711949	chr5	30275717	30275965	2.30	4.60	1.90	49.40	100.00	30275868	0.7
AR.N20.VII.1711950	chr5	31256917	31257112	3.40	15.90	0.00	52.80	100.00	31257049	1.2
AR.N20.VII.1711951	chr5	32210802	32210929	1.40	6.60	0.00	26.70	50.00	32210837	0.7
AR.N20.VII.1711952	chr5	36321808	36322040	2.40	8.50	2.00	62.70	87.50	36321912	0.6
AR.N20.VII.1711953	chr5	36409358	36409559	1.30	5.10	11.10	55.60	100.00	36409480	0.6
AR.N20.VII.1711954	chr5	37767002	37767262	6.60	15.70	0.00	49.30	97.10	37767140	1.9
AR.N20.VII.1711955	chr5	38151429	38151695	2.40	8.60	0.00	53.80	78.60	38151503	0.9

regionID	chrom	start	stop	RPM	fold	multi%	plus%	leftPlus%	peakPos	peakHeight
AR.N20.VII.1711956	chr5	38702906	38703167	9.00	42.90	0.00	41.80	92.70	38703006	2.4
AR.N20.VII.1711957	chr5	40342945	40343120	6.30	90.30	0.00	47.80	100.00	40343064	2.4
AR.N20.VII.1711958	chr5	40557323	40557512	2.80	19.90	0.00	40.00	100.00	40557412	0.9
AR.N20.VII.1711959	chr5	40685745	40685993	2.00	9.30	0.00	71.40	93.30	40685883	0.9
AR.N20.VII.1711960	chr5	40931952	40932100	1.00	5.10	16.70	61.60	100.00	40932015	0.6
AR.N20.VII.1711961	chr5	42497511	42497712	2.90	41.20	0.00	54.80	82.40	42497576	0.7
AR.N20.VII.1711962	chr5	46132094	46132236	1.60	23.20	2.90	65.70	100.00	46132176	0.9
AR.N20.VII.1711963	chr5	54070692	54070888	1.30	8.90	3.30	70.10	98.60	54070800	0.7
AR.N20.VII.1711964	chr5	54573528	54573657	1.10	8.00	0.00	41.70	100.00	54573595	0.5
AR.N20.VII.1711965	chr5	54967803	54967972	3.40	15.90	0.00	30.60	100.00	54967925	1.1
AR.N20.VII.1711966	chr5	55253276	55253474	3.10	14.60	0.00	51.50	76.50	55253353	0.9
AR.N20.VII.1711967	chr5	57409051	57409458	4.10	19.50	0.00	52.30	78.30	57409192	1.1
AR.N20.VII.1711968	chr5	58448961	58449136	2.10	9.70	0.00	50.00	72.70	58449060	1.2
AR.N20.VII.1711969	chr5	58563112	58563363	3.20	15.00	0.00	44.10	73.30	58563221	0.8
AR.N20.VII.1711970	chr5	58712402	58712606	2.30	33.20	4.00	74.00	43.20	58712444	0.7
AR.N20.VII.1711971	chr5	61332282	61332410	2.00	27.90	0.00	56.50	100.00	61332366	1.1
AR.N20.VII.1711972	chr5	62731780	62731931	2.60	10.80	8.30	51.40	96.80	62731866	0.9
AR.N20.VII.1711973	chr5	63830795	63830991	1.70	4.80	0.00	72.20	76.90	63830845	0.7
AR.N20.VII.1711974	chr5	65694737	65694992	2.30	16.70	0.80	54.20	100.00	65694953	0.8
AR.N20.VII.1711975	chr5	65697428	65697666	3.50	25.20	0.00	60.50	91.30	65697597	1.1
AR.N20.VII.1711976	chr5	66580426	66580570	3.50	16.80	0.00	52.60	80.00	66580473	1.6
AR.N20.VII.1711977	chr5	66967757	66967970	4.10	19.30	1.10	58.60	80.40	66967833	1
AR.N20.VII.1711978	chr5	67030356	67030547	3.10	43.80	0.00	57.60	68.40	67030427	0.7
AR.N20.VII.1711979	chr5	67330343	67330522	1.50	5.50	3.00	51.50	100.00	67330442	0.6
AR.N20.VII.1711980	chr5	67425146	67425395	2.90	20.60	0.00	38.70	75.00	67425223	0.9
AR.N20.VII.1711981	chr5	68362424	68362568	1.50	10.60	0.00	31.20	100.00	68362480	0.6
AR.N20.VII.1711982	chr5	70914805	70915189	3.60	12.90	0.00	38.50	66.70	70914925	1
AR.N20.VII.1711983	chr5	71080149	71080345	2.10	9.70	0.00	45.50	100.00	71080265	0.7
AR.N20.VII.1711984	chr5	71342031	71342293	4.10	19.30	1.10	42.50	89.20	71342132	1.1
AR.N20.VII.1711985	chr5	72938041	72938203	1.50	21.20	0.00	62.50	80.00	72938091	0.6
AR.N20.VII.1711986	chr5	73330126	73330367	3.60	25.90	0.00	43.60	100.00	73330226	1.2
AR.N20.VII.1711987	chr5	74165282	74165443	1.40	10.00	0.00	40.00	100.00	74165370	0.5
AR.N20.VII.1711988	chr5	74606209	74606346	1.30	18.60	0.00	42.90	100.00	74606318	0.6
AR.N20.VII.1711989	chr5	75827915	75828183	2.60	12.40	0.00	60.70	88.20	75828076	0.8
AR.N20.VII.1711990	chr5	75879160	75879385	2.40	8.40	1.00	55.40	71.40	75879243	0.7
AR.N20.VII.1711991	chr5	76660514	76660770	5.50	19.40	0.90	48.70	91.20	76660637	1.3
AR.N20.VII.1711992	chr5	76780991	76781144	2.00	9.30	0.00	50.00	100.00	76781106	0.7
AR.N20.VII.1711993	chr5	77426790	77426991	3.30	46.50	0.00	42.90	93.30	77426897	1.2
AR.N20.VII.1711994	chr5	79460736	79460905	2.30	6.60	0.00	40.00	100.00	79460759	0.9
AR.N20.VII.1711995	chr5	80308464	80308620	1.20	4.30	0.00	46.20	100.00	80308566	0.6
AR.N20.VII.1711996	chr5	81342351	81342509	1.10	15.90	0.00	33.30	100.00	81342462	0.7
AR.N20.VII.1711997	chr5	81496572	81496852	2.70	4.30	0.00	44.80	69.20	81496698	0.7
AR.N20.VII.1711998	chr5	90860463	90860668	1.40	19.90	0.00	60.00	66.70	90860584	0.6
AR.N20.VII.1711999	chr5	93723292	93723553	4.10	11.70	0.00	60.00	88.90	93723406	1.2
AR.N20.VII.1712000	chr5	93765014	93765264	7.90	112.80	0.00	61.20	82.70	93765153	2
AR.N20.VII.1712001	chr5	93979564	93979828	2.60	4.10	0.00	42.90	91.70	93979704	0.9
AR.N20.VII.1712002	chr5	95003398	95003633	6.20	29.70	0.00	46.30	90.30	95003490	1.4
AR.N20.VII.1712003	chr5	95351189	95351422	8.10	28.90	0.00	52.90	91.30	95351301	1.7
AR.N20.VII.1712004	chr5	95700163	95700308	2.10	14.60	0.00	43.50	80.00	95700212	0.7
AR.N20.VII.1712005	chr5	96862839	96863093	3.70	26.60	0.00	45.00	94.40	96862994	1.1
AR.N20.VII.1712006	chr5	104188694	104188875	3.40	15.90	0.00	47.20	100.00	104188785	1.2
AR.N20.VII.1712007	chr5	105262499	105262682	2.40	17.30	0.00	50.00	92.30	105262605	0.7
AR.N20.VII.1712008	chr5	106581473	106581662	2.00	13.90	0.00	33.30	85.70	106581583	0.7
AR.N20.VII.1712009	chr5	109351692	109351826	2.10	29.20	0.00	36.40	100.00	109351749	0.8
AR.N20.VII.1712010	chr5	109421807	109421976	1.50	10.60	0.00	37.50	100.00	109421932	0.6
AR.N20.VII.1712011	chr5	111145759	111145980	2.10	15.30	0.00	56.50	92.30	111145849	0.5
AR.N20.VII.1712012	chr5	113696156	113696363	1.70	4.80	0.00	27.80	80.00	113696271	0.6
AR.N20.VII.1712013	chr5	113837257	113837428	2.20	7.80	2.10	70.20	100.00	113837337	0.7
AR.N20.VII.1712014	chr5	114202717	114202930	4.20	14.90	0.00	37.80	94.10	114202785	1.2
AR.N20.VII.1712015	chr5	114854192	114854550	4.80	17.30	0.00	48.10	92.00	114854373	1.2
AR.N20.VII.1712016	chr5	114922276	114922503	1.90	8.90	0.00	50.00	100.00	114922397	0.6
AR.N20.VII.1712017	chr5	117742644	117742814	1.50	21.90	3.00	60.60	80.00	117742706	0.5
AR.N20.VII.1712018	chr5	118634513	118634828	3.30	46.50	0.00	37.10	100.00	118634662	0.9
AR.N20.VII.1712019	chr5	118816694	118816927	1.90	13.30	0.00	65.00	76.90	118816760	0.6
AR.N20.VII.1712020	chr5	119416857	119417069	15.70	111.50	0.00	54.80	88.00	119416934	3.6
AR.N20.VII.1712021	chr5	119447820	119448018	2.10	8.70	0.00	47.80	100.00	119447934	0.8
AR.N20.VII.1712022	chr5	121100737	121100910	2.20	31.30	2.50	50.90	100.00	121100826	0.8
AR.N20.VII.1712023	chr5	121141203	121141391	2.70	9.60	0.00	55.20	93.80	121141329	0.9
AR.N20.VII.1712024	chr5	121367844	121368104	3.10	29.30	12.30	47.10	93.60	121368029	0.9
AR.N20.VII.1712025	chr5	122761170	122761482	3.80	23.80	3.50	45.00	87.30	122761347	1
AR.N20.VII.1712026	chr5	123937267	123937436	1.70	6.00	0.00	50.00	90.00	123937385	0.7
AR.N20.VII.1712027	chr5	124019598	124019842	3.70	26.60	0.00	57.50	73.90	124019711	1.1
AR.N20.VII.1712028	chr5	124053329	124053627	3.10	22.40	2.20	44.40	93.30	124053448	1.2
AR.N20.VII.1712029	chr5	125546773	125547043	1.90	8.90	0.00	52.40	72.70	125546890	0.5
AR.N20.VII.1712030	chr5	126245817	126245943	1.90	13.30	0.00	30.00	100.00	126245912	0.7
AR.N20.VII.1712031	chr5	127013278	127013465	1.50	21.20	0.00	56.20	100.00	127013395	0.6
AR.N20.VII.1712032	chr5	127191148	127191297	1.50	21.20	0.00	35.30	100.00	127191225	0.7
AR.N20.VII.1712033	chr5	127680761	127680955	2.30	33.20	0.00	65.40	88.20	127680855	0.7
AR.N20.VII.1712034	chr5	128337532	128337769	2.10	9.70	0.00	50.00	90.90	128337647	0.9
AR.N20.VII.1712035	chr5	130523846	130524001	4.30	30.50	0.00	40.40	94.70	130523906	1.6
AR.N20.VII.1712036	chr5	130624593	130624795	2.70	38.50	0.00	34.50	100.00	130624678	1.1
AR.N20.VII.1712037	chr5	131665580	131665760	2.90	13.70	0.00	48.40	100.00	131665725	0.9
AR.N20.VII.1712038	chr5	132653680	132653912	3.20	11.30	0.00	41.20	92.90	132653832	1.6
AR.N20.VII.1712039	chr5	133830060	133830280	2.50	7.30	1.20	51.20	78.60	133830136	0.8
AR.N20.VII.1712040	chr5	134913715	134913857	1.50	21.20	0.00	50.00	100.00	134913811	0.7

regionID	chrom	start	stop	RPM	fold	multi%	plus%	leftPlus%	peakPos	peakHeight
AR.N20.VII.1712041	chr5	135314875	135315147	9.20	43.80	0.00	43.00	100.00	135315033	2.5
AR.N20.VII.1712042	chr5	136556038	136556380	4.20	19.90	0.00	51.10	78.30	136556179	1
AR.N20.VII.1712043	chr5	136679653	136679831	2.70	18.00	0.00	62.10	94.40	136679739	1.1
AR.N20.VII.1712044	chr5	136767642	136767908	2.10	9.70	0.00	45.50	100.00	136767808	0.6
AR.N20.VII.1712045	chr5	136988624	136988863	3.40	24.60	1.40	40.50	93.30	136988722	1.2
AR.N20.VII.1712046	chr5	137912313	137912518	2.30	11.10	0.00	72.00	83.30	137912433	0.8
AR.N20.VII.1712047	chr5	137973267	137973433	1.60	7.70	2.90	48.60	64.70	137973306	0.6
AR.N20.VII.1712048	chr5	139596025	139596295	4.60	16.30	0.00	51.00	96.00	139596170	1.2
AR.N20.VII.1712049	chr5	140726198	140726584	4.00	11.10	7.20	54.10	100.00	140726492	1.4
AR.N20.VII.1712050	chr5	142113035	142113314	4.70	33.20	0.00	54.00	92.60	142113169	1.3
AR.N20.VII.1712051	chr5	142177821	142178142	2.00	9.30	0.00	33.30	57.10	142177935	0.7
AR.N20.VII.1712052	chr5	142921052	142921292	7.00	49.80	0.00	52.00	97.40	142921229	1.8
AR.N20.VII.1712053	chr5	145262240	145262538	3.30	15.50	0.00	51.40	83.30	145262354	0.9
AR.N20.VII.1712054	chr5	145379983	145380204	6.00	42.50	1.60	53.10	97.10	145380091	1.4
AR.N20.VII.1712055	chr5	147271285	147271562	22.70	162.00	0.00	47.20	94.90	147271408	6.5
AR.N20.VII.1712056	chr5	147501420	147501705	5.50	78.30	0.00	47.50	57.10	147501558	1.4
AR.N20.VII.1712057	chr5	147758168	147758401	3.00	21.20	0.00	40.60	92.30	147758317	1.2
AR.N20.VII.1712058	chr5	148201429	148201668	4.20	20.10	0.70	49.60	95.70	148201560	1.4
AR.N20.VII.1712059	chr5	148326173	148326427	5.50	17.40	0.00	55.90	87.90	148326302	1.5
AR.N20.VII.1712060	chr5	148379013	148379237	2.40	34.50	3.80	34.60	100.00	148379147	0.6
AR.N20.VII.1712061	chr5	148960681	148960950	2.90	20.60	0.00	37.50	91.70	148960917	0.8
AR.N20.VII.1712062	chr5	149079589	149079700	1.20	17.30	0.00	46.20	100.00	149079669	0.5
AR.N20.VII.1712063	chr5	149217384	149217573	4.00	9.40	1.20	51.80	95.50	149217485	1.2
AR.N20.VII.1712064	chr5	149356353	149356571	4.20	30.20	1.10	52.70	100.00	149356474	1.1
AR.N20.VII.1712065	chr5	150774368	150774702	6.70	19.10	0.00	58.30	64.30	150774474	1.8
AR.N20.VII.1712066	chr5	156030318	156030492	3.10	14.60	0.00	66.70	90.90	156030400	1.4
AR.N20.VII.1712067	chr5	158545930	158546181	2.70	19.30	0.00	37.90	81.80	158546037	0.8
AR.N20.VII.1712068	chr5	158756751	158756920	1.80	8.40	0.00	47.40	88.90	158756792	0.6
AR.N20.VII.1712069	chr5	160531882	160532087	3.20	45.80	6.30	56.00	81.90	160531940	1
AR.N20.VII.1712070	chr5	160552729	160552971	4.00	28.50	0.00	44.20	94.70	160552836	1.1
AR.N20.VII.1712071	chr5	163150997	163151185	2.10	29.20	0.00	60.90	71.40	163151064	0.6
AR.N20.VII.1712072	chr5	163877778	163877999	2.10	30.50	0.00	39.10	88.90	163877935	0.9
AR.N20.VII.1712073	chr5	164687276	164687434	1.60	11.30	0.00	47.10	62.50	164687337	0.6
AR.N20.VII.1712074	chr5	165167953	165168190	1.90	26.60	0.00	60.00	75.00	165168070	0.6
AR.N20.VII.1712075	chr5	165422390	165422622	4.30	61.10	0.00	50.00	87.00	165422496	1.1
AR.N20.VII.1712076	chr5	165640486	165640751	2.00	5.70	1.60	60.90	61.50	165640570	0.6
AR.N20.VII.1712077	chr5	167712881	167713117	11.50	54.40	0.00	48.40	82.00	167713001	3.6
AR.N20.VII.1712078	chr5	169293383	169293574	3.30	23.20	0.00	54.30	100.00	169293455	1
AR.N20.VII.1712079	chr5	171742999	171743336	2.50	9.00	0.00	66.70	61.10	171743083	0.8
AR.N20.VII.1712080	chr5	172371280	172371489	7.80	55.80	0.00	49.40	92.90	172371387	2.3
AR.N20.VII.1712081	chr5	172831992	172832189	3.90	18.60	0.00	50.00	81.00	172832066	1.3
AR.N20.VII.1712082	chr5	174068978	174069168	10.90	154.70	0.40	50.20	89.80	174069076	3.7
AR.N20.VII.1712083	chr5	174957414	174957706	13.20	20.90	0.40	52.70	62.40	174957521	2.9
AR.N20.VII.1712084	chr5	176304023	176304190	1.80	12.60	0.00	36.80	100.00	176304150	0.5
AR.N20.VII.1712085	chr5	177254189	177254565	2.90	4.30	93.70	53.10	100.00	177254507	0.9
AR.N20.VII.1712086	chr5	177691298	177691587	3.20	5.70	1.40	63.80	59.10	177691422	0.7
AR.N20.VII.1712087	chr5	178109187	178109392	4.10	23.10	24.10	57.50	80.00	178109280	1.2
AR.N20.VII.1712088	chr5	178665776	178665928	1.70	11.90	0.00	33.30	100.00	178665901	0.8
AR.N20.VII.1712089	chr5	179266590	179266746	1.40	5.10	3.20	61.30	100.00	179266711	0.7
AR.N20.VII.1712090	chr5	179955134	179955464	5.40	6.40	0.90	53.00	67.20	179955314	1.3
AR.N20.VII.1712091	chr5	180006729	180007043	3.50	10.10	5.30	52.60	85.00	180006877	1
AR.N20.VII.1712092	chr5	180413040	180413304	1.80	5.00	0.00	65.00	84.60	180413121	0.7
AR.N20.VII.1712093	chr5	180533207	180533337	1.30	7.20	26.80	52.40	69.90	180533233	0.6
AR.N20.VII.1712094	chr5	180547283	180547503	1.90	4.10	35.40	52.30	47.50	180547303	0.5
AR.N20.VII.1712095	chr5	180548012	180548140	2.00	4.60	5.70	55.30	91.50	180548082	0.7
AR.N20.VII.1712096	chr5	180566424	180566564	2.10	13.10	45.70	62.70	57.70	180566466	0.7
AR.N20.VII.1712097	chr5	180582001	180582143	1.30	5.10	30.40	50.20	70.80	180582079	0.6
AR.N20.VII.1712098	chr5	180623363	180623579	4.50	53.10	0.00	37.50	94.40	180623459	1.7
AR.N20.VII.1712099	chr6	1497658	1497875	2.90	10.30	0.00	50.00	75.00	1497730	0.8
AR.N20.VII.1712100	chr6	1777990	1778315	3.90	13.90	0.00	42.90	77.80	1778116	1.2
AR.N20.VII.1712101	chr6	1784013	1784191	1.70	23.90	0.00	61.10	81.80	1784085	0.6
AR.N20.VII.1712102	chr6	3095317	3095454	1.70	6.00	0.00	27.80	100.00	3095387	0.7
AR.N20.VII.1712103	chr6	3452063	3452263	2.80	40.20	0.80	57.00	76.80	3452143	0.9
AR.N20.VII.1712104	chr6	3615186	3615383	2.00	5.60	0.00	42.90	88.90	3615306	0.7
AR.N20.VII.1712105	chr6	4683846	4684131	2.60	37.20	0.00	57.10	56.20	4683992	0.5
AR.N20.VII.1712106	chr6	5112845	5113050	4.90	70.40	0.00	54.70	82.80	5112901	1.6
AR.N20.VII.1712107	chr6	6266198	6266491	5.70	14.70	0.00	55.70	94.10	6266363	1.8
AR.N20.VII.1712108	chr6	6633608	6633901	3.20	6.50	1.40	47.80	69.70	6633687	0.8
AR.N20.VII.1712109	chr6	6695549	6695692	2.90	6.90	0.00	58.10	61.10	6695571	1.3
AR.N20.VII.1712110	chr6	7109990	7110155	1.60	5.80	0.00	54.30	89.50	7110025	0.7
AR.N20.VII.1712111	chr6	7921062	7921300	6.60	8.60	1.40	52.80	76.30	7921131	2.1
AR.N20.VII.1712112	chr6	8504276	8504482	4.40	15.60	0.00	48.90	82.60	8504359	1
AR.N20.VII.1712113	chr6	9061107	9061390	1.70	12.30	2.70	45.90	88.20	9061308	0.6
AR.N20.VII.1712114	chr6	9571560	9571848	2.10	15.30	0.00	58.30	71.40	9571734	0.5
AR.N20.VII.1712115	chr6	10619433	10619610	1.80	8.40	0.00	36.80	100.00	10619530	0.7
AR.N20.VII.1712116	chr6	10790844	10791106	4.60	21.70	0.00	49.00	95.80	10791029	1.4
AR.N20.VII.1712117	chr6	11041418	11041686	3.60	22.50	0.50	55.50	71.70	11041533	0.9
AR.N20.VII.1712118	chr6	11058320	11058664	3.90	27.90	0.00	64.30	74.10	11058486	0.9
AR.N20.VII.1712119	chr6	11396287	11396627	5.30	12.60	0.00	36.80	90.50	11396461	1.2
AR.N20.VII.1712120	chr6	13146732	13146901	1.30	18.60	0.00	64.30	100.00	13146812	0.5
AR.N20.VII.1712121	chr6	15561933	15562128	2.70	9.70	0.70	58.20	94.10	15562056	0.8
AR.N20.VII.1712122	chr6	18549585	18549763	1.50	10.60	0.00	43.80	100.00	18549735	0.6
AR.N20.VII.1712123	chr6	21293273	21293459	1.30	18.60	0.00	57.10	100.00	21293415	0.5
AR.N20.VII.1712124	chr6	21433584	21433729	2.10	29.50	5.40	36.50	73.20	21433609	0.7
AR.N20.VII.1712125	chr6	21475893	21476103	2.70	38.50	0.00	62.10	61.10	21475942	1

regionID	chrom	start	stop	RPM	fold	multi%	plus%	leftPlus%	peakPos	peakHeight
AR.N20.VII.1712126	chr6	21665207	21665453	2.10	29.20	0.00	40.90	100.00	21665349	0.6
AR.N20.VII.1712127	chr6	22629330	22629557	3.10	43.80	0.00	39.40	84.60	22629439	0.9
AR.N20.VII.1712128	chr6	24694262	24694390	1.10	4.60	26.00	26.60	100.00	24694325	0.6
AR.N20.VII.1712129	chr6	25069182	25069549	3.00	21.20	0.00	50.00	100.00	25069504	0.6
AR.N20.VII.1712130	chr6	25438233	25438505	6.60	47.10	0.00	53.50	89.50	25438367	1.5
AR.N20.VII.1712131	chr6	25555589	25555732	1.90	26.60	0.00	40.00	87.50	25555659	0.6
AR.N20.VII.1712132	chr6	26394710	26394816	2.10	5.30	50.30	50.90	100.00	26394789	0.7
AR.N20.VII.1712133	chr6	26413615	26413764	1.40	4.10	62.70	58.50	93.30	26413729	0.5
AR.N20.VII.1712134	chr6	26421279	26421479	1.90	6.10	47.20	59.40	74.80	26421345	0.6
AR.N20.VII.1712135	chr6	26438510	26438611	1.50	7.00	59.20	40.70	100.00	26438575	0.7
AR.N20.VII.1712136	chr6	26439605	26439801	2.60	5.80	31.20	56.40	100.00	26439715	0.7
AR.N20.VII.1712137	chr6	26661672	26661827	1.40	4.70	37.90	41.00	100.00	26661748	0.5
AR.N20.VII.1712138	chr6	26677041	26677142	1.10	5.00	17.60	55.50	85.10	26677098	0.6
AR.N20.VII.1712139	chr6	27182229	27182402	4.60	16.30	0.00	42.90	100.00	27182356	2.1
AR.N20.VII.1712140	chr6	27233852	27234009	1.50	6.20	50.30	64.10	92.20	27233917	0.6
AR.N20.VII.1712141	chr6	27369624	27369739	1.40	10.00	0.00	43.80	71.40	27369642	0.6
AR.N20.VII.1712142	chr6	27373722	27373867	1.50	4.90	61.60	46.80	97.90	27373801	0.5
AR.N20.VII.1712143	chr6	27408702	27408824	1.50	5.00	62.10	61.60	98.90	27408788	0.5
AR.N20.VII.1712144	chr6	27668543	27668707	2.60	10.60	39.60	42.20	91.60	27668657	0.9
AR.N20.VII.1712145	chr6	27978189	27978364	1.50	5.00	62.10	40.20	100.00	27978303	0.5
AR.N20.VII.1712146	chr6	28288748	28288941	2.20	4.40	32.20	58.30	60.00	28288799	0.6
AR.N20.VII.1712147	chr6	28534357	28534525	2.20	31.90	0.00	45.80	100.00	28534465	0.9
AR.N20.VII.1712148	chr6	28673098	28673259	1.80	4.80	62.80	35.40	67.20	28673128	0.5
AR.N20.VII.1712149	chr6	28733952	28734083	1.90	11.90	16.40	47.90	100.00	28734051	0.8
AR.N20.VII.1712150	chr6	28749565	28749697	1.90	10.20	35.00	44.00	100.00	28749670	0.6
AR.N20.VII.1712151	chr6	28818711	28818830	1.20	13.40	66.30	29.90	100.00	28818754	0.5
AR.N20.VII.1712152	chr6	28871698	28871831	1.30	12.10	19.20	55.50	73.90	28871715	0.6
AR.N20.VII.1712153	chr6	28892947	28893077	1.50	7.10	15.40	67.60	89.30	28893011	0.7
AR.N20.VII.1712154	chr6	28939353	28939565	1.90	4.90	29.50	42.10	100.00	28939511	0.8
AR.N20.VII.1712155	chr6	28957103	28957224	1.30	12.10	63.30	57.60	67.10	28957162	0.7
AR.N20.VII.1712156	chr6	29016730	29016941	2.60	9.40	21.10	56.40	91.60	29016857	0.6
AR.N20.VII.1712157	chr6	29020285	29020426	1.40	11.40	34.50	48.10	100.00	29020395	0.5
AR.N20.VII.1712158	chr6	32481601	32481781	1.80	25.20	0.00	57.90	63.60	32481621	0.6
AR.N20.VII.1712159	chr6	33789679	33789835	1.20	8.60	0.00	61.50	100.00	33789783	0.5
AR.N20.VII.1712160	chr6	33792995	33793214	2.40	8.60	0.00	53.80	92.90	33793127	1.1
AR.N20.VII.1712161	chr6	33806452	33806698	1.40	6.60	0.00	40.00	100.00	33806586	0.7
AR.N20.VII.1712162	chr6	34622525	34622743	3.10	6.30	0.00	54.50	94.40	34622666	0.8
AR.N20.VII.1712163	chr6	34671492	34671842	2.60	5.30	0.00	46.40	46.20	34671665	0.8
AR.N20.VII.1712164	chr6	34674569	34674769	3.20	22.60	0.00	58.80	95.00	34674669	1
AR.N20.VII.1712165	chr6	35677682	35677950	4.40	7.80	0.00	53.20	100.00	35677870	1.6
AR.N20.VII.1712166	chr6	35686671	35686940	7.50	21.20	0.00	57.50	97.80	35686835	1.8
AR.N20.VII.1712167	chr6	35798230	35798530	17.30	61.60	0.30	51.50	81.20	35798420	3.2
AR.N20.VII.1712168	chr6	35801420	35801673	2.40	4.80	0.00	38.50	70.00	35801537	0.6
AR.N20.VII.1712169	chr6	35803684	35804066	13.40	17.40	0.00	48.60	74.30	35803869	3.7
AR.N20.VII.1712170	chr6	35807719	35807891	6.90	19.60	0.00	44.60	75.80	35807771	2.9
AR.N20.VII.1712171	chr6	35854307	35854450	1.60	5.60	0.00	58.80	100.00	35854403	0.7
AR.N20.VII.1712172	chr6	35858237	35858429	5.10	10.40	0.00	52.70	82.80	35858352	1.5
AR.N20.VII.1712173	chr6	36425111	36425360	3.20	11.30	0.00	50.00	100.00	36425317	0.7
AR.N20.VII.1712174	chr6	36755274	36755445	2.50	9.00	0.00	40.70	81.80	36755368	0.9
AR.N20.VII.1712175	chr6	37049021	37049233	1.60	11.30	0.00	64.70	100.00	37049156	0.6
AR.N20.VII.1712176	chr6	37073775	37074073	1.90	5.30	0.00	45.00	66.70	37073859	0.5
AR.N20.VII.1712177	chr6	38246012	38246225	2.10	4.20	0.00	27.30	100.00	38246108	0.7
AR.N20.VII.1712178	chr6	38933660	38933905	2.20	10.60	0.00	58.30	64.30	38933750	0.7
AR.N20.VII.1712179	chr6	40472458	40472693	1.60	5.70	0.00	60.60	90.90	40472578	0.5
AR.N20.VII.1712180	chr6	41823244	41823640	3.50	7.20	0.00	34.20	69.20	41823493	0.8
AR.N20.VII.1712181	chr6	42121549	42121668	1.40	5.00	0.00	33.30	100.00	42121621	0.7
AR.N20.VII.1712182	chr6	42336827	42336943	1.30	6.20	0.00	53.30	75.00	42336894	0.6
AR.N20.VII.1712183	chr6	44639097	44639365	4.30	7.70	1.40	63.60	76.40	44639211	1.2
AR.N20.VII.1712184	chr6	44715853	44716108	1.50	21.20	0.00	50.00	87.50	44716012	0.6
AR.N20.VII.1712185	chr6	46897404	46897627	5.70	81.00	0.00	50.80	100.00	46897491	1.7
AR.N20.VII.1712186	chr6	49740569	49740835	6.10	43.50	0.80	51.10	67.20	49740640	1.5
AR.N20.VII.1712187	chr6	49982598	49982766	1.30	9.00	3.70	32.30	100.00	49982728	0.6
AR.N20.VII.1712188	chr6	51675761	51675877	1.10	5.30	0.00	66.70	87.50	51675816	0.6
AR.N20.VII.1712189	chr6	51816305	51816602	2.40	34.50	0.00	57.70	80.00	51816494	0.7
AR.N20.VII.1712190	chr6	51985981	51986163	3.90	55.80	0.00	42.90	100.00	51986039	1.6
AR.N20.VII.1712191	chr6	53113315	53113521	6.20	44.50	0.00	55.20	100.00	53113415	2.4
AR.N20.VII.1712192	chr6	53273849	53274010	2.10	30.50	0.00	73.90	76.50	53273908	0.8
AR.N20.VII.1712193	chr6	53406403	53406616	2.50	11.90	0.00	59.30	62.50	53406436	0.7
AR.N20.VII.1712194	chr6	53668443	53668608	4.50	31.90	0.00	56.20	100.00	53668551	1.5
AR.N20.VII.1712195	chr6	53677530	53677754	3.40	24.20	1.40	45.20	100.00	53677693	0.8
AR.N20.VII.1712196	chr6	53783977	53784186	1.90	13.30	0.00	35.00	85.70	53784108	0.6
AR.N20.VII.1712197	chr6	53916286	53916470	1.20	4.30	0.00	53.80	100.00	53916443	0.5
AR.N20.VII.1712198	chr6	55484013	55484191	2.60	18.60	0.00	59.60	88.20	55484102	0.9
AR.N20.VII.1712199	chr6	56487315	56487486	2.00	14.30	2.30	46.50	80.00	56487398	0.7
AR.N20.VII.1712200	chr6	57100618	57100795	5.30	38.00	2.10	54.10	98.40	57100708	1.8
AR.N20.VII.1712201	chr6	57351526	57351705	1.10	8.00	0.00	25.00	100.00	57351658	0.6
AR.N20.VII.1712202	chr6	57946589	57946787	5.10	39.70	17.00	53.50	88.60	57946670	1.6
AR.N20.VII.1712203	chr6	58551500	58551717	2.50	23.70	34.80	57.10	84.80	58551605	0.8
AR.N20.VII.1712204	chr6	62803866	62804146	2.40	34.50	0.00	53.80	78.60	62804000	0.7
AR.N20.VII.1712205	chr6	64260453	64260678	2.80	8.00	0.00	56.70	94.10	64260590	0.8
AR.N20.VII.1712206	chr6	68058919	68059094	2.40	11.50	0.00	57.70	100.00	68058980	0.8
AR.N20.VII.1712207	chr6	75520416	75520586	1.60	22.60	0.00	47.10	100.00	75520525	0.6
AR.N20.VII.1712208	chr6	76179895	76180095	1.50	21.20	0.00	43.80	100.00	76179999	0.6
AR.N20.VII.1712209	chr6	77183273	77183450	1.90	13.30	0.00	75.00	80.00	77183365	0.6
AR.N20.VII.1712210	chr6	79443072	79443309	1.60	14.90	41.90	54.70	73.40	79443147	0.7

regionID	chrom	start	stop	RPM	fold	multi%	plus%	leftPlus%	peakPos	peakHeight
AR.N20.VII.1712211	chr6	80585626	80585821	3.30	23.20	0.00	42.90	100.00	80585723	1.4
AR.N20.VII.1712212	chr6	82796818	82797011	2.50	35.80	0.00	63.00	58.80	82796873	0.7
AR.N20.VII.1712213	chr6	84661488	84661637	2.00	27.90	0.00	40.90	100.00	84661595	0.6
AR.N20.VII.1712214	chr6	86182676	86182874	2.10	29.20	0.00	50.00	90.90	86182736	0.6
AR.N20.VII.1712215	chr6	86674688	86674880	1.70	8.10	18.40	58.10	95.30	86674764	0.5
AR.N20.VII.1712216	chr6	90707836	90708030	4.10	58.40	0.00	50.00	86.40	90707925	1.3
AR.N20.VII.1712217	chr6	91135488	91135648	4.00	28.50	0.00	63.60	89.30	91135562	1.4
AR.N20.VII.1712218	chr6	93572806	93573022	8.40	39.80	0.00	55.60	96.00	93572898	2.3
AR.N20.VII.1712219	chr6	93871755	93871910	1.00	14.60	0.00	72.70	75.00	93871809	0.6
AR.N20.VII.1712220	chr6	94706917	94707207	7.70	110.20	0.00	62.70	61.50	94706989	2
AR.N20.VII.1712221	chr6	96099878	96100077	2.40	11.50	0.00	50.00	84.60	96099993	0.5
AR.N20.VII.1712222	chr6	97960818	97960960	1.10	5.30	0.00	33.30	100.00	97960880	0.5
AR.N20.VII.1712223	chr6	105856780	105857136	4.00	8.20	0.00	65.10	92.90	105857027	1.3
AR.N20.VII.1712224	chr6	105880975	105881139	2.20	15.90	0.00	66.70	75.00	105881017	0.8
AR.N20.VII.1712225	chr6	106624168	106624328	2.00	5.60	0.00	57.10	100.00	106624239	0.8
AR.N20.VII.1712226	chr6	106652281	106652481	4.70	22.10	0.00	40.00	95.00	106652379	1.5
AR.N20.VII.1712227	chr6	106690785	106690966	2.30	4.70	0.00	52.00	92.30	106690897	0.9
AR.N20.VII.1712228	chr6	107197132	107197477	4.00	26.50	13.40	52.90	81.10	107197212	1.6
AR.N20.VII.1712229	chr6	108218589	108218703	1.10	8.00	0.00	33.30	100.00	108218610	0.8
AR.N20.VII.1712230	chr6	109017180	109017406	4.50	15.90	0.00	56.20	100.00	109017363	1.2
AR.N20.VII.1712231	chr6	109798824	109798964	1.40	19.90	0.00	62.50	80.00	109798844	0.7
AR.N20.VII.1712232	chr6	110232610	110232801	1.40	19.90	0.00	62.50	80.00	110232705	0.6
AR.N20.VII.1712233	chr6	110244421	110244642	1.30	7.40	0.00	57.10	87.50	110244580	0.6
AR.N20.VII.1712234	chr6	110817739	110818027	2.00	4.70	5.50	63.40	78.80	110817862	0.5
AR.N20.VII.1712235	chr6	110945068	110945182	1.20	8.60	0.00	61.50	87.50	110945088	0.6
AR.N20.VII.1712236	chr6	111051135	111051327	2.10	7.30	0.00	45.50	100.00	111051282	0.8
AR.N20.VII.1712237	chr6	112869606	112869829	2.40	34.50	0.00	53.80	100.00	112869712	0.7
AR.N20.VII.1712238	chr6	112900347	112900554	2.70	19.30	0.00	55.20	93.80	112900451	0.8
AR.N20.VII.1712239	chr6	113557465	113557704	2.20	10.60	0.00	45.80	100.00	113557602	0.7
AR.N20.VII.1712240	chr6	114473926	114474082	2.90	8.20	1.60	58.10	61.10	114473962	0.9
AR.N20.VII.1712241	chr6	116539466	116539655	2.00	24.80	1.60	65.60	57.10	116539484	0.7
AR.N20.VII.1712242	chr6	116558427	116558646	1.80	25.20	0.00	63.20	100.00	116558567	0.6
AR.N20.VII.1712243	chr6	119564445	119564667	3.80	27.20	2.30	45.10	89.20	119564554	1.2
AR.N20.VII.1712244	chr6	122201905	122202091	2.70	19.60	1.70	40.70	100.00	122202008	1
AR.N20.VII.1712245	chr6	123134224	123134421	1.40	6.60	0.00	46.70	57.10	123134278	0.6
AR.N20.VII.1712246	chr6	125105844	125106121	2.30	6.50	2.00	49.00	83.30	125106006	0.9
AR.N20.VII.1712247	chr6	125517809	125517986	1.60	11.30	0.00	35.30	83.30	125517902	0.5
AR.N20.VII.1712248	chr6	126143059	126143198	1.60	6.30	53.00	29.80	95.80	126143124	0.6
AR.N20.VII.1712249	chr6	127495540	127495670	2.80	39.80	0.00	36.70	100.00	127495614	1.5
AR.N20.VII.1712250	chr6	127952054	127952250	3.10	11.00	0.00	61.80	85.70	127952138	1.3
AR.N20.VII.1712251	chr6	130371047	130371253	1.70	23.70	15.90	36.40	84.60	130371106	0.6
AR.N20.VII.1712252	chr6	131497318	131497495	1.50	10.60	0.00	62.50	100.00	131497438	0.6
AR.N20.VII.1712253	chr6	131588837	131589112	3.10	14.60	0.00	63.60	61.90	131588927	0.7
AR.N20.VII.1712254	chr6	131911352	131911540	1.60	11.30	0.00	70.00	92.90	131911491	0.9
AR.N20.VII.1712255	chr6	134993341	134993584	2.30	11.10	0.00	60.00	60.00	134993409	0.7
AR.N20.VII.1712256	chr6	135690187	135690399	1.80	12.60	0.00	47.40	100.00	135690293	0.6
AR.N20.VII.1712257	chr6	136701419	136701515	1.20	17.30	0.00	69.20	100.00	136701467	0.8
AR.N20.VII.1712258	chr6	137536883	137537088	2.70	38.50	0.00	62.10	100.00	137537000	0.9
AR.N20.VII.1712259	chr6	138236208	138236451	3.80	27.20	0.00	56.10	73.90	138236296	0.9
AR.N20.VII.1712260	chr6	138621906	138622188	7.70	54.80	0.60	49.10	88.90	138622059	1.7
AR.N20.VII.1712261	chr6	138855816	138855987	1.90	26.60	0.00	55.00	90.90	138855905	0.7
AR.N20.VII.1712262	chr6	139738139	139738429	2.40	11.50	0.00	53.80	85.70	139738253	0.7
AR.N20.VII.1712263	chr6	139848601	139848783	2.10	30.50	0.00	52.20	83.30	139848673	0.7
AR.N20.VII.1712264	chr6	142713251	142713422	2.90	41.20	0.00	41.90	100.00	142713336	1.1
AR.N20.VII.1712265	chr6	142738974	142739109	2.20	15.90	0.00	66.70	93.80	142739052	1
AR.N20.VII.1712266	chr6	144313727	144313903	1.00	6.30	0.00	54.50	83.30	144313816	0.6
AR.N20.VII.1712267	chr6	144774381	144774642	2.10	15.30	0.00	60.90	42.90	144774452	0.5
AR.N20.VII.1712268	chr6	145505854	145506084	3.20	45.10	0.00	64.70	100.00	145506029	0.9
AR.N20.VII.1712269	chr6	146532136	146532298	1.80	25.20	0.00	63.20	83.30	146532206	0.7
AR.N20.VII.1712270	chr6	147440111	147440321	2.60	12.40	0.00	50.00	71.40	147440207	0.8
AR.N20.VII.1712271	chr6	148620797	148620955	1.40	10.20	2.20	58.70	88.90	148620847	0.7
AR.N20.VII.1712272	chr6	150683210	150683469	8.90	42.00	0.00	54.20	94.20	150683360	2.4
AR.N20.VII.1712273	chr6	151387677	151387815	1.10	16.40	0.00	51.40	100.00	151387753	0.5
AR.N20.VII.1712274	chr6	151388042	151388272	3.70	13.30	0.00	52.50	100.00	151388173	1.1
AR.N20.VII.1712275	chr6	152719685	152719818	2.40	11.30	2.00	58.50	74.20	152719725	0.7
AR.N20.VII.1712276	chr6	156963181	156963365	1.90	27.20	2.40	56.10	100.00	156963303	0.6
AR.N20.VII.1712277	chr6	157179413	157179590	1.90	6.60	0.00	50.00	70.00	157179483	0.7
AR.N20.VII.1712278	chr6	157214009	157214203	1.50	10.60	0.00	75.00	75.00	157214090	0.6
AR.N20.VII.1712279	chr6	159149584	159149694	1.00	7.30	0.00	63.60	100.00	159149600	0.7
AR.N20.VII.1712280	chr6	160294659	160294869	1.90	8.90	0.00	40.00	87.50	160294748	0.7
AR.N20.VII.1712281	chr6	160513833	160514093	3.00	42.50	0.00	62.50	65.00	160513917	0.7
AR.N20.VII.1712282	chr6	160619947	160620121	1.80	12.60	0.00	31.60	66.70	160619999	0.5
AR.N20.VII.1712283	chr6	161295426	161295570	2.10	14.60	6.80	37.00	100.00	161295489	0.9
AR.N20.VII.1712284	chr6	163835269	163835528	2.80	13.30	0.00	53.30	87.50	163835417	0.8
AR.N20.VII.1712285	chr6	165885761	165885988	2.40	17.30	0.00	63.00	100.00	165885938	0.8
AR.N20.VII.1712286	chr6	165980630	165980893	3.20	9.20	1.40	44.90	87.10	165980722	0.9
AR.N20.VII.1712287	chr6	165981390	165981485	1.40	19.90	0.00	33.30	100.00	165981450	0.6
AR.N20.VII.1712288	chr6	166420768	166421044	8.80	15.70	0.50	48.20	95.70	166420980	1.7
AR.N20.VII.1712289	chr6	166538370	166538603	2.00	9.30	0.00	68.20	86.70	166538444	0.8
AR.N20.VII.1712290	chr6	167326250	167326450	2.60	7.40	0.00	46.40	100.00	167326380	1.2
AR.N20.VII.1712291	chr6	168050479	168050772	3.20	5.60	0.00	50.00	88.20	168050586	0.8
AR.N20.VII.1712292	chr6	168558317	168558544	4.40	15.60	0.00	45.80	90.90	168558464	1.4
AR.N20.VII.1712293	chr6	168670678	168670795	1.50	7.10	0.00	43.80	100.00	168670755	0.7
AR.N20.VII.1712294	chr6	168793258	168793543	4.50	12.70	0.00	43.80	95.20	168793398	1.2
AR.N20.VII.1712295	chr6	168976965	168977158	3.70	13.30	0.00	30.00	91.70	168977104	1.5

regionID	chrom	start	stop	RPM	fold	multi%	plus%	leftPlus%	peakPos	peakHeight
AR.N20.VII.1712296	chr6	169061932	169062076	4.20	59.70	0.00	44.40	65.00	169061968	1.3
AR.N20.VII.1712297	chr6_random	1464426	1464621	3.00	5.30	0.00	50.00	62.50	1464501	0.9
AR.N20.VII.1712298	chr7	1103409	1103640	4.70	13.30	0.00	46.00	95.70	1103534	1.6
AR.N20.VII.1712299	chr7	2837137	2837333	2.80	19.90	0.00	63.30	94.70	2837256	0.8
AR.N20.VII.1712300	chr7	2866843	2867083	7.30	17.30	0.00	60.30	93.60	2866951	1.9
AR.N20.VII.1712301	chr7	3526395	3526631	3.50	25.20	0.00	51.30	90.00	3526516	0.9
AR.N20.VII.1712302	chr7	4012960	4013094	2.10	15.30	0.00	65.20	100.00	4013058	0.9
AR.N20.VII.1712303	chr7	5206525	5206724	2.50	17.90	0.00	60.70	94.10	5206650	0.7
AR.N20.VII.1712304	chr7	5501895	5502122	3.70	8.90	0.00	56.10	91.30	5502022	0.9
AR.N20.VII.1712305	chr7	6275757	6275959	2.70	19.30	0.00	72.40	71.40	6275823	0.8
AR.N20.VII.1712306	chr7	7693106	7693316	2.70	12.80	0.00	62.10	100.00	7693223	0.8
AR.N20.VII.1712307	chr7	11234851	11235007	3.30	15.50	0.00	51.40	100.00	11234942	1.2
AR.N20.VII.1712308	chr7	11456497	11456777	3.40	12.30	0.00	60.50	60.90	11456553	0.8
AR.N20.VII.1712309	chr7	12721965	12722200	3.70	53.10	0.00	50.00	85.00	12722081	1.3
AR.N20.VII.1712310	chr7	12947769	12947967	2.80	39.80	0.00	60.00	100.00	12947874	1.2
AR.N20.VII.1712311	chr7	16284404	16284492	1.20	8.90	0.00	70.00	78.60	16284431	0.7
AR.N20.VII.1712312	chr7	19269955	19270196	1.50	5.30	0.00	31.20	100.00	19270023	0.5
AR.N20.VII.1712313	chr7	20600189	20600416	7.10	50.50	0.00	48.70	91.90	20600299	2.2
AR.N20.VII.1712314	chr7	20628086	20628204	1.30	18.60	0.00	73.30	63.60	20628123	0.6
AR.N20.VII.1712315	chr7	22011282	22011433	3.00	42.50	0.00	53.10	94.10	22011357	1.2
AR.N20.VII.1712316	chr7	22356998	22357212	2.50	11.90	0.00	51.90	100.00	22357093	0.7
AR.N20.VII.1712317	chr7	23107014	23107134	1.40	10.00	0.00	43.80	57.10	23107032	0.7
AR.N20.VII.1712318	chr7	23987894	23988176	2.80	20.20	1.60	62.30	100.00	23988137	0.6
AR.N20.VII.1712319	chr7	25255977	25256302	4.70	16.60	0.00	62.00	80.60	25256132	1.2
AR.N20.VII.1712320	chr7	25626409	25626639	3.20	15.30	1.40	49.30	94.10	25626513	0.9
AR.N20.VII.1712321	chr7	25669164	25669407	1.70	4.80	0.00	44.40	75.00	25669274	0.6
AR.N20.VII.1712322	chr7	25947239	25947379	2.40	17.30	0.00	53.80	92.90	25947340	1
AR.N20.VII.1712323	chr7	26419598	26419847	4.20	19.90	0.00	64.40	96.60	26419776	1.3
AR.N20.VII.1712324	chr7	27127102	27127338	2.10	10.20	0.00	56.50	92.30	27127207	0.7
AR.N20.VII.1712325	chr7	27532431	27532562	1.30	9.30	0.00	50.00	100.00	27532535	0.7
AR.N20.VII.1712326	chr7	27942682	27942999	2.70	38.50	0.00	37.90	54.50	27942747	0.7
AR.N20.VII.1712327	chr7	28011685	28011805	1.00	4.90	0.00	63.60	100.00	28011776	0.5
AR.N20.VII.1712328	chr7	28970307	28970573	2.70	5.40	1.80	50.90	100.00	28970446	1.1
AR.N20.VII.1712329	chr7	29218967	29219228	3.50	8.30	62.40	52.50	97.40	29219122	1
AR.N20.VII.1712330	chr7	30261300	30261432	1.30	9.30	0.00	50.00	85.70	30261321	0.5
AR.N20.VII.1712331	chr7	30540151	30540438	2.10	7.30	0.00	45.50	100.00	30540286	0.6
AR.N20.VII.1712332	chr7	30976779	30977050	7.00	16.70	0.70	57.60	90.80	30976902	2
AR.N20.VII.1712333	chr7	34204595	34204816	4.00	28.20	1.20	49.40	81.00	34204699	1
AR.N20.VII.1712334	chr7	34242216	34242543	8.40	39.70	35.30	52.40	72.30	34242363	1.9
AR.N20.VII.1712335	chr7	36134822	36135014	2.80	5.70	0.00	43.30	92.30	36134901	1
AR.N20.VII.1712336	chr7	36193062	36193289	5.90	27.90	0.00	50.80	87.50	36193171	1.8
AR.N20.VII.1712337	chr7	37677724	37677896	5.40	25.40	0.90	42.70	92.00	37677799	2.1
AR.N20.VII.1712338	chr7	42046276	42046392	1.50	7.10	0.00	31.20	80.00	42046298	0.6
AR.N20.VII.1712339	chr7	42076328	42076471	1.40	10.00	0.00	26.70	100.00	42076419	0.8
AR.N20.VII.1712340	chr7	44418266	44418405	1.20	8.60	0.00	46.20	100.00	44418320	0.7
AR.N20.VII.1712341	chr7	45930601	45930762	1.70	8.00	0.00	27.80	80.00	45930689	0.6
AR.N20.VII.1712342	chr7	46780807	46780948	1.40	19.90	0.00	46.70	85.70	46780868	0.6
AR.N20.VII.1712343	chr7	47260569	47260759	3.90	7.00	0.00	50.00	95.20	47260649	1.6
AR.N20.VII.1712344	chr7	47476807	47477007	3.10	21.90	0.00	63.60	85.70	47476925	1
AR.N20.VII.1712345	chr7	47545037	47545230	2.00	7.00	0.00	38.10	87.50	47545132	0.7
AR.N20.VII.1712346	chr7	47764086	47764270	2.80	5.70	0.00	53.30	68.80	47764153	0.8
AR.N20.VII.1712347	chr7	47983066	47983403	2.40	11.50	0.00	34.60	77.80	47983196	0.5
AR.N20.VII.1712348	chr7	48116428	48116735	3.80	13.60	0.00	43.90	100.00	48116622	1.2
AR.N20.VII.1712349	chr7	48305558	48305662	1.10	15.90	0.00	58.30	100.00	48305604	0.6
AR.N20.VII.1712350	chr7	49649385	49649550	1.80	25.20	0.00	40.00	75.00	49649444	0.6
AR.N20.VII.1712351	chr7	50543971	50544142	4.10	57.80	1.10	65.50	78.90	50544070	1.4
AR.N20.VII.1712352	chr7	50921383	50921549	1.90	27.00	6.60	51.60	100.00	50921492	0.7
AR.N20.VII.1712353	chr7	51641986	51642135	1.70	11.90	16.70	50.00	100.00	51642089	0.6
AR.N20.VII.1712354	chr7	51649075	51649296	2.20	10.60	0.00	70.80	76.50	51649198	0.6
AR.N20.VII.1712355	chr7	55110839	55110961	1.90	6.60	0.00	50.00	100.00	55110934	0.8
AR.N20.VII.1712356	chr7	55212929	55213281	10.50	18.70	0.40	58.10	78.80	55213089	1.8
AR.N20.VII.1712357	chr7	55467177	55467340	1.30	9.30	0.00	35.30	100.00	55467292	0.6
AR.N20.VII.1712358	chr7	56095980	56096166	2.30	5.90	33.60	50.20	100.00	56096090	0.8
AR.N20.VII.1712359	chr7	64095355	64095556	1.30	9.00	11.10	37.00	100.00	64095509	0.6
AR.N20.VII.1712360	chr7	64168711	64168919	3.10	21.90	88.90	52.70	89.90	64168804	1.2
AR.N20.VII.1712361	chr7	64862835	64863065	3.40	19.50	81.90	48.50	87.40	64862927	1.2
AR.N20.VII.1712362	chr7	66572804	66573134	9.70	138.10	0.00	52.80	91.10	66572997	2.9
AR.N20.VII.1712363	chr7	68699087	68699266	1.60	11.30	0.00	47.10	87.50	68699173	0.6
AR.N20.VII.1712364	chr7	68964223	68964387	2.00	9.30	0.00	66.70	71.40	68964287	0.8
AR.N20.VII.1712365	chr7	69566561	69566717	2.40	34.50	0.00	34.60	100.00	69566640	1
AR.N20.VII.1712366	chr7	72665092	72665315	4.10	14.40	1.10	56.30	91.80	72665226	1.3
AR.N20.VII.1712367	chr7	72802156	72802379	4.00	17.30	13.00	43.80	99.30	72802270	1.2
AR.N20.VII.1712368	chr7	75716747	75716993	9.50	19.30	0.50	51.20	96.20	75716861	3.1
AR.N20.VII.1712369	chr7	77135028	77135295	5.60	19.90	0.00	58.30	97.10	77135209	1.8
AR.N20.VII.1712370	chr7	79677752	79677967	1.90	13.60	2.40	43.90	100.00	79677912	0.6
AR.N20.VII.1712371	chr7	79745375	79745531	1.20	17.30	0.00	69.20	77.80	79745422	0.7
AR.N20.VII.1712372	chr7	80079139	80079346	1.60	11.30	0.00	64.70	90.90	80079273	0.5
AR.N20.VII.1712373	chr7	82734351	82734592	1.60	22.60	0.00	58.80	70.00	82734431	0.5
AR.N20.VII.1712374	chr7	86434292	86434457	1.60	11.30	0.00	66.70	58.30	86434360	0.5
AR.N20.VII.1712375	chr7	86811750	86811913	2.00	27.90	0.00	57.10	83.30	86811839	0.6
AR.N20.VII.1712376	chr7	89427514	89427645	4.00	57.10	0.00	51.20	100.00	89427618	1.7
AR.N20.VII.1712377	chr7	89534523	89534666	3.10	44.00	0.40	59.00	49.60	89534545	1
AR.N20.VII.1712378	chr7	89694615	89694829	4.50	31.90	0.00	46.90	95.70	89694758	1.5
AR.N20.VII.1712379	chr7	89698626	89698831	4.60	33.00	3.50	66.80	100.00	89698761	1.2
AR.N20.VII.1712380	chr7	90173636	90173840	3.80	54.40	0.00	51.20	95.20	90173736	1.4

regionID	chrom	start	stop	RPM	fold	multi%	plus%	leftPlus%	peakPos	peakHeight
AR.N20.VII.1712381	chr7	90832860	90833008	1.40	6.60	0.00	46.70	85.70	90832935	0.6
AR.N20.VII.1712382	chr7	91032723	91033287	6.00	8.50	1.60	43.80	80.40	91033106	1.7
AR.N20.VII.1712383	chr7	91719945	91720133	2.70	12.80	0.00	62.10	100.00	91720046	1
AR.N20.VII.1712384	chr7	92670796	92671006	3.40	16.20	1.40	58.70	100.00	92670941	1.3
AR.N20.VII.1712385	chr7	95012309	95012417	1.70	23.90	0.00	61.10	90.90	95012356	1
AR.N20.VII.1712386	chr7	95017458	95017756	8.90	31.50	0.00	46.90	77.80	95017569	2.5
AR.N20.VII.1712387	chr7	95054298	95054473	1.60	22.60	0.00	64.70	81.80	95054418	0.6
AR.N20.VII.1712388	chr7	95423045	95423269	4.30	30.50	0.00	41.30	94.70	95423194	1.2
AR.N20.VII.1712389	chr7	95816849	95817168	3.30	6.60	2.90	57.10	70.00	95816965	0.8
AR.N20.VII.1712390	chr7	95975790	95975936	1.40	19.90	0.00	66.70	80.00	95975870	0.7
AR.N20.VII.1712391	chr7	97641620	97641913	3.40	6.80	0.00	52.80	89.50	97641764	0.9
AR.N20.VII.1712392	chr7	98916651	98916878	1.40	19.90	0.00	66.70	100.00	98916781	0.5
AR.N20.VII.1712393	chr7	99262918	99263079	4.50	21.20	0.00	43.80	81.00	99262971	1.1
AR.N20.VII.1712394	chr7	99385436	99385644	1.60	22.30	10.60	69.20	74.20	99385580	0.7
AR.N20.VII.1712395	chr7	101092537	101092927	4.50	32.20	99.00	56.40	68.80	101092664	1
AR.N20.VII.1712396	chr7	101371913	101372082	2.60	9.30	0.00	64.30	88.90	101372002	0.7
AR.N20.VII.1712397	chr7	102417013	102417097	1.10	15.90	0.00	33.30	75.00	102417033	0.7
AR.N20.VII.1712398	chr7	103613091	103613348	3.70	26.20	3.80	61.70	68.00	103613203	1
AR.N20.VII.1712399	chr7	104218838	104219040	1.80	25.20	0.00	31.60	100.00	104218987	0.6
AR.N20.VII.1712400	chr7	104795232	104795480	3.80	17.90	1.20	38.50	100.00	104795422	0.8
AR.N20.VII.1712401	chr7	105390714	105390916	3.00	10.60	0.00	56.20	66.70	105390773	1
AR.N20.VII.1712402	chr7	105634653	105634817	1.60	4.50	0.00	50.00	55.60	105634734	0.6
AR.N20.VII.1712403	chr7	105644975	105645171	9.10	43.40	0.00	52.50	61.50	105645026	2.5
AR.N20.VII.1712404	chr7	107213726	107213905	3.30	23.20	2.90	60.00	100.00	107213843	1.1
AR.N20.VII.1712405	chr7	107239756	107239949	9.40	33.40	1.50	49.30	89.90	107239854	3.3
AR.N20.VII.1712406	chr7	108038958	108039201	2.10	7.30	0.00	54.50	75.00	108039073	0.5
AR.N20.VII.1712407	chr7	108042006	108042171	1.80	12.90	2.60	41.00	100.00	108042102	0.7
AR.N20.VII.1712408	chr7	109708809	109708934	2.10	14.60	0.00	56.50	61.50	109708835	0.7
AR.N20.VII.1712409	chr7	111230706	111230911	1.60	22.60	0.00	41.20	100.00	111230872	0.7
AR.N20.VII.1712410	chr7	111989387	111989621	5.40	19.30	0.00	47.50	100.00	111989496	2.4
AR.N20.VII.1712411	chr7	113141757	113141925	2.80	20.10	0.30	60.30	89.00	113141826	1.1
AR.N20.VII.1712412	chr7	115105350	115105507	1.70	11.90	0.00	44.40	87.50	115105450	0.5
AR.N20.VII.1712413	chr7	115744613	115744822	3.00	10.60	0.00	34.40	81.80	115744726	0.8
AR.N20.VII.1712414	chr7	116215917	116216105	2.10	29.20	0.00	63.60	92.90	116216009	0.7
AR.N20.VII.1712415	chr7	116463379	116463559	1.30	18.60	0.00	60.00	77.80	116463496	0.5
AR.N20.VII.1712416	chr7	117334744	117335018	2.90	10.30	0.00	32.30	100.00	117334965	0.8
AR.N20.VII.1712417	chr7	118899783	118899916	1.00	14.60	0.00	72.70	100.00	118899870	0.5
AR.N20.VII.1712418	chr7	119870025	119870162	3.00	14.20	0.00	40.60	100.00	119870133	1.1
AR.N20.VII.1712419	chr7	121037595	121037756	1.40	10.00	0.00	73.30	90.90	121037665	0.6
AR.N20.VII.1712420	chr7	122626388	122626608	1.90	26.60	0.00	50.00	100.00	122626478	0.6
AR.N20.VII.1712421	chr7	124129425	124129578	1.50	21.20	0.00	68.80	81.80	124129512	0.6
AR.N20.VII.1712422	chr7	124347115	124347252	1.30	18.60	0.00	71.40	60.00	124347150	0.6
AR.N20.VII.1712423	chr7	127093975	127094109	1.00	7.30	0.00	54.50	83.30	127094022	0.5
AR.N20.VII.1712424	chr7	127657174	127657376	1.60	5.80	2.90	54.30	78.90	127657307	0.5
AR.N20.VII.1712425	chr7	128571571	128571806	2.40	6.90	0.00	65.40	82.40	128571656	1.1
AR.N20.VII.1712426	chr7	129795920	129796132	6.20	21.90	0.00	51.50	73.50	129796001	2.6
AR.N20.VII.1712427	chr7	130619998	130620382	5.30	25.20	0.00	40.40	95.70	130620254	1.3
AR.N20.VII.1712428	chr7	131435922	131436049	2.70	37.80	1.80	71.90	100.00	131435998	1
AR.N20.VII.1712429	chr7	132718552	132718744	3.40	47.80	0.00	58.30	100.00	132718663	1.7
AR.N20.VII.1712430	chr7	134915434	134915610	2.00	27.90	0.00	47.60	100.00	134915540	0.6
AR.N20.VII.1712431	chr7	135298159	135298349	1.70	8.00	0.00	57.90	63.60	135298223	0.6
AR.N20.VII.1712432	chr7	135489121	135489344	2.40	8.60	0.00	34.60	100.00	135489281	0.7
AR.N20.VII.1712433	chr7	135738062	135738202	1.30	8.30	11.90	66.70	78.60	135738089	0.7
AR.N20.VII.1712434	chr7	136916975	136917184	2.90	41.20	0.00	41.90	100.00	136917090	0.7
AR.N20.VII.1712435	chr7	137431857	137432128	2.90	41.20	0.00	35.50	100.00	137432037	0.7
AR.N20.VII.1712436	chr7	138446515	138446728	2.10	29.20	0.00	63.60	64.30	138446536	0.8
AR.N20.VII.1712437	chr7	138675892	138676077	1.40	7.50	28.70	54.20	83.70	138675982	0.6
AR.N20.VII.1712438	chr7	139071390	139071647	3.40	16.40	0.00	54.10	50.00	139071444	0.8
AR.N20.VII.1712439	chr7	141512761	141512932	2.00	27.90	0.00	61.90	100.00	141512844	0.6
AR.N20.VII.1712440	chr7	142276224	142276411	4.50	8.00	0.00	47.90	91.30	142276325	1.4
AR.N20.VII.1712441	chr7	142302585	142302766	2.10	30.50	0.00	34.80	100.00	142302677	0.6
AR.N20.VII.1712442	chr7	142410220	142410420	3.60	12.90	0.00	48.70	100.00	142410316	1.1
AR.N20.VII.1712443	chr7	142919860	142919991	1.00	14.60	0.00	58.30	71.40	142919881	0.6
AR.N20.VII.1712444	chr7	143054133	143054499	5.70	11.60	99.20	54.10	78.80	143054314	1.1
AR.N20.VII.1712445	chr7	143144439	143144805	5.70	11.60	99.20	54.10	78.80	143144620	1.1
AR.N20.VII.1712446	chr7	143959927	143960052	1.50	7.20	0.00	57.10	100.00	143959978	0.6
AR.N20.VII.1712447	chr7	145544448	145544583	1.90	13.30	0.00	55.00	72.70	145544486	0.7
AR.N20.VII.1712448	chr7	145982129	145982245	2.30	33.20	0.00	61.50	100.00	145982218	0.8
AR.N20.VII.1712449	chr7	146320398	146320598	1.40	9.60	9.20	59.50	94.50	146320495	0.6
AR.N20.VII.1712450	chr7	147610472	147610677	2.60	12.40	0.00	46.40	100.00	147610575	0.9
AR.N20.VII.1712451	chr7	149688361	149688618	4.50	31.80	6.00	49.60	90.50	149688508	1.5
AR.N20.VII.1712452	chr7	150064103	150064294	3.90	27.40	0.80	63.70	88.60	150064206	1.4
AR.N20.VII.1712453	chr7	151096805	151096946	1.70	8.00	0.00	44.40	100.00	151096888	0.6
AR.N20.VII.1712454	chr7	151251612	151251859	3.80	18.20	0.40	49.00	95.00	151251788	1.1
AR.N20.VII.1712455	chr7	154901096	154901246	1.20	8.60	0.00	46.20	100.00	154901141	0.6
AR.N20.VII.1712456	chr7	156389091	156389276	6.40	10.20	0.00	42.00	100.00	156389189	2.1
AR.N20.VII.1712457	chr7	156978551	156978755	5.50	15.70	0.00	52.50	51.60	156978614	1.5
AR.N20.VII.1712458	chr8	512936	513115	1.50	4.20	0.00	56.20	100.00	512972	0.8
AR.N20.VII.1712459	chr8	1095222	1095356	2.00	13.90	0.00	45.50	100.00	1095324	0.7
AR.N20.VII.1712460	chr8	1882590	1882856	5.20	12.40	0.00	44.60	100.00	1882766	1.2
AR.N20.VII.1712461	chr8	6279174	6279405	2.30	16.60	0.00	48.00	100.00	6279346	0.7
AR.N20.VII.1712462	chr8	6377145	6377391	2.50	6.00	0.00	66.70	100.00	6377229	0.8
AR.N20.VII.1712463	chr8	6444419	6444620	1.70	24.30	1.80	58.60	91.20	6444514	0.6
AR.N20.VII.1712464	chr8	7297069	7297374	2.10	6.80	97.80	39.10	88.90	7297223	0.5
AR.N20.VII.1712465	chr8	7754028	7754337	2.10	6.80	97.80	63.00	65.50	7754184	0.5

regionID	chrom	start	stop	RPM	fold	multi%	plus%	leftPlus%	peakPos	peakHeight
AR.N20.VII.1712466	chr8	10383021	10383247	2.30	16.60	0.00	48.00	91.70	10383182	0.7
AR.N20.VII.1712467	chr8	11181751	11181994	2.20	31.90	0.00	50.00	100.00	11181842	0.6
AR.N20.VII.1712468	chr8	12697268	12697467	3.40	16.10	0.90	58.70	95.30	12697389	1
AR.N20.VII.1712469	chr8	17968604	17968867	2.00	9.30	0.00	52.40	63.60	17968626	0.6
AR.N20.VII.1712470	chr8	18081555	18081713	2.00	13.90	0.00	71.40	100.00	18081629	0.8
AR.N20.VII.1712471	chr8	18824512	18824705	1.70	4.80	5.60	58.30	52.40	18824593	0.6
AR.N20.VII.1712472	chr8	18856689	18856943	8.20	22.40	0.60	48.00	92.90	18856796	2.1
AR.N20.VII.1712473	chr8	19595943	19596118	2.00	13.90	0.00	47.60	50.00	19596008	0.6
AR.N20.VII.1712474	chr8	19596280	19596355	1.00	14.60	0.00	54.50	100.00	19596328	0.6
AR.N20.VII.1712475	chr8	22754133	22754329	4.00	14.30	0.00	53.50	82.60	22754263	1.4
AR.N20.VII.1712476	chr8	22936236	22936456	4.30	10.20	0.00	45.70	81.00	22936312	1.1
AR.N20.VII.1712477	chr8	23557172	23557514	7.50	21.30	0.40	49.80	85.00	23557334	1.7
AR.N20.VII.1712478	chr8	24216379	24216462	1.40	8.70	18.40	31.80	100.00	24216435	0.8
AR.N20.VII.1712479	chr8	24371452	24371598	1.10	5.30	0.00	41.70	100.00	24371517	0.6
AR.N20.VII.1712480	chr8	25273334	25273621	1.70	4.80	0.00	50.00	66.70	25273430	0.5
AR.N20.VII.1712481	chr8	25321677	25321897	10.00	23.70	0.00	54.60	91.50	25321811	2.4
AR.N20.VII.1712482	chr8	25392062	25392265	2.50	11.90	0.00	42.90	91.70	25392170	0.8
AR.N20.VII.1712483	chr8	26179438	26179648	2.00	5.60	0.00	59.10	92.30	26179569	0.6
AR.N20.VII.1712484	chr8	26358863	26359110	3.50	10.10	0.00	63.20	91.70	26359013	0.9
AR.N20.VII.1712485	chr8	27195957	27196182	7.80	110.90	0.60	52.10	77.00	27196041	2.2
AR.N20.VII.1712486	chr8	27312152	27312358	1.80	6.30	0.00	63.20	75.00	27312253	0.6
AR.N20.VII.1712487	chr8	27392520	27392786	5.20	12.10	3.30	69.00	87.00	27392658	2
AR.N20.VII.1712488	chr8	27509381	27509658	4.20	59.70	0.00	40.00	83.30	27509496	1.4
AR.N20.VII.1712489	chr8	28061631	28061852	1.90	13.50	1.60	50.80	100.00	28061717	0.5
AR.N20.VII.1712490	chr8	28261784	28261872	1.00	14.60	0.00	45.50	80.00	28261804	0.5
AR.N20.VII.1712491	chr8	30700141	30700269	1.40	19.90	0.00	26.70	100.00	30700187	0.7
AR.N20.VII.1712492	chr8	35633051	35633288	4.00	19.00	0.00	58.10	88.00	35633141	1.1
AR.N20.VII.1712493	chr8	37283844	37284014	2.30	6.60	0.00	56.00	100.00	37283948	0.7
AR.N20.VII.1712494	chr8	37287351	37287538	1.40	10.00	0.00	53.30	100.00	37287444	0.5
AR.N20.VII.1712495	chr8	37880583	37880836	2.20	6.40	0.00	62.50	93.30	37880718	0.8
AR.N20.VII.1712496	chr8	38291146	38291360	4.10	57.80	1.10	51.70	95.70	38291274	1.4
AR.N20.VII.1712497	chr8	38977969	38978145	2.00	27.90	0.00	75.00	94.40	38978075	0.8
AR.N20.VII.1712498	chr8	39808791	39809065	20.70	73.70	0.50	50.20	89.30	39808925	6.1
AR.N20.VII.1712499	chr8	41575039	41575179	1.50	10.60	0.00	75.00	83.30	41575073	0.6
AR.N20.VII.1712500	chr8	41586833	41587042	3.10	11.00	0.00	57.60	84.20	41586890	1.1
AR.N20.VII.1712501	chr8	41986947	41987113	5.00	71.70	0.00	46.30	60.00	41986968	1.9
AR.N20.VII.1712502	chr8	42884812	42884987	1.30	9.50	1.80	42.10	83.30	42884868	0.7
AR.N20.VII.1712503	chr8	47521845	47522062	1.90	8.90	0.00	54.40	90.90	47521999	0.5
AR.N20.VII.1712504	chr8	47601878	47602135	1.60	22.10	10.00	57.00	100.00	47602033	0.6
AR.N20.VII.1712505	chr8	48601271	48601432	3.70	10.60	0.00	35.00	100.00	48601373	1.4
AR.N20.VII.1712506	chr8	48734541	48734746	2.50	35.80	0.00	66.70	94.40	48734650	0.9
AR.N20.VII.1712507	chr8	48810295	48810507	15.80	74.80	0.00	47.50	92.90	48810384	5.5
AR.N20.VII.1712508	chr8	49724326	49724592	3.50	25.20	0.00	44.70	94.10	49724474	0.9
AR.N20.VII.1712509	chr8	49908496	49908724	2.80	13.30	0.00	50.00	73.30	49908555	0.6
AR.N20.VII.1712510	chr8	53502036	53502199	1.50	21.20	0.00	43.80	100.00	53502136	0.8
AR.N20.VII.1712511	chr8	54303130	54303315	11.10	52.70	0.00	49.60	95.00	54303218	3.1
AR.N20.VII.1712512	chr8	57094658	57094973	9.30	14.80	0.00	51.50	86.50	57094814	2.6
AR.N20.VII.1712513	chr8	57462757	57463060	3.00	14.20	0.00	68.80	50.00	57462861	0.7
AR.N20.VII.1712514	chr8	57470787	57470962	2.70	39.20	1.70	55.90	100.00	57470887	0.9
AR.N20.VII.1712515	chr8	59237229	59237445	2.20	15.90	0.00	29.20	85.70	59237326	0.7
AR.N20.VII.1712516	chr8	59361296	59361535	10.80	38.50	0.00	46.60	77.80	59361396	2.2
AR.N20.VII.1712517	chr8	59711743	59711942	2.10	15.30	0.00	55.90	61.50	59711784	0.6
AR.N20.VII.1712518	chr8	61975014	61975292	8.50	40.30	0.00	55.40	88.20	61975153	2.2
AR.N20.VII.1712519	chr8	63081241	63081486	2.60	37.20	0.00	53.40	100.00	63081376	0.6
AR.N20.VII.1712520	chr8	63733016	63733288	4.10	59.10	1.10	46.10	85.40	63733097	1.2
AR.N20.VII.1712521	chr8	64204168	64204318	1.00	14.60	0.00	27.30	100.00	64204264	0.5
AR.N20.VII.1712522	chr8	65931888	65932119	2.50	17.90	0.00	40.70	90.90	65932012	0.6
AR.N20.VII.1712523	chr8	66380027	66380236	2.00	27.90	0.00	47.60	70.00	66380118	0.7
AR.N20.VII.1712524	chr8	67188110	67188308	2.00	6.70	19.30	30.50	97.40	67188211	0.7
AR.N20.VII.1712525	chr8	69223524	69223716	1.90	26.60	0.00	40.00	100.00	69223599	0.7
AR.N20.VII.1712526	chr8	69806647	69806886	2.00	13.90	0.00	71.40	53.30	69806711	0.7
AR.N20.VII.1712527	chr8	69929252	69929497	4.20	19.90	0.00	69.60	78.10	69929393	1.1
AR.N20.VII.1712528	chr8	71742652	71742880	2.80	40.50	1.60	47.50	100.00	71742817	0.9
AR.N20.VII.1712529	chr8	72397315	72397467	2.40	17.30	0.00	61.50	81.20	72397380	1
AR.N20.VII.1712530	chr8	75651327	75651577	10.90	17.30	0.90	53.40	83.20	75651437	3.4
AR.N20.VII.1712531	chr8	77691784	77691934	1.40	19.90	0.00	66.70	90.00	77691858	0.8
AR.N20.VII.1712532	chr8	77764844	77765028	1.30	9.30	0.00	71.40	60.00	77764864	0.5
AR.N20.VII.1712533	chr8	78588000	78588210	2.90	41.20	0.00	38.70	83.30	78588044	0.9
AR.N20.VII.1712534	chr8	80981785	80981943	2.20	31.90	0.00	50.00	100.00	80981844	0.7
AR.N20.VII.1712535	chr8	81141451	81141575	1.70	8.00	0.00	38.90	85.70	81141527	0.7
AR.N20.VII.1712536	chr8	81153225	81153435	3.30	9.30	0.00	31.40	54.50	81153262	0.9
AR.N20.VII.1712537	chr8	81882773	81882937	1.00	7.30	0.00	66.70	87.50	81882819	0.6
AR.N20.VII.1712538	chr8	82198208	82198375	1.20	5.50	4.00	44.00	100.00	82198336	0.5
AR.N20.VII.1712539	chr8	82671810	82671953	1.50	21.20	6.20	37.50	100.00	82671866	0.8
AR.N20.VII.1712540	chr8	85443929	85444086	1.00	7.30	0.00	45.50	100.00	85443988	0.6
AR.N20.VII.1712541	chr8	85905222	85905470	2.60	18.60	1.20	35.30	90.00	85905340	0.8
AR.N20.VII.1712542	chr8	86412359	86412590	2.10	14.60	0.00	45.50	80.00	86412443	0.6
AR.N20.VII.1712543	chr8	87190130	87190283	1.70	11.90	0.00	61.10	72.70	87190188	0.7
AR.N20.VII.1712544	chr8	87498418	87498621	3.60	8.60	0.00	51.30	90.00	87498509	1
AR.N20.VII.1712545	chr8	90389245	90389375	2.50	35.80	3.70	37.90	100.00	90389284	1.1
AR.N20.VII.1712546	chr8	92016223	92016478	2.80	39.80	0.00	40.00	83.30	92016367	0.8
AR.N20.VII.1712547	chr8	93563310	93563525	2.10	29.20	0.00	63.60	92.90	93563417	0.9
AR.N20.VII.1712548	chr8	96041383	96041549	1.50	21.20	0.00	56.20	88.90	96041475	0.6
AR.N20.VII.1712549	chr8	96398937	96399148	3.10	44.50	1.50	59.20	52.40	96399043	0.7
AR.N20.VII.1712550	chr8	97941509	97941709	2.40	17.30	0.00	53.80	64.30	97941550	0.7

regionID	chrom	start	stop	RPM	fold	multi%	plus%	leftPlus%	peakPos	peakHeight
AR.N20.VII.1712551	chr8	98045629	98045736	1.10	11.50	4.30	34.80	75.00	98045694	0.5
AR.N20.VII.1712552	chr8	99449357	99449563	2.40	33.90	2.00	43.10	100.00	99449504	0.8
AR.N20.VII.1712553	chr8	99817310	99817522	1.30	18.60	0.00	64.30	100.00	99817437	0.5
AR.N20.VII.1712554	chr8	99994886	99995096	3.30	23.60	1.40	53.50	94.70	99994965	0.9
AR.N20.VII.1712555	chr8	100787268	100787446	5.20	74.30	0.00	51.80	100.00	100787368	1.9
AR.N20.VII.1712556	chr8	101099418	101099616	3.00	14.20	0.00	48.50	81.20	101099531	0.9
AR.N20.VII.1712557	chr8	101547285	101547472	1.70	23.90	0.00	33.30	83.30	101547385	0.6
AR.N20.VII.1712558	chr8	102359488	102359695	2.40	34.50	0.00	30.80	50.00	102359577	0.7
AR.N20.VII.1712559	chr8	102475049	102475139	1.00	7.30	0.00	45.50	100.00	102475079	0.5
AR.N20.VII.1712560	chr8	102505172	102505283	1.10	8.00	0.00	57.10	100.00	102505223	0.7
AR.N20.VII.1712561	chr8	102519898	102520150	9.20	26.30	0.00	50.50	78.40	102519967	2.8
AR.N20.VII.1712562	chr8	102586100	102586367	2.80	19.90	0.00	46.70	100.00	102586335	1.1
AR.N20.VII.1712563	chr8	102665345	102665523	2.20	15.90	0.00	58.30	92.90	102665456	0.7
AR.N20.VII.1712564	chr8	103244117	103244360	2.50	17.90	0.00	44.40	91.70	103244255	1
AR.N20.VII.1712565	chr8	103324037	103324182	1.80	25.20	0.00	42.10	87.50	103324084	0.8
AR.N20.VII.1712566	chr8	105061340	105061454	1.40	6.10	4.80	61.20	100.00	105061407	0.6
AR.N20.VII.1712567	chr8	105359957	105360203	3.40	19.60	2.30	60.60	82.10	105360079	1.5
AR.N20.VII.1712568	chr8	108696022	108696174	1.40	19.90	0.00	60.00	66.70	108696076	0.6
AR.N20.VII.1712569	chr8	112195658	112195860	3.20	22.90	1.40	53.60	83.80	112195763	1.5
AR.N20.VII.1712570	chr8	116885812	116885962	2.00	27.90	0.00	52.40	72.70	116885841	0.6
AR.N20.VII.1712571	chr8	118602262	118602515	5.20	8.30	0.00	54.40	93.50	118602420	2
AR.N20.VII.1712572	chr8	119690623	119690769	1.10	5.30	0.00	75.00	100.00	119690713	0.5
AR.N20.VII.1712573	chr8	121059000	121059134	1.30	18.60	0.00	50.00	100.00	121059037	0.6
AR.N20.VII.1712574	chr8	121298963	121299069	1.10	15.90	0.00	66.70	100.00	121299002	0.6
AR.N20.VII.1712575	chr8	121941132	121941262	1.70	11.90	0.00	33.30	100.00	121941177	0.7
AR.N20.VII.1712576	chr8	122400435	122400653	2.20	15.60	2.10	48.90	91.30	122400547	0.6
AR.N20.VII.1712577	chr8	124486974	124487243	11.50	82.00	0.40	57.50	46.50	124487041	2
AR.N20.VII.1712578	chr8	124522751	124523029	1.80	12.60	0.00	47.40	77.80	124522908	0.6
AR.N20.VII.1712579	chr8	125283084	125283319	3.10	44.50	1.50	43.30	93.10	125283179	1
AR.N20.VII.1712580	chr8	126285665	126285773	1.70	11.90	0.00	55.60	80.00	126285706	0.8
AR.N20.VII.1712581	chr8	128124685	128124843	1.30	4.60	0.00	42.90	100.00	128124773	0.6
AR.N20.VII.1712582	chr8	128930777	128930973	2.30	11.10	0.00	50.00	84.60	128930863	0.7
AR.N20.VII.1712583	chr8	128933976	128934280	2.60	12.40	0.00	53.60	80.00	128934127	0.6
AR.N20.VII.1712584	chr8	128960979	128961090	1.50	21.60	0.00	57.00	100.00	128961051	0.8
AR.N20.VII.1712585	chr8	129223268	129223600	3.70	6.60	0.00	55.00	100.00	129223498	1
AR.N20.VII.1712586	chr8	129238790	129239048	9.60	45.60	0.50	53.90	91.00	129238914	2.6
AR.N20.VII.1712587	chr8	134220850	134221053	2.00	13.90	0.00	38.10	100.00	134220962	0.7
AR.N20.VII.1712588	chr8	134536949	134537427	7.70	12.20	0.00	59.90	82.00	134537270	2.2
AR.N20.VII.1712589	chr8	135948440	135948648	3.10	5.80	0.00	57.60	84.20	135948560	1.3
AR.N20.VII.1712590	chr8	135968013	135968212	4.60	21.90	1.00	51.50	100.00	135968159	0.9
AR.N20.VII.1712591	chr8	140858768	140858927	1.40	10.00	0.00	40.00	100.00	140858862	0.6
AR.N20.VII.1712592	chr8	143755710	143756124	5.40	6.40	0.00	46.60	81.50	143755962	1.6
AR.N20.VII.1712593	chr8	144208707	144209009	2.20	10.60	16.70	49.00	74.50	144208844	0.5
AR.N20.VII.1712594	chr8	145309040	145309213	2.00	4.60	0.00	57.10	50.00	145309060	0.6
AR.N20.VII.1712595	chr9	484848	485142	2.90	13.70	0.00	62.50	95.00	485026	0.8
AR.N20.VII.1712596	chr9	561177	561411	3.10	43.80	0.00	64.70	100.00	561341	1
AR.N20.VII.1712597	chr9	2467757	2467991	2.30	16.30	2.00	59.20	48.30	2467818	0.7
AR.N20.VII.1712598	chr9	4574728	4574947	3.60	25.90	0.00	59.00	95.70	4574867	1.2
AR.N20.VII.1712599	chr9	4784876	4785066	2.10	14.60	0.00	36.40	87.50	4784924	0.6
AR.N20.VII.1712600	chr9	4793791	4793948	1.80	12.60	0.00	55.00	81.80	4793841	0.6
AR.N20.VII.1712601	chr9	4856349	4856492	1.60	22.60	5.90	61.80	95.20	4856458	0.5
AR.N20.VII.1712602	chr9	13024013	13024204	1.80	8.40	5.30	55.30	90.50	13024078	0.8
AR.N20.VII.1712603	chr9	13268426	13268760	3.00	5.30	0.00	59.40	57.90	13268544	0.6
AR.N20.VII.1712604	chr9	13478025	13478231	1.90	13.30	0.00	50.00	100.00	13478140	0.7
AR.N20.VII.1712605	chr9	14017258	14017423	6.50	15.40	0.70	39.20	100.00	14017363	2.2
AR.N20.VII.1712606	chr9	14467971	14468134	1.30	18.60	0.00	66.70	90.00	14468075	0.7
AR.N20.VII.1712607	chr9	14690567	14690813	2.10	10.20	0.00	69.60	93.80	14690721	0.6
AR.N20.VII.1712608	chr9	18198228	18198440	2.40	34.50	0.00	69.20	50.00	18198310	0.6
AR.N20.VII.1712609	chr9	22819346	22819553	1.60	11.30	0.00	41.20	100.00	22819511	0.7
AR.N20.VII.1712610	chr9	22945053	22945259	2.10	9.80	5.40	58.60	92.30	22945186	0.7
AR.N20.VII.1712611	chr9	24371298	24371583	10.20	72.50	2.00	39.20	97.70	24371457	2.1
AR.N20.VII.1712612	chr9	31325890	31326071	3.30	23.20	0.00	57.10	90.00	31325953	1.1
AR.N20.VII.1712613	chr9	33153046	33153277	8.60	40.90	0.50	54.60	86.10	33153151	2.3
AR.N20.VII.1712614	chr9	33868692	33868976	3.10	11.00	9.70	46.10	70.70	33868819	0.8
AR.N20.VII.1712615	chr9	34565852	34566006	1.60	11.30	0.00	70.60	91.70	34565963	0.7
AR.N20.VII.1712616	chr9	35647638	35648044	5.00	5.30	1.80	47.90	59.50	35647778	1
AR.N20.VII.1712617	chr9	36089826	36090038	2.90	41.20	0.00	58.10	88.90	36089938	0.9
AR.N20.VII.1712618	chr9	37046171	37046364	1.60	11.60	14.30	45.70	100.00	37046292	0.6
AR.N20.VII.1712619	chr9	37690900	37691168	2.10	30.50	0.00	60.90	92.90	37691043	0.6
AR.N20.VII.1712620	chr9	40996947	40997153	2.20	21.50	98.80	55.10	93.50	40997042	0.7
AR.N20.VII.1712621	chr9	41232055	41232262	1.70	14.30	98.10	64.20	94.30	41232156	0.7
AR.N20.VII.1712622	chr9	41812207	41812413	2.20	21.50	98.80	40.90	94.20	41812294	0.7
AR.N20.VII.1712623	chr9	43485338	43485545	1.70	14.30	98.10	64.20	94.30	43485439	0.7
AR.N20.VII.1712624	chr9	44923576	44923897	12.10	44.20	99.00	47.40	95.90	44923777	2.6
AR.N20.VII.1712625	chr9	45610367	45610688	12.10	44.20	99.00	47.40	95.90	45610568	2.6
AR.N20.VII.1712626	chr9	45996552	45996873	12.10	44.20	99.00	47.40	95.90	45996753	2.6
AR.N20.VII.1712627	chr9	46287460	46287781	12.00	42.30	99.30	50.60	66.00	46287556	2.6
AR.N20.VII.1712628	chr9	46816178	46816384	2.20	21.50	98.80	55.10	93.50	46816273	0.7
AR.N20.VII.1712629	chr9	65776819	65777019	2.20	12.90	42.70	51.70	93.30	65776913	1.2
AR.N20.VII.1712630	chr9	66972062	66972237	1.70	7.20	49.10	37.70	87.10	66972167	0.9
AR.N20.VII.1712631	chr9	67390368	67390696	11.80	41.50	98.90	49.30	64.80	67390471	2.6
AR.N20.VII.1712632	chr9	71307758	71307970	2.20	31.90	0.00	62.50	80.00	71307859	0.7
AR.N20.VII.1712633	chr9	72224746	72224936	2.20	6.40	0.00	58.30	85.70	72224839	0.7
AR.N20.VII.1712634	chr9	72285489	72285759	16.30	77.40	0.60	47.20	78.90	72285603	3.6
AR.N20.VII.1712635	chr9	72406391	72406632	5.40	10.90	0.00	43.50	96.00	72406528	2

regionID	chrom	start	stop	RPM	fold	multi%	plus%	leftPlus%	peakPos	peakHeight
AR.N20.VII.1712636	chr9	72995959	72996173	2.20	10.60	0.00	37.50	55.60	72995998	0.6
AR.N20.VII.1712637	chr9	73068178	73068567	4.30	30.50	0.00	38.40	94.40	73068428	1.5
AR.N20.VII.1712638	chr9	78604118	78604362	2.80	39.80	0.00	60.00	88.90	78604275	0.7
AR.N20.VII.1712639	chr9	82737775	82737955	2.20	15.90	0.00	54.20	92.30	82737837	0.7
AR.N20.VII.1712640	chr9	83336363	83336555	2.60	6.20	0.60	32.40	98.20	83336487	0.9
AR.N20.VII.1712641	chr9	83392949	83393147	4.20	10.00	0.00	50.00	82.60	83393024	1.7
AR.N20.VII.1712642	chr9	83619203	83619399	3.10	14.60	0.00	30.30	90.00	83619338	0.9
AR.N20.VII.1712643	chr9	84526440	84526619	2.10	14.60	0.00	39.10	100.00	84526572	0.6
AR.N20.VII.1712644	chr9	84937612	84937824	5.40	25.70	0.00	60.30	80.00	84937697	1.4
AR.N20.VII.1712645	chr9	86703044	86703164	1.30	6.20	0.00	57.10	75.00	86703078	0.6
AR.N20.VII.1712646	chr9	88210017	88210249	7.50	107.50	0.00	53.10	97.70	88210170	1.9
AR.N20.VII.1712647	chr9	91469707	91469948	10.80	22.00	0.00	44.90	88.70	91469812	2.9
AR.N20.VII.1712648	chr9	92723275	92723477	9.30	33.20	0.00	58.00	81.00	92723380	2.4
AR.N20.VII.1712649	chr9	92922365	92922599	3.80	18.10	0.00	42.90	100.00	92922556	1.1
AR.N20.VII.1712650	chr9	95937442	95937632	4.60	13.00	0.00	56.60	60.70	95937521	1.4
AR.N20.VII.1712651	chr9	96810474	96810631	1.90	13.60	2.40	39.00	87.50	96810566	1
AR.N20.VII.1712652	chr9	97523432	97523624	5.20	18.60	0.00	53.60	96.70	97523543	1.3
AR.N20.VII.1712653	chr9	97870680	97870888	4.20	29.90	0.00	37.80	100.00	97870829	1.3
AR.N20.VII.1712654	chr9	98406062	98406259	2.40	11.50	0.00	53.80	92.90	98406166	0.9
AR.N20.VII.1712655	chr9	100134560	100134749	3.30	23.60	1.40	56.30	100.00	100134700	0.9
AR.N20.VII.1712656	chr9	101627031	101627269	1.80	5.00	0.00	42.10	100.00	101627088	0.6
AR.N20.VII.1712657	chr9	102087876	102088070	2.00	14.20	1.60	37.50	100.00	102087978	0.7
AR.N20.VII.1712658	chr9	103223865	103224081	2.80	8.00	0.00	48.40	93.30	103223977	0.8
AR.N20.VII.1712659	chr9	104008581	104008841	4.70	33.20	0.00	35.30	94.40	104008751	1.3
AR.N20.VII.1712660	chr9	107374560	107374801	2.80	39.80	3.30	46.70	71.40	107374639	0.7
AR.N20.VII.1712661	chr9	109177895	109177995	1.50	21.20	0.00	68.80	100.00	109177927	0.8
AR.N20.VII.1712662	chr9	109628113	109628242	1.70	23.90	0.00	38.90	100.00	109628212	0.6
AR.N20.VII.1712663	chr9	109944943	109945154	2.00	5.60	0.00	71.40	93.30	109945067	0.6
AR.N20.VII.1712664	chr9	110370292	110370467	3.80	18.00	1.60	39.70	100.00	110370387	1.7
AR.N20.VII.1712665	chr9	110591899	110592194	5.50	39.50	0.80	50.40	73.30	110592040	1.3
AR.N20.VII.1712666	chr9	110696399	110696598	2.70	10.80	5.30	49.10	89.30	110696507	0.8
AR.N20.VII.1712667	chr9	111103236	111103441	2.40	34.50	0.00	46.20	83.30	111103339	0.8
AR.N20.VII.1712668	chr9	111690365	111690486	1.20	8.60	0.00	46.20	83.30	111690409	0.6
AR.N20.VII.1712669	chr9	111705583	111705802	7.60	36.10	0.60	54.60	80.90	111705650	2.1
AR.N20.VII.1712670	chr9	111991216	111991428	1.60	5.60	0.00	61.10	100.00	111991357	0.6
AR.N20.VII.1712671	chr9	112516493	112516790	3.90	55.80	0.00	59.50	100.00	112516654	1.3
AR.N20.VII.1712672	chr9	114199067	114199215	1.70	12.00	27.90	43.50	94.00	114199165	0.7
AR.N20.VII.1712673	chr9	114584404	114584596	3.00	19.60	0.60	40.40	85.20	114584513	1
AR.N20.VII.1712674	chr9	115283559	115283823	6.20	17.50	0.00	48.50	96.90	115283712	1.8
AR.N20.VII.1712675	chr9	115484722	115484871	1.70	4.80	0.00	66.70	100.00	115484791	0.7
AR.N20.VII.1712676	chr9	115915345	115915547	2.50	9.00	0.00	46.40	84.60	115915446	0.7
AR.N20.VII.1712677	chr9	117452139	117452335	2.30	8.30	0.00	60.00	93.30	117452284	1.1
AR.N20.VII.1712678	chr9	121670863	121671131	5.60	10.00	0.00	45.00	77.80	121670962	1.6
AR.N20.VII.1712679	chr9	122679921	122680044	1.30	6.20	0.00	57.10	100.00	122680003	0.6
AR.N20.VII.1712680	chr9	122718742	122719004	4.00	8.20	0.00	39.50	58.80	122718806	1
AR.N20.VII.1712681	chr9	122744966	122745103	2.30	33.20	0.00	56.00	92.90	122745035	0.8
AR.N20.VII.1712682	chr9	125481824	125482041	2.70	7.70	0.00	62.10	83.30	125481945	1
AR.N20.VII.1712683	chr9	125573858	125574130	4.90	69.70	1.00	54.30	100.00	125574021	1.6
AR.N20.VII.1712684	chr9	128891833	128892003	2.30	11.10	0.00	48.00	50.00	128891868	0.7
AR.N20.VII.1712685	chr9	128980833	128981045	2.30	6.50	0.00	61.20	80.00	128980927	0.9
AR.N20.VII.1712686	chr9	128999658	128999905	1.90	8.90	0.00	60.00	75.00	128999776	0.6
AR.N20.VII.1712687	chr9	129857882	129858075	1.20	5.50	4.00	60.00	93.30	129858018	0.5
AR.N20.VII.1712688	chr9	129905255	129905485	2.90	6.90	0.00	58.10	72.20	129905342	1.2
AR.N20.VII.1712689	chr9	130664551	130664795	2.20	4.60	0.00	40.00	100.00	130664714	0.7
AR.N20.VII.1712690	chr9	131234894	131235094	4.30	6.10	0.00	63.00	96.60	131234994	1.3
AR.N20.VII.1712691	chr9	132738555	132738713	2.00	9.30	0.00	57.10	100.00	132738646	0.7
AR.N20.VII.1712692	chr9	133334741	133334886	1.40	6.60	0.00	40.00	66.70	133334800	0.6
AR.N20.VII.1712693	chr9	134029621	134029843	2.70	12.80	0.00	41.40	100.00	134029782	0.7
AR.N20.VII.1712694	chr9	134954439	134954659	3.30	9.40	12.30	52.60	67.70	134954541	1
AR.N20.VII.1712695	chr9	134979871	134980050	2.10	4.90	0.00	56.50	69.20	134979966	0.8
AR.N20.VII.1712696	chr9	136314770	136315181	3.80	6.00	0.00	29.30	58.30	136314910	0.7
AR.N20.VII.1712697	chr9	136994104	136994275	1.80	13.10	3.50	69.40	69.60	136994214	0.5
AR.N20.VII.1712698	chr9	137425410	137425535	1.30	6.20	0.00	50.00	71.40	137425459	0.5
AR.N20.VII.1712699	chr9	138012626	138012908	3.60	5.40	0.90	36.50	100.00	138012795	1
AR.N20.VII.1712700	chr9	139626570	139626795	8.10	14.40	0.00	52.90	89.10	139626679	2.2
AR.N20.VII.1712701	chrX	2606697	2606921	2.80	40.20	98.40	46.20	92.90	2606833	0.8
AR.N20.VII.1712702	chrX	7002433	7002656	1.20	17.70	17.50	47.50	92.10	7002490	0.5
AR.N20.VII.1712703	chrX	9031152	9031323	1.60	11.30	0.00	47.10	62.50	9031199	0.5
AR.N20.VII.1712704	chrX	9834905	9835013	1.20	8.60	0.00	46.20	100.00	9834977	0.6
AR.N20.VII.1712705	chrX	9976952	9977262	7.60	27.20	0.00	44.00	83.80	9977052	2.2
AR.N20.VII.1712706	chrX	10867450	10867684	2.20	15.90	0.00	66.70	100.00	10867580	0.7
AR.N20.VII.1712707	chrX	11392425	11392658	3.20	45.10	0.00	58.80	60.00	11392501	0.7
AR.N20.VII.1712708	chrX	12016476	12016728	2.80	19.90	0.00	40.00	83.30	12016606	0.8
AR.N20.VII.1712709	chrX	12805416	12805648	7.70	110.20	0.00	53.60	95.60	12805528	1.9
AR.N20.VII.1712710	chrX	12992714	12993021	1.80	25.90	2.60	30.80	100.00	12992972	0.6
AR.N20.VII.1712711	chrX	15189673	15189853	3.70	26.60	0.00	70.00	78.60	15189715	1.4
AR.N20.VII.1712712	chrX	15642684	15642858	1.60	11.30	0.00	58.80	70.00	15642748	0.6
AR.N20.VII.1712713	chrX	19264847	19264988	2.60	37.20	0.00	51.70	100.00	19264907	1.4
AR.N20.VII.1712714	chrX	21662242	21662476	3.00	21.20	0.00	37.50	91.70	21662361	0.9
AR.N20.VII.1712715	chrX	22305867	22305992	1.40	19.90	0.00	33.30	100.00	22305942	0.7
AR.N20.VII.1712716	chrX	35705556	35705720	1.60	20.00	16.40	42.30	96.50	35705630	0.6
AR.N20.VII.1712717	chrX	36777561	36777788	2.50	35.80	0.00	37.00	100.00	36777668	0.6
AR.N20.VII.1712718	chrX	40709479	40709682	1.30	18.60	0.00	57.10	87.50	40709594	0.7
AR.N20.VII.1712719	chrX	43151987	43152174	1.10	6.80	89.40	58.80	93.20	43152071	0.6
AR.N20.VII.1712720	chrX	43451983	43452403	4.20	29.90	0.00	53.30	75.00	43452273	0.9

regionID	chrom	start	stop	RPM	fold	multi%	plus%	leftPlus%	peakPos	peakHeight
AR.N20.VII.1712721	chrX	48032401	48032685	1.50	8.40	24.80	61.40	75.80	48032515	0.5
AR.N20.VII.1712722	chrX	51075947	51076162	2.20	21.20	10.40	42.00	100.00	51076074	0.8
AR.N20.VII.1712723	chrX	51283033	51283271	2.20	21.20	8.30	60.40	100.00	51283151	0.7
AR.N20.VII.1712724	chrX	53117612	53117863	27.60	65.60	2.20	51.70	96.60	53117729	6.6
AR.N20.VII.1712725	chrX	54088695	54088882	1.80	25.20	0.00	60.00	83.30	54088810	0.7
AR.N20.VII.1712726	chrX	55508018	55508253	1.80	10.10	100.00	56.40	95.50	55508136	0.5
AR.N20.VII.1712727	chrX	55551266	55551501	1.80	10.40	97.40	43.60	100.00	55551384	0.5
AR.N20.VII.1712728	chrX	56044049	56044247	3.50	33.60	0.00	65.80	92.00	56044164	1.3
AR.N20.VII.1712729	chrX	64909425	64909644	4.00	20.20	39.20	60.70	94.20	64909549	1.5
AR.N20.VII.1712730	chrX	64967894	64968066	2.20	15.90	0.00	52.00	76.90	64967984	1.1
AR.N20.VII.1712731	chrX	66242068	66242271	2.50	17.90	0.00	40.70	90.90	66242193	0.8
AR.N20.VII.1712732	chrX	66883871	66883989	1.90	26.60	0.00	45.00	88.90	66883941	0.7
AR.N20.VII.1712733	chrX	68451244	68451352	1.20	8.60	0.00	38.50	100.00	68451281	0.7
AR.N20.VII.1712734	chrX	69085053	69085280	8.70	31.00	0.30	57.10	75.60	69085142	2.2
AR.N20.VII.1712735	chrX	71757213	71757484	10.50	37.50	0.00	47.80	79.60	71757310	2.4
AR.N20.VII.1712736	chrX	83108111	83108259	1.00	14.60	0.00	50.00	100.00	83108227	0.5
AR.N20.VII.1712737	chrX	96551766	96551884	1.30	18.60	0.00	66.70	90.00	96551857	0.5
AR.N20.VII.1712738	chrX	106871741	106871910	2.20	15.90	0.00	54.20	53.80	106871783	0.7
AR.N20.VII.1712739	chrX	107646305	107646455	1.30	17.90	0.00	33.30	77.80	107646341	0.5
AR.N20.VII.1712740	chrX	108809805	108810019	2.30	32.50	2.00	49.00	100.00	108809931	0.8
AR.N20.VII.1712741	chrX	109125079	109125350	2.60	12.40	0.00	50.00	100.00	109125257	0.8
AR.N20.VII.1712742	chrX	109212066	109212304	1.70	23.90	0.00	61.10	72.70	109212180	0.6
AR.N20.VII.1712743	chrX	116562006	116562134	1.10	15.90	0.00	66.70	87.50	116562061	0.6
AR.N20.VII.1712744	chrX	117602225	117602443	2.00	14.50	4.00	49.70	87.70	117602299	0.7
AR.N20.VII.1712745	chrX	121048972	121049143	1.80	12.60	0.00	73.70	78.60	121049048	0.7
AR.N20.VII.1712746	chrX	128804269	128804434	1.40	19.90	0.00	40.00	100.00	128804317	0.7
AR.N20.VII.1712747	chrX	129159290	129159476	3.20	18.40	5.50	45.60	93.70	129159346	1.4
AR.N20.VII.1712748	chrX	129164221	129164327	1.10	8.00	0.00	58.30	100.00	129164288	0.5
AR.N20.VII.1712749	chrX	130633626	130633743	1.20	8.60	0.00	30.80	50.00	130633646	0.5
AR.N20.VII.1712750	chrX	131804631	131804822	3.40	15.90	0.00	36.10	100.00	131804711	0.9
AR.N20.VII.1712751	chrX	134118853	134119071	1.60	22.10	97.00	53.00	96.20	134118951	0.5
AR.N20.VII.1712752	chrX	134176660	134176878	1.60	22.10	97.00	50.00	94.00	134176781	0.5
AR.N20.VII.1712753	chrX	138453953	138454121	2.70	12.80	0.00	65.50	100.00	138454040	0.7
AR.N20.VII.1712754	chrX	142843357	142843467	1.30	17.90	11.10	59.30	75.00	142843374	0.6
AR.N20.VII.1712755	chrX	152511700	152511927	1.50	7.10	0.00	68.80	100.00	152511834	0.5
AR.N20.VII.1712756	chrY	2606697	2606921	2.80	40.20	98.40	46.20	92.90	2606833	0.8
AR.N20.VII.1712757	chrY	7513987	7514203	2.30	22.70	65.30	51.60	82.80	7514047	0.7
AR.N20.VII.1712758	chrY	8539953	8540094	4.10	28.90	1.10	65.20	72.40	8540001	1.6
AR.N20.VII.1712759	chrY	10454718	10454909	1.70	10.90	35.50	35.50	100.00	10454872	0.6
AR.N20.VII.1712760	chrY	13150624	13150728	1.00	7.30	0.00	72.70	100.00	13150690	0.6
AR.N20.VII.1712761	chrY	19217755	19217895	1.90	26.60	97.50	42.50	100.00	19217852	0.9
AR.N20.VII.1712762	chrY	19345054	19345194	1.90	26.60	97.50	60.00	95.80	19345097	0.9
AR.N20.VII.1712763	chrY	24935962	24936157	2.00	17.50	97.70	54.80	57.20	24936003	0.5
AR.N20.VII.1712764	chrY	25845076	25845246	1.90	17.10	99.00	46.30	100.00	25845206	0.5

Appendix E

Chromatin Immunoprecipitation Protocol for LNCaP Cells Used to Generate Initial ChIP-Seq Dataset

Chromatin Immunoprecipitation of Androgen Receptor in LNCaP Cells as Performed for Chapter 4 ChIP-Seq Experiment. (adapted from Wold lab ChIP protocol[1,2] and protocol used by Nicholas G. Nickols for AR ChIP[3])

Reagents/Equipment and Vendors Utilized

LNCaP cells (ATCC Cat. No. CRL-1740)

175 cm^2 Falcon Tissue Culture Plates (BD Biosciences Cat. No. 353112)

Trypsin (Invitrogen Cat. No. 25200056)

RPMI 1640 (Invitrogen Cat. No. 21870)

Fetal Bovine Serum (Omega Scientific Cat No. FB-01)

100X L-glutamine (Invitrogen Cat. No. 25030)

50 mL conical tubes (BD Biosciences Cat. No. 352098)

15 mL conical tubes (BD Biosciences Cat. No. 352097)

25 mL pipettes (VWR Cat. No. 101093-952)

10 mL pipettes (VWR Cat. No. 101093-962)

5 mL pipettes (VWR Cat. No. 101093-976)

Phosphate buffered saline pH 7.2 (Invitrogen Cat. No. 20012)

10X PBS pH 7.4 (make from salts and autoclave)

KCl (Biology stockroom)

NaCl (Biology stockroom)

Na_2HPO_4 (Biology stockroom)

KH_2PO_4 (Biology stockroom)

15 cm BD Falcon tissue culture plates (BD Biosciences Cat. No. 353025)

Charcoal-dextran treated FBS (Omega Scientific Cat No. FB-04, Lot No. 103365)

Dihydrotestosterone (Sigma-Aldrich Cat. No. A8380; this is a schedule III drug and requires extra time/steps/approval for ordering)

1.7 mL microcentrifuge tubes (Sorensen, DNase, RNase-free, Cat. No. 11700)

Absolute Ethanol (can be purchased in the Chemistry stockroom)

16% formaldehyde (Ted Pella Product No. 18505)

Dynabeads M-280, Sheep anti-Rabbit IgG, (Invitrogen Cat. No. 112-03D for 2 mL bottle and 112-04D for 10 mL bottle)

Bovine serum albumin, fraction V (Amresco Cat. No. 0903)

Magnet (Invitrogen Cat No. 123-21D is currently manufactured)

Santa Cruz Biotech SC-816 (N-20) polyclonal antibody (1 mL vials)

Glycine (Fluka Cat. No. 50046) – use to make 2.5 M stock of glycine; store at -20 ºC

PMSF (Roche Cat. No. 10236608001)

LiCl (Sigma-Aldrich Cat. No. L9650)

$NaHCO_3$ (can be purchased Biology stockroom)

SDS (Fluka Cat. No. 71727)

Sodium deoxycholate (Sigma-Aldrich Cat. No. D6750)

Isopropanol

Razor blades (can purchase on campus at VWR stock room)

Protease inhibitor cocktail tablets: Complete, EDTA-free, Roche Cat No. 11873580001 for tablets that make 50 mL 1X and Roche Cat No. 11836170001 for tablets that make 10 mL 1X PIC (Complete, mini, EDTA-free)

Farnham Lysis Buffer

RIPA Buffer

LiCl IP Wash Buffer

Elution buffer

Tris base (Biology stockroom)

0.5M EDTA pH 8.0 (Invitrogen Cat. No. 15575-020)

Branson Sonifier S-450D

Cary UV-Vis

Disposable clear plastic cuvettes (Biology stockroom)

BSA concentration standards (Bio-Rad Cat. No. 500-0207)

1X Bradford Reagent (Bio-Rad Cat. No. 500-0205)

0.15M NaCl (make using crystalline NaCl and Millipore water)

end-over-end rotator (VWR Cat. No. 13916-822)

O-ring screw-cap microcentrifuge tubes

1X TE buffer pH 8.0 (make from Tris base and EDTA)

phenol/$CHCl_3$/isoamyl alcohol (Invitrogen Cat. No. 15593-031)

Qiagen Buffer PM (Cat. No. 19083)

Qiagen QIAquick PCR Purification Kit (Cat. No. 28104 for 50 tubes, and 28106 for 250 tubes)

FastStart Universal SYBR Green Master (Rox) (Roche Cat. No. 04913914001 for 10 x 5 mL tubes)

IDT DNA primers

USB Ultrapure water, RNase-Free, DEPC Treated (USB Cat. No. 70783)

Buffer Compositions

<u>10X PBS pH 7.4</u>

Dissolve the following into 800 mL deionized Millipore H_2O:

80 g of NaCl

2.0 g of KCl

14.4 g of Na_2HPO_4

2.4 g of KH_2PO_4

Adjust pH to 7.4.

Adjust volume to 1L in volumetric flask with additional deionized Millipore H_2O.

Sterilize by autoclaving.

<u>Farnham Lysis Buffer</u> (make in 100 mL volumetric flask)

5 mM PIPES pH 8.0 (from 100 mM PIPES pH 8.0 stock in Millipore water; sterile filter

with 0.2 μm filter)

85 mM KCl (from 850 mM KCl stock in Millipore water; sterile filter with 0.2 μm filter)

0.5% NP-40 (from 10% NP-40 stock)

Roche Complete, EDTA-free (added immediately prior to use)

RIPA Buffer (make in 100 mL volumetric flask)

1X PBS (from 10X PBS stock)

1% NP-40 (from 10% NP-40 stock in Millipore water)

0.5% Sodium Deoxycholate (from powder or from 10% stock in Millipore water; powder was used exclusively for these studies)

0.1% SDS (from 10% SDS stock in Millipore water)

Roche Complete, EDTA-free (added immediately prior to use)

LiCl IP Wash Buffer (make in 100 mL volumetric flask)

100 mM Tris (from 1 M Tris base in Millipore water; do not adjust pH after making Tris; must autoclave 1 M Tris base prior to use)

500 mM LiCl (from 5M LiCl stock in Millipore water stored at -20 ºC)

1% NP-40 (from 10% NP-40 stock in Millipore water)

1% Sodium Deoxycholate (from powder or from 10% stock in Millipore water; powder was used exclusively for these studies)

Elution buffer

1% SDS (from 10% stock in Millipore water)

0.1 M $NaHCO_3$ (from 1 M stock in Millipore water)

1X TE Buffer pH 8.0

1 mL 1M Tris-HCl pH 8.0

0.2 mL 0.5 M EDTA pH 8.0

998.8 mL Millipore water

Autoclave

Plating LNCaP Cells **Day 1**

1. 85–90% Confluent LNCaP cells grown in five 175 cm^2 Falcon plates were trypsinized by (1) decanting the RPMI 1640 from each plate, (2) rinsing each plate with 37 ºC PBS, (3) adding 5 mL trypsin, (4) decanting the trypsin from each plate, (5) incubating the plates at 37 ºC for five minutes, and (6) adding fresh, complete RPMI 1640 (Invitrogen Product No. 21870; supplemented with 10% FBS (Omega Scientific Cat No. FB-01) and 2 mM L-glutamine (Invitrogen Product No. 25030)) to collect the detached cells.
2. Detached LNCaP cells were collected in a 50 mL conical tube to give 50 mL total volume of cells. The cell suspension was aspirated in a 25 mL pipette to ensure even distribution. A 5 mL pipet is useful for disrupting clumped LNCaP cells. 10 mL of the 50 mL cell suspension was used to seed five new 175-cm^2 Falcon plates in 30 mL total volume per plate (complete RPMI 1640 used). An additional 10 mL complete RPMI 1640 was added to the 50 mL conical tube to yield a 50 mL volume once again.
3. 1 mL of the 50 mL volume was diluted to 10 mL using PBS in a separate 15 mL conical tube. The 1:10 dilution was counted by hemocytometer, and the cell concentration was noted.
4. 42 million LNCaP cells (sufficient for ~21 15-cm plates) were added to a solution of complete RPMI 1640 (defined in step 1) to give a total volume of 525 mL.
5. LNCaP cells, each at 2 million cells per plate in 25 mL complete RPMI 1640 were seeded into 15 cm tissue culture plates. A total of 20 plates were made.
6. After adding cells to each cells were dispersed by a horizontal sliding motion made along a single vector while standing.
7. Cell culture plates were placed in the 37 ºC incubator containing 5 % CO_2 and were allowed to grow for 72 hours.

Swapping Medium of LNCaP cells to CT-FBS **Day 4**

8. Cell culture plates were moved from the incubator to the cell culture hood and decanted. Each plate was carefully washed with 37 ºC PBS by angling the plate and adding PBS to the sidewall of the plate nearest the floor of the cell culture hood. The PBS was then decanted from each plate. A minimum of cells were detached resulting from the wash.
9. 25 mL RPMI 1640 (the RPMI 1640 used is Invitrogen Product No. 21870; supplemented with 10% CDT-FBS (Omega Scientific Cat No. FB-04, Lot No. 103365) and 2 mM L-glutamine (Invitrogen Product No. 25030)) was added to each plate as per the procedure in step 8, to minimize dislodging attached LNCaP cells.
10. The plates were returned to the 37 ºC, 5% CO_2 incubator for 48 hours.

Inducing LNCaP cells with Dihydrotestosterone **Day 6**

11. 500nM dihydrotestosterone (DHT) was prepared by aliquoting a 5-10 mg sample of DHT into a 1.5 mL microcentrifuge tube. 1 mL EtOH was added to the 1.5 mL microcentrifuge tube. A serial dilution ensued using absolute EtOH, with each dilution reducing DHT concentration 10-fold. The final three dilutions utilized are as follows: (1) 900 µL PBS + 100 µL previous dilution, (2) 900 µL PBS + 100 µL previous dilution, (3) (1000 – x) µL PBS + x µL previous dilution. A vehicle supplement was created as well by mimicking the final three dilutions but replacing step (1) with 900 µL PBS + 100 µL EtOH.
12. To each 25 mL plate of LNCaP cells was added 50 µL vehicle (10 plates) or 50 µL, 500 nM DHT (1 nM DHT final concentration to 10 plates).
13. Plates were allowed to incubate 16 hours with DHT treatment prior to formaldehyde fixation (step 22).

Coupling Antibody to Magnetic Beads (everything performed at 4 ºC) Day 6

14. Add 100 µL resuspended (read: VORTEX) magnetic bead slurry (Invitrogen Dynabeads M-280, Sheep anti-Rabbit IgG, Cat No. 112-03D for 2 mL bottle and 112-04D for 10 mL bottle) to 1.5 mL Eppendorf tube. (For other experiments, be sure to match the bead type to the organism of the antibody and try starting with 50 µL bead slurry).
15. Add 1 mL PBS + 5 mg/mL BSA (fraction V, prepare fresh + syringe filter; measure concentration of BSA in PBS using A_{280} = 6.61 for 10 mg / mL)
16. Place tube on magnet (Invitrogen Cat No. 123-21D is currently manufactured) for 5 minutes. Remove supernatant.
17. Add 1 mL PBS + 5 mg/mL BSA to beads. Mix on end-over-end rotator for 10 minutes.
18. Place tube on magnet for 5 minutes. Remove supernatant.
19. Repeat steps 17–18 two more times.
20. Add 10 µg of Santa Cruz Biotech SC-816 (N-20) polyclonal antibody (50 µL of 200 µg / mL) (If other antibodies, try 5 µg polyclonal antibody (25 µL of 200 µg / mL) or 1 µg of monoclonal antibody (5 uL of 200 ug / mL) to AR; inevitably titration of antibody will be necessary).
21. Allow beads to incubate with antibody for 24 hours while mixed on end-over-end rotator (16–24 hours have been utilized with good results).

Formaldehyde Cell Fixation Day 7

22. Decant medium from 15 cm plates.
23. Wash each plate with ~20 mL 37 ºC PBS.
24. To each plate add 20 mL 1% formaldehyde in RPMI 1640 (no L-glut, no FBS, no P/S, warmed to room temperature)
25. Fix at room temperature for 10 minutes on rocker.

26. Stop cross-linking reaction by adding 1 mL 2.5 M glycine (final concentration ~ 0.125 M; RPMI 1640 solution turns yellow in color)
27. Rock for 5 minutes.
28. Decant medium from plates.
29. Wash plates with ~20 mL 4 ºC PBS.
30. Add 2 mL 4 ºC PBS supplemented with 1/200 vol. 100 mM PMSF in isopropanol (PMSF added immediately before use) to each plate of cells.
31. Scrape cells off plate with razor blade, and transfer them to a conical Falcon tube on an ice-water bath (4 ºC).
32. Pellet cells at 2,000 RPM for 5 minutes (4 ºC). Decant supernatant.
33. Resuspend cell pellet in 5 mL / plate Farnham Lysis Buffer (add PIC (Roche, Protease inhibitor cocktail: Complete, EDTA-free, Cat No. 11873580001 for tablets that make 50 mL 1X and Cat No. 11836170001 for tablets that make 10 mL 1X PIC) fresh prior to use). Mix gently on rocker for 15 minutes at 4 ºC (cold room).
34. Centrifuge crude nuclear prep at 2000 RPM for 5 minutes (4 ºC). Decant. (if necessary, cell pellet can be frozen in LN_2 and stored at -80 ºC prior to use)

Sonication of Isolated Cell Pellets **Day 7**

From here down, everything is done in the Cold Room (4 ºC)

35. Resuspend pellet in 1.0 mL RIPA Buffer (add PIC fresh prior to use) and transfer to 1.7 mL Eppendorf tube.
36. Sonicate on -80 ºC EtOH bath (50 mL conical tube with EtOH stored on dry ice or in freezer). Sonicate 30 times 30 sec. (30 secs on, 30 secs off; be consistent with total number of cycles) at 25% amplitude. The EtOH bath should be switched for a fresh, cold EtOH bath every 5 sonication cycles (a cycle = 30 secs on, 30 secs off). Be careful that you do not froth the solution. Work quickly so that the initial solution does not freeze.

37. Microcentrifuge sheared solution at 14,000 RPM for 15 mins at 4 ºC. Decant supernatant to a new tube. If any of the pellet transfers to the new Eppendorf tube, repeat the centrifugation, and transfer the supernatant to a new Eppendorf tube.
38. If sheared chromatin is not to be used immediately, the samples may be frozen in LN_2 and stored at -80 ºC prior to use. To thaw frozen samples, allow them to warm in the cold room on ice. If time is short, samples may be centrifuged at 14,000 RPM for 10 mins at 4 ºC. The thawed sample should be aspirated several times to ensure it is evenly mixed.

Bradford Assay to Determine Protein Concentration (at room temperature) Day 7

39. Turn on Cary UV-Vis at least 1 h prior to use.
40. For each sample of chromatin to be measured, make a stock solution (30 μL), a 1:5 dilution (50 μL) in RIPA buffer and a 1:10 dilution (100 μL) in RIPA buffer. Make a 1 mL tube of RIPA buffer to use in the blank.
41. Use disposable clear plastic cuvettes (2 cuvettes per measured condition). For the blanks, add 10 μL RIPA buffer, 90 μL 0.15M NaCl. For the standard curve (2.0 mg/mL BSA, 1.5 mg/mL BSA, 1.0 mg/mL BSA, 0.75 mg/mL BSA, and 0.5 mg/mL BSA, all available in Bio-Rad Cat. No. 500-0207), add 10 μL standard, 10 μL RIPA buffer, and 80 μL 0.15M NaCl. For the samples to be measured, add 10 μL sample, 90 μL 0.15M NaCl. When all cuvettes are ready, add 1 mL 1X Bradford Reagent to each tube, in the order they are to be scanned (blanks, then standards, then samples). Wait at least 5 but no more than 50 minutes prior to scanning samples in the UV-Vis.
42. Open the Simple Reads application. Click setup and set the wavelength to 595 nm. Add the blank to the UV-Vis and click zero. Use the second blank to ensure the machine reads close to 0.0. Measure the standard curve first. Then measure the individual samples. If the absorbance for an individual sample does not fit within

the range of measured absorbances for the standard curve, the sample cannot be interpolated.

43. Use a linear regression to fit the standards to a line. Use the resulting least-squares fitted line to interpolate the quantity of the individual samples. Make sure to multiply the appropriate dilution factor by the resulting concentration. Each sample's concentration will be determined.

Addition of Chromatin to Antibody-incubated Beads (in 4 ºC room) Day 7

44. Wash magnetic beads from Day 6 three times (steps 17–18). Prior to pelleting on the magnet each time, briefly spin the tube(s) in the microcentrifgue (short spin to no more than 2000 RPMs).
45. To fully decanted beads, add 100 μL PBS+BSA (fresh) to beads. Add 1 mg total protein concentration (determined from steps 39-43). Add RIPA to make the total volume in the tube 1 mL.
46. Save some of the material from step 37 (50 uL is sufficient) for use as input DNA for qPCR.
47. Incubate step 45 on the end-over-end rotator at 4 ºC for 24 h (16–24 h is sufficient).

LiCl IP Wash of Chromatin-incubated Beads Day 8

Still in the cold room (4 ºC)

48. Briefly spin the tube to remove any liquid / beads from the cap of the microcentrifuge tube. Pellet on magnet for 5 minutes. Decant all of the liquid from the tube.
49. Wash pellet 5 times with 1 mL LiCl IP Wash Buffer with 10 min mixing between washes and 5 minute pellet against magnet. Prior to each pelleting, briefly centrifuge the tube to remove any liquid / beads from the cap of the microcentrifuge tube. Decant all of the liquid from the tube.

50. Wash pellet once with 1 mL TE. Spin briefly. Pellet on magnet 5 minutes. Decant all of the liquid from the tube. **Outside of cold room**
51. Resuspend beads in 200 μL IP Elution buffer. (To 50 μL input from step 46, add 150 μL IP Elution buffer)
52. Elute immune complexes by incubating in 65 ºC water bath for 1 h, vortexing every 15 mins to resuspend magnetic beads.
53. Spin at 14,000 RPM for 3 mins to pellet beads. Save the supernatant as the IP.
54. Continue cross-link reversal by incubating IP in O-ring screw-cap microcentrifuge tubes at 65 ºC on the heated shaker (1400 RPM). Allow to proceed overnight (~16 h should be sufficient).

Workup / purification of IP **Day 9**

55. Extract once with 200 μL phenol/$CHCl_3$/isoamyl alcohol, vortex thoroughly, and centrifuge at 14,000 RPM for 3 minutes.
56. Save aqueous phase. Back extract organic phase once (for IP only, for input it is unnecessary) with 100 μL elution buffer and pool both aqueous phases.
57. Add three volumes of Qiagen Buffer PM.
58. Add half of the solution (if IP, otherwise all if input) to Qiagen PCR Cleanup Kit spin column. Spin 30 secs at 14,000 RPM. Repeat with second half of solution. Discard all flow through.
59. Wash column with 750 μL Buffer PE. Spin 30 secs. Discard flow through. Spin 1 minute at 14,000 RPM.
60. Elute IP columns with 100 μL warmed Buffer EB (~55 ºC) and input DNA columns with 200 μL warmed Buffer EB. For IP columns, run eluate through column again for second elution.

qPCR Verification of Enriched Loci **Day 9**

All conditions are run in technical quadruplicate. Each PCR reaction consists of:

5 μL template DNA

5 μL Forward + Reverse primers (each at 1.8 μM concentration)

10 μL Roche FastStart Universal SYBR Green Master (Rox)

A standard curve must be run for each set of primers and for each unique input sample (i.e., vehicle treated, 1 nM DHT treated, etc.). If there are more than 20 experimental samples to analyze for a single primer pair (more than a single plate is required for a single primer set), the standard curve must be repeated on each plate. The standard curve consists of wells containing 50 ng, 5 ng, 500 pg, and 50 pg input DNA (i.e., the concentrations must be 10 ng/μL, 1 ng/μL, 100 pg/μL, and 10 pg/μL; adjust to these concentrations by using the NanoDrop UV/Vis to sample the concentration of your input samples).

Quantification of IP'd DNA **Day 9**

The Quant-iT™ PicoGreen® dsDNA Assay Kit (Invitrogen Cat. No. P11496) was used as directed to quantitate concentration of immunoprecipitated chromatin. The Sternberg lab NanoDrop fluorometer was used to generate a standard curve and to measure fluorescence emission of the PicoGreen dye. Typical concentrations for a single IP experiment were ~1 ng IP'd DNA.

Preparation of DNA for ChIP-Seq Submission

Five IP'd experiments for 1 nM DHT-induced LNCaP cells were examined by qPCR. The three most strongly enriched samples were combined, and the sample was quantified by PicoGreen assay. The input DNA sample (≥ 500 ng material, as determined by NanoDrop UV-Vis) and 1 nM DHT-induced pooled IP sample were each SpeedVac'd to ≤ 75 μL. For submission, a paper including my name, reference to the Dervan

laboratory, my sample labels (JWP VII-171 1 nM DHT induced input, JWP VII-171 1 nM DHT induced IP), and sample concentrations / total amount (and how they were measured: 3 ng IP'd solution measured by PicoGreen assay)

Primers Used

PSA ARE III F: 5'-GGATTGAAAACAGACCTACTCTGG-3'

PSA ARE III R: 5'-CAACAGATTTGTTTACTGTCAAGGA-3'

PSA ARE II F: 5'-CTGGTCTCAGAGTGGTGCAG-3'

PSA ARE II R: 5'-AGACCCAGTGTGCCCTAAGA-3'

PSA ARE I F: 5'-TGCATCCAGGGTGATCTAGT-3'

PSA ARE I R: 5'-ACCCAGAGCTGTGGAAGG-3'

PSA HRE F: 5'-GGTGTTGCTGTCTTTGCTCA-3'

PSA HRE R: 5'-GAGGCAATTCTCCATGGTTC-3'

FKBP5 intron-L F: 5'-AGCAATTTTGTTTTGAAGAGCA-3'

FKBP5 intron-L R: 5'-CTGTCAGCACATCGAGTTCA-3'

Neg1 F: 5'-AAAGACAACAGTCCTGGAAACA-3'

Neg1 R: 5'-AAAAATTGCTCATTGGAGACC-3'

Neg2 F: 5'-CCAGAAAACTGGCTCCTTCTT-3'

Neg2 R: 5'-TAGAAGGGGGATAGGGGAAC-3'

Primers were designed using Primer3[4] and checked for specific amplification by BLAST,[5] and the UCSC *in silico* PCR[6] prior to ordering. Each primer pair has had its concentration optimized. Primers were screened for unique product formation by quantitative PCR melting temperature examination and by running the primers on a native 4.0% agarose gel and visualizing the products relative to a 25 bp ladder (Invitrogen TrackIt Cat. No. 10488022).

References

(1) Johnson, D. S.; Mortazavi, A.; Myers, R. M.; Wold, B. *Science* **2007**, *316*, 1497–502.

(2) Mortazavi, A.; Leeper Thompson, E. C.; Garcia, S. T.; Myers, R. M.; Wold, B. *Genome Res.* **2006**, *16*, 1208–21.

(3) Nickols, N. G.; Dervan, P. B. *Proc. Natl. Acad. Sci. U. S. A.* **2007**, *104*, 10418–23.

(4) Rozen, S.; Skaletsky, H. *Methods Mol. Biol.* **2000**, *132*, 365–86.

(5) Johnson, M.; Zaretskaya, I.; Raytselis, Y.; Merezhuk, Y.; McGinnis, S.; Madden, T. L. *Nucleic Acids Res.* **2008**, *36*, W5–9.

(6) Kent, W. J.; Sugnet, C. W.; Furey, T. S.; Roskin, K. M.; Pringle, T. H.; Zahler, A. M.; Haussler, D. *Genome Res.* **2002**, *12*, 996–1006.